

AD-A085 859

DAYTON UNIV ON RESEARCH INST

F/S 11/4

QUICK REACTION EVALUATION OF MATERIALS FOR SYSTEMS APPLICATIONS--ETC (11)

APR 80 D R ASKINS, R R CERVAY, D L HART

F33615-78-C-5002

UNCLASSIFIED

UDR-TR-80-12

AFWAL-TR-80-4025

ML

1 of 4

AD-A085 859



11/4

5c (2) ~~SECRET~~
AFWAL-TR-80-4025

ADA 085859

QUICK REACTION EVALUATION OF MATERIALS
FOR SYSTEMS APPLICATIONS

D. R. Askins, R. R. Cervay, D. L. Hart, and B. H. Wilt
University of Dayton Research Institute
Dayton, Ohio 45469

April 1980

Technical Report AFWAL-TR-80-4025
Final Report Period 3 January 1978 to 31 March 1980

Approved for public release; distribution unlimited.

AIR FORCE MATERIALS LABORATORY
AIR FORCE WRIGHT AERONAUTICAL LABORATORIES
AIR FORCE SYSTEMS COMMAND
WRIGHT-PATTERSON AIR FORCE BASE, OHIO 45433

FILE COPY

80 6 20 151

NOTICE

When Government drawings, specifications, or other data are used for any purpose other than in connection with a definitely related Government procurement operation, the United States Government thereby incurs no responsibility nor any obligation whatsoever; and the fact that the Government may have formulated, furnished, or in any way supplied the said drawings, specifications, or other data, is not to be regarded by implication or otherwise as in any manner licensing the holder or any other person or corporation, or conveying any rights or permission to manufacture, use, or sell any patented invention that may in any way be related thereto.

This technical report has been reviewed by the Information Office (IO) and is releasable to the National Technical Information Service (NTIS). At NTIS, it will be available to the general public, including foreign nations.

This technical report has been reviewed and is approved for publication.

Albert Olevitch

MR. ALBERT OLEVITCH, Chief
Project Engineer

FOR THE COMMANDER:

Albert Olevitch

MR. ALBERT OLEVITCH, Chief
Materials Engineering Branch
Materials Support Division
Air Force Materials Laboratory

Copies of this report should not be returned unless return is required by security considerations, contractual obligations, or notice on a specific document.

UNCLASSIFIED

SECURITY CLASSIFICATION OF THIS PAGE (When Data Entered)

REPORT DOCUMENTATION PAGE		READ INSTRUCTIONS BEFORE COMPLETING FORM
1. REPORT NUMBER AFWAL-TR-80-4025	2. GOVT ACCESSION NO. AD-A085 859	3. REPORT'S CLASSIFICATION NUMBER
4. TITLE (and Subtitle) QUICK REACTION EVALUATION OF MATERIALS FOR SYSTEMS APPLICATIONS		5. TYPE OF REPORT & PERIOD COVERED Final Tech. Report 3 Jan. 1978-31 March 1980
7. AUTHOR(s) D. R. Askins, R. R. Cervay, D. L. Hart and B. H. Wilt		6. PERFORMING ORGANIZATION NUMBER UDR-TR-80-12
9. PERFORMING ORGANIZATION NAME AND ADDRESS University of Dayton Research Institute 300 College Park Avenue Dayton, Ohio 45469		8. CONTRACT OR GRANT NUMBER(s) F33615-78-C-5002
11. CONTROLLING OFFICE NAME AND ADDRESS Air Force Wright Aeronautical Laboratories Materials Laboratory (AFWAL/MLSE) Wright-Patterson AFB, Ohio 45433		10. PROGRAM ELEMENT PROJECT AREA & WORK UNIT NUMBERS 2421-03-05
12. MONITORING AGENCY NAME & ADDRESS (if different from Controlling Office) 12-71		11. REPORT DATE 11 Apr 1980
		13. NUMBER OF PAGES 370
		15. SECURITY CLASSIFICATION Unclassified

Approved for public release; distribution unlimited.

17. DISTRIBUTION STATEMENT (of the abstract entered in Block 20, if different from Report)

14. SUPPLEMENTARY NOTES

19. KEY WORDS (Continue on reverse side if necessary and identify by block number)

Nondestructive inspection Paris Equation
Crack initiation Walker Equation
Slack-quenched Hyperbolic Sine Equation
Mechanical properties Failure analysis
Fatigue crack growth rate Molybdenum-Disulfide (Moly-D) grease

20. ABSTRACT (Continue on reverse side if necessary and identify by block number)

This report is divided into four sections summarizing the engineering studies completed under contract to the Air Force Wright Aeronautical Laboratories, Materials Support Division. A variety of materials evaluations were completed under the categories of Alloys and Composites, Electronic Failure Analysis, Elastomers, and Plastics, Adhesives, and Composites.

DD FORM 1473
1 JAN 73

EDITION OF 1 NOV 65 IS OBSOLETE

UNCLASSIFIED

SECURITY CLASSIFICATION OF THIS PAGE (When Data Entered)

UNCLASSIFIED

SECURITY CLASSIFICATION OF THIS PAGE(When Data Entered)

19. Key Words (Concluded)

Lubrication characteristics
Dielectric constant
O-ring seals
Sealants
Primers
Chalking
Hydrolytic stability

Reticulated foams
Adhesives
Stress cracking
Polycarbonate
Potting compounds
Composites
Environmental aging

UNCLASSIFIED

SECURITY CLASSIFICATION OF THIS PAGE(When Data Entered)

PREFACE

This summary report covers work performed under Air Force Contract F33615-78-C-5002 during the period from 3 January 1978 to 31 March 1980. The contract was initiated under Project Number 2421-03-05, "Materials Application." The work was administered under the direction of the Air Force Materials Laboratory, Materials Support Division, Wright-Patterson Air Force Base, Ohio. Mr. A. Olevitch (AFML/MXE) acted as Project Engineer.

This work was conducted under the general supervision of Mr. D. Gerdeman, Project Supervisor. University of Dayton personnel who made major contributions to the program include: D. R. Askins, R. R. Cervay, D. L. Hart, J. J. Ruschau, B. H. Wilt, Research Engineers; and D. R. Byrge, S. J. Caldwell, J. R. Conner, J. N. Dues, T. Dusz, J. H. Eblin, T. A. Elmore, R. J. Kuhbander, A. L. Logue, S. C. Macy, R. J. Marton, J. C. McKiernan, D. S. Opela, L. D. Pike, P. J. Proshek, R. A. Rondeau, D. W. Wolesslagle, Research Technicians. This report was submitted in February 1980. The contractor's report number is UDR-TR-80-12.

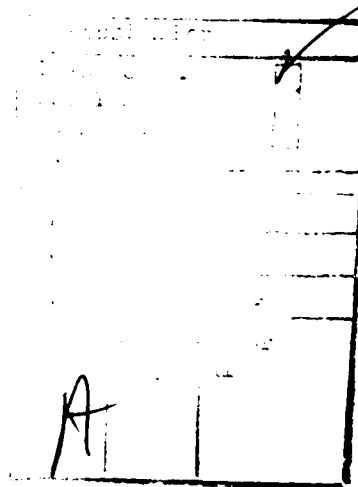


TABLE OF CONTENTS

<u>SECTION</u>		<u>PAGE</u>
1	ENGINEERING DATA ON ALLOYS AND COMPOSITES	1
1.1	F-100 Engine NDI Program	1
1.2	A Thorough Mechanical Property Investigation of Slack-Quenched ("Soft") Aluminum Alloy 2124-T851 Plate	3
1.3	Tensile Properties of Six Slack-Quenched Aluminum Alloy Rolled Plates	28
1.4	Computer Assisted Test Control and Data Acquisition	39
1.5	Software Development for the DEC PDP-11/34 Minicomputer	41
1.6	Complete Fatigue Crack Growth Rate Curves for Aluminum Alloy 2124-T851 Including Crack Growth Modeling	44
1.7	Crack Length Determination for the Elongated Compact Type Specimen Using Compliance Techniques	58
1.8	Spectrum Fatigue Testing of 10 Ni Steel	69
1.9	Failure Analysis Investigation of Bomb Link Assembly	78
1.10	Mechanical Property Data on CE 9000/7781 E-Glass Composite System	83
1.11	Lubrication Characteristics of Aerospace Greases on Fasteners	97
1.12	Torque/Tension Relationships for High Strength Threaded Fasteners Lubricated with Graphite Grease and Moly-D Grease	102
1.13	Comparison of Manually and Machine Developed Torque/Tension Data	109
1.14	Some Torque/Tension Data for Threaded Fasteners	119
1.15	Determination of Test Technique on K_{ISCC} Values for Aluminum 7075-T651 in a 3.5 Percent NaCl Environment	128
2	ELECTRONIC FAILURE ANALYSIS	137
2.1	Variable Reluctance Stepper Motor	137
2.2	Sensitive Push-Button Switch	139
2.3	Precision Variable Resistors	147
2.4	The Determination of the Dielectric Constant and Dissipation Factor of Two Dielectric Materials	142

TABLE OF CONTENTS (Concluded)

SECTION		PAGE
3	ELASTOMERS	145
3.1	Fluorosilicone O-Ring Seals	145
3.2	Dynamic Evaluation of MIL-P-83461 O-Rings	146
3.3	Volume Change of MIL-P-83461 O-Rings in Toluene	146
3.4	Evaluation of O-Ring Kits	156
3.5	Elastomers/JP-9 Compatibility Evaluation	159
3.6	Chalking of MIL-S-83430 Fuel Tank Sealants	170
3.7	Chalking of Sealants in Turbine Fuels Containing Anti-Static Additives	177
3.8	MIL-S-83430C Sealant on MIL-C-27725 and MIL-P-23377 Coatings	178
3.9	Purging Fluids	185
3.10	Evaluation of Aliphatic Naptha in MIL-C-38736 Cleaner	189
3.11	Channel Sealants	189
3.12	Hydrolytic Stability Tests of F-15 Fuel Tank Foams	218
3.13	Compatibility of Reticulated Foams with Turbine Fuels Containing Anti-Static Additives	230
3.14	RTV-133	251
3.15	MIL-A-8625 Anodized Aluminum Pnaels	251
4	PLASTICS, ADHESIVES, AND COMPOSITES	258
4.1	Stress Cracking of Polyethersulfone	258
4.2	Evaluation of "Tuffak" Polycarbonate	274
4.3	Thinwall Nylon Tensile Tests	274
4.4	Uralite 3130-Urethane Cast Elastomer	278
4.5	Characterization of Resin Matrix Systems	280
4.6	Determination of Temperature Profile in Potting Compounds	280
4.7	Vespel (Polyimide) Compatibility with JP-8 and JP-4	283
4.8	Core Splice Evaluation	283
4.9	Evaluation of F-178 Resin	283
4.10	Compression Properties of Shelter Potting Compound	283
4.11	Shelter Adhesive Retest Program	286
4.12	Shelter Repair Adhesive Evaluation	309
4.13	Evaluation of SCAR Specimen Design	310
4.14	Compatibility of Phosphoric Acid Anodizing with 350°F (177°C) Curing Adhesive Primers	325
4.15	AEDC End Cap Adhesive Evaluation	329
4.16	Durability Testing of Adhesives	331
4.17	Flexural Testing of PMR-15/Glass Panels	346
	REFERENCES	349

LIST OF ILLUSTRATIONS

<u>FIGURE</u>		<u>PAGE</u>
1	Through-the-Thickness Tensile Results for Slack-Quenched Aluminum 2124-T851	9
2	Compressive Stress-Strain Curves for Slack-Quenched and Baseline Aluminum 2124	11
3	Smooth Fatigue Results for Slack-Quenched Aluminum 2124-T851	13
4	Notched Fatigue Results for Slack-Quenched Aluminum 2124-T851	14
5	Hardness versus Cycles to Failure Curves of Notched Fatigue Data for Slack-Quenched Aluminum 2124-T851	17
6	Conductivity versus Cycles to Failure Curves of Notched Fatigue Data for Slack-Quenched Aluminum 2124-T851	19
7	R-Curves for Slack-Quenched Aluminum 2124-T851	20
8	Fatigue Crack Growth Data for Specimens CG-1-A and CG-1-B	22
9	Fatigue Crack Growth Data for Specimens CG-2-A and CG-2-B	23
10	Baseline and Affected Stress-Corrosion Cracking Test Specimens After 3,000 Hours in Test	26
11	Load versus Displacement Records for Slack-Quenched Lap-Shear Tensile Specimens	27
12	Fracture Toughness and Fatigue Crack Growth Specimens	46
13	Constant Amplitude Fatigue Crack Growth Rate Curves for Aluminum Alloy 2124-T851 at R-ratio of +0.1	49
14	Constant Amplitude Fatigue Crack Growth Rate Curves for Aluminum Alloy 2124-T851 at R-ratio of +0.5	50
15	Paris Model Equation for Aluminum Alloy 2124-T851 at R-ratios of +0.1 and +0.5	52

LIST OF ILLUSTRATIONS (Continued)

<u>FIGURE</u>		<u>PAGE</u>
16	Walker Model Equation for Aluminum Alloy 2124-T851	54
17	Forman Model Equation for Aluminum Alloy 2124-T851	56
18	Hyperbolic Sine Model Equation for Aluminum Alloy 2124-T851 at R-ratios of +0.1 and +0.5	57
19	Elongated Compact (WOL) Specimen Used for Fatigue Crack Growth Rate Testing	60
20	Calibration Curve for Elongated Compact (WOL) Specimen	64
21	Fatigue Crack Growth Rate Data for Aluminum 2124-T851, 0.75 Inch (19.0 mm) Thick, R = +0.1	65
22	Fatigue Crack Growth Rate Data for Aluminum 2124-T851, 1.50 Inch (38.1 mm) Thick, R = +0.1	66
23	Photomicrographs of Fatigue Fracture Face of Aluminum 2124-T851, 0.75 Inch (19.0 mm) Thick	67
24	Photomicrograph of Fracture Face of Aluminum 2124-T851, 1.50 Inch (38.1 mm) Thick	67
25	Fatigue Crack Growth Rate Data for Aluminum 2124-T851, 0.375 Inch (9.5 mm) Thick, R = +0.5	68
26	Double-Edge-Notched Specimen	70
27	Corner Crack Specimen for Crack Initiation Tests	71
28	Stress Spectra Graphically Presented	73
29	Crack Length versus Flights for Crack Initiation Specimens	77
30	Fracture Face of Corner Crack Specimen C-2-M1-4	78
31	Swivel Assembly	80
32	Photograph of Test Swivel Assembly (left) and Failed Swivel Assembly	80
33	Swivel Assembly Loading Fixture	81

LIST OF ILLUSTRATIONS (Continued)

<u>FIGURE</u>		<u>PAGE</u>
34	Test Specimen Layouts for Both A and B Panels	85
35	Composite Tensile Specimen Geometry	86
36	Three-Point Flexural Specimen Geometry	87
37	Short Beam Shear Specimen Geometry	87
38	Comparison of Graphite and Moly-D Grease	101
39	Effect of Changing Grease on Clamp-Up Force	103
40	Tension versus Torque for 5/8 Inch (15.9 mm) Diameter Fasteners with Dry Film Lubricant per MIL-N-8984 on Nuts	106
41	Tension versus Torque for 3/4 Inch (19.0 mm) Diameter Fasteners with Dry Film Lubricant per MIL-N-8984 on Nuts	107
42	Tension versus Torque for 7/8 Inch (22.2 mm) Diameter Fasteners with Dry Film Lubricant per MIL-N-8984 on Nuts	108
43	Comparison of Torque/Tension Characteristics for 5/8 Inch (15.9 mm) Diameter Fasteners With and Without Dry Film Lubricant on the Nuts	110
44	Comparison of Machine Developed (Data Points) and Manually Developed (Solid Curve) Torque/Tension Data	115
45	Comparison of Machine Developed (Data Points) and Manually Developed (Solid Curve) Torque/Tension Data	116
46	Comparison of Machine Developed (Data Points) and Manually Developed (Solid Curve) Torque/Tension Data	117
47	Individual Data Points and Best Fit Curve for Manually Developed Torque/Tension Data for 5/8 Inch (15.9 mm) Bolts Lubricated with Moly-D	118
48	Torque/Tension Results for 5/8 Inch (15.9 mm) Bolts	125

LIST OF ILLUSTRATIONS (Continued)

<u>FIGURE</u>		<u>PAGE</u>
49	Torque/Tension Results for 3/4 Inch (19.0 mm) Bolts	126
50	Torque/Tension Results for 7/8 Inch (22.2 mm) Bolts	127
51	Typical Load versus Crack Opening Displacement Traces	131
52	Compliance Curve Obtained for Bolt-Loaded Specimen	131
53	Stress Corrosion Cracking Results for Aluminum Alloy 7075-T651	134
54	Plastic Rotating Band Specimen	260
55	Tensile Stress-Rupture Specimen Immersed in Solvent and Under Load	262
56	Effect of Stress on Stress Craze Behavior of Polyethersulfone in Isopropanol	265
57	Effect of Stress on Stress Craze Behavior of Polyethersulfone in Acetic Acid	266
58	Effect of Stress on Stress Craze Behavior of Polyethersulfone in Methoxyethanol	267
59	Effect of Stress on Stress Fracture Behavior of Polyethersulfone in Isopropanol	268
60	Effect of Stress on Stress Fracture Behavior of Polyethersulfone in Acetic Acid	269
61	Effect of Stress on Stress Fracture Behavior of Polyethersulfone in Methoxyethanol	270
62	Typical Craze in PES Rotating Bands on 20 mm Projectiles	271
63	Tensile Stress-Strain Curves of Cast Resin Matrix Systems	282
64	Lap Shear Specimens (from ASTM)	293
65	Floating Roller ("Bell") Peel Specimen and Fixture (from ASTM)	293

LIST OF ILLUSTRATIONS (Concluded)

<u>FIGURE</u>		<u>PAGE</u>
66	Lap Shear Specimen and Stress Durability Fixture (from ASTM)	295
67	Thick Adherend Double Cantilever Beam (DCB) Crack Extension Specimen (from AFML-TR-76-173)	295
68	Lap Shear Specimens (from ASTM)	311
69	SCAR Specimen	318
70	Form and Dimensions of Test Specimen	319
71	Durability Test Apparatus	321
72	Specimen Mounting Cells for the Durability Test Apparatus	334
73	Specimen Mounting Cell Being Inserted Into Humidity Cabinet	335
74	Overall View of Durability Test Apparatus	336
75	Single Lap Shear Adhesive Specimen	338
76	Environmental Degradation Behavior of Machined Single Lap Shear Adhesive Joints	341
77	Comparative Environmental Stress-Rupture Time-to-Failure Behavior of Three 350°F (177°C) Curing Adhesive Systems at 140°F (60°C) and 95-100% Relative Humidity	345

LIST OF TABLES

<u>TABLE</u>		<u>PAGE</u>
1	Longitudinal Tensile Data, 2124-T851 5.5 Inch Plate	6
2	Transverse Tensile Data, 2124-T851 5.5 Inch Plate	7
3	Through-Thickness Longitudinal Tensile Properties Through 5.5 Inch 2124-T851 Slack- Quenched Aluminum Plate	8
4	Compression Strength Data for 2124-T851 5.5 Inch Slack-Quenched Aluminum Plate	10
5	Bearing Strength Data ($E/D = 2.0$) for 2124- T851 5.5 Inch Slack-Quenched Aluminum Plate	12
6	Smooth Fatigue Data 2124-T851 5.5 Inch Slack-Quenched Aluminum Plate	15
7	Notched ($K_t = 2.43$) Fatigue Data 2124-T851 5.5 Inch Slack-Quenched Aluminum Plate	16
8	Stress Corrosion Test Results for 2124-T851 5.5 Inch Thick Plate, Constant Stress, Alternate Immersion	24
9	Stress Corrosion Cracking Test Results from 2124-T851 5.5 Inch Thick Plate, L-T Orientation, Continuous Immersion	26
10	Fastener Fatigue Results	29
11	Longitudinal Tensile Properties 2124-T851 Slack-Quenched Aluminum Plate 2.750 Inches (70 mm) Thick	31
12	Longitudinal Tensile Properties 2024-T351 Slack-Quenched Aluminum Plate 2.00 Inches (51 mm) Thick	31
13	Longitudinal Tensile Properties of 2124-T851 Slack-Quenched Aluminum Plate 5.50 Inches (140 mm) Thick	32
14	Transverse Tensile Properties of 2124-T851 Slack-Quenched Aluminum Plate 5.50 Inches (140 mm) Thick	33

LIST OF TABLES (Continued)

<u>TABLE</u>		<u>PAGE</u>
15	Through the Thickness Longitudinal Properties of 2124-T851 Slack-Quenched Aluminum Plate 5.50 Inches (140 mm) Thick	33
16	Through the Thickness Longitudinal Tensile Properties of ALCOA Aluminum Company Alloy 2124-T851 Plate, 5.50 Inches (140 mm) Thick	34
17	Through the Thickness Longitudinal Tensile Properties of Kaiser Aluminum Company Alloy 2124-T851 Plate, 5.0 Inches (127 mm) Thick	34
18	Longitudinal Tensile Properties of Alloy 7075-T7351 Aluminum Slack-Quenched Plate 4.00 Inches (102 mm) Thick	35
19	Transverse Tensile Properties of Alloy 7075-T7351 Slack-Quenched Aluminum Plate 4.00 Inches (102 mm) Thick	36
20	Through the Thickness Longitudinal Tensile Properties of Alloy 7075-T7351 Aluminum Plate 4.00 Inches (102 mm) Thick	36
21	Longitudinal Tensile Properties of Alloy 7075-T651 Slack-Quenched Aluminum Plate 1.250 Inches (32 mm) Thick	37
22	Transverse Tensile Properties of Alloy 7075-T651 Slack-Quenched Aluminum Plate 1.250 Inches (32 mm) Thick	38
23	Longitudinal Tensile Properties of Alloy 7075-T7351 Slack-Quenched Aluminum Plate 0.50 Inch (13 mm) Thick	38
24	Tensile Properties of Aluminum Alloy 2124-T851 Two Inch (50.8 mm) Thick Plate	48
25	Fracture Toughness Properties of Aluminum Alloy 2124-T851 Two Inch (50.8 mm) Thick Plate	48
26	General Dynamics Flight by Flight Fatigue Test Spectra	72
27	Fatigue Spectrum Results on 10 Ni Steel, Double Edge-Notch Specimens	74

LIST OF TABLES (Continued)

<u>TABLE</u>		<u>PAGE</u>
28	Results for Tensile Tests on Swivel Assemblies	82
29	Physical Properties of Glass Reinforced Composite System CE 9000/7781 E-Glass, Panels A and B	88
30	Room Temperature Tensile Test Results for Composite Material CE 9000/7781 E-Glass	90
31	Elevated Temperature [380°F (193°C)] Tensile Test Results for Composite Material CE 9000/7781 E-Glass	91
32	Three-Point Flexural Test Results for CE 9000/7781 E-Glass Material, Warp Direction	93
33	Short Beam Shear Results for CE 9000/7781 E-Glass Material, Warp Direction	94
34	Test Results on CE 9000/7781 Double-Lap Shear Specimens Bonded With FM-400 Adhesive	95
35	Test Conditions for Fasteners	100
36	Test Results for a 5/8 Inch (15.9 mm) Bolt Lubricated with Moly-D and Tested at Constant Rotational Rate	113
37	Average Values of Test Results for 5/8 Inch (15.9 mm) Bolt	114
38	Torque/Tension Values for 5/8 Inch (15.9 mm) Bolts, Dry Film Lubricant	122
39	Torque/Tension Values for 3/4 Inch (19.0 mm) Bolts, Dry Film Lubricant	122
40	Torque/Tension Values for 7/8 Inch (22.2 mm) Bolts, Dry Film Lubricant	123
41	Torque/Tension Values for 5/8 Inch (15.9 mm) Bolts, No Lubricant	123
42	Torque/Tension Values for 3/4 Inch (19.0 mm) Bolts, No Lubricant	124
43	Torque/Tension Values for 7/8 Inch (22.2 mm) Bolts, No Lubricant	124

LIST OF TABLES (Continued)

<u>TABLE</u>		<u>PAGE</u>
44	Fluorosilicone O-Rings (Tensile Strength and Elongation)	147
45	Fluorosilicone O-Rings (Flexibility)	148
46	Evaluation of Fluorosilicone O-Rings	151
47	Parker N756-75 Dynamic Tests to MIL-P-83461	153
48	Houghton 10V75-440 Dynamic Tests to MIL-P-83461	154
49	Parco 4367-70 Dynamic Tests to MIL-P-83461	155
50	Volume Swell of 83461 O-Rings in Toluene for 24 Hours	157
51	National Kit OK 311	160
52	Aerocustom Kit ACOK 311	161
53	Elastomers/JP-9 Compatibility Evaluation, O-Rings	164
54	Elastomers/JP-9 Compatibility Evaluation, Polysulfide Sealants	169
55	Elastomers/JP-9 Compatibility Evaluation, Sheet Materials	171
56	Elastomers/JP-9 Compatibility Permeation Evaluations	173
57	Sealant Chalking Tests	175
58	Results of Chalking Tests	176
59	Evaluation of MIL-P-23377D Panels	179
60	MIL-S-83430 Sealant Evaluation on MIL-C-27725 and MIL-P-23377 Coating	180
61	Evaluation of Elastomeric Materials in JP-4/Soltrol 220	186
62	Volume Change Determination on Elastomers in JP-5	187
63	Evaluation of Aliphatic Naptha in MIL-C-38736 Cleaner	190

LIST OF TABLES (Continued)

<u>TABLE</u>		<u>PAGE</u>
64	Channel Sealants (Volume Change, Density, and Weight Loss)	194
65	Channel Sealants (Volume Change, Density, and Weight Loss)	195
66	Channel Sealants (Flatwise Tension)	200
67	Channel Sealants (Low Temp. Flex.)	208
68	Channel Sealants (Pressure Rupture)	212
69	Channel Sealants (Corrosion)	214
70	Channel Sealants (Non-Volatile Content)	215
71	Channel Sealants (Thermal Extrusion)	216
72	Channel Sealants (Extrusion Rate)	217
73	Channel Sealants (Volume Change, Weight Change, and Specific Gravity)	219
74	Channel Sealants (Flatwise Tension)	222
75	Hydrolytic Stability of Foams	224
76	Hydrolytic Stability of Foams W258R (1-1) Red Foam Re-Test, 120°F (49°C) + 95% R.H.	228
77	Hydrolytic Stability of Foams	231
78	Compatibility of Reticulated Foams in Fuels W236R Blue Foam	235
79	Compatibility of Reticulated Foams in Fuels W258R (1-1) Red Foam	243
80	Compatibility of Reticulated Foams in Fuels W901P Red Foam (Fluid No. 10)	247
81	Compatibility of Reticulated Foams in Fuels W402-2 Blue Foam (Fluid No. 10)	248
82	Compatibility of Reticulated Foams in Fuels W403-2 Orange Foam (Fluid No. 10)	249
83	Compatibility of Reticulated Foams in Fuels W404-2 Red Foam (Fluid No. 10)	250

LIST OF TABLES (Continued)

<u>TABLE</u>		<u>PAGE</u>
84	RTV-133	252
85	Peel Strength	256
86	Polyethersulfone Tensile Stress Cracking Behavior	264
87	Effect of Paint on Tensile Stress Cracking Behavior of Polyethersulfone	273
88	Mechanical and Thermal Properties of Tuffak Polycarbonate	275
89	General Data on Tuffak Polycarbonate	276
90	Optical Quality Data on Tuffak Polycarbonate	276
91	Environmental Data on Tuffak Polycarbonate	277
92	Coefficient of Thermal Conductivity of Tuffak Polycarbonate	277
93	Tensile Properties of Thinwall Nylon	279
94	Hardness Measurements	280
95	Gel Times of Various Urethane Mix Ratios at 72°F (22°C)	281
96	Effect of Fuel Immersion of Vespel Polyimide	284
97	Tube Shear Test Results for Core Splice Adhesives	285
98	Lap-Shear Test Results on F-178 Resin	285
99	Effect of Environmental Aging on the Compressive Strength of Potting Compounds	287
100	Adhesive Lap Shear Test Results on 6061T6 Adherends with Machined Specimens	297
101	Adhesive Lap Shear Test Results on 5052H34 Adherends with Machined Specimens	299

LIST OF TABLES (Continued)

<u>TABLE</u>		<u>PAGE</u>
102	Adhesive Lap Shear Test Results on 6061T6 Adherends with Preslotted Specimens	301
103	Adhesive Lap Shear Test Results on 5052H34 Adherends with Preslotted Specimens	302
104	Adhesive Floating Roller Peel Test Results	304
105	Adhesive Stress-Durability Test Results	305
106	DCB Crack Extension Results	307
107	Shelter Repair Program, Phase I: Baseline Lap-Shear Data on 5052-H34 Adherends	312
108	Shelter Repair Program, Phase I: Baseline Lap-Shear Data on 6061-T6 Adherends	313
109	Phase II: Stress-Durability Test Results on 5052-H34 Adherends Exposed at 200°F (93°C), 95-100% R.H.	314
110	Phase II: Stress-Durability Test Results on 6061-T6 Adherends Exposed at 200°F (93°C), 95-100% R.H.	315
111	Phase III: Stress-Durability Test Results on 5052-H34 Adherends Exposed at 140°F (60°C), 95-100% R.H.	316
112	Phase III: Stress-Durability Test Results on 6061-T6 Adherends Exposed at 140°F (60°C), 95-100% R.H.	317
113	Static Lap Shear Test Results for SCAR Design Evaluation	322
114	Stress-Durability Test Results Using the Sharp Fixture for SCAR Design Evaluation	323
115	Stress-Durability Test Results Using the Durability Test Apparatus for SCAR Design Evaluation	324
116	Lap Shear Data Summary	327
117	Floating Roller Peel Data Summary	328

LIST OF TABLES (Concluded)

<u>TABLE</u>		<u>PAGE</u>
118	Wedge Crack-Propagation Data Summary	329
119	"T"-Type Tensile Test Results	330
120	Lap Shear Test Results on Polyimide/Aluminum Specimens Bonded with DC3145 Adhesive	330
121	Test Results Obtained on AF-143 Adhesive Bonded Joints	332
122	Test Results Obtained on AF-143 Adhesive Bonded Joints	333
123	Single Lap Shear Strength of Adhesive Joints	339
124	Environmental Stress-Rupture Lap Shear Behavior of Adhesive Joints	340
125	Flexural Properties of PMR-15/Glass Laminates	348

SUMMARY

This report presents the results of engineering evaluations of a wide variety of materials of interest to the U.S. Air Force. To facilitate presentation of the data, the report is divided into four major sections: Alloys and Composites, Electronic Failure Analysis, Elastomers, and Plastics, Adhesives and Composites.

The first section, Engineering Data on Alloys and Composites, includes material properties evaluations of metal alloys and composite structural components. Included are data on the investigation of improperly quenched, rolled aluminum alloys, the determinations of fatigue crack growth rate of aluminum and steel, mechanical properties of CE 9000/7781 E-Glass composites, and lubrication characteristics of aerospace greases. Nondestructive test capabilities in determining engine cracks and the development of computer codes to assist fatigue test capabilities are also discussed.

The second section, Electronic Failure Analysis, discusses failure analyses of a variety of electronic components including stepper motors, mini-switches, variable resistors, and dielectric materials.

Section 3, Elastomers, includes the physical and dynamic evaluations of fluorosilicone O-ring seals for the prediction of useful seal life, the evaluation of MIL-P-83461 O-ring seals, and the evaluation of O-ring kits in use by the Air Force. Included also are the results of compatibility determinations of fuel tank sealants and fuel tank reticulated foams in fuels and fuel additives, and the effect of JP-9 fuel on a variety of elastomeric materials.

Section 4, Plastics, Adhesives and Composites, summarizes the results of mechanical and environmental testing of plastics including transparent materials, injection molded and cast materials. Adhesives investigations include adhesives for use in portable tactical shelters, high temperature applications, and

aircraft structural uses. Evaluations of composite materials for high temperature applications are also discussed.

SECTION 1

ENGINEERING DATA ON ALLOYS AND COMPOSITES

The mechanical response of materials of interest to the United States Air Force includes fracture mechanics properties that are affected by environmental conditions, i.e., temperature and relative humidity. Test programs range from several man-hours to evaluate hydraulic tubing failures in the A-10 aircraft to as much as two man-years to assess the nondestructive test capabilities used in the manufacture and maintenance of the F-100 engine.

Approximately 70 percent of the materials that undergo test in the laboratory are high strength alloyed structural metals: steel, titanium, aluminum, magnesium, and nickel. The remainder are either polymeric or composite structural materials that use glass fibers, graphite cloth, or metal fibers in a metal or polymeric matrix.

Joint designs are usually the most vulnerable to mechanical failure. Various joint designs that have undergone evaluation include the seam fold and stitching pattern influence on parachute seam strength, the influence of drilled hole size on the ultimate load carrying capability of a blind hole rivet joint, the C-141 interference fit fastener corrosion fatigue, and the weld repair procedure for cracked turbine blades. Included in this section are summations of some of the significant projects conducted on structural materials and/or system components.

1.1 F-100 ENGINE NDI PROGRAM

This program was conducted in cooperation with the Failure Analysis Group of the Air Force Materials Laboratory. Flawed specimens were prepared to assist Pratt and Whitney Aircraft Company in assessing their nondestructive inspection facilities capability of finding very small cracks in complex engine configurations. Nineteen specimen configurations were selected for

the program to simulate an equal number of potential fatigue cracking trouble areas that exist in the F-100 engine. The specimen blanks were initially machined and supplied by the Pratt and Whitney Aircraft Company. Five different materials were used to make the 19 various specimen configurations, depending on the material used in fabricating the actual piece of engine hardware being modeled. The five materials were: titanium alloys 6-2-4-6 and 8-1-1; and nickel alloys IN-100, ASTRALLOY, and WASPALLOY. A spot welding machine was used to create a stress concentration dimple which served as a fatigue crack initiator in the appropriate area of the specimen blank. A usual procedure for all configurations was to fracture open three precracked specimens to determine the fatigue crack aspect ratio, i.e., flaw depth to surface trace. This relationship was subsequently relied upon to determine what flaw depth would remain in the specimen after final machine removal of a specified amount of surface material and contouring the specimen to be identical to the engine component being modeled. All of the final machining was performed by the base machine shop. Approximately 70 percent of the exotic tooling required was furnished by the Pratt and Whitney Aircraft Company and the remainder was procured locally by the UDRI. Nine flawed specimens were produced for each of the 19 specimen configurations; there were three different flaw sizes (maximum depth), 0.005, 0.010, and 0.020 inch (0.125, 0.254, and 0.508 mm, respectively) for each of the 19 specimen geometries. Before shipment to Pratt and Whitney Aircraft Company, the specimens were examined by the AFML Nondestructive Inspection Laboratory (NDI), AFML/MXA. The NDI laboratory verified that the cracks were still present in the flawed specimens and had not been machined away or that material had not been smeared over the flaw so as to obscure or mask it. Four control specimens were included with each of the 19 specimen geometry sets when they were shipped back to Pratt and Whitney Aircraft; the control specimens either contained

no flaws or they contained a much larger, readily found crack in the particular specimen configuration's region of interest. Also, additional specimen blanks were machined to the final configuration and returned to Pratt and Whitney Aircraft to aid them in attempts to model the fatigue cracked flawed specimens with an Electrical Discharge Machining (EDM) induced flaw. The EDM would then be used to develop custom contoured eddycurrent nondestructive inspection probes for the problem crack initiation areas in the F-100 engine.

Initially, there were several specimen configurations that were questionable as to the feasibility of being able to precrack and then control the flaw shape and size well enough to define the end product flaw size following machining. All of these configurations were successfully fatigue cracked. Due to the extensive alteration of the flaw area by the multiple machining operations performed on these several configurations, exact definition of the final flaw shape/size can only be verified after the Pratt and Whitney Aircraft Company is finished with the specimens. When returned they will be failed open for verification.

This program was one of the largest efforts ever conducted in the engineering and design data area. The program was a concentrated effort from March through August 1979 and represents approximately two and one-half man-years effort expended in six months period of time.

1.2 A THOROUGH MECHANICAL PROPERTY INVESTIGATION OF SLACK-QUENCHED ("SOFT") ALUMINUM ALLOY 2124-T851 PLATE

In the summer of 1979 a German airframe manufacturer, while preparing a large aluminum plate for a future aircraft component, became aware of areas in the final machine part which, when anodized, appeared dark in comparison to a normal aluminum anodized surface. Investigations later revealed these areas to contain substantially lower hardness and higher electrical conductivities

than acceptable for this particular aluminum alloy and heat treatment condition. The problem was traced back to the producer's heat treatment facility. This facility had apparently been producing plates containing improperly quenched areas for some time. These areas were found to possess low strength properties. Very briefly, a water spray unit in a heat treatment line was unable to rapidly quench areas of a plate from the solutionizing temperature, leaving regions on one surface of the plate somewhere between an annealed and properly solution heat-treated condition. A survey of material delivered throughout the industry indicated that many plates contained these slack-quenched or "soft" regions and, up to this time, had been undetected.

Because of the serious implication of inferior aircraft components for both civilian and commercial use, an immediate mechanical property investigation was conducted. A number of aluminum plates, discovered with soft regions, have been examined for tensile strength property degradation in the inferior regions, with results published in UDR-TM-79-23.^[1] This report consumes a thorough investigation of several mechanical properties of one such plate, a 5.5 inch (140 mm) thick plate of aluminum 2124-T851 which was diverted from being machined into a final bulkhead component.

It should be stated that several phases or terms have been used to describe the areas of inferior quality. The term "slack-quench" was originally coined to describe the regions; terms later evolved such as "soft" and "affected" aluminum, all referring to these inferior regions on one surface of the rolled plate. (Note: Because both sides of a plate are always water quenched, the top surface opposite the soft or affected surface was properly heat treated and displayed little or no loss in hardness or increase in electrical conductivity over the entire surface.) Throughout this report, specimens removed from either surface will be designated with the letter "A" if removed from the affected plate surface, or "B" (baseline) if removed from the properly heat treated surface.

The mechanical properties investigated were both longitudinal and transverse tensile, compression, bearing, smooth and notched ($K_t = 2.4$) fatigue, fatigue crack growth, stress corrosion, fracture, stress corrosion cracking, and fatigue and tensile properties of fastened elemental joints. These properties were examined both in the affected regions and the normal, baseline side of the plate.

In addition to determining the mechanical property degradation, hardness and electrical conductivity measurements were taken on all specimens prior to test (when possible) in an attempt to link these nondestructive type test results to the level or degree of inferiority. This was a major emphasis, since the ability to discover, or proof, already installed aircraft components could obviously insure the integrity of the aircraft for its remaining design life.

The results of the tensile tests, as performed in accord with ASTM Standard E8-78, are presented in Table 1 for the longitudinal oriented specimens, and Table 2 for the transverse oriented specimens. Presented for each specimen is the range in hardness taken at each specimen end (obtained after the test in a little or no plastic-strained region on the test coupon) and the average electrical conductivity, EC, prior to testing. Also presented is the recommended^[2] minimum hardness and conductivity range for this aluminum/heat treatment.

While all of the baseline (B) specimen results meet the appropriate recommended specifications, the affected (A) side tensile results indicate a dramatically inferior strength (yield and ultimate) when compared to those same specifications. In comparing the affected to the baseline test results, there is as much as a 30 percent loss in the ultimate and a 39 percent loss in the yield strength for the longitudinal oriented series of specimens. For the transverse oriented (surface region) specimens there is a maximum 30 percent loss in the ultimate and a 46 percent loss in the yield strength, when comparing the affected to the baseline test data. These grossly inferior

TABLE 1
LONGITUDINAL TENSILE DATA,
2124-T851 5.5 inch PLATE

Specimen I.D.	UTS, KSI	Yield, KSI	Elong. in 2.0" G.L.	RA (%)	Hardness, R _B	EC, % IACS*
TL-1A	44.5	32.8	8.7	20.6	40/36	46/46
TL-2A	44.8	33.6	9.1	18.9	48/39	46/46
TL-3A	44.9	32.7	8.3	23.3	39/36	46/46
TL-4A	48.9	37.5	7.7	24.6	50/47	45/45
TL-5A	50.5	38.5	8.5	24.9	48/58	45/44
TL-6A	49.1	37.4	8.6	19.6	49/47	45/45
TL-7A	48.4	36.2	8.4	27.2	47/47	45/45
TL-8A	49.6	37.6	8.5	22.3	47/48	45/45
TL-9A	49.3	37.1	8.8	24.5	47/49	45/45
TL-10A	<u>50.9</u>	<u>39.2</u>	<u>8.3</u>	<u>25.2</u>	<u>47/54</u>	<u>45/45</u>
Average	48.1	36.3	8.5	23.1	46.2	45.2
Specif.	63	54	5	--	74	35.0-42.5
TL-1B	69.1	61.3	7.4	20.4	77/74	41/41
TL-2B	69.6	61.8	7.2	17.7	78/77	41/41
TL-3B	69.5	61.3	7.7	18.0	75/74	41/41
TL-4B	68.8	60.8	7.4	12.5	75/74	41/41
TL-5B	69.6	62.0	7.2	13.1	77/79	41/41
TL-6B	69.8	61.9	7.1	20.8	79/80	41/41
TL-7B	69.7	61.8	8.4	17.4	79/80	41/41
TL-8B	69.5	61.4	6.6	15.6	80/80	41/41
TL-9B	70.1	62.2	8.1	17.4	80/80	41/41
TL-10B	<u>70.3</u>	<u>62.1</u>	<u>7.6</u>	<u>18.0</u>	<u>79/79</u>	<u>41/41</u>
Average	69.6	61.7	7.5	17.1	77.8	41.0
Specif.	63	54	5	--	74	35.0-42.5

* IACS: International Annealed Copper Standard.

TABLE 2
TRANSVERSE TENSILE DATA
2124-T851 5.5 inch PLATE

Specimen I.D.	UTS, KSI	Yield, KSI	Elong. in 2.0" G.L.	RA (%)	Hardness R _B	EC % IACS
TT-1A	47.2	31.1	8.2	13.7	53/42	45/45
TT-2A	44.5	27.3	9.6	20.3	39/38	46/46
TT-3A	<u>46.3</u>	<u>29.2</u>	<u>9.5</u>	<u>15.3</u>	<u>53/40</u>	<u>45/45</u>
Average	46.0	29.2	9.1	16.4	44.2	45.3
Specif.	63	54	4	--	74	35.0-42.5
TT-1B	69.3	61.6	6.9	9.3	77/79	41/41
TT-2B	69.4	61.7	5.4	8.8	79/78	41/41
TT-3B	<u>69.1</u>	<u>60.5</u>	<u>7.7</u>	<u>10.1</u>	<u>79/79</u>	<u>41/41</u>
Average	69.3	61.3	6.7	9.4	78.5	41.0
Specif.	63	54	4	--	74	35.0-42.5

strength properties are further substantiated by the extremely low hardness and high conductivity readings taken on each affected specimen. For both longitudinal and transverse affected specimens the ductility was noticeably increased, as was expected.

A through-thickness, longitudinal tensile strength profile was obtained, with results presented in Table 3. The dimension to the left of the table represents the depth of the specimen's centerline as measured from the affected side. As can be readily observed, the depth of the soft or affected region extends through the majority of the plate thickness. In the chart shown in Figure 1, the effect of the inferior quench is strikingly evident where the yield and ultimate strengths fall below the minimum allowables at depths over 70 percent of the total thickness as measured from the affected side. Again, as expected, the hardness readings indicate the same trend, while

TABLE 3
THROUGH-THICKNESS LONGITUDINAL TENSILE PROPERTIES
THROUGH 5.5 inch 2124-T851 SLACK
QUENCHED ALUMINUM PLATE

Depth From Soft Side (In.)	Specimen I.D. \	UTS KSI	Yield KSI	Hardness R _B	EC % IACS
1/8	TL-2-A	44.8	33.6	48/39	45.8
3/4	TL-2-1	44.9	33.8	44/38	45.3
1-1/4	TL-2-2	56.9	48.0	60/64	42.5
1-3/4	TL-2-3	58.5	49.8	65.5	42.4
2-1/4	TL-2-4	59.7	51.4	68.5	42.2
2-3/4	TL-2-5	59.8	51.9	69.0	42.2
3-1/4	TL-2-6	60.4	50.3	68.5	42.2
3-3/4	TL-2-7	62.4	52.4	70.0	42.1
4-1/4	TL-2-8	64.6	55.1	74.0	41.8
4-3/4	TL-2-9	67.8	59.3	77.0	41.2
5-3/8	TL-2-B	69.6	61.8	77.5	41.0
Specification		63.0	54.0	74.0	35.0-42.5

the EC readings are less conservative. By noting only the curve of EC versus depth into the plates, one would expect the effect of the soft region to exist to a depth less than 25 percent of the plate thickness. This is obviously not the case. However, all results obtained do indicate that the most drastic drop in tensile strength is somewhat shallow, less than 20 percent into the plate thickness. The strength levels in the central section of the plate tend to level out at values that are typically 10 to 15 percent below the minimum strength specifications, at a depth range of 1 to 4 inches (25 to 102 mm) from the affected side.

The results of compression testing, conducted in accord with ASTM Standard E9-77, are presented in Table 4. The average compressive yield strength obtained for the affected regions represents a decrease in excess of 55 percent of the average compressive yield strength value obtained for the baseline side; the loss in average yield strength is equal to 46 percent of the minimum

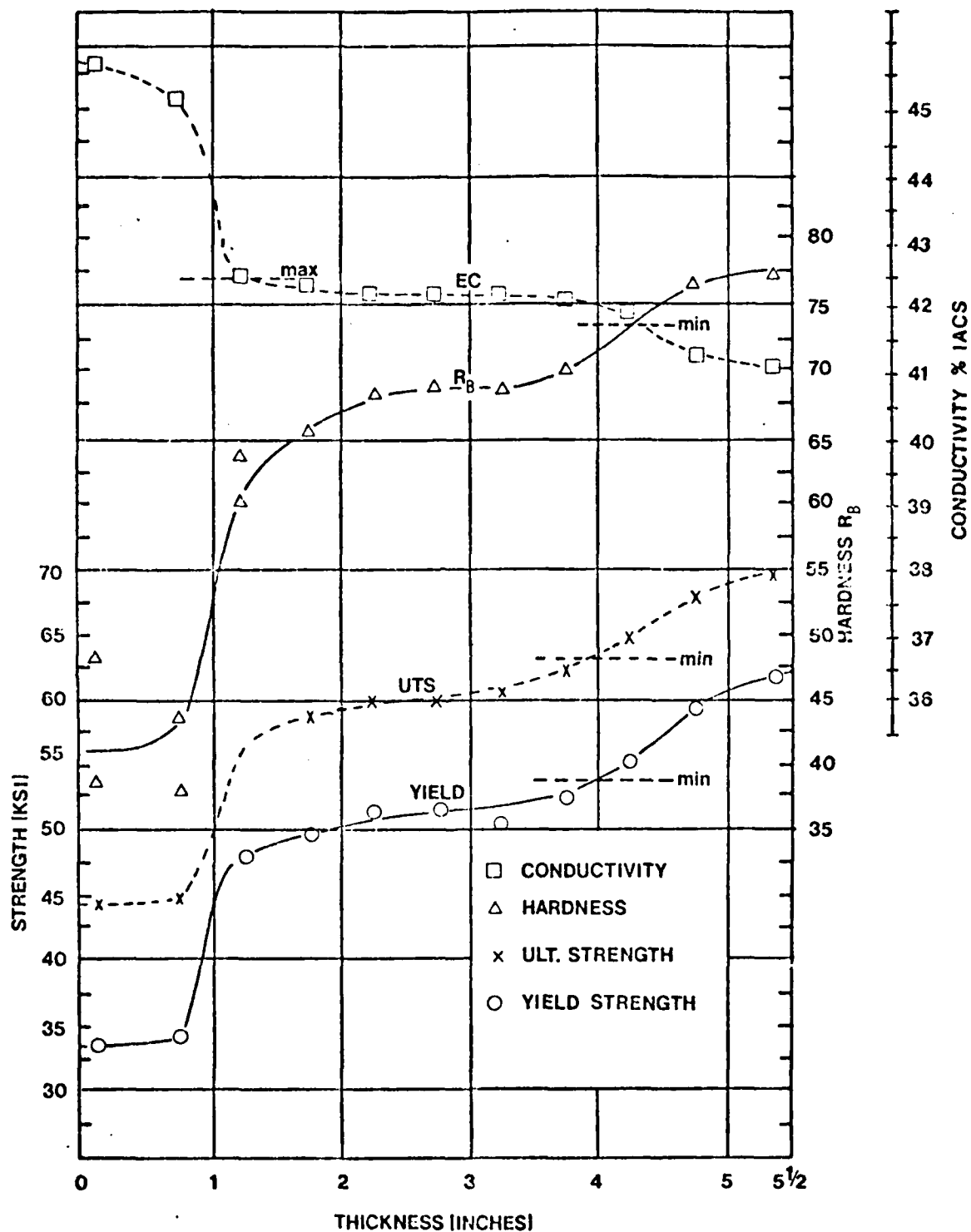


Figure 1. Through-the-Thickness Tensile Results for Slack-Quenched Aluminum 2124-T851.

TABLE 4
COMPRESSION STRENGTH DATA FOR 2124-T851
5.5 inch SLACK-QUENCHED ALUMINUM PLATE

Specimen I.D.	Yield Strength KSI	Hardness R _B	EC % IACS
C-1A	24.7	39.2	45.5
C-2A	26.0	51.0	45.4
C-3A	32.1	62.5	44.2
Average	27.6	50.9	45.0
C-1B	62.9	80.0	40.5
C-2B	62.3	80.5	40.8
C-3B	62.0	80.5	40.6
Average	62.4	80.3	40.6
Specification	51.0	74.0	35.0-42.5

specification. Both the hardness and EC readings for the three affected specimens indicate all three to be vastly substandard, with specimen C-1A being the lowest in strength. The stress-strain curves obtained for specimens C-2A and B, presented in Figure 2, clearly illustrate the inferior compressive strength properties in the affected regions.

The results of bearing tests conducted following guidelines set forth in ASTM Standard E238-68 are presented in Table 5. The results from specimens removed from the affected side of the plate show a significant loss in both bearing yield and ultimate strengths, approximately 26 and 16 percent, respectively, in comparison with the minimum specification values. All baseline specimens exceeded those minimum requirements listed in the table. Finally, the hardness and EC readings clearly pointed out all affected specimens to be inferior.

An important note to keep in mind for all types of test results is the property degradation with respect to the location in the plate. These bearing test specimens were not removed from

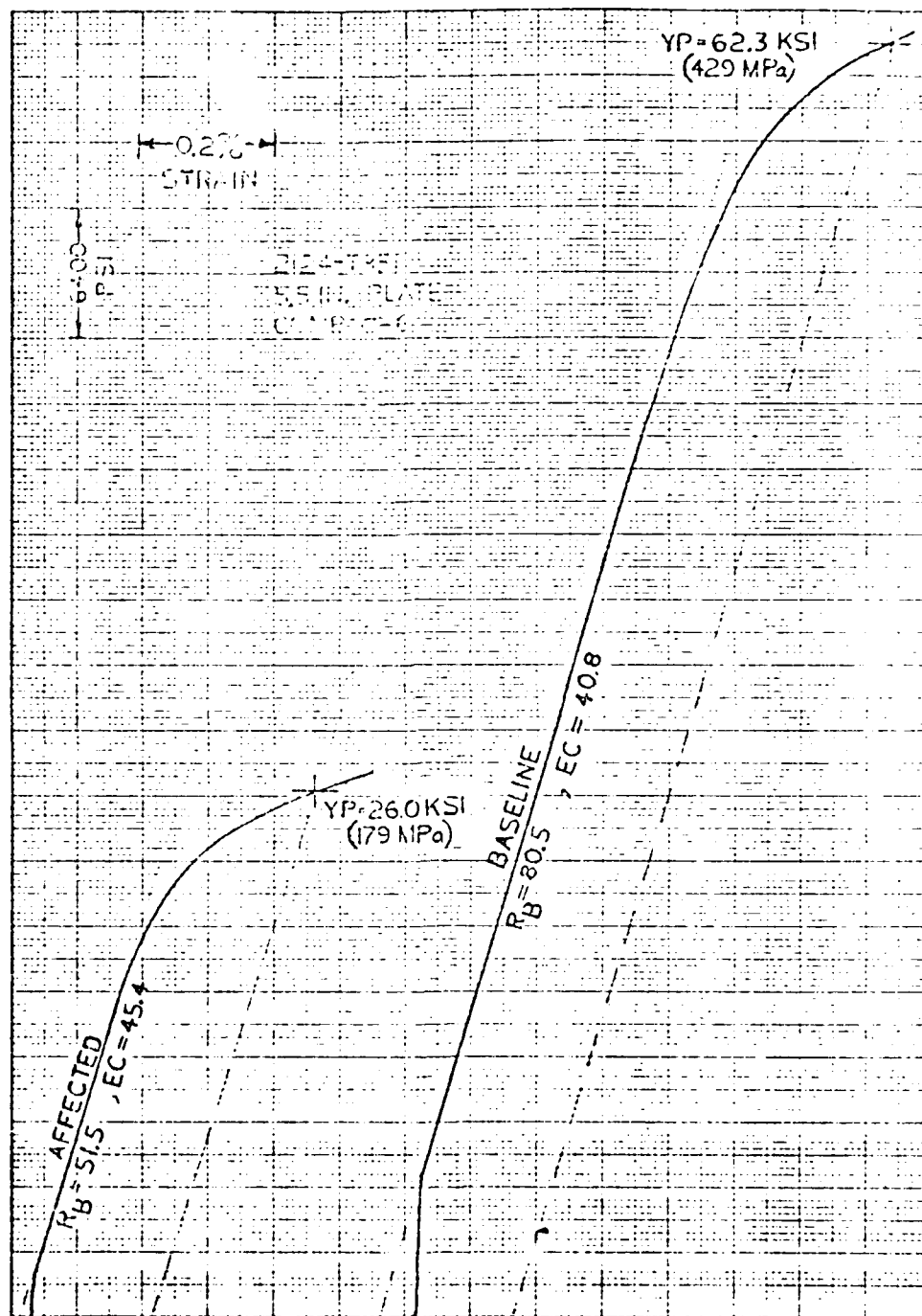


Figure 2. Compressive Stress-Strain Curves for Slack-Quenched and Baseline Aluminum 2124.

TABLE 5

BEARING STRENGTH DATA (E/D=2.0) FOR 2124-T851
5.5 inch SLACK-QUENCHED ALUMINUM PLATE

Specimen I.D.	Yield Strength KSI	Ultimate Strength KSI	Hardness R _B	EC % IACS
BE-1A	71.6	103.0	59-60	43.8
BE-2A	66.3	102.0	56-56	43.7
BE-3A	67.0	98.0	55-55	44.2
Average	68.3	101.0	56.8	43.9
BE-1B	99.6	132.0	76-77	40.7
BE-2B	97.0	129.0	77-77	40.6
BE-3B	98.7	131.0	78-77	40.9
Average	98.4	130.7	77.0	40.7
Specifi.	93.0	121.0	74.0	35.0-42.5

the "softest" location of the plate, as evident from the layout photo and hardness and EC readings. The farther away from the center of the soft spot, the less influence the inferior quench will have on any mechanical properties. However, it is important to note that bearing properties can be noticeably undermined by the inferior quench.

The results of both smooth and notched fatigue testing are presented as S-N (stress versus cycle life) plots in Figures 3 and 4, respectively. The same results are tabularized along with individual specimen hardness and conductivity in Table 6 for smooth fatigue and Table 7 for the notched fatigue results. The effect in fatigue properties is not clearly evident upon viewing these plots. This is possibly due to the fact that the specimens were removed from different locations in the plate and, as stated earlier, the effect on mechanical properties is dependent on the nearness to the affected region. By replotting the notched fatigue data in terms of hardness versus life, as shown in Figure 5, the effect of the slack quench becomes more apparent. The cyclic life is slightly proportional to the hardness, i.e., the closer

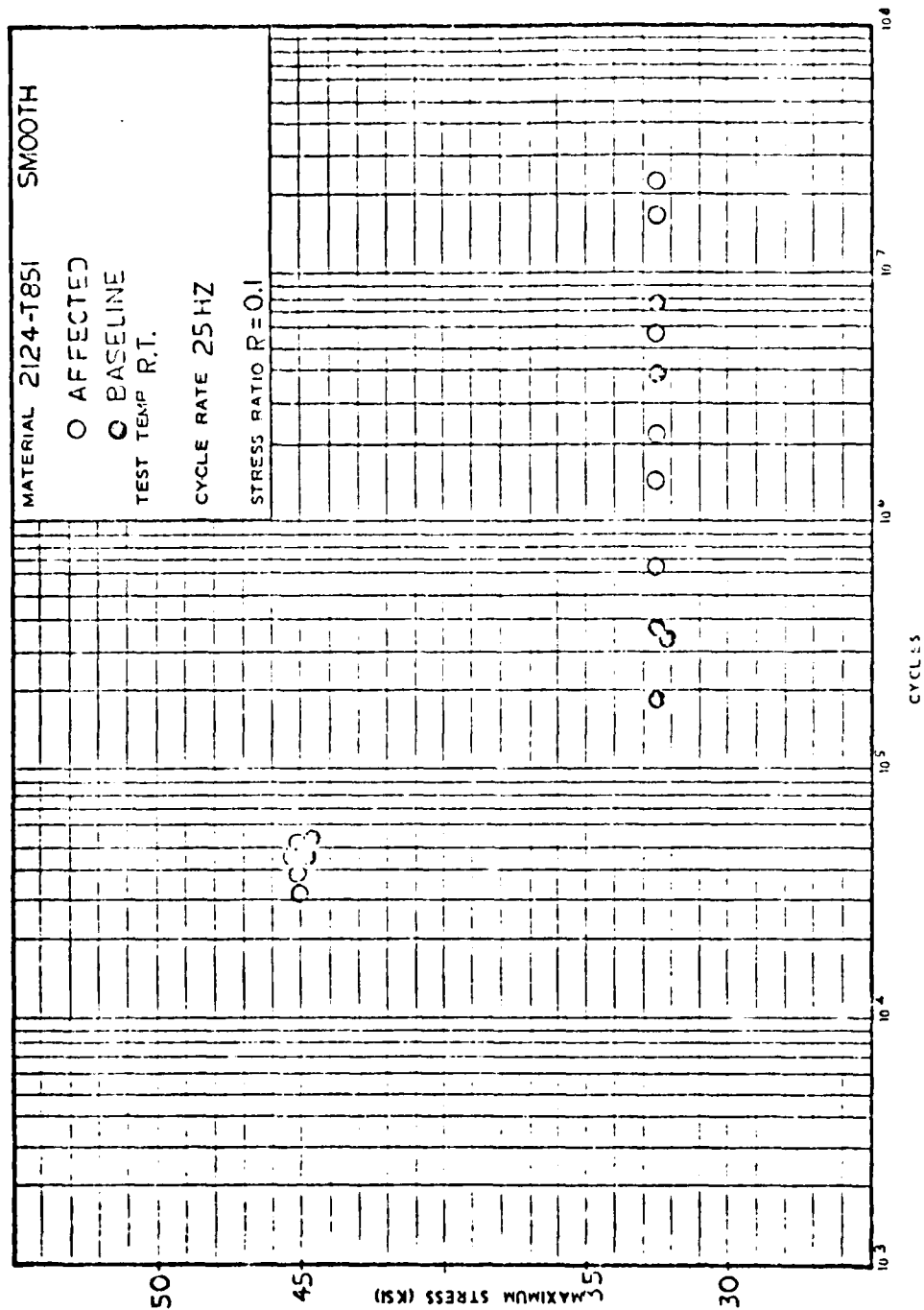


Figure 3. Smooth Fatigue Results for Slack-Quenched Aluminum 2124-T851.

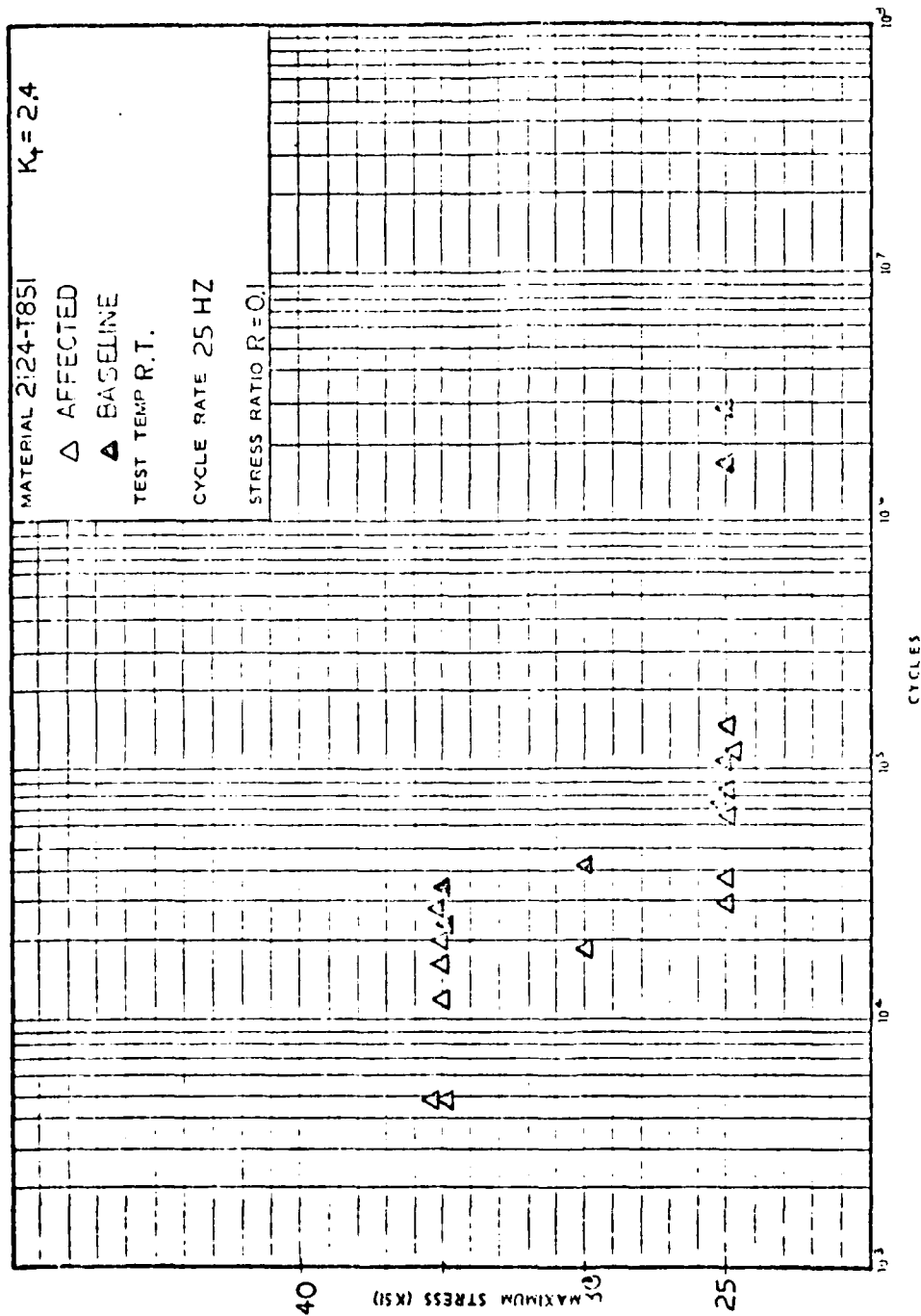


Figure 4. Notched Fatigue Results for Slack-Quenched Aluminum 2124-T851.

TABLE 6
SMOOTH FATIGUE DATA 2124-T851 5.5 Inch
SLACK-QUENCHED ALUMINUM PLATE

Specimen No.	Max. Stress (KSI)	Cycles to Failure	Hardness Before Test, R_B (Avg.)	Conductivity % IACS
FS-1A	45.0	3.1×10^4	58.5	43.7
FS-1B	45.0	4.5×10^4	79.0	40.6
FS-2A	45.0	3.7×10^4	63.0	43.8
FS-2B	45.0	4.4×10^4	79.0	40.7
FS-3A	32.5	1.4×10^6	68.5	43.0
FS-3B	32.5	7.8×10^6	81.5	40.9
FS-4A	32.5	2.2×10^6	73.0	42.5
FS-4B	32.5	3.2×10^5	79.5	40.6
FS-5A	45.0	5.1×10^4	75.0	42.0
FS-5B	45.0	5.2×10^4	80.0	40.8
FS-6A	32.5	2.2×10^7	74.0	42.0
FS-6B*	32.5	1.8×10^5	79.0	40.7
FS-7A	32.5	6.2×10^5	72.0	42.6
FS-7B	32.5	3.5×10^5	80.0	41.0
FS-8A	32.5	5.4×10^6	71.0	42.3
FS-8B	32.5	3.9×10^6	78.0	40.9

* FS-6B--Failed in Radius.

TABLE 7
 NOTCHED ($K_t = 2.43$) FATIGUE DATA 2124-T851
 5.5 Inch SLACK-QUENCHED ALUMINUM PLATE

Specimen No.	Max. Stress (KSI)	Cycles to Failure	Hardness Before Test, R_B (Avg.)	Conductivity % IACS
FN-1A	30	1.95×10^4	63.0	43.6
FN-1B	30	4.2×10^4	79.0	40.5
FN-2A	35	1.2×10^4	65.0	43.4
FN-2B	35	2.6×10^4	81.0	40.5
FN-3A	25	8.3×10^4	68.0	42.9
FN-3B	25	1.8×10^6	80.0	40.5
FN-4A	25	1.1×10^5	70.0	42.4
FN-4B	25	1.0×10^5	80.5	40.6
FN-5A	35	2.0×10^4	73.0	41.7
FN-5B	35	3.3×10^4	80.0	40.8
FN-6A	25	6.6×10^4	73.5	41.8
FN-6B	25	7.2×10^4	79.5	41.0
FN-7A	35	1.6×10^4	70.0	43.0
FN-7B	35	2.3×10^4	80.0	40.7
FN-8A	25	1.4×10^5	70.0	42.5
FN-8B	25	2.9×10^6	80.5	40.8
FN-TL-1A	35	5.0×10^3	44.0	45.2
FN-TL-7A	35	5.0×10^3	52.0	44.9
FN-TL-3A	25	3.0×10^4	46.0	45.0
FN-TL-8A	25	3.7×10^4	51.0	44.9

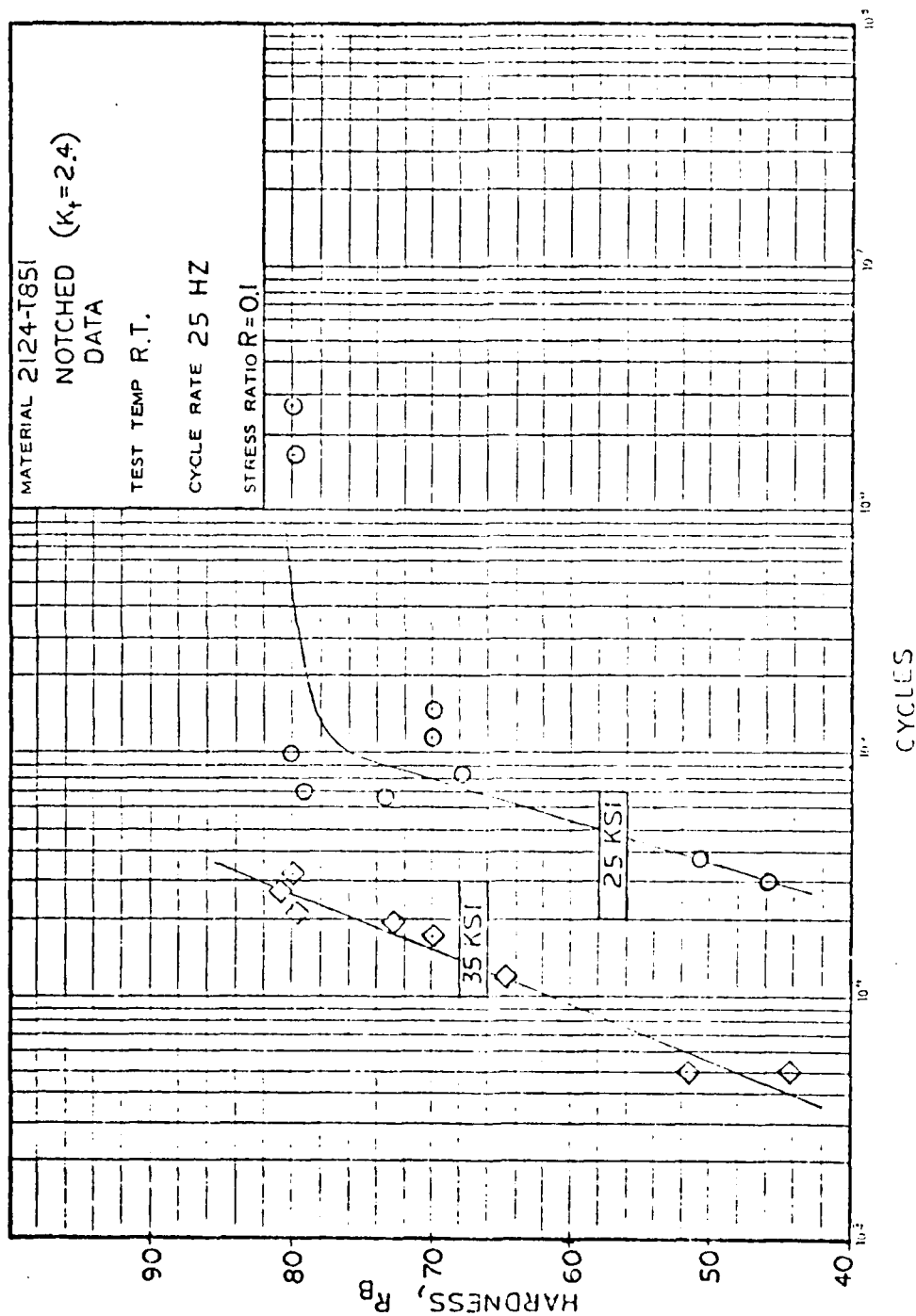


Figure 5. Hardness versus Cycles to Failure Curves of Notched Fatigue Data for Slack-Quenched Aluminum 2124-T851.

to the soft spot the lower the notched fatigue life, for both stress levels examined. A similar trend is observed in the replot of conductivity versus cyclic life shown in Figure 6; the fatigue life is inversely proportional to the electrical conductivity. However, for the latter replot, there is a much larger scatter in the EC versus cycles, indicating again that conductivity as an inspection criteria is not nearly as effective in determining the extent of property degradation as are the hardness readings.

Though not shown, a similar plot of the hardness versus cycles and EC versus cycles data for the smooth data showed no conclusive trend in fatigue life. This was due to large data scatter. Based on these results, it is unknown what effect, if any, the slack quench has on the smooth fatigue properties. Perhaps additional testing on specimens containing vastly different hardness and conductivity readings would substantiate what effect the slack quench would have on smooth fatigue life.

Because the depth of the soft region was originally unknown, the standard toughness test for linear elastic materials, ASTM Standard E999, could not be used. To obtain a valid plane strain stress intensity value for this material, a thick, uniform specimen is required; e.g., thickness greater than 1 inch (22 mm). To obtain some meaningful indication of toughness, it was decided the only valid test for toughness was the R-curve method as described in ASTM Standard E561-76T. An R-curve is a continuous record of toughness developed plotted against the crack extension for a specimen being loaded under a continuously increasing stress intensity factor.

The R-curves developed for two baseline specimens and two affected specimens, superimposed on a common set of axes are shown in Figure 7. For stress intensities below approximately $45 \text{ KSI}\sqrt{\text{in}}$ ($49 \text{ MPa}\sqrt{\text{m}}$) the two sets of data appear nearly equal, thereby implying an equal resistance to crack extension. Beyond this maximum value of stress intensity, the curve for the baseline material shows a continual increase in resistance with respect to

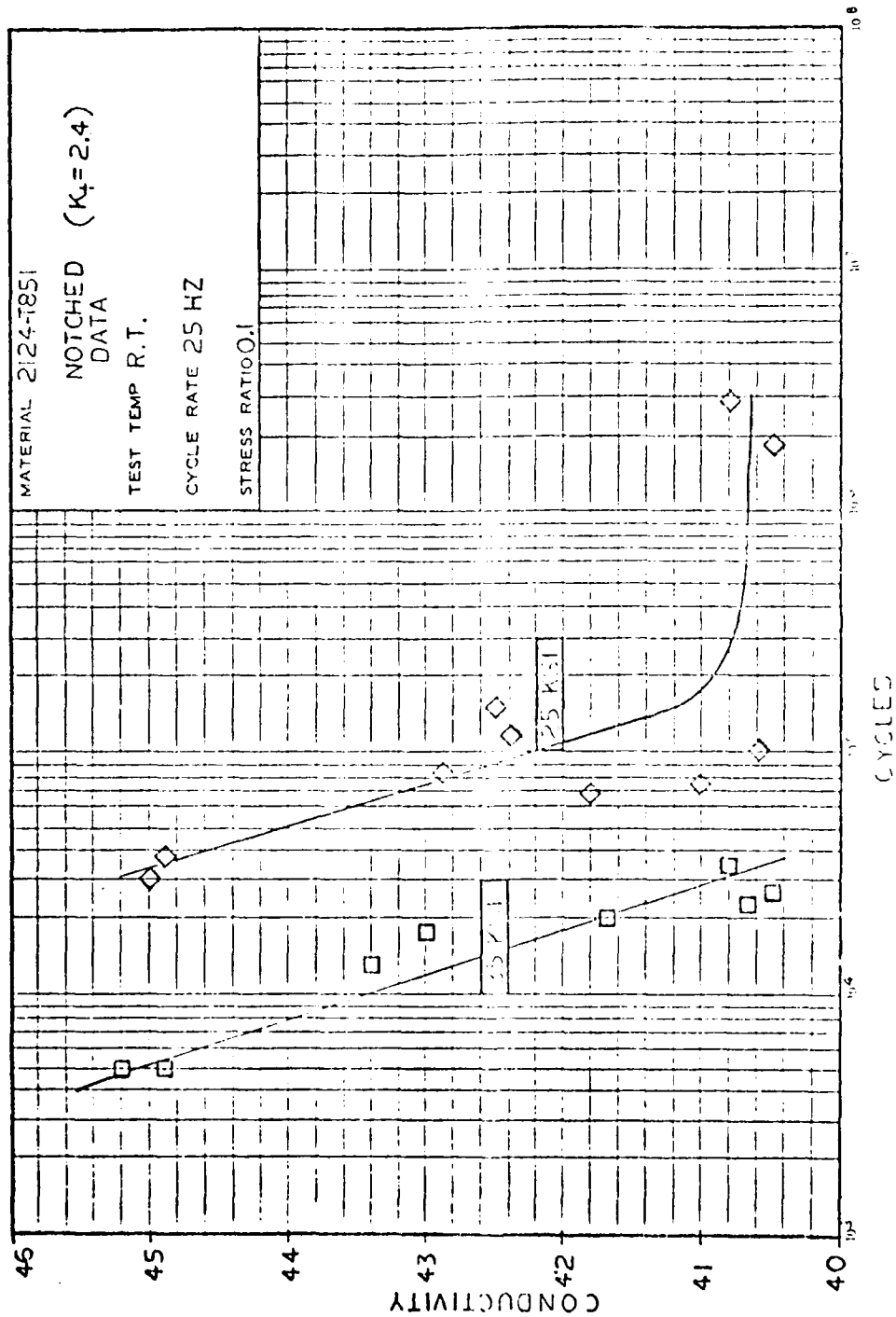


Figure 6. Conductivity versus Cycles to Failure Curves of Notched Fatigue Data for Slack-Quenched Aluminum 2124-T851.

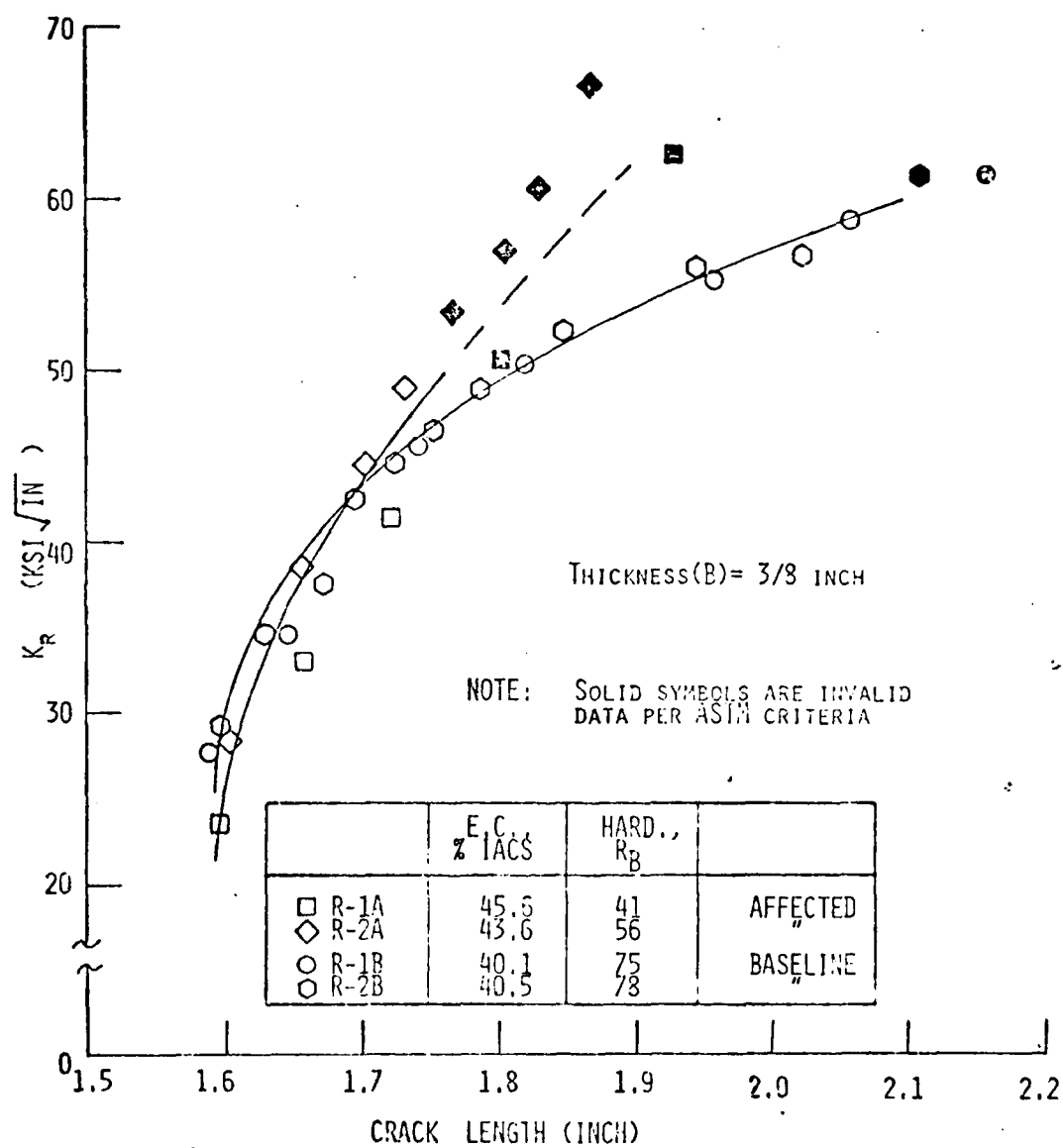


Figure 7. R-Curves for Slack-Quenched Aluminum 2124-T851.

crack extension but at a lesser rate, while the affected material's R-curve, though invalid by ASTM criteria, displays a greater increase in resistance. If some credibility is given to the invalid data, it could be inferred that the affected material is able to absorb more energy than the baseline material, therefore being tougher to some degree. It is, however, apparent the affected material shows no loss or degradation and is equal or superior to the baseline material's toughness.

The fatigue crack growth rate test results on two sets of affected and baseline specimens (CG-1A and B, and CG-2A and B) are presented in Figures 8 and 9. All testing was conducted in accordance with the current tentative ASTM E647-78T procedures, with crack length monitored by means of a 30X traveling microscope. An R-ratio of +0.1 was investigated at a test frequency of 25 Hz. The results for both sets of samples indicate little or no increase in crack growth rate properties for the affected material over the baseline material. Also, the baseline material results agree well with reference data^[3] on this same material.

Smooth tensile bars removed from the affected and baseline material were loaded to high stress levels and exposed to an alternating immersion; ten minutes of each hour fully submerged in a 3.5 weight percent environment followed by 50 minutes in lab air. Times to failure were recorded for specimens machined from the longitudinal and short-transverse orientations of the affected plate as shown in the layout sketch. Due to time considerations, maximum exposure time was limited to approximately 600 hours.

The results of this effort are presented in Table 8. Because of difficulties encountered in obtaining consistent hardness and EC readings, they are not reported. As can be readily observed for those samples which failed, the specimens removed from the affected regions showed consistently lower stress rupture lives than did the samples machined from the baseline, properly quenched material. This conclusion was reached for specimens removed from both orientations.

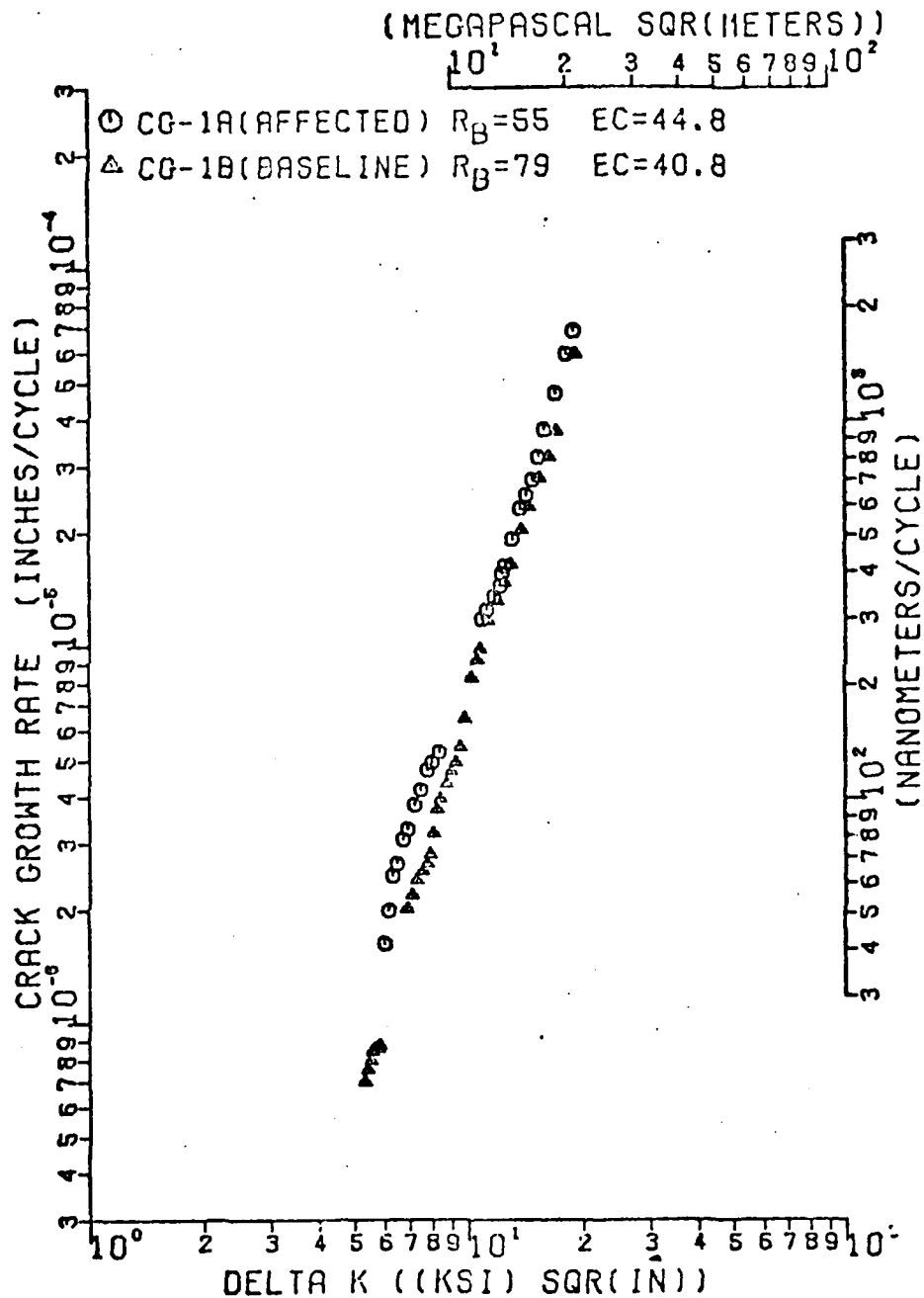


Figure 8. Fatigue Crack Growth Data for Specimens CG-1-A and CG-1-B.

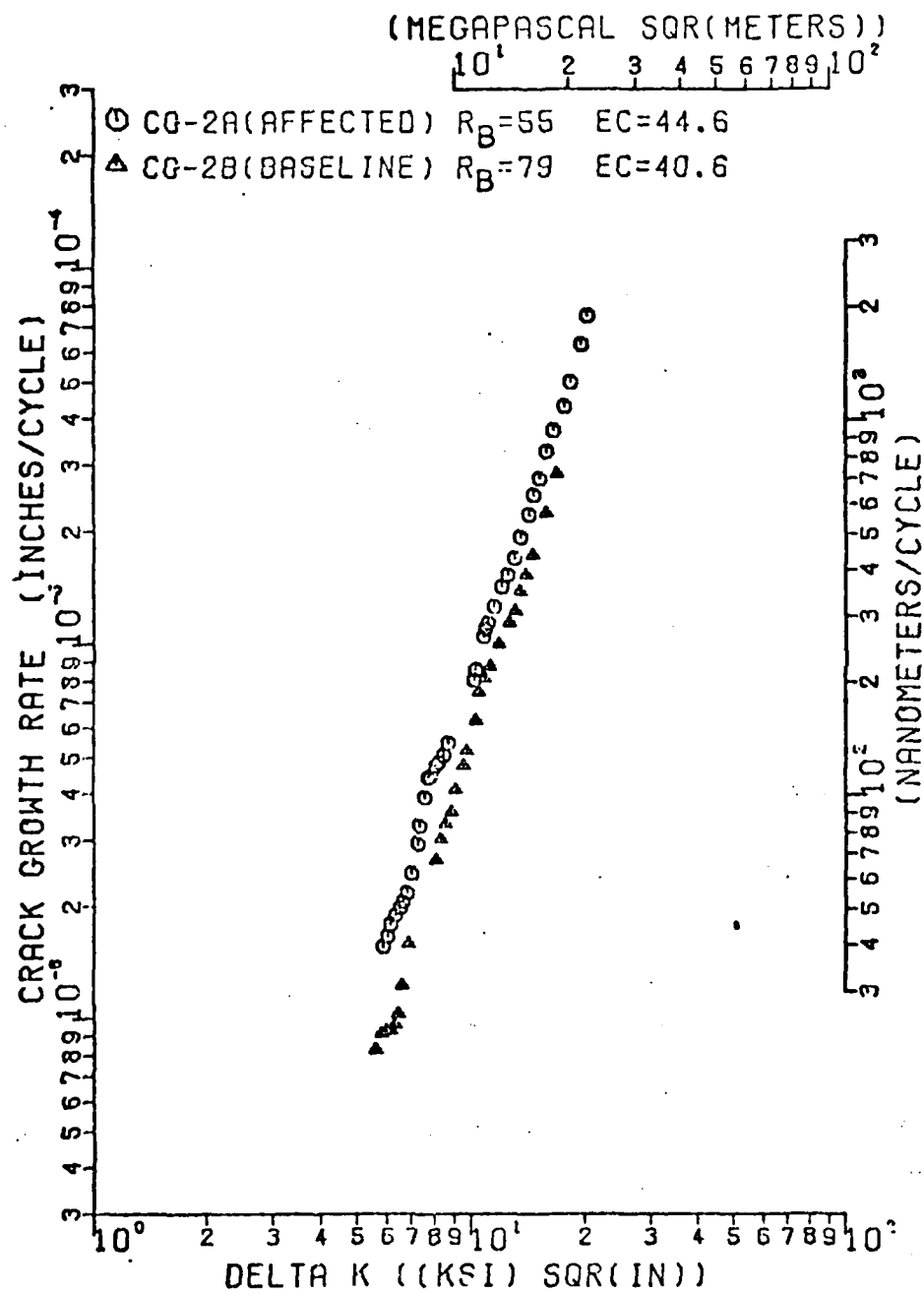


Figure 9. Fatigue Crack Growth Data for Specimens CG-2-A and CG-2-B.

TABLE 8

STRESS CORROSION TEST RESULTS FOR 2124-T851 5.5 inch
THICK PLATE, CONSTANT STRESS, ALTERNATE IMMERSION

Specimen Number	Orientation	Stress (KSI)	Percent of Yield Strength*	Exposure Time (hrs)	Fail?
S-1A	Longitudinal	45.0	83	317	Yes
S-1B	Longitudinal	45.0	83	677	No
S-4A	Short Trans.	45.0	88	547	Yes
S-5B	Short Trans.	45.0	88	625	Yes
S-6A	Short Trans.	45.0	88	386	Yes
S-6B	Short Trans.	45.0	88	593	Yes
S-5A	Short Trans.	38.2	75	600	No
S-4B	Short Trans.	38.2	75	600	No

* Yield Strength per MIL-HDBK-5; Longitudinal = 54 KSI
Short Trans. = 51 KSI

Two precracked compact type specimens, one machined from the affected material, one from the baseline material, were loaded at an initial stress intensity of approximately 22 KSI $\sqrt{\text{in}}$ (24 MPa $\sqrt{\text{m}}$) in a 3.5 weight percent NaCl solution to test the material's resistance to stress corrosion cracking. The exposure was continuous, with lab air bubbled through the solution to provide oxygen to the corrosive medium and to help maintain a homogeneous NaCl mixture.

The results of these tests are presented in Table 9. For specimens loaded at approximately 70 percent of the expected K_{IC} value, no stress corrosion cracking failures were experienced after 3,000 hours in test, suggesting that stress corrosion properties are not seriously altered by the improper quench. Both specimens exhibited little or no crack propagation, though the appearances of each sample differed noticeably. As shown in the photo presented in Figure 10, the baseline material was extensively pitted on the surfaces, while the fatigue crack tip remained sharp. On the other hand, the soft or affected material displayed little pitting on the surface; however, the crack's fracture faces were definitely corroded and the crack tip severely blunted as displayed in Figure 10. The affect of such crack tip blunting is to diminish the stress intensity by reducing the severity of the stress concentration.

Single lap shear fastener specimens were fabricated from both the affected and baseline regions of the plate to study the effect of the improper quench on an elemental structure. Tensile and fatigue properties were evaluated.

The results of the tensile test are best presented as plots in Figure 11, showing the load as a function of specimen displacement [measured with a 2 inch (50 mm) extensometer across the lapped joint] for both affected and baseline fabricated joint specimens. Results indicate a lower maximum load-carrying capability for the affected material than for the baseline masterial which failed as a result of the fastener failing. Likewise, more relative displacement between the two joined specimen halves

TABLE 9
STRESS CORROSION CRACKING TEST RESULTS FROM
2124-T851 5.5 inch THICK PLATE,
L-T ORIENTATION, CONTINUOUS IMMERSION

Specimen Number	K _{initial} KSI√in	Time (hrs)	Fail?	Hardness, R _B	EC % IACS
K-1A	22	3000	No	42.0	45.6
K-2A				52.0	45.2
K-1B	22	3000	No	79.5	40.6
K-2B				79.5	40.8

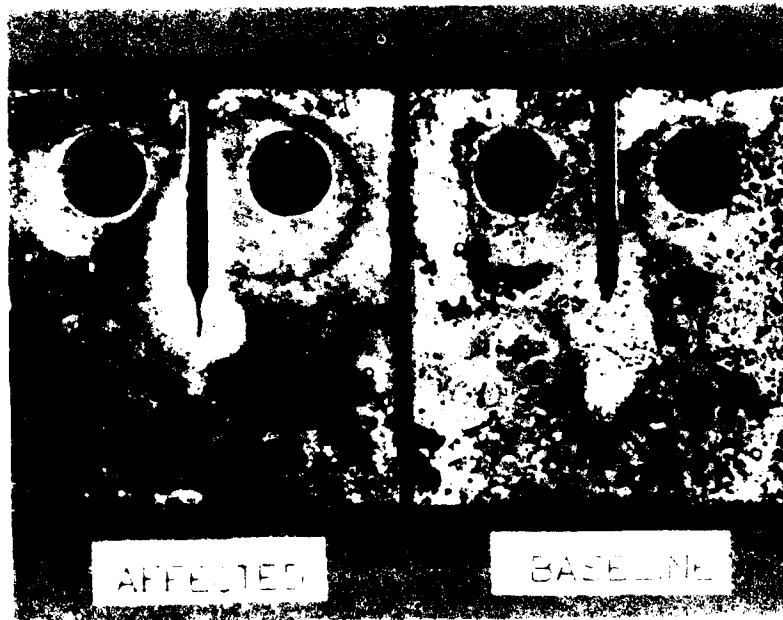


Figure 10. Baseline and Affected Stress-Corrosion Cracking Test Specimens After 3,000 Hours in Test.

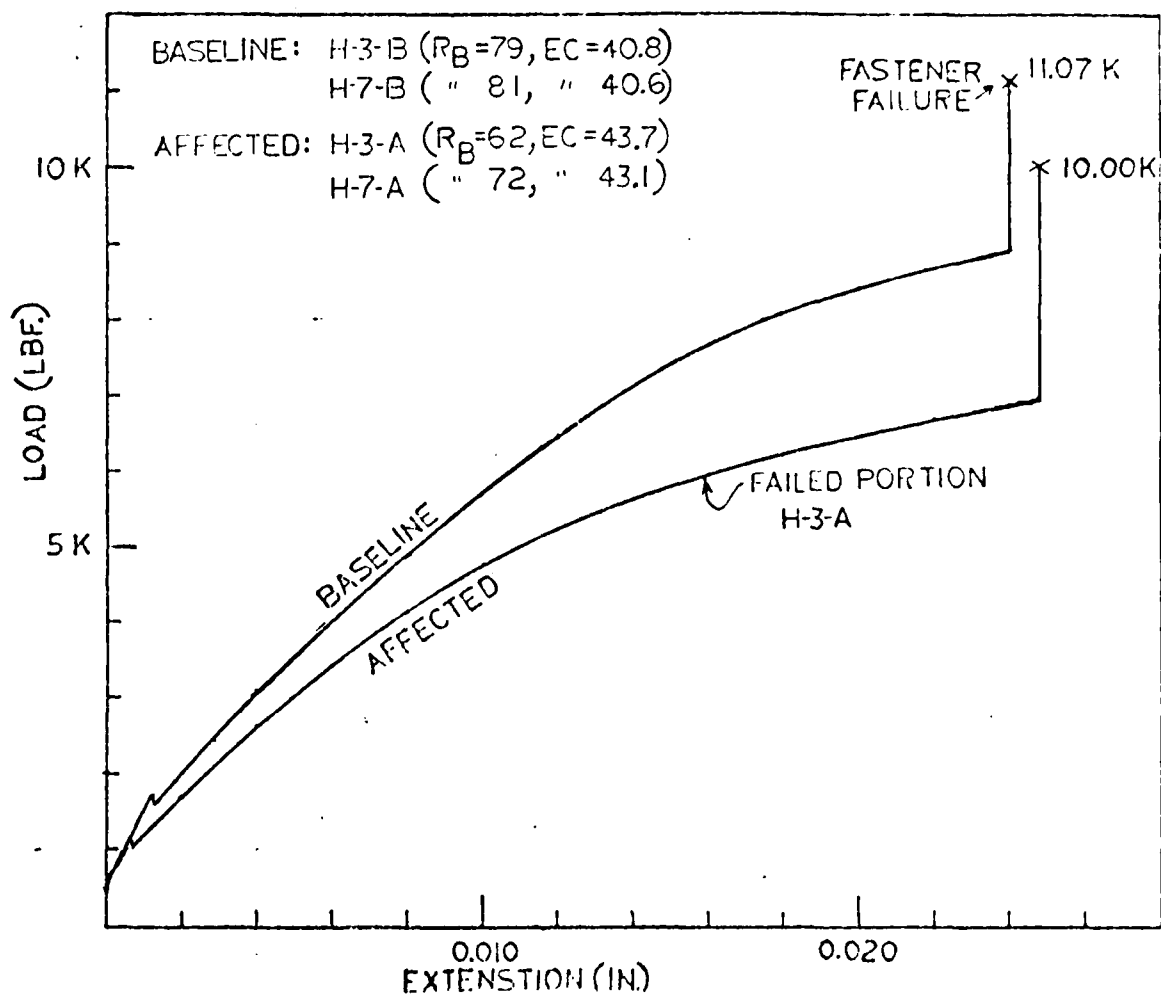


Figure 11. Load versus Displacement Records for Slack-Quenched Lap-Shear Tensile Specimens.

was experienced for the affected specimens than for the baseline specimens, somewhat expected due to the lower bearing and yield strengths of the affected material. Special notice should be made to the small differences in both the hardness and conductivities of the two lap shear specimens; the affected specimen (specimen halves H-3-A and H-7-A) were fabricated from material removed a substantial distance from the softest region, resulting in a lesser degree of degradation. Consequently, any mechanical property degradation would be expected to be lesser than if the specimens were removed from the softest (e.g., $R_B = 50$) region.

The results of the fastener fatigue tests are presented in Table 10. A sandwich type restraint was employed on all fatigue tests. Because initial fatigue tests on bare, untreated aluminum specimens resulted in fatigue failure due to fretting, the remaining specimens' faying surfaces received an ~ 0.001 inch (0.025 mm) epoxy primer coating. Results in Table 10 reflect both types of test results. These limited results for the specimens of the indicated hardness and conductivity values shows no consistent differences in the fatigue lives between the affected and baseline fabricated specimens. Therefore, no conclusive statement can be made regarding the affect of the inferior quench on the fatigue life of an actual assembly.

1.3 TENSILE PROPERTIES OF SIX SLACK-QUENCHED ALUMINUM ALLOY ROLLED PLATES

The AFML requested tensile property data on several 2000 and 7000 series aluminum alloy plates which had also been identified as containing "soft" spots or regions of reduced tensile properties. The main interest in the slack-quenched plates was to assess the anticipated problem of a reduction in the yield strength in the "soft" spot region and to establish acceptance/rejection criteria for suspect aluminum plates. The combined results of paragraph 1.1 and of this continued evaluation have been reported in AFML-TR-79-4205.[4]

TABLE 10
FASTENER FATIGUE RESULTS

MAX STRESS = 15 KSI (GROSS AREA), R = +0.1, 25 Hz
SINGLE LAP, HIGH LOAD TRANSFER

Specimen Number	Cycles (x10 ³)	Failed Portion	Hardness on Failed Portion, R _B	E.C.(%) on Failed Portion
<u>Bare Faying Surface</u>				
H-1-B/H-5-B	85.5	H-1-B(F)	79.2	40.9
H-1-A/H-5-A	100.2	H-5-A(F)	69.3	43.1
<u>Epoxy Primer Coating</u>				
H-2-B/H-6-B	109.9	H-2-B(F)?	81.2	41.0
H-2-A/H-6-A	193.1	H-2-A	61.0	44.0
H-4-B/H-8-B	197.6	H-4-B	80.2	40.4
H-4-A/H-8-A	87.2	H-4-A	57.0	43.4

NOTE: (F) Indicates failure due to fretting.

All tests run with "sandwich" type restraint.

The six slack-quenched aluminum alloy plates used in this program were: (1) 2024-T851; 2.75 inches (60 mm) thick, (2) 2024-T351; 2.00 inches (51 mm) thick, (3) 2124-T851; 5.50 inches (140 mm) thick, (4) 7075-T7341; 4.00 inches (102 mm) thick, (5) 7075-T651; 1.25 inches (32 mm) thick, and (6) 7075-T7351; 0.50 inch (13 mm) thick.

Two additional properly heat treated plates were procured, one from Kaiser Aluminum Company and one from the Aluminum Company of America (ALCOA), for the purpose of comparison. Both of these additional reference plates were alloy 2124-T851; the Kaiser Aluminum Company produced plate is 5.0 inches (127 mm) thick and the ALCOA plate was 5.50 inches (140 mm) thick.

All of the tensile tests were performed using the same 10,000 pound Instron tensile machine. The tests were conducted at room temperature in compliance with the appropriate ASTM test standard, Method E8-78.

Hardness and conductivity measurements were also made and are reported in the tables with the tensile data. The conductivity measurements were made prior to the tensile test and the hardness measurements on the Rockwell "B" scale were performed after completion of the tensile test. The hardness measurements were made on both halves of the failed tensile specimen in the tapered region between the gripping area and the gage section, a region that would have undergone little or no plastic deformation.

All of the tensile test results for the six slack-quenched aluminum plates and the two properly heat treated reference plates are presented in Tables 11 through 23. The electrical conductivity, EC, and the surface hardness measurements on the Rockwell "B" scale, R_B , for each failed test specimen half are also presented in these tables along with the tensile data. When a conductivity range is given in the tables, it includes the high and low value of six measurements made on each specimen prior to the tensile test.

TABLE 11
LONGITUDINAL TENSILE PROPERTIES 2124-T851
SLACK-QUENCHED ALUMINUM PLATE
2.750 Inches (70 mm) Thick

	Specimen No.	Ult. Tensile Strength KSI (MPa)	0.2% Yield Strength KSI (MPa)	% Elong. 2 in G.L.	RA (%)	R _B	EC %IACS
Affected	2	59.9 (413)	52.8 (364)	6.0	12.6	73	40.9
	5	56.8 (392)	47.1 (325)	7.7	11.3	74	41.4
	6	64.0 (441)	57.3 (395)	8.9	17.2	75	39.9
Base	1	72.0 (496)	60.3 (416)	8.9	14.9	82	38.5
	3	70.0 (483)	66.2 (456)	9.6	17.2	84	38.6
	6	70.5 (486)	66.5 (458)	8.9	13.3	82	38.6
Specifi- cations		65.0 (448)	57.0 (393)	6	--	74	35.0- 42.5

TABLE 12
LONGITUDINAL TENSILE PROPERTIES 2024-T351
SLACK-QUENCHED ALUMINUM PLATE
2.00 Inches (51 mm) Thick

	Specimen No.	Ult. Tensile Strength KSI (MPa)	0.2% Yield Strength KSI (MPa)	% Elong. 2 in G.L.	RA (%)	R _B	EC %IACS
Base	Y1B	69.9 (482)	53.0 (365)	13.0	23.6	77-78	30.0-30.4
	Y2B	69.7 (481)	53.8 (371)	17.7	24.4	77-78	30.1-30.3
	Y3B	69.7 (481)	54.1 (373)	19.8	24.4	78-79	30.0-30.4
Middle	Y1M	73.3 (505)	57.4 (396)	15.5	19.9	76-77	30.8-31.0
	Y2M	73.3 (505)	57.0 (393)	13.6	16.2	77-78	31.0-31.0
	Y3M	72.9 (503)	57.7 (398)	13.0	15.3	77-78	31.0-31.0
Affected	Y1T	65.6 (452)	52.1 (359)	13.9	23.0	73-76	30.8-33.9
	Y2T	65.7 (453)	52.6 (363)	12.1	21.2	76-77	30.6-34.0
	Y3T	65.3 (450)	52.1 (359)	13.0	19.8	72-73	31.0-33.8
Specifi- cations		62.0 (427)	47.0 (324)	6	--	63	28.5-32.5

TABLE 13
LONGITUDINAL TENSILE PROPERTIES OF 2124-T851
SLACK-QUENCHED ALUMINUM PLATE
5.50 Inches (140 mm) Thick

	Specimen No.	Ult. Tensile Strength KSI (MPa)	0.2% Yield Strength KSI (MPa)	% Elong. 2 in G.L.	RA (%)	R _B	EC 3IACS
Affected	TL-1A	44.5 (307)	32.8 (226)	8.7	20.6	36-40	46-46
	TL-2A	44.8 (309)	33.6 (232)	9.1	18.9	39-48	46-46
	TL-3A	44.9 (310)	32.7 (225)	8.3	23.3	36-39	46-46
	TL-4A	48.9 (337)	37.5 (259)	7.7	24.6	47-50	45-45
	TL-5A	50.5 (348)	38.5 (265)	8.5	24.9	48-58	45-44
	TL-6A	49.1 (338)	37.4 (258)	8.6	19.6	47-49	45-45
	TL-7A	48.4 (334)	36.2 (250)	8.4	27.2	47-47	45-45
	TL-8A	49.6 (352)	37.6 (259)	8.5	22.3	47-48	45-45
	TL-9A	49.3 (340)	37.1 (256)	8.8	24.5	47-49	45-45
	TL-10A	50.9 (351)	39.2 (270)	8.3	25.2	47-54	45-45
Base	TL-1B	69.1 (476)	61.3 (423)	7.4	20.4	74-77	41-41
	TL-2B	69.6 (480)	61.8 (426)	7.2	17.7	77-78	41-41
	TL-3B	69.5 (479)	61.3 (423)	7.7	18.0	74-75	41-41
	TL-4B	68.8 (474)	60.8 (419)	7.4	12.5	74-75	41-41
	TL-5B	69.6 (480)	62.0 (427)	7.2	13.1	77-79	41-41
	TL-6B	69.8 (474)	61.9 (427)	7.1	20.8	79-80	41-41
	TL-7B	69.7 (481)	61.8 (426)	8.4	17.4	79-80	41-41
	TL-8B	69.5 (479)	61.4 (423)	6.6	15.6	80-80	41-41
	TL-9B	70.1 (483)	62.2 (429)	8.1	17.4	80-80	41-41
	TL-10B	70.3 (484)	62.1 (428)	7.6	18.0	79-79	41-41
Specifi- cations		63.0 (434)	54.0 (372)	5.0	--	74	35.0-42.5

TABLE 14
TRANSVERSE TENSILE PROPERTIES OF 2124-T851
SLACK-QUENCHED ALUMINUM PLATE
5.50 Inches (140 mm) Thick

	Specimen No.	Ult. Tensile Strength KSI (MPa)	0.2% Yield Strength KSI (MPa)	% Elong. 2 in G.L.	RA (%)	R _B	EC %IACS
Affected	TT-1A	47.2 (325)	31.1 (214)	8.2	13.7	42-53	45-45
	TT-2A	44.5 (307)	27.2 (188)	9.6	20.3	38-39	46-46
	TT-3A	46.3 (319)	29.2 (201)	9.5	15.3	40-53	45-45
Base	TT-1B	69.3 (478)	61.6 (425)	6.9	9.3	77-79	41-41
	TT-2B	69.4 (479)	61.7 (425)	5.4	8.8	78-79	41-41
	TT-3B	69.1 (476)	60.5 (417)	7.7	10.1	79-79	41-41
Specifi- cations		63.0 (434)	54.0 (372)	4.0	--	74	35.0-42.5

TABLE 15
THROUGH THE THICKNESS LONGITUDINAL TENSILE
PROPERTIES OF ALLOY 2124-T851 SLACK-
QUENCHED ALUMINUM PLATE
5.50 Inches (140 mm) Thick

Depth From Top Surface (Inches)	Specimen No.	Ult. Tensile Strength KSI (MPa)	0.2% Yield Strength KSI (MPa)	% Elong. 2 in G.L.	RA (%)	R _B	EC %IACS Avg.
	Affected						
1/8	TL-2-A	44.8 (309)	33.6 (231)	9.1	18.8	39-48	45.8
3/4	TL-2-1	44.9 (310)	33.8 (233)	9.2	20.5	38-44	45.3
1-1/4	TL-2-2	56.9 (392)	48.0 (330)	7.1	15.9	60-64	42.5
1-3/4	TL-2-3	58.5 (403)	44.8 (343)	6.1	11.6	64-66	42.4
2-1/4	TL-2-4	59.7 (412)	51.4 (354)	5.7	9.5	68-69	42.2
2-3/4	TL-2-5	59.8 (412)	51.9 (358)	5.0	7.3	69-69	42.2
3-1/4	TL-2-6	60.4 (416)	50.3 (347)	5.5	9.8	68-69	42.2
3-3/4	TL-2-7	62.4 (430)	52.4 (361)	7.2	16.6	70-70	42.1
4-1/4	TL-2-8	64.6 (445)	55.1 (380)	6.9	16.8	74-74	41.8
4-3/4	TL-2-9	67.8 (467)	59.3 (409)	7.4	14.7	77-77	41.2
5-3/8	TL-2-B	69.6 (480)	61.8 (426)	7.2	17.7	77-78	41.0
	Base						
Specification		63.0 (434)	54.0 (372)	5.0	--	74	35.0-42.5

TABLE 16

THROUGH THE THICKNESS LONGITUDINAL TENSILE
 PROPERTIES OF ALCOA ALUMINUM COMPANY ALLOY
 2124-T851 PLATE, 5.50 Inches (140 mm) Thick

Depth From Top Surface (Inches)	Specimen No.	Ult. Tensile Strength KSI (MPa)	0.2% Yield Strength KSI (MPa)	% Elong. 2 in G.L.	RA (%)	R _B	EC % IACS
0.25	A1T	72.9 (503)	67.9 (468)	8.5	21.2	84-84	41-41
1.50	A2	69.1 (476)	62.0 (427)	7.4	16.7	79-80	41-42
2.75	A3	68.9 (475)	61.1 (421)	7.3	16.6	78-79	42-42
4.00	A4	68.9 (475)	61.8 (426)	7.1	17.4	79-80	42-42
5.25	A5-B	73.0 (503)	68.1 (470)	6.0	24.5	83-84	41-42
Specification		63.0 (434)	54.0 (372)	5.0	--	74	35.0-42.5

TABLE 17

THROUGH THE THICKNESS LONGITUDINAL TENSILE
 PROPERTIES OF KAISER ALUMINUM COMPANY ALLOY
 2124-T851 PLATE, 5.0 Inches (127 mm) Thick

Depth From Top Surface (Inches)	Specimen No.	Ult. Tensile Strength KSI (MPa)	0.2% Yield Strength KSI (MPa)	% Elong. 2 in G.L.	RA (%)	R _B	EC % IACS
0.25	K-1T	70.8 (488)	65.5 (452)	7.8	24.6	82-82	41-41
1.00	K-2	65.5 (452)	58.0 (400)	7.3	21.6	75-76	42-42
1.75	K-3	64.8 (447)	56.7 (391)	6.5	16.4	76-76	42-42
2.50	K-4	64.1 (442)	56.6 (390)	6.7	14.1	74-76	42-42
3.25	K-5	65.1 (449)	57.1 (394)	7.0	17.2	76-77	42-42
4.00	K-6	66.1 (456)	58.8 (405)	7.7	20.8	77-78	42-42
4.75	K-7B	71.2 (491)	66.4 (458)	7.9	23.9	78-82	41-41
Specification		63.0 (434)	54.0 (372)	5.0	--	74	35.0-42.5

TABLE 18
LONGITUDINAL TENSILE PROPERTIES OF ALLOY 7075-T7351
ALUMINUM SLACK-QUENCHED PLATE
4.00 Inches (102 mm) Thick

	Specimen No.	Ult. Tensile Strength KSI (MPa)	0.2% Yield Strength KSI (MPa)	% Elong. 2 in G.L.	RA (%)	RB	EC % IACS
Base	P1B	73.9 (509)	63.3 (436)	9.3	13.6	82-83	39-39
	P2B	73.6 (507)	62.8 (433)	7.3	14.5	82-83	39-39
	P3B	73.3 (505)	62.3 (430)	7.3	16.4	82-83	39-39
	P4B	73.5 (407)	62.6 (432)	8.3	15.6	78-82	39-39
	P5B	73.4 (406)	63.1 (435)	7.8	14.5	90-83	39-39
	P6B	73.1 (504)	62.3 (430)	7.4	14.0	79-82	39-39
	P7B	72.3 (505)	61.7 (425)	6.9	14.8	82-83	39-39
	P8B	72.8 (501)	61.6 (425)	7.0	12.0	82-83	39-39
	P9B	72.7 (501)	62.3 (430)	7.4	13.4	82-83	39-39
	P10B	72.5 (500)	61.3 (423)	7.6	16.6	84-84	39-39
Affected	P1A	71.7 (494)	60.7 (418)	7.9	15.9	78-81	39-41
	P2A	70.8 (488)	59.5 (410)	7.4	15.1	81-80	39-41
	P3A	70.4 (485)	58.6 (404)	6.7	11.6	81-82	39-40
	P4A	71.6 (493)	60.7 (418)	8.4	14.4	79-81	39-41
	P5A	71.2 (490)	60.2 (415)	8.0	14.9	76-81	39-41
	P6A	71.9 (496)	60.6 (418)	7.4	16.6	76-81	39-40
	P7A	71.7 (494)	60.4 (416)	7.1	16.0	82-83	39-39
	P8A	71.9 (496)	60.5 (417)	7.9	13.3	83-83	39-40
	P9A	71.2 (490)	59.6 (411)	8.0	14.3	82-82	39-40
	P10A	70.5 (486)	58.6 (404)	8.4	16.9	80-81	39-41
Specifi- cations		*63.0 (434)	*49.0 (338)	6.0	--	81	40-44

*From Reference 1, MIL-HDBK-5, "A" values for a 2.5-3.0 Inch Thick Plate.

TABLE 19
TRANSVERSE TENSILE PROPERTIES OF
ALLOY 7075-T7351 SLACK-QUENCHED ALUMINUM PLATE
4.00 Inches (102 mm) Thick

	Specimen No.	Ult. Tensile Strength KSI (MPa)	0.2% Yield Strength KSI (MPa)	% Elong. 2 in G.L.	RA (%)	R _B	EC %IACS
Affected	G-1-A	69.7 (480)	59.0 (407)	7.5	17.0	82-83	39-41
	G-2-A	71.1 (494)	60.3 (416)	9.2	17.7	81-81	39-40
	G-3-A	69.8 (481)	58.3 (402)	9.2	19.1	80-81	39-40
	G-4-A	69.4 (478)	58.6 (404)	8.3	18.3	80-80	39-40
Base	G-1-B	72.1 (490)	61.7 (425)	9.5	19.7	82-83	39-39
	G-2-B	71.5 (493)	61.1 (421)	9.0	20.0	83-83	39-39
	G-3-B	72.0 (496)	62.1 (428)	9.5	18.0	83-83	39-39
	G-4-B	72.1 (490)	61.8 (426)	9.1	26.3	83-84	39-39
Specifi- cations		*64.0 (441)	*49.0 (338)	6.0	--	81	40-44

* From Reference 1, MIL-HDBK-5, "A" Values for a 2.5-3.0 Inch Thick Plate.

TABLE 20
THROUGH THE THICKNESS LONGITUDINAL TENSILE
PROPERTIES OF ALLOY 7075-T7351 ALUMINUM PLATE
4.00 Inches (102 mm) Thick

Depth From Top Surface (Inches)	Specimen No.	Ult. Tensile Strength KSI (MPa)	0.2% Yield Strength KSI (MPa)	% Elong. 2 in G.L.	RA (%)	R _B	EC %IACS
	Affected						
0.125	P-5-A	71.2 (490)	60.2 (415)	8.0	14.9	76-81	39-41
0.661	P-5-1	62.0 (427)	48.1 (332)	8.0	14.1	72-74	40-41
1.197	P-5-2	61.4 (423)	48.2 (332)	7.6	11.8	70-71	40-41
1.733	P-5-3	64.4 (444)	52.6 (362)	6.3	11.4	73-74	40-40
2.269	P-5-4	63.7 (439)	53.2 (367)	6.4	10.0	74-75	40-40
2.805	P-5-5	63.7 (439)	50.3 (347)	6.6	10.9	74-74	40-40
3.341	P-5-6	68.4 (472)	56.1 (387)	7.6	11.4	77-78	39-40
3.875	P-5-B	73.4 (406)	63.1 (435)	7.8	14.5	80-83	39-39
	Base						
Specifications		*63.0 (434)	*49.0 (338)	6.0	--	81	40-44

* From Reference 1, MIL-HDBK-5, "A" Values for a 2.5-3.0 Inch Thick Plate.

TABLE 21
LONGITUDINAL TENSILE PROPERTIES OF ALLOY 7075-T651
SLACK-QUENCHED ALUMINUM PLATE
1.250 Inches (32 mm) Thick

	Specimen No.	Ult. Tensile Strength KSI (MPa)	0.2% Yield Strength KSI (MPa)	% Elong. 2 in G.L.	RA (%)	R _B	EC %IACS
Affected	L-1A	70.0 (469)	58.6 (392)	10.0	15.9	78-78	34-35
	L-2A	70.0 (469)	60.0 (402)	8.6	18.8	80-82	33-35
	L-3A	69.8 (467)	58.3 (390)	11.0	18.5	82-84	33-35
	L-4A	68.8 (467)	56.6 (379)	10.4	20.2	81-82	34-35
	L-5A	68.6 (459)	55.8 (374)	11.3	21.1	81-81	34-34
	L-6A	69.1 (462)	58.2 (390)	10.5	18.8	84-84	33-35
	L-7A	70.7 (473)	61.5 (412)	7.5	18.6	82-85	33-35
	L-8A	70.7 (473)	59.7 (400)	10.2	19.4	81-85	33-35
	L-9A	70.2 (470)	58.2 (390)	11.1	21.6	81-83	34-34
	L-10A	70.3 (471)	58.4 (391)	11.5	18.4	78-79	33-34
Middle	L-4M	81.0 (542)	72.0 (482)	10.3	12.2	82-85	33-33
	L-5M	80.2 (537)	71.0 (475)	9.1	12.6	81-85	33-33
	L-6M	80.4 (538)	70.6 (473)	10.3	14.7	82-84	33-33
Base	L-1B	74.8 (401)	64.9 (435)	10.6	18.1	82-83	35-35
	L-2B	77.1 (516)	70.2 (470)	8.6	22.6	84-85	32-32
	L-3B	76.9 (515)	67.5 (452)	9.3	19.0	84-86	32-32
	L-4B	78.1 (523)	69.2 (463)	11.5	21.3	85-86	31-32
	L-5B	78.7 (527)	69.9 (466)	11.6	20.0	85-86	31-32
	L-6B	79.1 (530)	70.5 (472)	11.6	20.0	85-86	31-32
	L-7B	78.1 (523)	68.4 (458)	12.6	19.7	85-87	32-32
	L-8B	77.7 (520)	68.6 (459)	13.2	17.3	85-88	31-32
	L-9B	79.5 (532)	70.8 (474)	13.4	23.1	87-90	31-32
	L-10B	81.8 (548)	75.8 (507)	7.2	17.9	84-87	31-32
Specifi- cations		76.0 (509)	69.0 (562)	6.0	--	84	31-36

TABLE 22
TRANSVERSE TENSILE PROPERTIES ALLOY 7075-T651
SLACK-QUENCHED ALUMINUM PLATE
1.250 Inches (32 mm) Thick

	Specimen No.	Ult. Tensile Strength KSI (MPa)	0.2% Yield Strength KSI (MPa)	% Elong. 2 in G.L.	RA (%)	R _B	EC %IACS
Affected	X-1A	71.2 (477)	56.8 (380)	10.0	17.8	79.0	34-34
	X-2A	69.6 (466)	54.7 (366)	9.2	16.5	77.5	34-34
	X-3A	69.6 (466)	54.2 (363)	10.6	15.2	79.9	34-34
Base	X-1B	79.6 (528)	66.5 (445)	9.7	16.1	87.5	32-32
	X-2B	80.2 (537)	67.7 (453)	9.9	14.6	86.0	32-32
	X-3B	79.8 (534)	66.1 (442)	9.6	15.7	86.5	31-32
Specifi- cations		75.0 (502)	65.0 (435)	6.0	--	84.0	31-36

TABLE 23
LONGITUDINAL TENSILE PROPERTIES OF ALLOY 7075-T7351
SLACK-QUENCHED ALUMINUM PLATE
0.50 Inch (13 mm) Thick

	Specimen No.	Ult. Tensile Strength KSI (MPa)	0.2% Yield Strength KSI (MPa)	Elong. 2 in G.L.	RA (%)	R _B	EC %IACS Avg.
	H1	65.6 (439)	56.3 (377)	12.5	27.6	78-79	42.2
	H2	65.7 (440)	56.3 (377)	11.0	30.0	79-80	41.3
	H3	65.3 (437)	55.8 (374)	11.0	30.2	79-79	41.6
Specifi- cations		70.0 (469)	59.0 (395)	6.0	--	78	40-44

1.4 COMPUTER ASSISTED TEST CONTROL AND DATA ACQUISITION

During the contractual period the Air Force Materials Laboratory's Engineering and Design Data Laboratory, AFML/MXA, has procured two minicomputers and their associated peripheral devices, i.e., line printers, flexible disk and hard disk drives, and I/O devices used to interface the computer to the control console of the test machine. The two units are a Hewlett-Packard 9825A and a DEC PDP-11/34 minicomputer. The units were procured to expand the capabilities of the laboratory in the form of: (1) automated data acquisition, allowing important test data to be taken continuously at a faster rate, more accurately and consistently than is humanly possible; (2) automated test machine control to conduct complex spectra fatigue tests; and (3) to aid the laboratory in processing new data into a final, presentable form, i.e., quality plots, tabularized results, statistical analysis, etc. The units are being implemented to operate on a 24-hour basis performing test control and/or data acquisition. This has increased the laboratory's productivity and reduced personnel requirements for continuous attention.

The DEC PDP-11/34 minicomputer was procured to supplement the previously available paper tape reader used to control a test machine to apply a limited random flight spectrum on a test article. The University has generated software programs for the new minicomputer that facilitates implementing far more sophisticated spectrum loading fatigue testing programs than could be performed with the tape reader. One such spectrum the Air Force is particularly interested in is the Fighter Aircraft Loading Standard for Fatigue or "FALSTAFF", a complex flight spectrum containing 200 unique flights each of which contains typically 175 end points. An electrical interface has been implemented so that the PDP-11/34 computer can handle the job of controlling any one of the Engineering and Design Data Laboratory's seven hydraulic test machines under the FALSTAFF spectrum.

The unit is programmed to control in a quasi-closed-loop with minimal control by laboratory personnel to periodically inspect the output signal to insure load accuracy. The computer is typically capable of running the FALSTAFF spectrum at approximately 10 Hz with exceptional accuracy, e.g, less than 0.5 percent error with a typical test article. A more detailed technical discussion of this software development is presented in Paragraph 1.5.

A histogram recorder was procured and one of the University staff acquired a histogram of the FALSTAFF spectrum for each of the NATO countries participating in the cooperative spectrum fatigue program. When the programming for Engineering and Design Data Laboratory's DEC minicomputer was completed, the same equipment was used to record a histogram for the FALSTAFF program. The applied spectrum flight loading accuracy for the Design Data Laboratories is equal to the performance of the better NATO member laboratories conducting FALSTAFF flight load testing.

An additional program was written to collect and store a histogram summary and subsequently print it out for each flight. These two programs have the long-term benefit of allowing the AFML/MXA Engineering and Design Data Laboratory to represent the United States Air Force as a full participant in the future NATO countries spectrum fatigue round-robin testing program.

Another aircraft spectrum that has been acquired for use in the DEC PDP-11/34 flight loads computer program is the A-10 attack aircraft, wing spectrum number 3. This program is even larger than the FALSTAFF flight loads spectrum program. The A-10 spectrum, when implemented, will fully tax the present capabilities of the computer by totally filling the hard disk pack storage capacity. Minor programming changes are yet to be accomplished to allow this spectrum to be rendered fully operational.

The second minicomputer, the Hewlett-Packard 9825A minicomputer has been interfaced to the majority of the test machines in the laboratory to act as a universal data acquisition system for virtually any type of test presently conducted. One example of implementing this system is for low cycle strain controlled fatigue testing. In the present configuration, the system possesses the capability of monitoring the load versus strain record of an on-going fatigue test and can output any significant change in either parameter. Also, the maximum and minimum parameters are printed after a predetermined number of elapsed load cycles in the event that no significant change occurs to insure a steady state test condition. The advantages of such a system are to insure the proper load-controlling parameter and to observe what effect the cycling straining has on the dependent parameter, i.e., load. Materials which either undergo cyclic softening or hardening (or remain unchanged) during fatigue loading become readily apparent by observing the maximum load values, a far more accurate and reliable method than measuring the bandwidth, or load amplitude of a strip chart recorder. Finally, by utilizing a multiple relay card in the computer system, the test can be halted if a predetermined condition, such as a percent change in maximum steady state load, is encountered.

1.5 SOFTWARE DEVELOPMENT FOR THE DEC PDP-11/34 MINICOMPUTER

UDRI has provided a number of items of software for the PDP-11/34 to support the mission of the AFML Systems Support Group. This software includes general systems software, control software for the MTS machines, and special software related to specific programs.

UDRI personnel have obtained the computer codes and documentation required to generate the FALSTAFF standard load sequence. The FALSTAFF computer code was obtained in the form of a paper tape. UDRI provided computer codes to read the paper tape and verify its contents. UDRI personnel then converted the FALSTAFF data set generator, GENESIS, to run on a large CDC

mainframe computer, and then to run correctly on the PDP-11/34. Versions of the code were generated to produce tabular output and to produce a special data set on an RK05 cartridge disk. UDRI provided a special computer code, MTSFRM, to convert the FALSTAFF data set to a format allowing faster access. The integrity of the load sequence was verified at each step of the conversion, using the computer codes SAMCHK, which reads the same input file as MTSFRM and produces a histogram and summary of each flight, and FALDMP, which prints portions of the FALSTAFF tables in the same format used in the FALSTAFF report.

UDRI has provided several computer codes to aid in the calibration of the MTS machine control systems. The CALMTS computer code provides a predetermined load level into the MTS machine controller which allows static testing of the D/A converter, the MTS machine console, the load cell and associated signal conditioning electronics and the A/D converter. The MTSZER computer code sets the MTS machine load to zero to unload the test stand as quickly as possible. The MTSTST computer code exercises the MTS machine by producing a single quarter cycle of a haversine forcing function. This code is used, together with a storage oscilloscope, to measure the lag and overshoot or undershoot of the load cell feedback signal compared with the forcing function, which allows calibration of the gain and range controls. The MTST02 computer code produces a train of four half-cycles of the haversine forcing function. It is used in the same way as MTSTST. The MTST03 computer code exercises and tests the MTS machine's response by producing an arbitrary number of half-cycles of a constant amplitude forcing function and plotting the forcing function and the load cell feedback on the line printer. The feedback function is held to a user-specified tolerance. The codes MTSCl1 and DACHEK are used to test the D/A converter under static and dynamic conditions. The code MTSDRV produces an arbitrary number of cycles of the constant amplitude haversine forcing function for calibration or to warm up the machine.

The MTS machine "production" software includes the UDRI computer code, MTSPRG, which controls the MTS machine through an experiment simulating an arbitrary number of flights, each consisting of 1,023 or fewer load levels. UDRI software engineers designed and implemented MTSPRG using modern top-down modular design techniques. The computer code is implemented as a hierarchy of modules. Each module performs a single task, calling lower level modules to perform subtasks.

The top level module, MTSPRG, initializes the system, then, for each end point, generates the forcing function to reach that end point, calculates the error and obtains the next end point. When the end of the simulation occurs, MTSPRG unloads the MTS machine and halts.

The first module called by MTSPRG is GETHAV. GETHAV conducts a dialogue with the experiment operator to set up the experiment parameters, then builds the haversine table used to produce the forcing function.

The program, IGETEP, retrieves a single end point from the load spectrum data set each time it is called. It buffers the end points internally, reading an entire flight from the storage disk at a time. The first time IGETEP is called, it obtains the name, length, and other information about the data set from the user and opens the RT-11 direct access file containing the data set.

The module RUNMTS controls the MTS machine through a single excursion from the current end point to the next end point. It accomplishes this excursion as a series of steps on a quarter cycle of a haversine curve connecting the end points. At each step, it applies the control signal to the machine, waits for a short time, then reads and stores the feedback signal from the load cell.

The module CHEKEP determines if the current end point is a peak as a trough calculates the error (overshoot or undershoot) of the previous excursion, and calculates a correction factor to be applied to the next excursion.

The module WAITMT causes the computer to wait a short period of time (from several tens of microseconds to a millisecond). It is used to introduce short "busy" waits in the MTS control program to allow time for the electronics and hydraulics systems to become stable after a load change, and to control the speed of some processes.

1.6 COMPLETE FATIGUE CRACK GROWTH RATE CURVES FOR ALUMINUM ALLOY 2124-T851 INCLUDING CRACK GROWTH MODELING

Due to the increasingly wide usage of aluminum alloy 2124-T851 in present Air Force systems, there currently exists the need to thoroughly document a variety of mechanical properties for this structural material. One important mechanical property of interest for this alloy is its fatigue crack growth rate characteristics. Prior to these results, no consistent data set, produced by a single source, existed that documents the entire da/dN -curve from the threshold up to a growth rate where K_{max} is approaching the critical fracture toughness. Also, due to the ever increasing nondestructive inspecting capabilities, fatigue crack growth rate properties at or near the threshold for crack propagation are becoming of prime concern to the designers and life prediction analysts. It is because of a lack of a consistent data set for 2124-T851 that this program was initiated.

The complete fatigue crack growth rate curves were obtained for aluminum alloy 2124-T851 for two stress ratios. Threshold values of stress intensity range were determined for each stress ratio investigated. The effect of specimen thickness on crack growth properties were examined for both stress ratios. A variety of mathematical models currently employed in the technical community were also statistically fitted to the data sets and examined. These data were published in AFML-TR-78-155.[5]

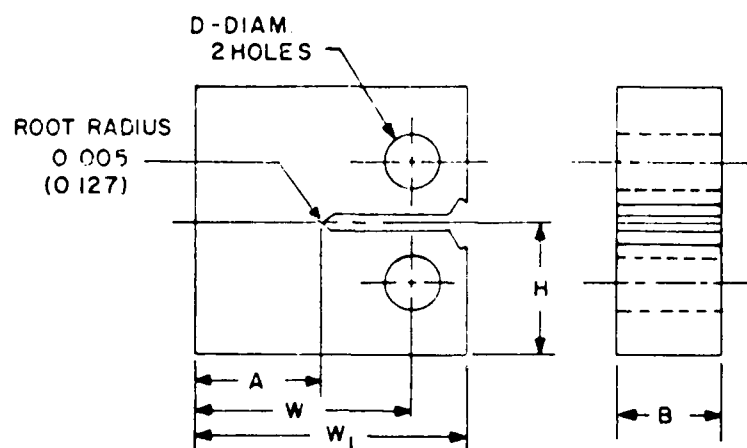
The test material used in this investigation was a single 2.0 inch (50.8 mm) thick plate of aluminum alloy 2124-T851.

Tensile specimens were removed from the longitudinal orientation of the test plate. Two inch (50.8 mm) thick compact type (CT) fracture toughness specimens were removed from the test plate having longitudinal-transverse orientation (L-T) (Figure 12). Elongated compact type specimens ($H/W = 0.486$) for crack growth investigations were likewise machined from the same orientation (L-T) and machined to the dimensions shown in Figure 12. These specimens were machined in three thicknesses, holding the profile dimensions constant, so the effect of specimen thickness on fatigue crack growth properties could be examined. Because of occasional out-of-plane cracking problems experienced with this specimen geometry during the course of testing, particularly at a stress ratio of $R = +0.5$, the elongated CT specimens were later remachined to the configuration of a CT specimen ($H/W = 0.60$) by reducing the specimen width (W in Figure 12).

Tensile testing was performed on a Baldwin Wiedemann tensile testing machine. Strain was obtained with a 1.0 inch (25.4 mm) Instron extensometer. Tensile testing was carried out in accordance with ASTM Standard E8-69.

Fracture toughness testing was accomplished using a Tinius-Olsen tensile testing machine following guidelines set forth in ASTM E399-74. Crack opening-displacement (COD) was monitored with a clip-on gage as described in the test standard.

All fatigue crack growth rate testing was carried out with a 2.5 KIP (11.1 kN) MTS hydraulic fatigue testing machine operating in a load-controlled mode. Two stress ratios were employed in this program: $R = +0.1$ and $+0.5$. Test frequency was limited to 30 Hz and all testing was conducted at room temperature. To minimize intralaboratory effects, humidity chambers were fashioned from plexiglass, with humidity limited to less than 10 percent using a dessicant material. Procedures outlined in the proposed standard for constant amplitude fatigue crack growth rate testing^[6] were adhered to as close as possible. The K-Increasing Constant-Amplitude-Load Control method was employed for all specimens.



DIMENSIONS INCHES (mm)

SPECIMEN TYPE	A	B	W	W ₁	H	D
FRACTURE TOUGHNESS	2.250 (57.15)	2.000 (50.80)	4.000 (101.60)	4.625 (117.48)	2.400 (60.96)	0.625 (15.87)
CRACK* GROWTH	1.785 (45.3)	0.375 (9.52)	2.550 (64.8)	3.188 (80.9)	1.240 (31.5)	0.500 (12.7)
CRACK* GROWTH	1.785 (45.3)	0.750 (19.05)	2.550 (64.8)	3.188 (80.9)	1.240 (31.5)	0.500 (12.7)
CRACK* GROWTH	1.785 (45.3)	1.500 (38.1)	2.550 (64.8)	3.188 (80.9)	1.240 (31.5)	0.500 (12.7)

* ELONGATED COMPACT SPECIMEN

Figure 12. Fracture Toughness and Fatigue Crack Growth Specimens.

Crack length was obtained using a 30X traveling microscope to measure the fatigue crack length on each surface of the specimen. After a predetermined number of load cycles [sufficient to yield an estimate crack extension of 0.010 to 0.020 inch (0.25 to 0.50 mm)] the test machine was halted, a mean load applied to enhance the fatigue crack tip, and a visual measurement of crack length taken, after which the testing machine was restarted. This procedure was continued until complete specimen fracture. A crack curvature correction factor was determined using the same guidelines for crack length correction set forth in ASTM 399 for Fracture Toughness Testing. This correction was added to each visual trace previously taken, along with the length of the starter notch (from centerline of loading holes to notch tip) to obtain the raw crack growth data set of crack length "a", and corresponding number of load cycles, "N". These data were then reduced to the standard accepted form (crack growth rate, da/dN , as a function of change in stress intensity, ΔK) in the manner prescribed in the aforementioned proposed test standard. This method fits a second-order polynomial to a seven-point data subset, and in turn calculates the slope at the midpoint of the subset. The midpoint crack length is used to calculate the ΔK value, while the slope is the corresponding da/dN value. This procedure is applied throughout the entire raw data set to generate the da/dN versus ΔK curve.

Upon generation of the entire crack growth rate curves, a variety of mathematical models, developed to describe the constant amplitude crack growth relationship, were statistically fitted to the data and compared for best fit. Models investigated were the Paris Power Law equation, the Walker equation, the Forman equation, and a form of the hyperbolic sine equation.[7]

The tensile test results for specimens tested in the longitudinal orientation are presented in Table 24 and are in good agreement with published data.[8,9] Fracture toughness test results for longitudinal-transverse oriented specimens

TABLE 24
TENSILE PROPERTIES OF ALUMINUM ALLOY
2124-T851 TWO INCH (50.8 mm) THICK PLATE

Specimen No.	Yield Strength KSI (MPa)	Ultimate Strength KSI (MPa)	Elongation in 1.0 inch (25.4 mm) Gage Length	Reduction in Area (%)
X1	65.6 (452)	71.9 (496)	9.0	21.5
X2	67.0 (462)	72.5 (500)	9.1	22.6
X3	66.7 (460)	71.9 (496)	9.0	21.2
Avg.	66.4 (458)	72.1 (497)	9.0	21.7

are listed in Table 25 and are also in agreement with References [8] and [9].

TABLE 25
FRACTURE TOUGHNESS PROPERTIES OF ALUMINUM ALLOY
2124-T851 TWO INCH (50.8 mm) THICK PLATE

Specimen No.	Orientation	K_{IC} KSI \sqrt{in} (MPa \sqrt{m})
1C	Long.-Transverse	30.1 (33.1)
2C	Long.-Transverse	30.9 (34.0)
3C	Long.-Transverse	30.4 (33.4)
Avg.		30.5 (33.5)

The fatigue crack growth rate curves for aluminum alloy 2124-T851 for R-ratios of +0.1 and +0.5 are presented in Figures 13 and 14, respectively. The curves presented in both figures represent data obtained from 16 specimens per R-ratio. The curves obtained for both R-ratios demonstrate unstable crack propagation occurring when K_{max} is approximately 30 KSI \sqrt{in} (33 MPa \sqrt{m}), which coincidentally is the critical fracture toughness, K_{IC} , for this material.

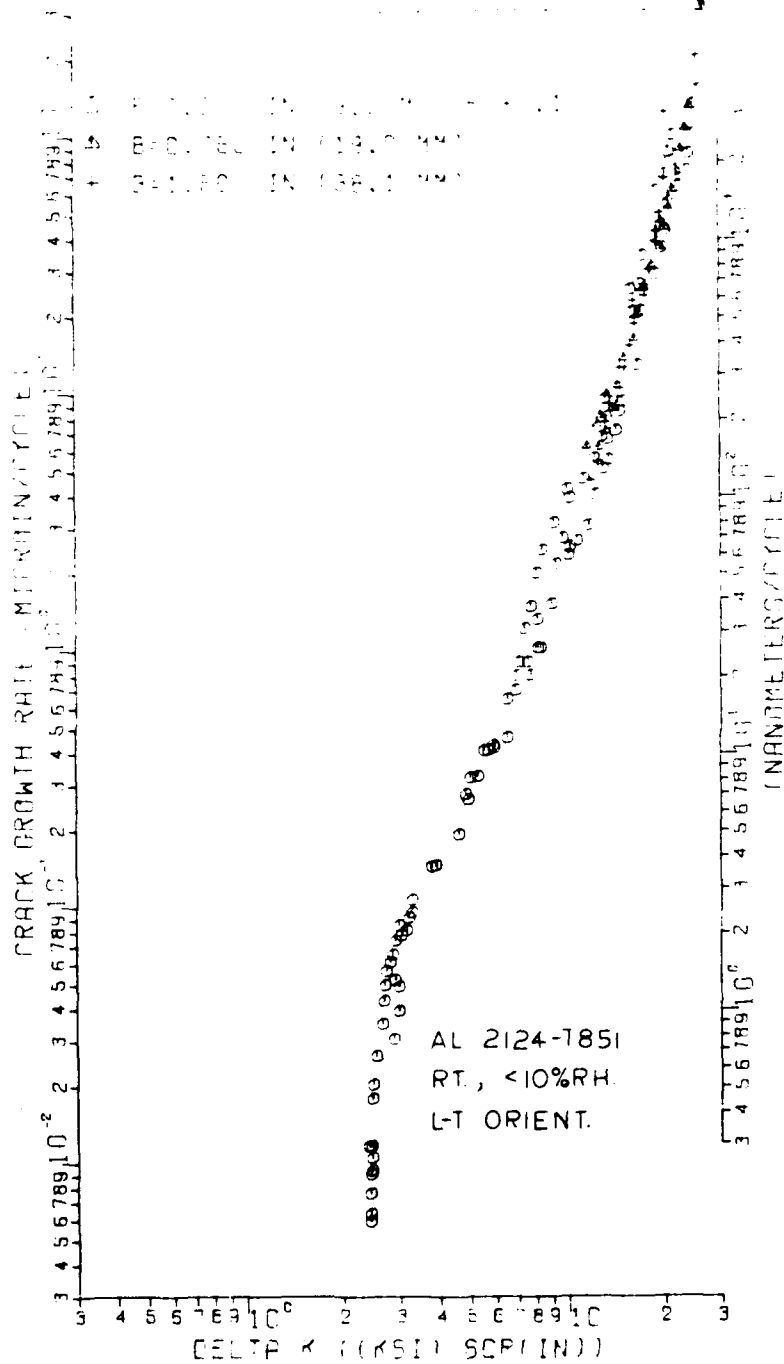


Figure 13. Constant Amplitude Fatigue Crack Growth Rate Curves for Aluminum Alloy 2124-T851 at R-Ratio of +0.1.

THIS PAGE IS BEST QUALITY PRACTICABLE
FROM COPY FURNISHED TO JMC

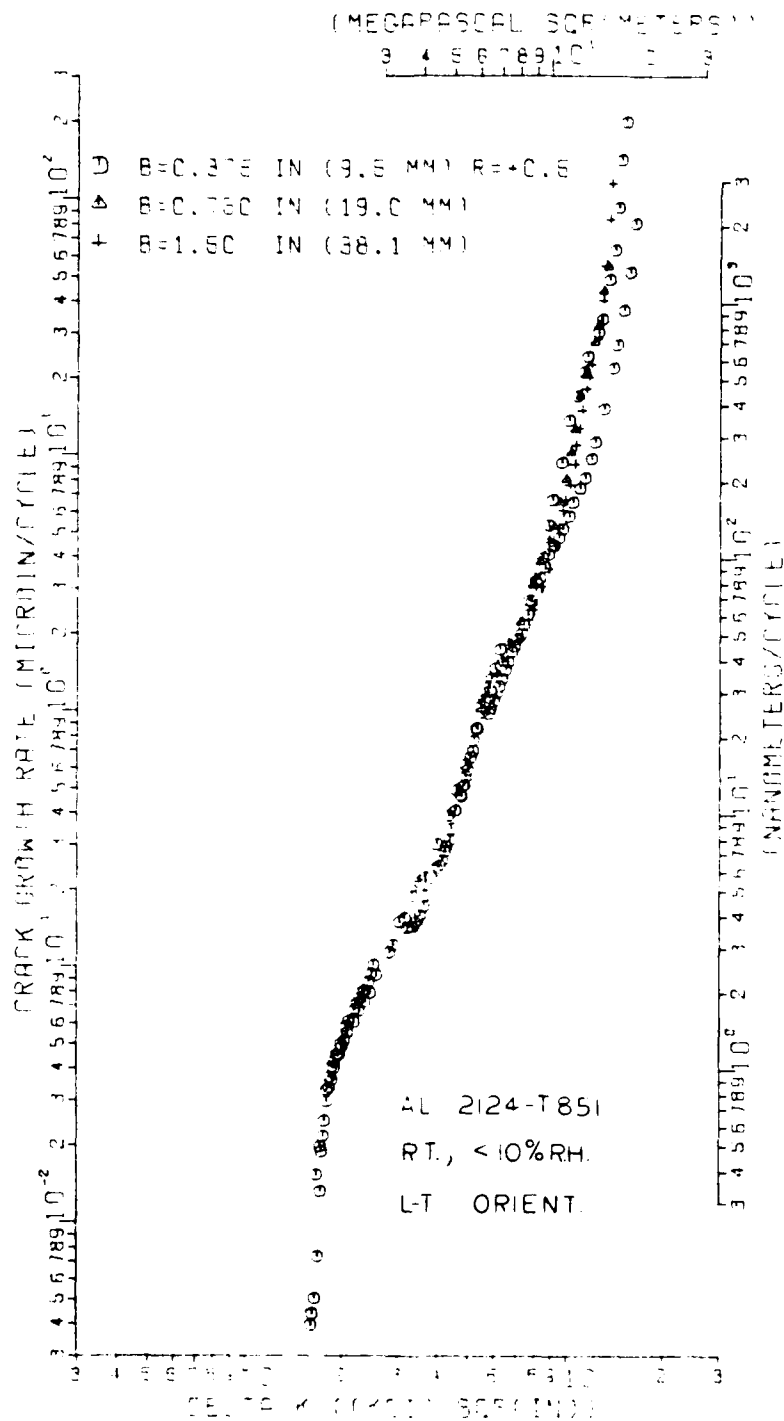


Figure 14. Constant Amplitude Fatigue Crack Growth Rate Curves for Aluminum Alloy 2124-T851 at R-Ratio of +0.5.

The effect of specimen thickness on fatigue crack growth was examined only at growth rates above 10^{-6} in./cyc. (25.4 nm/cyc.) since it was felt it would be more difficult to maintain a symmetric crack front at low ΔK values for the thicker specimens. For the three thicknesses investigated there does not appear to be any thickness effect on crack growth rates below 10^{-4} in./cyc. (2.5×10^3 nm/cyc.). This fact is in good agreement with the findings of Reference [6] where it was noted that any apparent variation in fatigue crack growth rate data due to thickness results from inaccuracies in the crack length measurements due to nonsymmetric crack front curvature or tunneling.

A number of constant amplitude fatigue crack growth rate model equations were statistically fitted to the data obtained from the 0.375-inch (9.52 mm) thick specimens. The most familiar is the Paris Power Law equation, illustrated in Figure 15. The curves illustrated in Figure 15 were fitted to the test data at R-ratios above both 10^{-7} in./cyc. (2.5 nm/cyc.) and below 10^{-5} in./cyc. (254 nm/cyc.). Crack growth rates are in terms of inches per cycles, while stress intensity range is in $\text{KSI}\sqrt{\text{in.}}$.

The Paris equation has the definite advantage of being a compact yet accurate model when considering only the linear portion of the crack growth rate curve; however, it does have limitations. One major shortcoming of this equation is that by making it short and concise, it contains no expression to account for such parameters as varying R-ratios. Consequently, different parameters must be used for each different possible R-ratio.

Walker, [10] in his investigation of stress ratio effects on fatigue crack propagation, developed an expression for an effective stress (\bar{S}):

$$\bar{S} = S_{\max} (1-R)^m$$

where S_{\max} is the maximum cyclic stress, and m is an empirically determined constant. This effective stress concept was used to

develop an effective stress intensity which, when substituted in the Paris equation, yielded the following equation:

$$da/dN = c(K_{max}(1-R)^m)^p$$

where K_{max} is the maximum cyclic stress intensity, and C , p , and m are the empirically derived constants. This equation was fitted to the data developed from the 0.375 inch (9.52 mm) thick specimens used at $R = +0.1$ yielding the following expression:

$$da/dN = 1.483 \times 10^{-9} [K_{max}(1-R)^{0.297}]^{3.14}$$

where da/dN is again in terms of inches/cycle and K_{max} is in terms of $KSI\sqrt{in}$. Again data were limited to greater than 10^{-7} in./cyc. (2.5 nm/cyc.) and less than 10^{-5} in./cyc. (254 nm/cyc.). Note that when $R = +0.1$ the equation is identical to the Paris equation previously obtained. This equation is graphically depicted in Figure 16 for R -ratios of +0.1 and +0.5. The Walker model handles the curve shift due to different R -ratios reasonably well as exemplified in the figure.

The Walker equation is more versatile than the Paris equation since only the one equation is needed to define the crack growth rate curve at any stress ratio; however, like the Paris equation, it is applicable only to the linear portion of the da/dN versus ΔK curve. It does not account for either the upper or lower portions of the curve and therefore can lead to large errors if extrapolated beyond its limits.

Forman, et al. [11] developed an expression to handle the acceleration of fatigue crack growth at high stress intensity values for any stress ratio, which has the form

$$da/dN = \frac{C \Delta K^p}{(1-R) K_C^{-\Delta K}}$$

where the numerator is simply the Paris equation and K_C is the maximum fracture toughness value at the onset of unstable crack propagation, determined from the vertical asymptote at the upper portion of the da/dN versus ΔK curve. This equation was

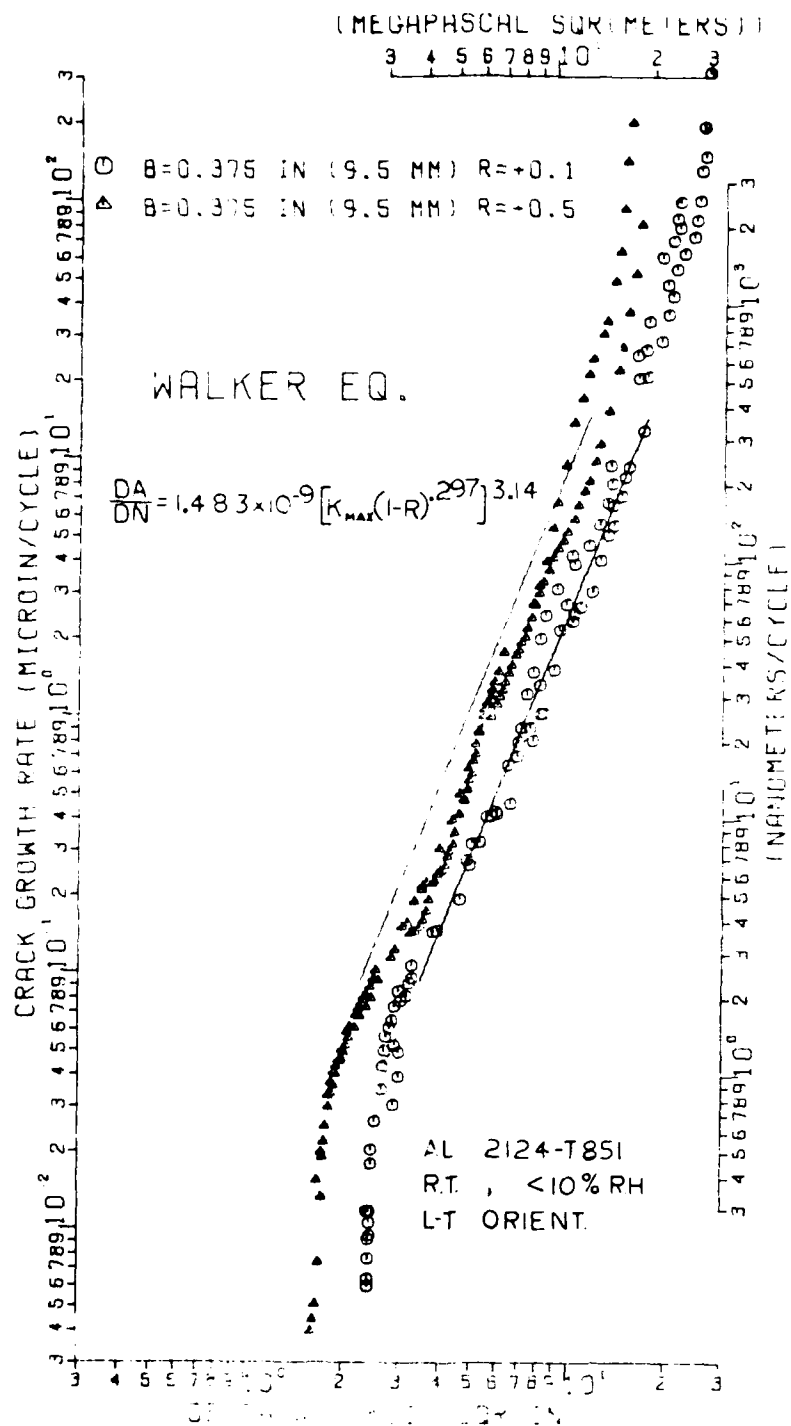


Figure 16. Walker Model Equation for Aluminum Alloy 2124-T851.

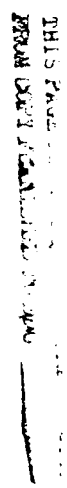
fitted to the $R = +0.1$ data (above 10^{-7} in./cyc. [2.5 nm/cyc.]) and is presented in Figure 17 for both R-ratios (+0.1 and +0.5) for a value of K_C of $30.5 \text{ KSI}\sqrt{\text{in}}$ ($33.5 \text{ MPa}\sqrt{\text{m}}$). In addition to handling well the R-ratio shift, the Forman equation accurately models the upper portion as well as the linear portion of the crack growth rate curve. However, as in the case of the two previously mentioned models, it fails to model crack growth rates near the threshold.

A number of investigators have looked at the hyperbolic trigonometric functions as a possible choice for a model since both the hyperbolic sine (\sinh) and hyperbolic tangent (\tanh) expressions yield a sigmoidally-shaped curve. Annis, et al.[7] developed a hyperbolic sine model of the form:

$$\log(da/dN) = C_1 \sinh(C_2(\log(\Delta K) + C_3)) + C_4,$$

where the coefficients are functions of test frequency, stress ratio, and temperature. This expression was fitted to both data sets and the coefficients were statistically determined via the regression technique used for the previously mentioned models. The value C_1 , which controls the vertical "stretch" of the S-shaped curve, is reported to be a fixed value for a given material. For IN-100 material, C_1 has a value of 0.5,[7] while limited experience with titanium indicated a value of 0.9 yields the best curve.[12] For this investigation C_1 was varied between 0.5 and 1.5, with results indicating a value of C_1 equal to 0.97 produces the best fit. The results of this analysis are presented in Figure 18. Each curve adequately represents its respective data set throughout the entire da/dN range. The effect of R-ratio is seen as a shift of the curve to the left and slightly down for increasing R-ratio. This same trend was noted by Annis, et al. for IN-100 material tested at various R-ratios.

The following conclusions are based on test results from a single 2 inch (50.8 mm) thick plate of aluminum alloy 2124-T851. All model equations obtained can be considered accurate only over the ranges specified in this report and should not be extrapolated.



57

1. The thresholds for constant amplitude fatigue crack growth for this material tested at R-ratios of +0.1 and +0.5 are 2.4 and 1.6 KSI $\sqrt{\text{in}}$ (2.63 and 1.76 MPa $\sqrt{\text{m}}$), respectively.

2. Increasing R-ratio has the effect of increasing the crack growth rate for a given stress intensity range; the threshold stress intensity range decreased with increasing R-ratio.

3. There was no effect of specimen thickness on the fatigue crack growth rate for either R-ratio investigated.

4. No effect of specimen geometry on fatigue crack growth data was observed for the compact type and the elongated compact type specimen. However, the elongated CT specimens were prone to out-of-plane cracking, while the CT specimens were not.

5. The following model equations were obtained for this material undergoing constant amplitude fatigue crack growth testing:

a. Paris Equation

$$\begin{aligned}\frac{da}{dN} &= 1.86 \times 10^{-9} \Delta K^{3.14} @ R = +0.1 \\ &= 2.86 \times 10^{-9} \Delta K^{3.35} @ R = +0.5\end{aligned}$$

b. Walker Equation

$$\frac{da}{dN} = 1.48 \times 10^{-9} [K_{\max}(1-R)^{0.297}]^{3.14}$$

c. Forman Equation

$$\frac{da}{dN} = \frac{1.014 \times 10^{-7} \Delta K^{2.63}}{30.5(1-R) - \Delta K}$$

d. Hyperbolic Sine Equation

$$\log \frac{da}{dN} = 0.97 \sinh (2.92(\log \Delta K - 0.86)) - 5.97 @ R = +0.1$$

$$\log \frac{da}{dN} = 0.97 \sinh (2.88(\log \Delta K - 0.63)) - 6.39 @ R = +0.5$$

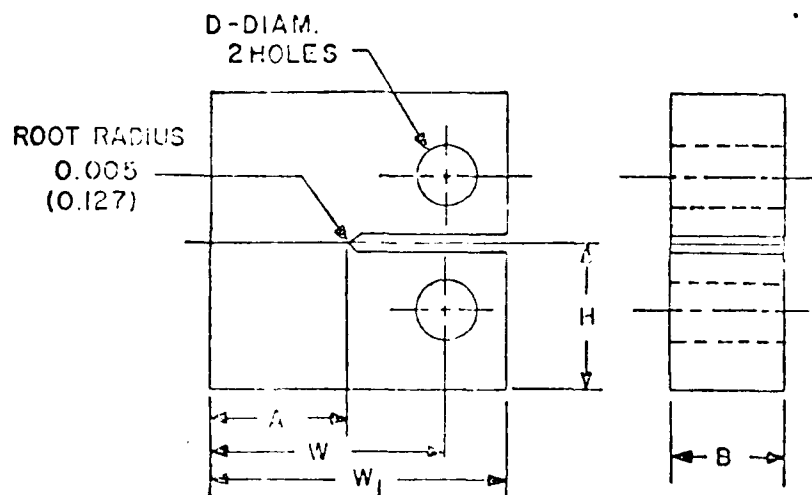
1.7 CRACK LENGTH DETERMINATION FOR THE ELONGATED COMPACT TYPE SPECIMEN USING COMPLIANCE TECHNIQUES

After the crash of one of the Air Force's F-111 aircraft in 1969, attributed to brittle fracture, the field of fracture mechanics

was vastly expanded. This and other brittle fractures led to decisions to incorporate fracture mechanics related design policies in all subsequent aircraft designs, exemplified by the Air Force's Damage Tolerance Mil. Spec. 83444. Because of the lack of extensive data bases on some materials, there currently exists the need to generate large amounts of fracture design data for materials currently existing in the Air Force's inventory, as well as materials under consideration for use by the Air Force.

A recently completed round robin ASTM program has determined that most variability found in fatigue crack growth rate data obtained from different laboratories results from the experimental procedures used to obtain the raw test data.[13] Assuming the testing machine is properly calibrated, the source for such variability lies solely in the crack length measuring procedure. The purpose of this report is to outline an automated crack growth rate data generation technique, one which has the potential for continuous crack length monitoring. This technique utilizes a clip gage which measures displacements to determine crack length via an electronic signal during a loading cycle. Such a procedure can be adapted to interface a data acquisition system, i.e., minicomputer, to yield crack growth rate data while the test is running, thus eliminating all lengthy data reduction requirements, overnight shutdowns, etc. A "hands-off" system such as this also eliminates possible human error and lengthy specimen preparation, and minimizes personnel requirements.

The material used in this investigation was aluminum alloy 2124-T851 2 inch (50 mm) thick plate. The geometry of the fatigue crack growth specimens used is presented in Figure 19. Three thicknesses were examined as indicated in Figure 19. Constant amplitude fatigue crack growth testing was conducted at two stress ratios: $R = +0.1$ and $R = +0.5$, with test machine frequency limited to 30 Hz. All testing was carried out on an MTS hydraulic fatigue testing machine operating in load controlled mode. Two methods are employed to gather the necessary test data and are outlined



DIMENSIONS: INCHES
(mm)

A	B	W	W ₁	H	D
1.785 (45.3)	0.375 (9.52)	2.550 (64.8)	3.188 (80.9)	1.240 (31.5)	0.500 (12.7)
↓	0.750 (19.1)	↓	↓	↓	↓
↓	1.500 (38.1)	↓	↓	↓	↓

Figure 19. Elongated Compact (WOL) Specimen Used for Fatigue Crack Growth Rate Testing.

in the following paragraphs. Crack growth rate obtained from the data were finally compared to stress intensity range, $K_{I\max}$, to plot a compliance factor at the fracture stage.

Crack growth was widely used by the majority of testing engineers. Employing a VAX traveling microscope to measure the crack length on each surface of the specimen. After a selected number of load cycles (sufficient to yield an estimated crack extension of 0.010 to 0.020 in. (0.25 to 0.50 mm), the test machine was halted, a mean load applied to enhance the fatigue crack tip, and a visual measurement of crack length taken, after which the testing machine was restarted. This procedure was continued until complete specimen fracture. Finally, a crack curvature correction factor was determined using the same guidelines for crack length correction set forth in ASTM 399 for Fracture Toughness Testing. This correction was added to each visual trace previously taken, along with the length of the starter notch (from centerline of loading holes to notch tip). This data set, crack length "a", and corresponding number of load cycles, "N", was then used to compute the crack growth rate da/dN as a function of stress intensity range. Methods for this computation routine are described in many technical publications, [13,14] usually consisting of fitting some curve through a small section of the "a versus N" data curve and calculating the slope at the mid-point of this data subset. This slope is the crack growth rate while the midpoint crack length is used to compute the corresponding stress intensity range.

While the previously described testing procedures were being applied, fatigue crack length measurements were simultaneously being recorded in a different fashion using a compliance technique which relates crack length as a function of crack opening displacement (COD). Hardened steel knife edges were affixed to the specimen and an MTS clip gage used to monitor specimen COD. The signal from the clip gage was

inputted to an X-Y recorder; COD to the X-axis, load to the Y-axis. Each time the cyclic loading was halted for a visual crack length measurement, a trace of specimen COD versus load was recorded. To obtain this, the load was slowly applied to approximately 90 percent of the maximum cyclic load. After completing this trace, fatigue testing was resumed and the same procedures applied after crack extension of approximately 0.010 inch (0.254 mm). Values of crack length were then calculated from the slopes of the COD versus load trace using the necessary compliance curve. Crack growth rate data were obtained from these data, using the same computation routines used to reduce the visually obtained data.

The compliance curve was generated using two specimen thicknesses: 0.375 inch (9.52 mm) and 0.75 inch (19.0 mm). This procedure involved precracking ($R = +0.1$) to a certain crack length an elongated compact (WOL) specimen instrumented with the clip gage. Load was then applied slowly and a trace of load versus COD was obtained with an X-Y recorder. Care was again taken so this load never exceeded 90 percent of the maximum cyclic load in order to avoid any retardation effects. The specimen was then further precracked to a different crack length and the same technique repeated. A series of curves were obtained for the $\frac{a}{w}$ (crack length/specimen width) range of 0.35 to 0.65. Normalized values of crack opening displacement and crack length were then plotted and an expression developed relating the specimen COD to crack length.

Normalized values of crack length with corresponding normalized values of crack-opening displacement were obtained for a number of elongated compact (WOL) specimens of various thicknesses. A third degree polynomial was fitted to the data yielding the following expression:

$$\frac{E \cdot B \cdot COD}{P} = -348.6 + 2492 \left(\frac{a}{w}\right) - 5512 \left(\frac{a}{w}\right)^2 + 4431 \left(\frac{a}{w}\right)^3$$

or

$$\frac{a}{w} = 0.0677 + 0.00894 \left(\frac{E \cdot B \cdot \text{COD}}{P} \right) - 0.000049 \left(\frac{E \cdot B \cdot \text{COD}}{P} \right)^2 \\ + 0.000000101 \left(\frac{E \cdot B \cdot \text{COD}}{P} \right)^3$$

where E is the material's modulus of elasticity, B is the specimen thickness, COD is the displacement as measured by the clip gage, and P is the applied load.

The first equation is illustrated in the computer-prepared curve shown in Figure 20 along with a similar curve^[15] developed for compact (CT) specimen machined from aluminum alloys 7075-T6 and 2024-T351, titanium 6Al-4V, and 4340 steel. Deviation between the two curves is small over the range of $\frac{a}{w}$ from 0.35 to 0.60. For crack length/width ratios above this, differences between the two curves become greater with increasing values of $\frac{a}{w}$.

Crack growth rate data obtained employing the "visual" method are presented in Figures 21 and 22 for a stress ratio of $R = +0.1$. Also presented on each curve are the crack growth rate data obtained using the compliance (COD) technique. For both thicknesses investigated, the results are identical over the range tested. Photomicrographs obtained with the scanning electron microscope (SEM) for both thicknesses at a stress intensity of approximately $15 \text{ KSI}\sqrt{\text{in}}$ ($16.5 \text{ MPa}\sqrt{\text{m}}$) are presented in Figures 23 and 24. These results, also presented in Figures 21 and 22, verify both procedures as accurate methods. Results for a stress ratio of $R = +0.5$ are similarly presented in Figure 25 for specimen thickness of 0.375 inch (9.50 mm). Again, the results for the compliance method are in excellent agreement with those obtained via the visual trace method. Because of a poor fracture face topography for this particular sample, a microscopic investigation could not be accomplished.

The results of this report cover a small portion of the normal data-taking range for constant amplitude fatigue crack growth rate testing. This range was limited due to the lack of

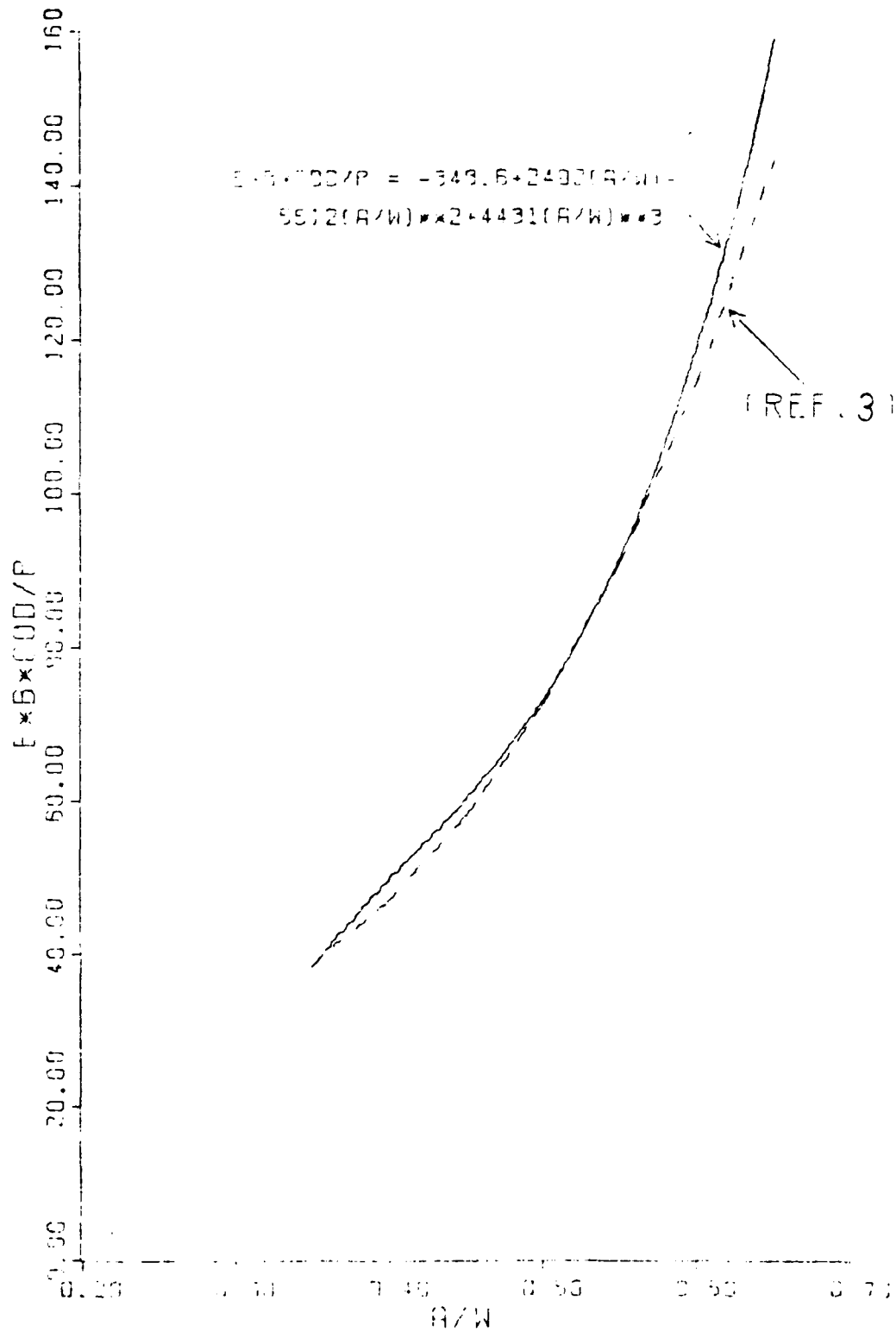
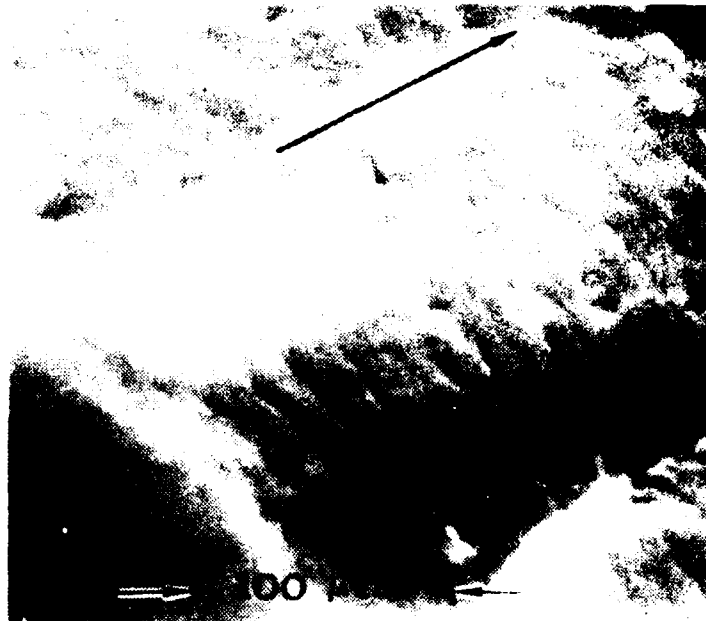


Figure 20. Calibration Curve for Elongated Compact (WOL) Specimen.



$\Delta K = 15.2 \text{ KSI}\sqrt{\text{in}} \text{ (16.7 MPa}\sqrt{\text{m}}\text{)}$

Figure 23. Photomicrograph of Fatigue Fracture Face of Aluminum 2124-T851, 0.75 Inch (19.0 mm) Thick.



$\Delta K = 15.0 \text{ KSI}\sqrt{\text{in}} \text{ (16.5 MPa}\sqrt{\text{m}}\text{)}$

Figure 24. Photomicrograph of Fracture Face of Aluminum 2124-T851, 1.50 Inch (38.1 mm) Thick.

MEMORANDUM FOR THE RECORD

100 0 4 5 5 5 5 10

⊙ R / 1500

Δ R / 1500

B = 0.375 in. (9.5mm)

R = +0.5

30 Hz

Figure 25. Fatigue Crack Growth Rate Data for Aluminum 2124-T851, 0.375 Inch (9.5 mm) Thick, R = +0.5.

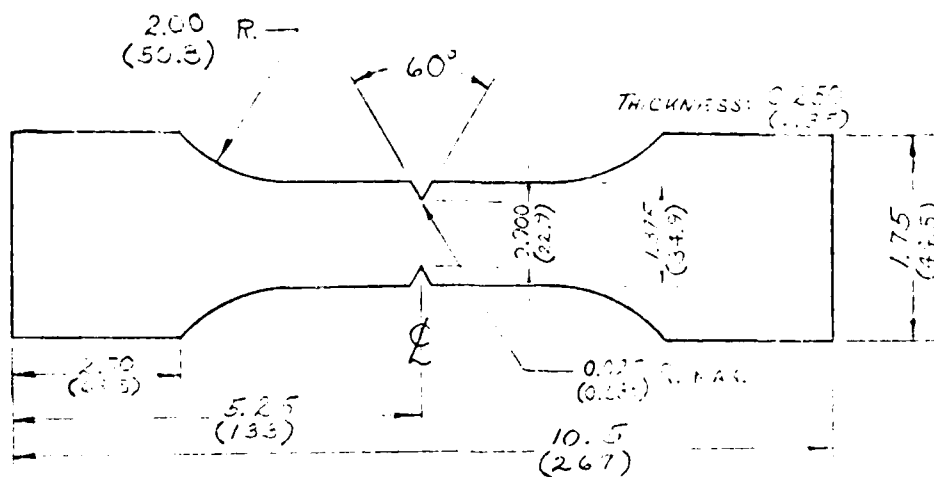
sensitivity of the clip gage employed in this investigation. More sophisticated fatigue clip gages currently on the market with accuracies on the order of ± 0.0001 inch (± 0.0025 mm) would naturally increase accuracy and extend this data range. Likewise, additional accuracy could be achieved and efficiency increased if the outputs from the clip gage and load cell were analyzed via a minicomputer or some other data acquisition system, rather than the graphical manipulation as was accomplished in this program. However, over the range investigated, the normalized COD calibration curve obtained is an accurate representation for the elongated compact (WOL) specimen at any thickness. Also, the calibration curve obtained for this specimen is in good agreement with the calibration curve derived for the ASTM compact specimen over the majority of the range examined. The COD calibration method lends itself well to a completely automated data acquisition system for constant amplitude fatigue crack growth rate testing.

1.8 SPECTRUM FATIGUE TESTING OF 10 Ni STEEL

A request was made by the Advanced Metallic Structures/Advanced Development Program (AMS/ADP) office to conduct spectrum fatigue tests on double-edge-notched specimens fabricated from 10 Ni steel. This material was originally developed by U.S. Steel under contract to the U.S. Navy. The four stress spectra employed in this study were furnished by the General Dynamics Corporation, Fort Worth, Texas (Ref. pg. 13 FZM-5999, Add. 1. August 1974). One additional stress spectrum, which was identical to one of the four spectra originally furnished but with one stress level altered, was also used for crack growth investigations on specimens with different fatigue crack starter notches.

Specimens were supplied to AFML machined to the configuration shown in Figure 26. Two additional specimens of a different geometry were also furnished, both with two notches machined in them; one notch was produced by a wire saw, the other notch

THIS PAGE IS BEST QUALITY PRACTICABLE
FROM COPY FURNISHED TO DDC



DIMENSIONS: inches
(mm)

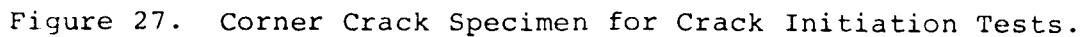
Figure 26. Double-Edge-Notched Specimen.

by an electric discharge machine (EMD). See Figure 27 for these latter specimens. It was requested that both notches be monitored during spectrum testing for crack initiation and growth.

All spectrum testing was performed on an MTS 50 KIP (222 KN) electrohydraulic servo-controlled fatigue testing machine which is equipped with hydraulic grips. Load signals were generated by an EMR load profiler equipped with a Talley paper tape reader. Mylar tape was used rather than the standard computer paper tape since the latter could not endure the rigorous wind/rewind cycles of the tape reader. A Weston Instruments Limit Detector was used in conjunction with the EMR load profiler to insure proper loading conditions were being maintained during the tests. Load was simultaneously recorded as a function of time on a Honeywell 1508 Visicorder. For those tests where crack growth was monitored, a 30X Gaertner traveling microscope with a digital readout unit was employed.

The four basic spectra investigated are presented in Table 26, and identified as A, A*, B, and B*. Each spectrum is also graphically depicted in Figure 28 with stress as a

- 5 -



All testing was performed in lab air, with a maximum cyclic loading frequency limited to 5 Hz. To minimize lengthy testing periods, after the first test all stresses in each of the four spectra were increased 10 percent, and are hence referred to as 110 percent A, etc. Also, all stresses were based on the net area of the gage section. For the crack initiation studies of the specimens shown in Figure 27, the basic A-Spectrum was employed with one change: the maximum stress at load step 28 was reduced from 100 KSI (689 MPa) to 70 KSI (483 MPa).

The results of the fatigue spectrum testing of double-edge-notched 10 Ni steel specimens are presented in Table 27. With the exception of specimen C-1-3-45D, the resultant total lives obtained for each spectrum are in good agreement. An explanation for the longer life obtained for this particular specimen is presented later in this section.

TABLE 26
GENERAL DYNAMICS FLIGHT BY FLIGHT
FATIGUE TEST SPECTRA

Flight No.	Stress Spectrum A & A*				Frequency Specimen A/A* (Hz)	Stress Spectrum B & B*			
	Max (G)	Min (G)	Cycle Count	Frac. Cycles		Max (G)	Min (G)	Cycle Count	Frac. Cycles
1	0	-8.4	G	G	RAMP	0	-9.5	G	G
2	92.4	55.9	1.01	1.01	6	79.7	48.4	1.01	1.01
3	84.4	55.9	0.1	0.10		71.8	48.4	1.01	1.01
4	64.4	55.9	1.00	2.00		55.6	48.4	1.00	2.00
5	55.9	45.0	1.00	1.00		48.4	39.5	1.00	1.00
6	69.7	61.7	0	2.00		56.7	53.3	0	2.00
7	66.1	39.3	1.00	1.00	180	57.0	39.4	1.00	1.00
8	54.8	48.3	1.00	2.00		47.3	41.7	1.00	2.00
9	45.7	19.0	1.00	1.00		31.9	14.6	1.00	1.00
10	53.6	43.7	1.00	2.00		39.2	31.9	0	2.00
11	43.7	37.2	1.00	2.00		31.9	27.7	0	2.00
12	56.8	31.7	1.00	1.00	6	43.0	22.8	1.00	1.00
13	31.2	12.3	1.00	1.00		22.8	9.5	1.00	1.00
14	42.3	31.2	1.00	53.00		30.1	22.8	0	53.00
15	31.2	26.4	1.00	53.00		22.8	19.3	0	53.00
16	69.2	22.4	1.00	1.00		74.3	27.7	1.00	1.00
17	41.1	23.3	1.00	1.00	60	56.7	38.7	1.00	1.00
18	50.9	42.4	0.10	0.10		70.2	52.3	0.10	0.10
19	48.4	24.6	1.00	1.00		59.8	39.4	1.00	1.00
20	39.7	30.3	0	7.00		48.9	37.5	0	7.00
21	42.7	7.1	1.00	1.00		52.7	8.9	1.00	1.00
22	28.2	15.9	1.00	132.00		34.9	19.6	1.00	132.00
23	25.1	-3.9	1.00	1.00		31.1	-4.7	1.00	1.00
24	17.2	7.4	0	132.00		21.2	9.1	0	132.00
25	57.5	3.3	1.00	1.00		70.9	4.0	1.00	1.00
26	43.5	6.0	9.00	2.00		53.7	7.3	9.00	2.00
27	28.2	12.3	95.0	95.00		34.9	15.2	95.0	95.00
28	108.0	56.1	0.01	0.01	6	86.3	48.4	0.01	0.01
29	90.0	-15.0	0.10	0.10		77.7	12.9	0.10	0.10
30	77.4	56.1	1.00	1.00		66.8	48.4	1.00	1.00
31	0	-8.4	G	G	RAMP	0	-9.5	G	G
32	79.5	53.6	1.00	1.00	6	68.6	46.3	1.00	1.00
33	74.4	43.7	1.00	1.00		54.4	31.9	1.00	1.00
34	56.1	37.5	1.00	1.00		48.4	32.4	1.00	1.00
35	65.0	56.1	1.00	19.0		56.1	48.4	1.00	19.0
36	56.1	50.1	1.00	19.0		48.4	43.2	1.00	19.0
37	83.4	52.0	1.00	1.00	180	72.0	44.9	1.00	1.00
38	71.3	61.0	0	4.00		61.5	52.6	0	4.00
39	72.8	36.5	1.00	1.00		62.8	31.5	1.00	1.00
40	65.8	43.3	9.00	9.00		56.8	37.4	9.00	9.00
41	62.3	46.8	48.0	48.0		53.8	40.4	48.0	48.0
42	57.5	50.1	0	294.0		49.6	43.2	0	294.0

NOTES: ¹Cyclic frequencies applicable to sump tank water tests only. Tests in Lab Air or Dry Air should be run at most convenient frequencies.
²"G" means ramp to minimum stress shown at convenient rate.
³Apply fractional cycles every 10th and 100th flights, respectively.

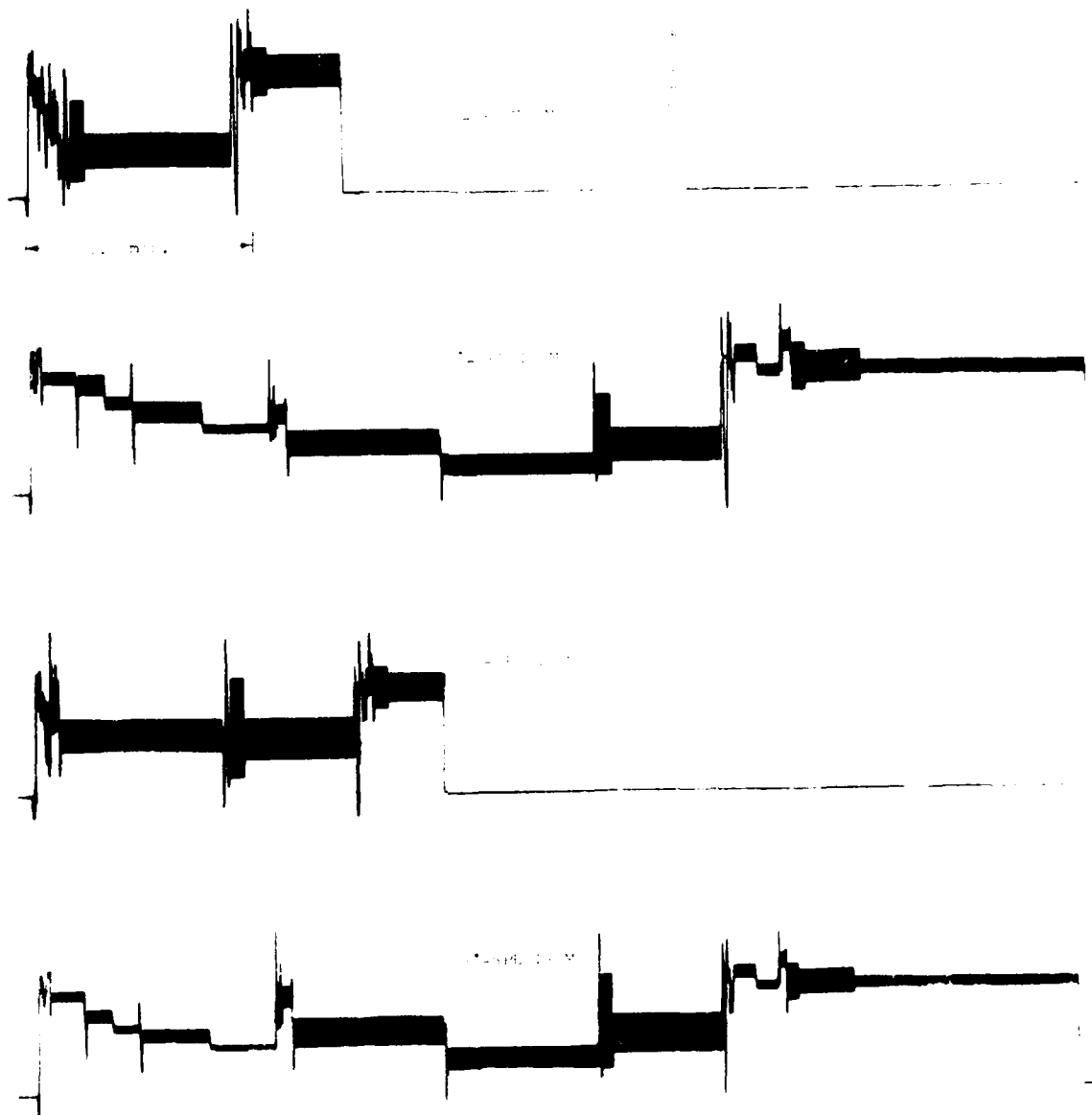


Figure 28. Stress Spectra Graphically Presented.

TABLE 27
FATIGUE SPECTRUM RESULTS ON 10 Ni STEEL,
DOUBLE EDGE-NOTCH SPECIMENS

Specimen I.D.	Stress Spectrum	Total Flights Completed	Flight Number When Crack First Observed
C-1-3-46C	A	1481	<780
C-1-3-44C	110% A	879	N.A.
C-1-3-45C	110% A	867	410
C-1-3-43A	110% A	759	350
C-1-3-44A	110% A (1)	799 (1)	300-500 (2)
C-1-3-45A	110% A	739	254
C-1-3-43B	110% B	594	265
C-1-3-44B	110% B	618	300
C-1-3-45B	110% B	592	275
C-1-3-43D	110% B	527	210
C-1-3-44D	110% B	539	250
C-1-3-45D	110% B	557	340

(1) Actual stresses \approx 107% A due to error in set-up.

(2) Range between no observed crack and large observed crack
[0.075 in. - 1.0 mm].

AD-A085 859

DAYTON UNIV OH RESEARCH INST

F/O 11/4

QUICK REACTION EVALUATION OF MATERIALS FOR SYSTEMS APPLICATIONS--ETC (11)

APR 80 D R ASKINS, R R CERVAY, D L HART

F33615-78-C-5002

UNCLASSIFIED

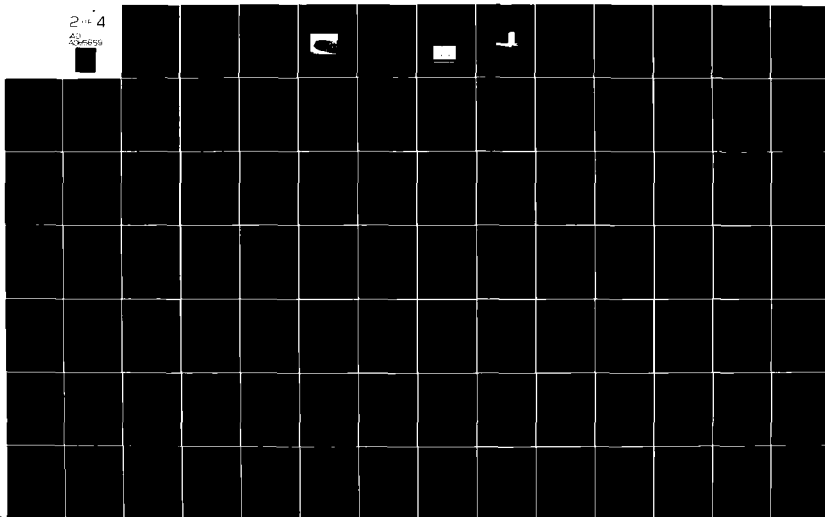
UDR-TR-80-12

AFWAL-TR-80-4025

ML

2 of 4

AD
Address



The results indicate that for a spectrum comparison, the A and A* spectra are less severe than the B and B* spectra. These results were not immediately apparent when first studying the stress spectra (Table 26) since the maximum stresses in spectra A and A* are generally greater than those maximum stresses in B and B* for the same load step. Also, the number of cycles per flight is the same for the A* and B* spectra yet the lives determined for each indicate the B* spectrum is much more severe.

Other interesting results worth noting are the differences in lives obtained between the A and A* spectra and also the B and B* spectra. As explained previously in this section, the "star" spectra are similar to the "non-star" spectra in regards to stress levels, differing only in the number of times each stress level is applied throughout a flight. The A spectrum contains approximately 187 cycles per flight, while the A* spectrum contains over 975 cycles per flight. Although the number of cycles differ greatly, the difference in lives in terms of total flights is not so great, indicating the effect of repetitious load cycles is small. The same observations are made for the B and B* spectra, which contain 314 and 979 cycles per flight, respectively.

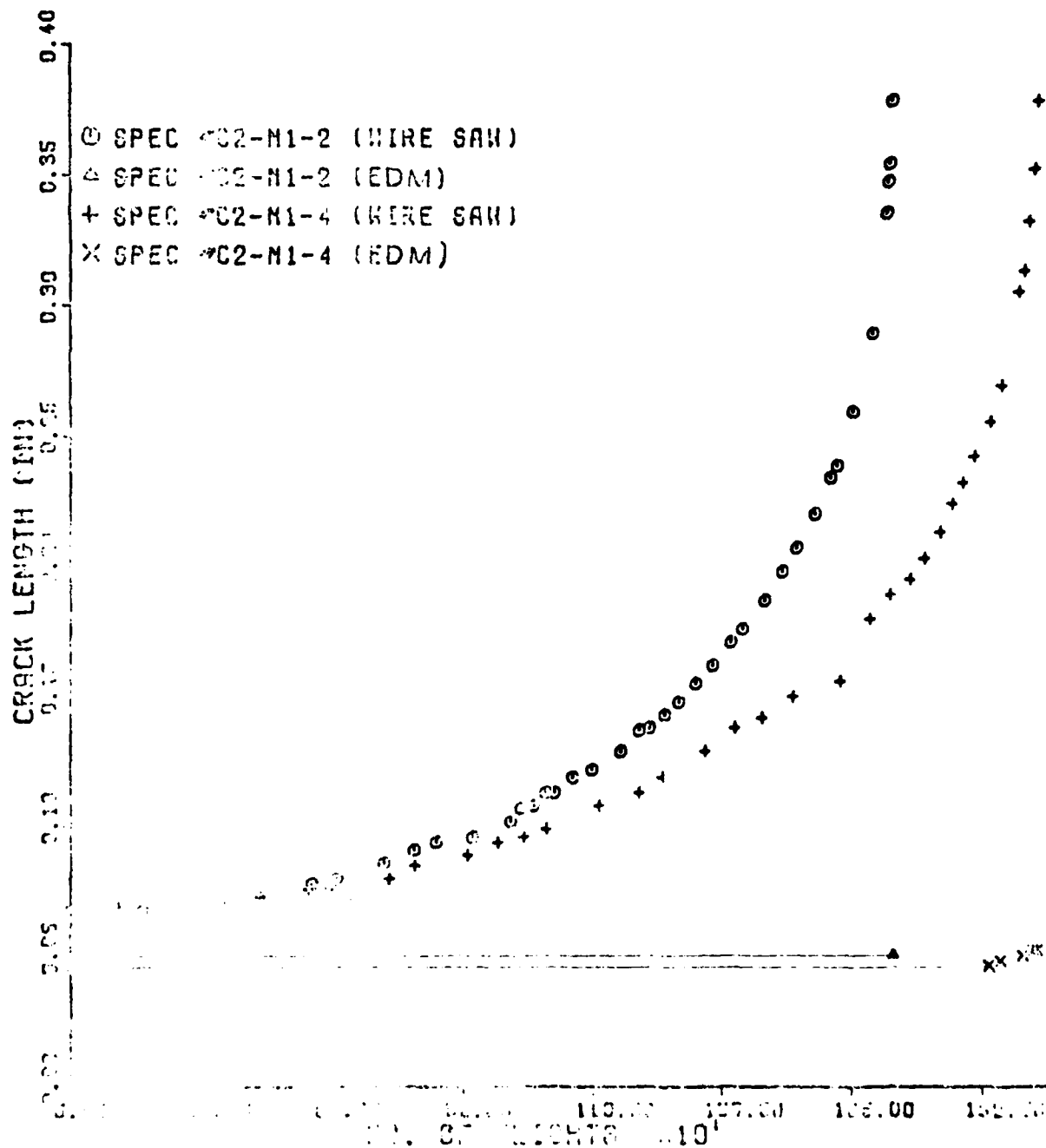
These above mentioned results clearly demonstrate the significant effect of load interaction or retardation on spectrum loading. Many investigators have found that a high load applied to a cracked structure can in many instances increase the life of the structure or, more exactly, retard crack growth. The effect of a high load excursion is often thought of as a "blunting" of the crack tip. Thus, the stress spectrum which contains the greatest magnitude stresses is not necessarily the most severe spectrum. Similarly, the effect of load sequence, i.e., high to low or low to high, can also significantly alter the resultant life of a structure undergoing variable amplitude loading. Repeated stress cycles have little or no effect on a material when following one or more significantly higher stress excursions. This could explain why the life difference between the star and

non-star spectra is not as great as would be expected when a large difference in the number of cycles per flight is compared.

During the course of fatigue testing, the double-edge-notch specimens were periodically examined under low power magnification for first signs of fatigue crack initiation. These results are also presented in Table 27. In all but one of the tests conducted, fatigue cracks [greater than 0.005 inch (0.127 mm)] were first observed at slightly less than half of the total life of the specimen, indicating a crack nucleation period of half-life. Again, the only exception is specimen C-1-3-45D. For this specimen, a fatigue crack did not initiate until well beyond the time for initiation obtained for the two other specimens undergoing the 110 percent B* program. However, the remaining life, i.e., the number of flights to failure after a crack is present, is approximately the same as the other two specimens under 110 percent B* loading, that being about 300 flights. Thus, it appears that the longer life for this specimen is due to the longer crack incubation period. This might be attributed to any number of factors; a slight variation in machining process for this particular specimen could produce such an effect.

The results of the crack initiation study conducted on the two dogbone-shaped specimens with starter notches are presented in Figure 29 as a series of curves of total crack length versus number of completed flights. Crack length measurements were made on the front sides of the specimens only, with the crack lengths measured from the edge of the specimen to the crack tip. The horizontal lines indicate the length of the starter notch only, i.e., no fatigue crack.

The results show that for both specimens, fatigue cracks first initiated at the wire saw notch. This was anticipated since the wire saw notch was longer than the EDM notch. For specimen C-2-M1-2, a 0.010 inch (0.245 mm) fatigue crack was first observed at 508 flights and grew to critical size in 1,738 flights. A 0.004 inch (0.102 mm) fatigue crack was first



observed in specimen C-2-M1-4 at 400 flights before growing to critical size in 2,043 flights. In both cases the fatigue crack grew in a "quarter-circle" shape until reaching the back side, whereupon the crack front changed rapidly to that of an edge crack configuration. A photograph of the fracture face of specimen C-2-M1-4 is presented in Figure 30, illustrating this rapid growth transition through the very distinct and widely spaced fatigue crack striations.

Specimen C-2-M1-4 yielded a fatigue crack from the EDM produced notch only after 1,963 flights or 96 percent of total life. A fatigue crack did not initiate from the EDM produced notch in specimen C-2-M1-2.



Figure 30. Fracture Face of Corner Crack Specimen C-2-M1-4.

1.9 FAILURE ANALYSIS INVESTIGATION OF BOMB LINK ASSEMBLY

A request was made to the Air Force Materials Laboratory to conduct a failure analysis investigation on a component identified as a swivel assembly. The requesting organization,

the Armament and Development Test Center at Eglin Air Force Base, furnished the failed component in question along with identical additional virgin assemblies.

The function of swivel subassembly is to arm the GBU-15 guided bomb upon its release from the aircraft. Arming is accomplished by means of pulling a lanyard which is attached to the swivel assembly. The lanyard pulls a plunger which activates the detonation and guidance systems. Since the force required to pull this plunger is designed to be less than 60 lbf. (276 N), the swivel assembly is designed to withstand a minimum load of 80 lbf. (356 N) but not to exceed 150 lbf. (667 N). After a recent arming failure during a test run at the White Sands Missile Range, two components of the bomb system were suspected of causing the problem: either the plunger assembly failed to pull out at or below its required maximum design load, or the swivel assembly failed below its minimum design load of 80 lbf. (356 N). It was the purpose of this investigation to empirically determine the probable load at which failure of the swivel occurred.

A sketch of the swivel assembly is presented in Figure 31. The head of the swivel eye is designed to shear off upon reaching the design maximum load. The swivel link is supported by the bomb rack, while the swivel eye engages the lanyard which attaches to the plunger assembly. A photo of the swivel assembly under investigation is presented in Figure 32 alongside an unused assembly. Deformation of the failed swivel link is readily observable.

To determine the maximum load sustained by the swivel assembly in question, it was decided to incrementally load a number of virgin test assemblies. At each load increment, the samples were removed from the test machine and measurements made of the permanent deformation. The deformation measurements "L" and "W" (see Figure 31) were obtained via a toolmaker's microscope with 50X magnification. Load was applied by an Instron tensile testing machine using a crosshead speed of approximately 2 in./min.

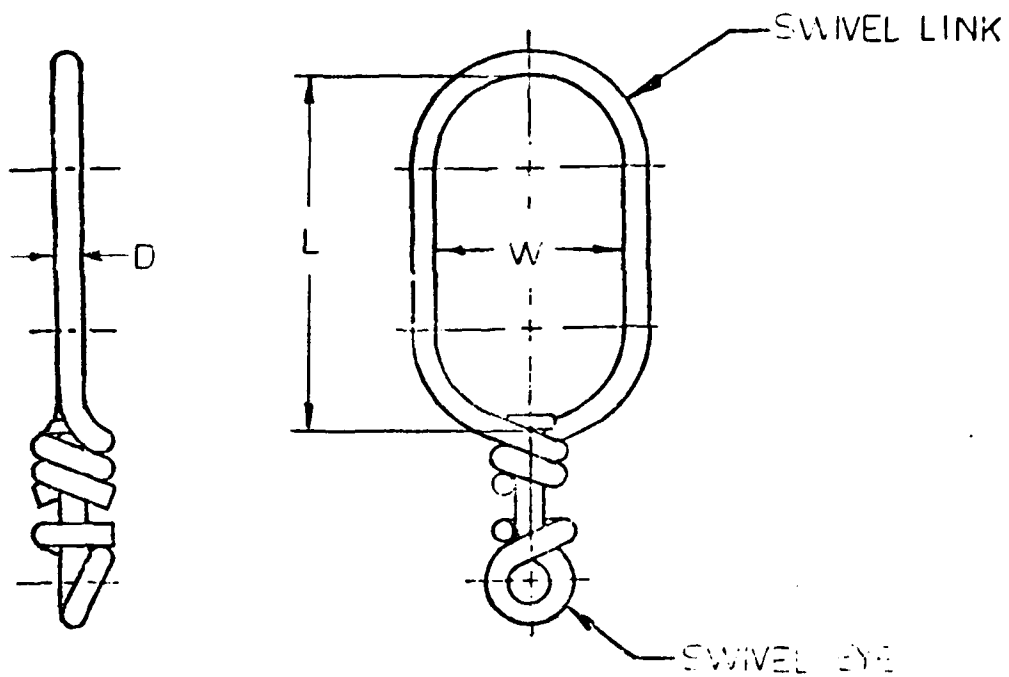


Figure 31. Swivel Assembly.

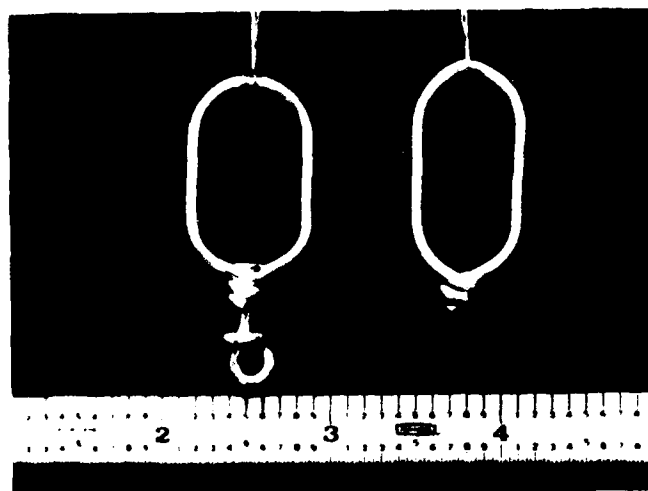


Figure 32. Photograph of Test Swivel Assembly (left) and Failed Swivel Assembly.

(0.85 mm/s). For the six articles tested, measurements were taken at 20 lbf. (89 N) increments until failure occurred.

The assembly which failed in service was attached to the bomb rack by means of a 0.250 inch (6.35 mm) diameter steel ball arrangement butted tightly against a flat plate. To simulate this condition, a fixture was manufactured to support the assembly in the testing machine. A photo of this fixture is presented in Figure 33. For the eye swivel portion, a 0.125 inch (0.031 mm) diameter rod was used to simulate the lanyard.

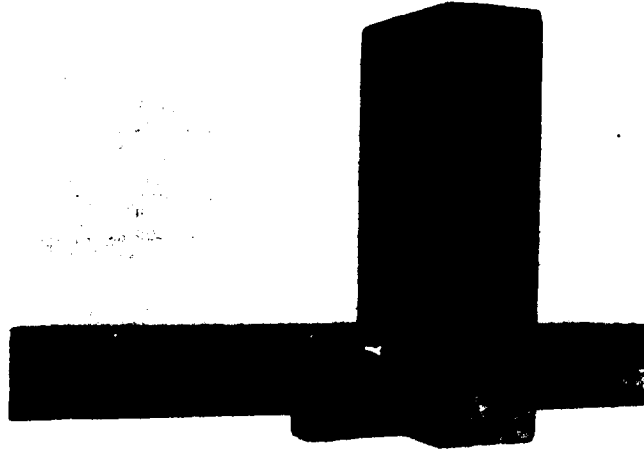


Figure 33. Swivel Assembly Loading Fixture.

The results of the tensile testing are presented in Table 28 with load and corresponding deformation measurements presented for each of the six test assemblies furnished. Also listed, are the deformation measurements taken for the failed assembly in question.

Results show that the test articles reached similar permanent deformation as the failed assembly after 100 lbf (445 N). At 80 lbf. (356 N), the minimum load required of the swivel assembly, permanent deformation of the swivel link was negligible

TABLE 28
RESULTS FOR TENSILE TESTS ON SWIVEL ASSEMBLIES*

<div> <div>FAILED</div> <div>ASSEMBLY</div> <div> L = 1.151 (29.2) W = 0.506 (12.9) D = 0.080 (2.03) </div> </div>							
<div>TEST ASSEMBLIES</div> <div>0 lbf. (0 N.)</div>							
SPEC #	1	2	3	4	5	6	AVG.
L	1.074(27.3)	1.077(27.4)	1.077(27.4)	1.075(27.3)	1.077(27.4)	1.071(27.2)	1.075(27.3)
W	0.597(15.2)	0.605(15.4)	0.605(15.4)	0.600(15.2)	0.600(15.2)	0.600(15.2)	0.599(15.2)
D	0.680(2.03)	0.077(1.96)	0.077(1.96)	0.077(1.96)	0.079(2.01)	0.078(1.93)	0.078(1.95)
40 lbf. (178 N.)							
SPEC #	1	2	3	4	5	6	AVG.
L	1.076(27.3)	1.079(27.4)	1.074(27.3)	1.073(27.2)	1.077(27.4)	1.075(27.3)	1.076(27.3)
W	0.598(15.2)	0.594(15.1)	0.603(15.3)	0.596(15.1)	0.600(15.2)	0.601(15.3)	0.598(15.2)
60 lbf. (267 N.)							
SPEC #	1	2	3	4	5	6	AVG.
L	1.072(27.2)	1.073(27.3)	1.081(27.4)	1.083(27.5)	1.089(27.7)	1.078(27.4)	1.079(27.4)
W	0.594(15.1)	0.591(15.0)	0.598(15.2)	0.597(15.1)	0.595(15.1)	0.597(15.2)	0.595(15.1)
80 lbf. (356 N.)							
SPEC #	1	2	3	4	5	6	AVG.
L	1.087(27.6)	1.097(27.9)	1.097(27.9)	1.098(27.9)	1.098(27.9)	1.094(27.8)	1.096(27.8)
W	0.575(14.6)	0.585(14.4)	0.575(14.6)	0.580(14.7)	0.583(14.8)	0.577(14.6)	0.578(14.6)
100 lbf. (445 N.)							
SPEC #	1	2	3	4	5	6	AVG.
L	1.120(28.4)	1.110(28.2)	1.130(28.7)	1.118(28.4)	1.126(28.6)	1.120(28.4)	1.121(28.5)
W	0.545(13.8)	0.542(13.8)	0.538(13.7)	0.542(13.6)	0.558(14.0)	0.542(13.8)	0.544(13.8)
FAILURE LOADS							
SPEC #	1	2	3	4	5	6	AVG.
Max. Load	1103.4(24.7)	1121.2(25.1)	1121.2(25.1)	1116.4(24.9)	1123.5(25.1)	1121.5(25.0)	1120.4(25.0)
L	1.137(28.8)	1.137(28.8)	1.137(28.8)	1.137(28.8)	1.137(28.8)	1.137(28.8)	1.137(28.8)
W	0.497(12.1)	0.497(12.1)	0.497(12.1)	0.497(12.1)	0.497(12.1)	0.497(12.1)	0.497(12.1)

* All dimensions are in inches (mm).

for all six assemblies tested. All assemblies withstood static loads of 110 lbf. (489 N) or better, well above the minimum requirements. Thus, from the above observations, it would appear that the failed swivel assembly withstood the minimum requirement of 80 lbf. (356 N) before failure, with the failure load being in the vicinity of 110 lbf. (489 N). These results are based on the tacit assumption that the swivel assembly in question was, before use, of similar dimensions to the test samples before testing.

A final important point to consider is the effect of loading rate on the deformation of the assembly. The assembly under actual service conditions experienced a high loading rate as the bomb was jettisoned at about 6 ft/sec. (1.8 m/s). The test articles were loaded three orders of magnitude slower than would be experienced in service. In general, plastic flow, i.e., deformation, is dependent on loading rate; as loading rate increases, deformation decreases. Thus, if the test articles could have been loaded at the same rate the failed assembly experienced it could be expected to withstand a higher failure load and the deformations at each load level would most likely be less. Similarly at lower temperatures [as experienced by an aircraft traveling at 30,000 feet (7,620 m)] plastic flow would likewise be reduced. Therefore, it is likely that the conclusions obtained in this investigation are not only accurate, but are somewhat conservative when the parameters of loading rate and service temperature are taken into consideration.

1.10 MECHANICAL PROPERTY DATA ON CE 9000/7781 E-GLASS COMPOSITE SYSTEM

The use of composite materials in place of their metallic counterparts has long been recognized as a successful approach in greatly reducing the weight and accompanying stresses in a particular component, thereby increasing the overall life and performance of the system. One such example where glass-reinforced

materials are being substituted in place of former metal components is the large supersonic wind tunnel at the Arnold Engineering and Development Center in Tullahoma, Tennessee, where composite compressor blades and blade spacers have either been installed or are in some developmental stage for four of the five compressor stages. The AFML has been supporting this reblading effort by characterizing a number of composite systems either currently being used or intended for use as either blade or spacer material.

One such glass-reinforced epoxy resin system was CE 9000/7781 E-Glass. This material, intended for use as spacer material in the C-1 compressor stage, was supplied to the AFML by the Composite Horizon Company in the form of two panels. Mechanical properties investigated were tensile, flexural, and interlaminar shear at both room and 380°F (193°C) temperatures. Also furnished were adhesively bonded double-lap joint specimens to determine the integrity of the FM-400 adhesive bond as applied to this particular composite system.

The two panels delivered for test were 24 by 24 inches (51 by 51 mm) each of 15 ply, prepreg laminate. A sketch of the specimen layout for each panel is presented in Figure 34. Tensile, three-point flex, and short beam shear specimens were machined from the panels to the test geometries illustrated in Figures 35, 36, and 37, respectively. The first letter of each specimen identification code indicates from which panel (A or B) it was removed. The following letter of the identification code identifies the specimen type (T=tensile, F=flex, R=physical properties), the third (or third and fourth) digit indicates the orientation of the specimen's major axis (0=Warp, 90=Fill), while the final number is the individual sample identification.

Physical property data (specific gravity, fiber content, and resin content) obtained on samples from two locations per panel (see Figure 34) were determined, the results of which are presented in Table 29. The fiber and resin densities listed were supplied by the manufacturer of the prepreg material. Judging from these data, the two panels appear nearly identical with

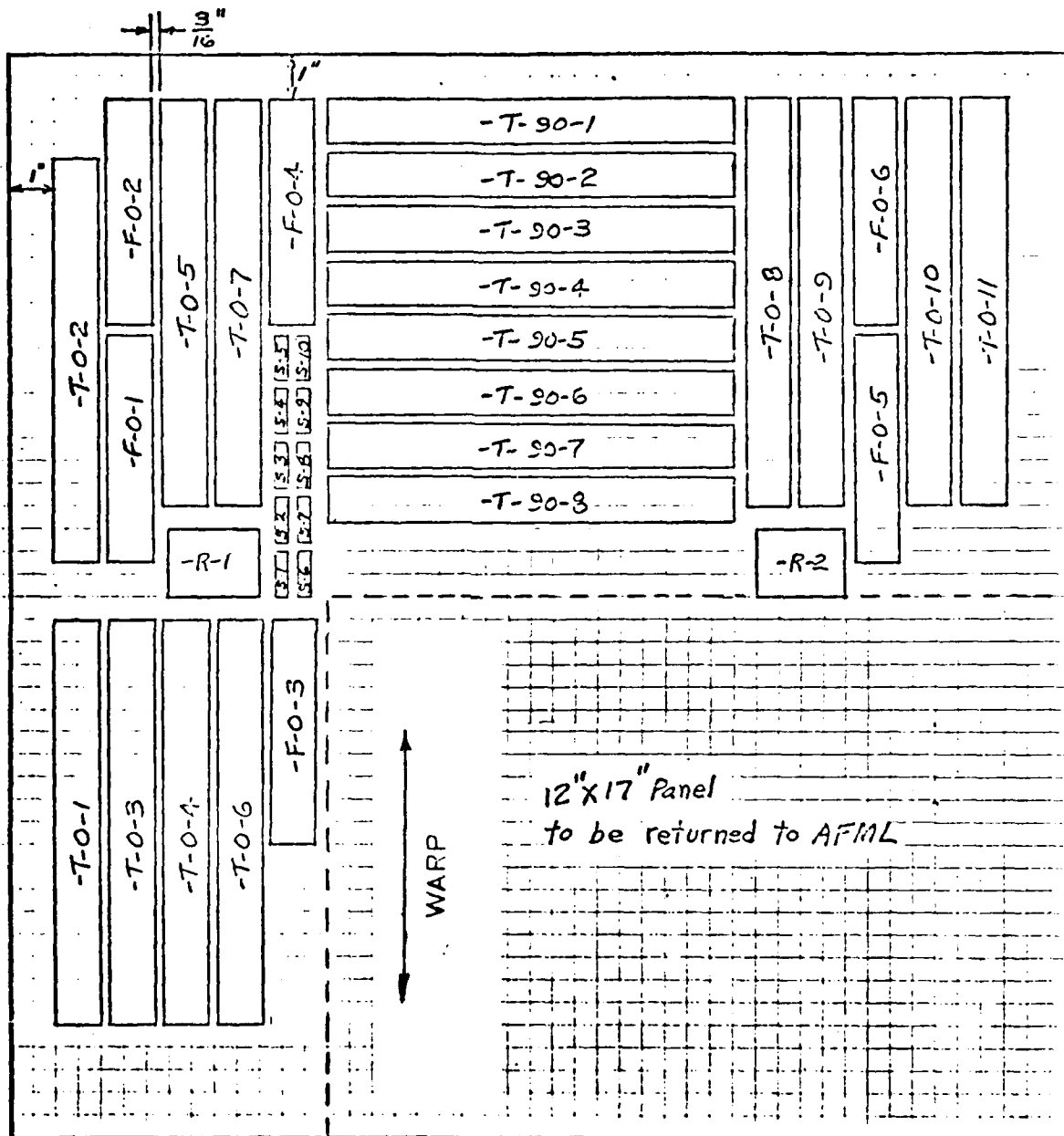


Figure 34. Test Specimen Layouts for Both A and B Panels.

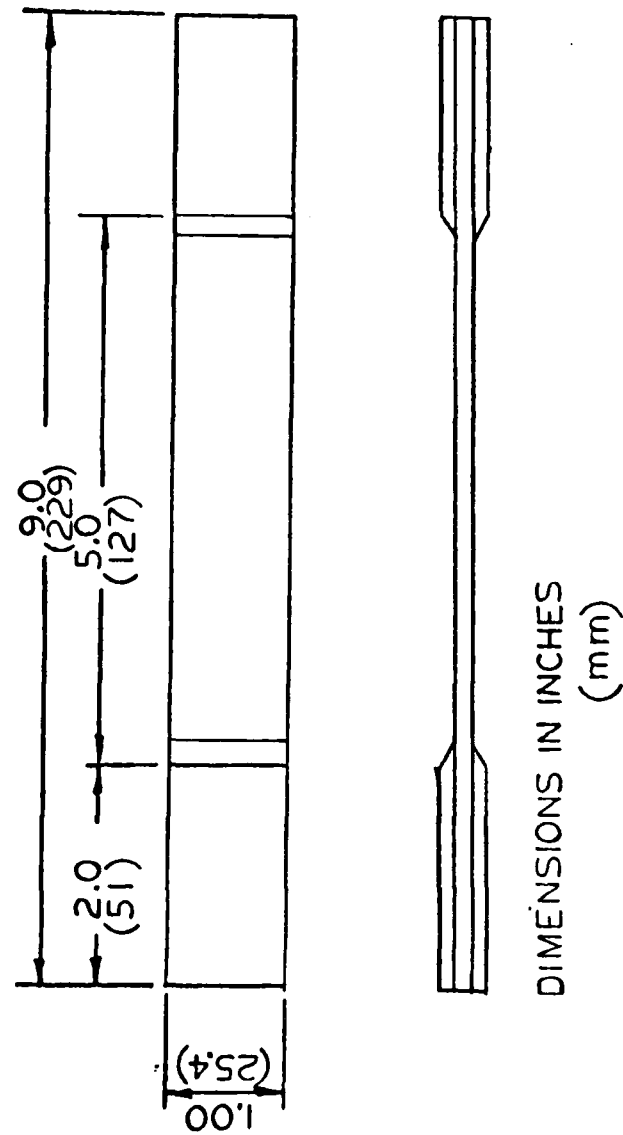


Figure 35. Composite Tensile Specimen Geometry.

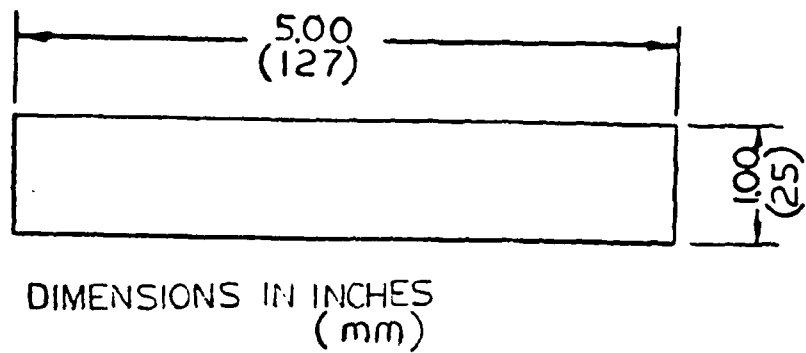


Figure 36. Three-Point Flexural Specimen Geometry.

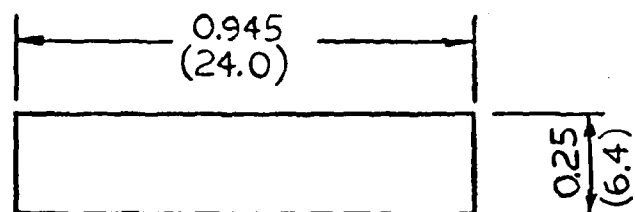


Figure 37. Short Beam Shear Specimen Geometry.

TABLE 29
PHYSICAL PROPERTIES OF GLASS REINFORCED COMPOSITE
SYSTEM CE 9000/7781 E-GLASS, PANELS A AND B

Specimen Number	Specific Gravity	Fiber Density (gm/cc)	Resin Density (gm/cc)	Fiber Content Weight %	Resin Content Weight %	Void Content*
AR-1	1.93			67.55	32.45	0
AR-2	<u>1.93</u>			<u>67.17</u>	<u>32.83</u>	0
Avg.	1.93	2.54	1.25	67.36	32.64	
BR-1	1.92			67.23	32.77	0
BR-2	<u>1.92</u>			<u>67.06</u>	<u>32.94</u>	0
Avg.	1.92	2.54	1.25	67.14	32.86	

* Based on ASTM recommended practice D2734, negative values obtained indicate no void content.

respect to fiber and resin content and specific gravity. Void content measurements and ultrasonic inspections performed on each panel indicated no delaminations or major internal voids present. However, the ultrasonic, as well as later visual examinations, revealed small resin-rich areas on panel A. Consequently, specimen locations were carefully selected from this panel to avoid these resin-rich areas.

In addition to the two panels, ten double-lap shear adhesively-bonded specimens were also furnished. Each bonded lap joint, bonded with FM-400 adhesive, was typically 1 inch (25 mm) wide and 0.5 inch (12.5 mm) long. Because none of these specimens contained any identification they were arbitrarily assigned identification labels #1 through #10.

Tensile testing was carried out following guidelines set forth in the ASTM Standard D3039-76, "Tensile Properties of Oriented Fiber Composites." All testing, including flexural, short beam shear, and double lap shear, was accomplished using

an Instron tensile testing machine equipped with a Conrad Missimer environmental chamber for the elevated temperature test conditions. Crosshead speed was maintained at 0.05 in./min (1.27 mm/min) for all tests, while specimen extension was monitored via an Instron 2 inch (50.8 mm) extensometer.

Flexural testing was conducted in accordance with ASTM Standard D790-71, "Flexural Properties of Plastics and Electrical Insulating Materials," employing a three-point loading method. The loading fixture was set with a span equal to 4 inches (102 mm). Again the crosshead speed was maintained at 0.05 in./min (1.27 mm/min), while crosshead displacement was equated to specimen deflection for flex modulus determination.

Interlaminar shear (short-beam-shear) testing was carried out at both room temperature and 380°F (193°C) using the guidelines described in ASTM Standard D2344-76, "Apparent Horizontal Shear Strength of Reinforced Plastics by Short Beam Method." A span-to-depth ratio was set equal to approximately 5.

The double-lap shear, adhesively bonded specimens were tested in a similar fashion as the tensile specimens, recording only the maximum load specimens were pin loaded to insure accurate alignment. The crosshead rate was again held at 0.05 in./min (1.27 mm/min) for both temperatures investigated.

The results of the tensile tests performed at room temperature and 380°F (193°C) on CE 9000/7781 E-Glass material are presented in Tables 30 and 31, respectively. The results at both test temperatures indicate both test panels to be nearly equal in terms of maximum strength and modulus in both the warp and fill directions of the test panels. The tensile strength in the fill direction is approximately 60 percent that of the warp direction for both panels. However, care must be exercised when interpreting the ultimate strength for each panel, particularly in the warp direction, since the majority of tensile fractures occurred in the tabbed portion of the specimens, resulting from the stress concentration imposed by the gripping

TABLE 30
ROOM TEMPERATURE TENSILE TEST RESULTS FOR
COMPOSITE MATERIAL CE 9000/7781 E-GLASS

Specimen I.D.	Orientation	Max. Stress KSI (MPa)	Modulus MSI (GPa)	Location of Fracture*
AT-0-2	Warp	58.4 (402)	4.1 (28.3)	T
AT-0-4	Warp	58.2 (401)	3.9 (26.9)	T
AT-0-6	Warp	60.5 (417)	4.0 (27.6)	T
AT-0-8	Warp	59.6 (411)	4.1 (28.3)	T
AT-0-10	Warp	<u>60.2 (415)</u>	<u>4.4 (30.3)</u>	T
Avg.		59.4 (409)	4.10 (28.3)	
AT-90-2	Fill	45.8 (316)	3.6 (24.8)	T
AT-90-4	Fill	45.5 (314)	3.6 (24.8)	G
AT-90-6	Fill	45.1 (311)	3.8 (26.2)	G
AT-90-8	Fill	<u>45.5 (314)</u>	<u>3.8 (26.2)</u>	G
Avg.		45.5 (314)	3.70 (25.5)	
BT-0-2	Warp	62.3 (430)	4.5 (31.0)	T
BT-0-4	Warp	60.7 (418)	4.0 (27.6)	T
BT-0-6	Warp	60.4 (416)	4.0 (27.6)	T
BT-0-8	Warp	62.0 (427)	4.0 (27.6)	G
BT-0-10	Warp	<u>60.1 (414)</u>	<u>3.9 (26.9)</u>	T
Avg.		61.1 (421)	4.08 (28.1)	
BT-90-2	Fill	43.6 (301)	3.8 (26.2)	T
BT-90-4	Fill	47.1 (325)	3.6 (24.8)	G
BT-90-6	Fill	45.4 (313)	3.8 (26.2)	G
BT-90-8	Fill	<u>46.5 (321)</u>	<u>3.6 (24.8)</u>	T
Avg.		45.6 (315)	3.70 (25.5)	

* T - indicates failure in tabbed, gripped area.
G - indicates failure in gage section.

TABLE 31
ELEVATED TEMPERATURE [380°F(193°C)] TENSILE
TEST RESULTS FOR COMPOSITE MATERIAL
CE 9000/7781 E-GLASS

Specimen I.D.	Orientation	Max. Stress KSI (MPa)	Modulus MSI (GPa)	Location of Fracture*
AT-0-1	Warp	59.5 (410)	3.5 (24.1)	T
AT-0-3	Warp	60.6 (418)	3.3 (22.8)	T
AT-0-5	Warp	58.0 (400)	3.4 (23.4)	T
AT-0-7	Warp	58.8 (405)	3.3 (22.8)	T
AT-0-9	Warp	<u>59.7 (412)</u>	<u>3.1 (21.4)</u>	T
Avg.		59.3 (409)	3.32 (22.9)	
AT-90-1	Fill	43.9 (303)	2.9 (20.0)	G
AT-90-3	Fill	45.7 (315)	3.0 (20.7)	G
AT-90-5	Fill	45.0 (310)	2.6 (17.9)	G
AT-90-7	Fill	<u>40.8 (281)</u>	<u>2.8 (19.3)</u>	T
Avg.		43.8 (302)	2.82 (19.5)	
BT-0-1	Warp	56.1 (387)	3.1 (21.4)	T
BT-0-3	Warp	57.0 (393)	3.4 (23.4)	T
BT-0-5	Warp	60.8 (419)	3.0 (20.7)	T
BT-0-7	Warp	58.7 (405)	3.2 (22.1)	T
BT-0-9	Warp	<u>60.6 (418)</u>	<u>3.6 (24.8)</u>	G
Avg.		58.6 (404)	3.26 (22.5)	
BT-90-1	Fill	45.0 (310)	2.6 (17.9)	G
BT-90-3	Fill	43.4 (299)	2.6 (17.9)	G
BT-90-5	Fill	41.5 (286)	2.8 (19.3)	T
BT-90-7	Fill	<u>46.5 (321)</u>	<u>3.0 (20.7)</u>	G
Avg.		44.1 (304)	2.75 (19.0)	

* T - indicates failure in tabbed, gripped area.
G - indicates failure in gage section.

apparatus. The actual ultimate strength properties for these panels may be equal to or may exceed those presented in the tables. However, when successful failures (fracture in the gage section) did occur, the associated ultimate strength values achieved were nearly equal to the invalid specimen test results, suggesting the invalid ultimate strength levels reached are quite close to the actual ultimate strength for this material.

The test temperature of 380°F (193°C) had no effect on the maximum load-carrying capability of either panel, although a decrease of approximately 20 percent was observed in the warp modulus, and a 25 percent drop experienced in the fill modulus from their respective room temperature values.

The results of the three-point flexural tests are listed in Table 32 for both room and 380°F (193°C) test temperatures. Room temperature results indicate panel A to be slightly superior in both strength and modulus to panel B; however, at the elevated test temperature, the opposite trend is observed. The flex strength of panel A decreased by 17 percent at 380°F (193°C), while only a 6 percent decrease was observed in panel B. The flexural modulus of each panel is likewise diminished by approximately the same proportions.

The results of the short beam shear tests conducted at both room temperature and 380°F (193°C) are presented in Table 33. For all tests, the span-to-depth ratio employed resulted in an interlaminar shear mode of failure. The average room temperature shear strengths were 7.69 KSI (53.0 MPa) for panel A, and 7.54 KSI (52.0 MPa) for panel B. The test temperature of 380°F (193°C) lowered the maximum interlaminar shear strengths of both panels by roughly 33 percent.

The double-lap shear test specimens, fabricated and supplied by the Composites Horizons Company along with the two test panels, were tested at both room temperature and 380°F (193°C). The adhesive system utilized was FM-400. The results of this effort are presented in Table 34. The average maximum shear strength

TABLE 32
THREE-POINT FLEXURAL TEST RESULTS FOR
CE 9000/7781 E-GLASS MATERIAL,
WARP DIRECTION

Specimen Number	Test Temperature		Flexural Strength		Flexural Modulus	
	°F	(°C)	KSI	(MPa)	MSI	(GPa)
A-F-0-2	70	(21)	85.0	(586)	3.63	(25.0)
A-F-0-4	70	(21)	83.5	(576)	3.72	(25.6)
A-F-0-6	70	(21)	<u>83.9</u>	<u>(578)</u>	<u>3.60</u>	<u>(24.8)</u>
Avg.			84.13	(580)	3.650	(25.2)
B-F-0-2	70	(21)	80.4	(554)	3.61	(24.9)
B-F-0-4	70	(21)	77.0	(531)	3.63	(25.0)
B-F-0-6	70	(21)	<u>80.4</u>	<u>(554)</u>	<u>3.64</u>	<u>(25.1)</u>
Avg.			79.27	(546)	3.627	(25.0)
AF-0-1	380	(193)	68.4	(472)	3.25	(22.4)
AF-0-3	380	(193)	69.3	(478)	3.15	(21.7)
AF-0-5	380	(193)	<u>71.6</u>	<u>(494)</u>	<u>3.23</u>	<u>(22.3)</u>
Avg.			69.77	(481)	3.210	(22.1)
BF-0-1	380	(193)	75.9	(523)	3.48	(24.0)
BF-0-3	380	(193)	76.8	(529)	3.52	(24.3)
BF-0-5	380	(193)	<u>71.0</u>	<u>(489)</u>	<u>3.28</u>	<u>(22.6)</u>
Avg.			74.57	(514)	3.427	(23.6)

TABLE 33
SHORT BEAM SHEAR RESULTS
FOR CE 9000/7781 E-GLASS MATERIAL
WARP DIRECTION

Specimen Number	Test Temperature °F (°C)		Shear Stress KSI (MPa)		Failure Mode
A-2	70	(21)	8.10	(55.8)	Interlaminar Shear ↓
A-4	70	(21)	6.99	(48.2)	
A-6	70	(21)	7.90	(54.5)	
A-8	70	(21)	7.69	(53.0)	
A-10	70	(21)	<u>7.75</u>	<u>(53.4)</u>	
Avg.			7.686	(53.0)	
B-2	70	(21)	7.71	(53.2)	Interlaminar Shear ↓
B-4	70	(21)	7.47	(51.5)	
B-6	70	(21)	7.73	(53.3)	
B-8	70	(21)	7.28	(50.2)	
B-10	70	(21)	<u>7.50</u>	<u>(51.7)</u>	
Avg.			7.538	(52.0)	
A-1	380	(193)	5.27	(36.3)	Interlaminar Shear ↓
A-3	380	(193)	4.82	(33.2)	
A-5	380	(193)	5.19	(35.8)	
A-7	380	(193)	5.30	(36.5)	
A-9	380	(193)	<u>5.28</u>	<u>(36.4)</u>	
Avg.			5.172	(35.7)	
B-1	380	(193)	4.98	(34.3)	Interlaminar Shear ↓
B-3	380	(193)	5.03	(34.7)	
B-5	380	(193)	4.78	(33.0)	
B-7	380	(193)	4.97	(34.3)	
B-9	380	(193)	<u>4.91</u>	<u>(33.8)</u>	
Avg.			4.934	(34.0)	

TABLE 34
 TEST RESULTS ON CE 9000/7781
 DOUBLE-LAP SHEAR SPECIMENS
 BONDED WITH FM-400 ADHESIVE

Specimen I.D.	Test Temperature		Maximum Shear Stress	
	°F	(°C)	KSI	(MPa)
1	70	(21)	2.16	(14.9)
4	70	(21)	2.06	(14.2)
5	70	(21)	---	
6	70	(21)	1.77	(12.2)
8	70	(21)	<u>2.11</u>	<u>(14.5)</u>
Avg.			2.02	(13.9)
2	380	(193)	1.22	(8.4)
3	380	(193)	1.48	(10.2)
7	380	(193)	1.06	(7.3)
9	380	(193)	1.02	(7.0)
10	380	(193)	<u>1.08</u>	<u>(7.4)</u>
Avg.			1.17	(8.1)

was diminished by 42 percent, resulting in 1.17 KSI (8.1 MPa) maximum shear strength. Not surprisingly, all failures occurred at the bonded interface.

The following conclusions are based on the results obtained from two, 15-ply test panels of the CE 9000/7781 E-Glass composite systems, as well as the FM-400 adhesively bonded lap joint specimens furnished along with the panels.

1. The physical properties of each panel, A and B, are equal with regards to specific gravity, fiber content, and resin content. Neither panel contained any significant voids or delaminations.

2. The tensile properties of each panel appear similar. The tensile strength in the fill direction is approximately 60 percent that of the warp direction for both panels.

3. The 380°F (193°C) test temperature had little or no effect on the maximum load-carrying capability of either panel, while a slight loss in modulus was experienced.

4. The maximum flexural strength of panel A at room temperature is approximately 84 KSI (500 MPa) for panel A, and 79 KSI (545 MPa) for panel B. The 380°F (193°C) test environment decreased the flex strength of panel A by 17 percent, and that of panel B only 6 percent.

5. The room temperature interlaminar shear strength of each panel is approximately the same, 7.5 KSI (52 MPa). The 380°F (193°C) test environment reduced each panel's shear strength by one-third.

6. For the adhesively bonded test specimens, the 380°F (193°C) test temperature reduced the maximum load-carrying capability to one-half that of room temperature values.

1.11 LUBRICATION CHARACTERISTICS OF AEROSPACE GREASES ON FASTENERS

One of the standard lubricants used on high-strength threaded fasteners on Air Force systems is graphite grease, MIL-T-5544B. The lubricating characteristics of this grease are good, but concern has been raised over corrosion problems associated with its use. The potential for such problems was voiced over a decade ago and the major contributor to the corrosion was identified as galvanic corrosion with the couple occurring between the graphite and the metallic parts. Because of the corrosion problems, a substitute lubricant has been proposed to replace the graphite grease. However, before such a substitute can be used, its lubricating characteristics must be catalogued.

Throughout the aerospace industry much time and money has been spent empirically developing the torque and tension relationships of high strength fasteners lubricated with MIL-T-5544B. These data are presented in tabular form as stress induced in the fastener versus fastener size, with the empirical torque values filling in the matrix. Designers, manufacturing personnel, and maintenance personnel use these tables. Therefore, before switching from one lubricant to another, one of two sets of data must be developed. The first, and less time-consuming to develop, is a small set of data that shows the proposed substitute lubricant has similar lubricating qualities to a standard lubricant. Then the torque/tension tables for the standard lubricant can be used. The second approach is for lubricants that do not display lubricating properties similar to those of a standard. In this case a complete two-dimensional set of tests must be performed. The two variables are bolt size and stress induced in the bolt. For each size/stress combination a number of tests must be conducted.

This program^[16] was initiated to determine whether Molybdenum-Disulfide (Moly-D) grease could be substituted for graphite grease without developing completely new torque/tension tables. There are data in the literature that indicate there

are similarities in the lubricating characteristics of the two greases. Therefore, a limited data generation program was undertaken to substantiate the data in the literature and to use the data to make a decision whether or not to allow the direct substitution of the Moly-D for the graphite grease without developing new tables.

This test program concerned itself with two fastener sizes, 9/16 inch (14.3 mm) and 5/8 inch (15.9 mm) diameter. All bolts and nuts were new and each bolt/nut pair was kept as a pair throughout the test program. The graphite grease was Graphite-Petrolatum, MIL-T-5544B, which came in a one-pound can and the Moly-D came as a powder defined as Lubricant Grade Molybdenum Disulfide, MIL-M-78665. The Moly-D was mixed with an equal amount by weight of petrolatum to form the grease.

Testing was performed by incrementally torquing the fasteners. Torque increments were 20 percent of the pre-determined maximum torque for each fastener size. At each increment the torquing was stopped and the torque and axial load were recorded. At the maximum torques the loads were allowed to remain on the bolts for approximately three minutes at which time they were unloaded and the unloading torque recorded.

A minimum of five runs were performed at each condition (a run is defined as incrementally torquing to full scale and unloading). Between each run new grease was applied to the bolts, nuts, and washers. Two types of tests were conducted. In one case the load transducer and disk of the test rig was allowed to rotate as the torque was applied (free). All mating surfaces of the rig were polished and lubricated and, in general, rotational slip took place between the mating surfaces of the rig. Under these conditions the interactions between the fastener system and the component being fastened are minimized. In the other tests all components of the test apparatus were pinned together (restrained) and rotational slip took place between the nut/washer/test rig interfaces. These latter tests

are considered to give more realistic values that reflect actual service usage.

Table 35 lists the fasteners, tests and test conditions for this program. The predominance of tests were conducted with the test fixture pinned together (restrained). For four of the bolts, numbers 12, 15, 22, and 25, five test runs were conducted and then the bolts were cleaned in an ultrasonic cleaner and the opposite lubricant applied before retesting. The intent was to ascertain whether any compatibility problems would occur if such a change in lubricant were effected during an overhaul of a system.

Test results comparing the lubricity of the two greases are shown in bar graph format in Figure 38. All of the data represent the average values for the first five runs on the bolt/nut pairs. As indicated in the foregoing, the most significant data are the "restrained" data where the rotational slip took place between either the nut/washer interface or the washer/test rig interface. There are very few component configurations in real hardware where the components being fastened together would be able to allow rotational slip to occur. For the restrained condition, two bolts were used for each condition of bolt size and lubricant. The 9/16 and 5/8 inch (14.3 and 15.9 mm) fasteners with graphite grease exhibited the better lubricity. The average clamp-up force at 100 percent torque for the smaller fasteners with graphite grease was 11 percent higher than the average value for the Moly-D. For the larger fasteners the difference was 16 percent.

When tests were performed under "free" conditions, where rotational slip was allowed to occur between the mating parts of the test rig, the smaller fasteners exhibited similar characteristics irrespective of the lubricant. In the first set of data, bolts 8, 9, and 10, the clamp-up force at 100 and 80 percent maximum torque values for the Moly-D coated fastener fell in between the values for the two graphite coated bolts. For the second set of small diameter "free" tests, bolts 21 and

TABLE 35
TEST CONDITIONS FOR FASTENERS

Bolt No.	Diameter		Identification	Test Condition*	Run Nos.	Lubricant
	in	mm				
8	9/16	14.3	MS21297	Free	1-5	Graphite
9	↓	↓	↓	Free	1-5	Graphite
10	↓	↓	↓	Free	1-5	Moly-D
11	5/8	15.9	EWB22-10-80	Free	1-5	Moly-D
12	↓	↓	↓	Restrained	1-5	Moly-D
	↓	↓	↓	Restrained	6-10	Graphite
13	↓	↓	↓	Restrained	1-5	Moly-D
14	↓	↓	↓	Free	1-5	Graphite
15	↓	↓	↓	Restrained	1-5	Graphite
	↓	↓	↓	Restrained	6-10	Moly-D
16	↓	↓	↓	Restrained	1-5	Graphite
21	9/16	14.3	LWB22-9-70	Free	1-5	Moly-D
22	↓	↓	↓	Restrained	1-5	Moly-D
	↓	↓	↓	Restrained	6-10	Graphite
23	↓	↓	↓	Restrained	1-5	Moly-D
24	↓	↓	↓	Free	1-5	Graphite
25	↓	↓	↓	Restrained	1-5	Graphite
	↓	↓	↓	Restrained	6-10	Moly-D
26	↓	↓	↓	Restrained	1-5	Graphite

* Free: All parts of test rig were lubricated and free to rotate and rotational slip generally took place between mating surfaces of rig.

Restrained: Test rig pinned. Rotational slip forced to occur between nut/washer/test rig interfaces.

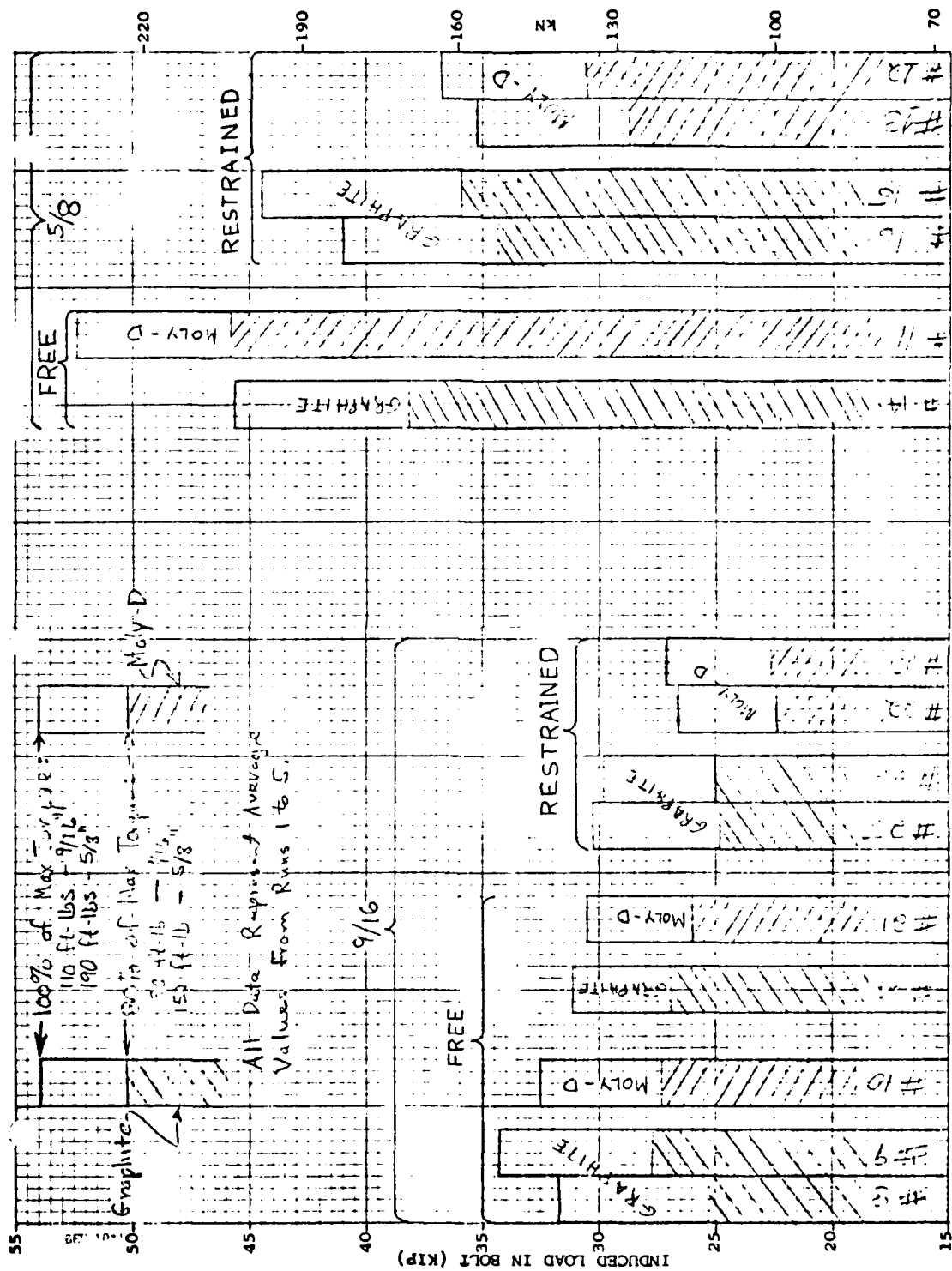


Figure 38. Comparison of Graphite and Moly-D Grease.

24, the difference in clamp-up force at 100 percent maximum torque was less than 2 percent. The "free" condition in all cases resulted in higher load values than the restrained values for a given lubricant, i.e., bolts 8, 9, and 24 versus bolts 25 and 26 for the graphite and bolts 10 and 21 versus bolts 22 and 23 for the Moly-D. This, of course, indicates the nut/washer/component interfaces play an important role in determining the magnitude of the clamp-up force. In all of the restrained tests the washers were new and were kept as part of the nut/bolt pair.

The "free" test results for the large fasteners appear to contradict the results for the small fasteners. However, it was noted during the tests of the graphite lubricated 5/8 inch (15.9 mm) bolt that the components of the test rig did not slip during these runs except during the first incremental loading of the first run and during the last increment of loading during the second run. These results, therefore, more closely parallel those of the "restrained" test results. A comparison of the "free" Moly-D data to the "free" graphite data is not in order. The cause of the lack of turning of the test fixture is not known.

The same trends noted for the smaller fasteners in the free and restrained condition for a given lubricant hold true for the larger bolts. For both the Moly-D and graphite lubricants the free test results were higher than the restrained test results.

Test results for the case where the lubricant was switched after the first five runs are presented in Figure 39. In three of the four cases switching the grease caused an increase in clamp-up force. The Moly-D lubricated 9/16 inch (14.3 mm) fastener showed a slight decrease in clamp-up force. It can be concluded that switching lubricants will not produce an undesirable effect.

1.12 TORQUE/TENSION RELATIONSHIPS FOR HIGH STRENGTH THREADED FASTENERS LUBRICATED WITH GRAPHITE GREASE AND MOLY-D GREASE

In Paragraph 1.11, the lubricating characteristics of two aerospace thread lubricants were discussed. The effort

involved graphite grease and molybdenum disulfide (Moly-D) grease which were applied to high-strength aerospace threaded fasteners. Subsequent to that effort, a requirement developed for similar data for the same lubricants on additional threaded fasteners.[17]

The impetus for both efforts stemmed from the desire to change from the standard graphite grease to the Moly-D which was motivated by concern over corrosion problems caused by the former grease. Before the changeover can be effected, a new torque/tension table must be developed for bolts lubricated with the Moly-D grease. The development of the new torque/tension table was a cooperative effort with General Dynamics, Fort Worth, Texas. General Dynamics developed data for fastener sizes up through 5/8 inch (15.9 mm) to supplement the results obtained by UDRI for 5/8, 3/4, and 7/8 inch (15.9, 19.0, and 22.2 mm, respectively). bolts.

The two lubricants used in this investigation were graphite/petrolatum grease (MIL-T-5544) and molybdenum disulfide/petrolatum grease (MIL-M-7866B). Both lubricants were supplied by General Dynamics and were from the same batches used by that company to develop similar data on smaller fasteners. The greases were produced by mixing the powder (graphite or Moly-D) into an equal weight of petrolatum.

The fastener systems used were supplied by General Dynamics. All of the bolts were MS21297 while the associated nuts were identified as MS21084. The nuts had a dry film lubricant coating and were procured per MIL-N-8984 which does not specify a dry lubricant but does indicate a qualification procedure for the dry film lubricant manufacturer. Two different washers were used on each bolt. The washer under the head of the fastener had a chamfer to allow room for the blending radius at the shank-head interface and the washer under the nut was a conventional flat washer made from stainless steel. Neither the washers nor the bolts had a dry film lubricant on them.

A Lebow Bolt Force Sensor and Lebow Transducer Indicator, interfaced to both a recorder and a digital voltmeter provided

both a permanent record and an instantaneous display of the load. As before, torque was applied by hand using digital torque wrenches that had peak memory.

One basic difference in test procedure between this program and that of Paragraph 1.11 is that torque was applied until a preselected tension was induced in the bolt, while previously, the criteria were based on stopping at specific torque values. Loads, induced by torquing, were incrementally applied to 20, 40, 60, 80, and 100 percent of full scale. At each load the digitized torque and load values (from the torque wrench and voltmeter) were written on the autographic record of load versus time. Each fastener system was loaded (torqued) five times to full scale. Between each run all threads and both surfaces of the washer under the nut were recoated with grease. As with the previous tests, the nuts were turned while the bolt was held stationary relative to the test fixture. The test fixturing was such that rotational slip, excluding that of the threads, was constrained to occur at either the nut/washer interface or the washer/test apparatus interface.

Two bolt/nut/washer sets were used at each test condition. This resulted in ten data points for every combination of load, lubricant, and fastener diameter. Every component of each fastener system was new at the beginning of the testing and all parts were kept together and treated as one test sample.

Graphical presentations of the test results are presented in Figures 40 through 42. The data represent the 60, 80, and 100 percent of full load data. The curves represent a second degree polynomial least squares fit for the individual data points.

It is apparent that the graphite grease possesses superior lubricity. The clamp-up force for a given torque is in all cases higher for the graphite than for the Moly-D. Each data set is sufficiently distinct that there is not an overlap of the data points at any place on the curves.

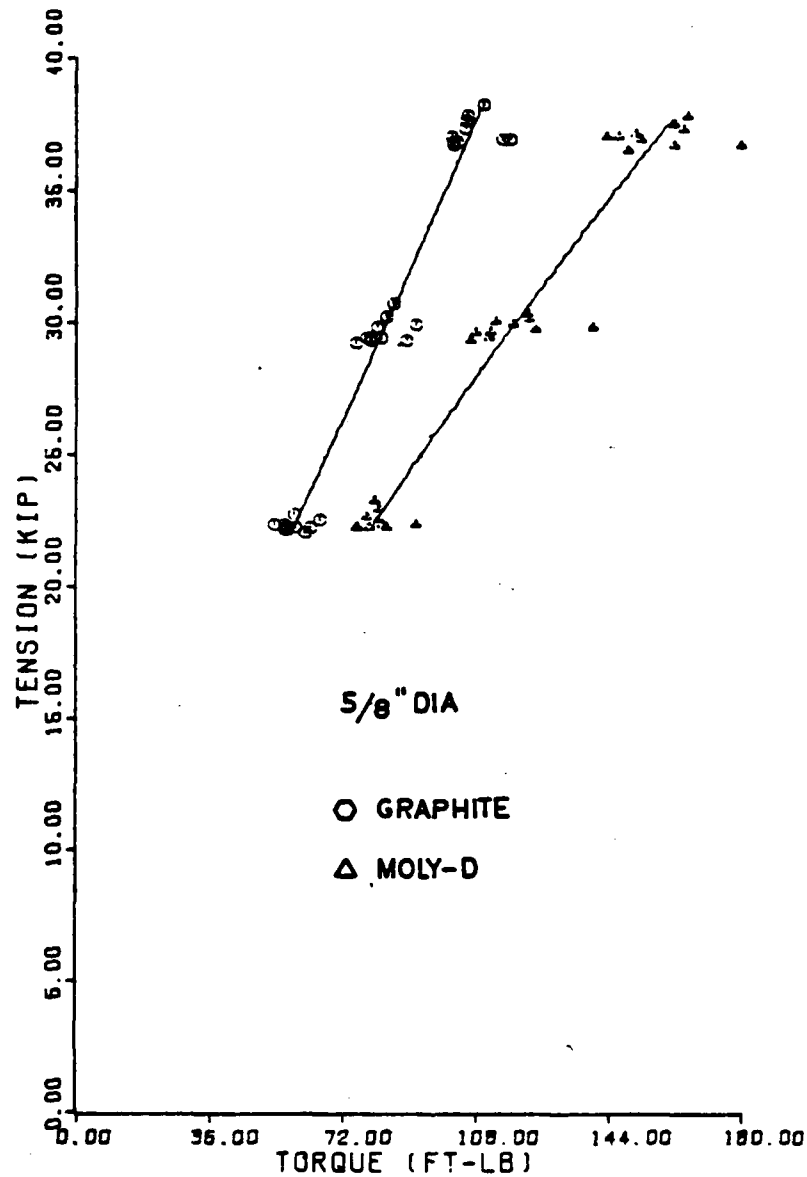


Figure 40. Tension Versus Torque for 5/8 Inch (15.9 mm) Diameter Fasteners With Dry Film Lubricant per MIL-N-8984 on Nuts.

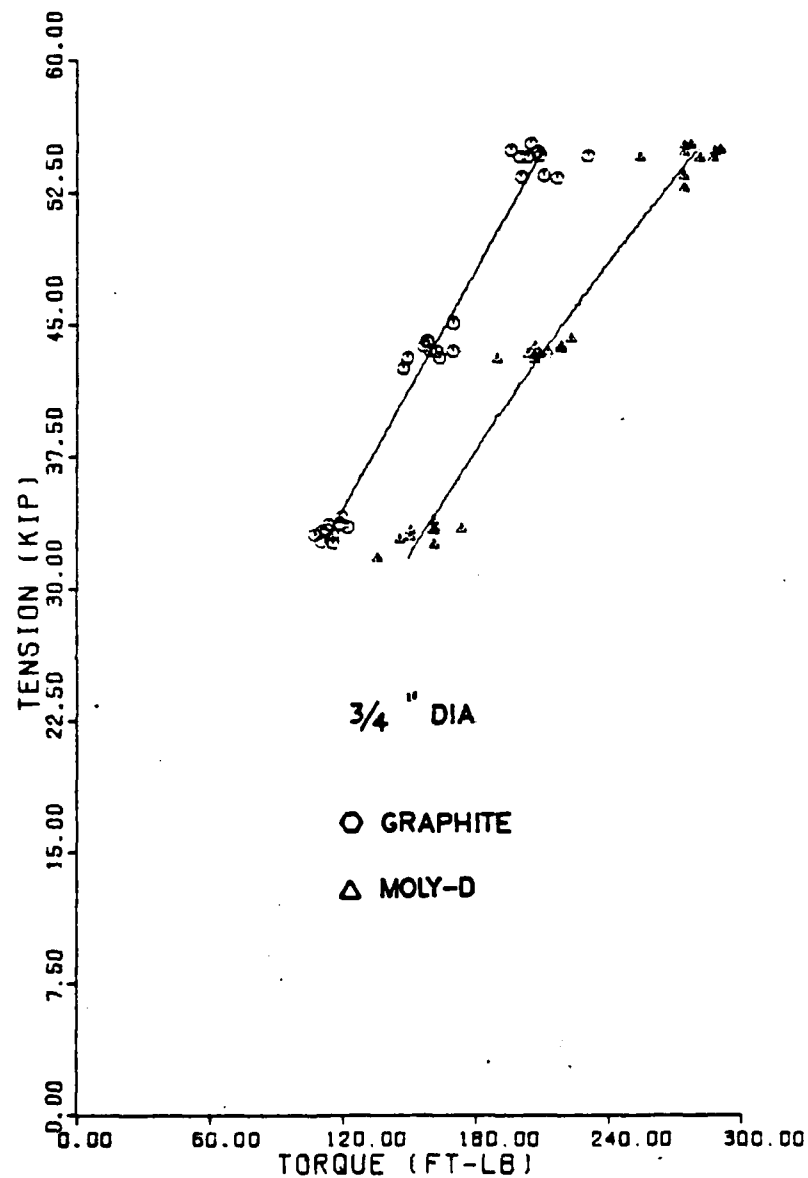


Figure 41. Tension Versus Torque for 3/4 Inch (19.0 mm) Diameter Fasteners with Dry Film Lubricant per MIL-N-8984 on Nuts.

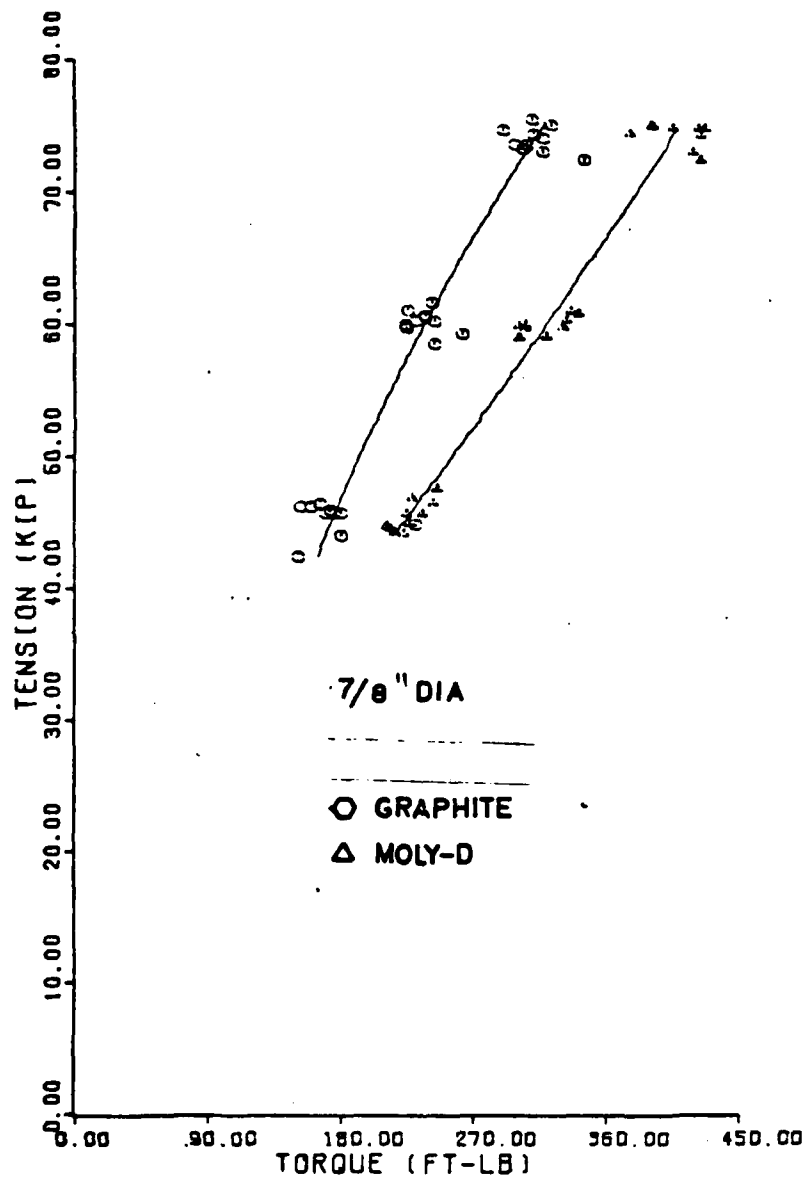


Figure 42. Tension Versus Torque for 7/8 Inch (22.2 mm) Diameter Fasteners with Dry Film Lubricant per MIL-N-8984 on Nuts.

An inspection of the best fit curves reveals that they are both concave and convex. It is apparent that the equations representing the data are only good in the range for which they were developed. Extrapolation outside the range could lead to major errors. This can also be seen from an inspection of the first constant in each equation defining the curves which represents the point where each curve intersect the torque (X) axis. These vary from -121 to 80 ft-lbs (-164 to 108 N-m).

Aside from the distinct difference in the lubricating characteristics of the two greases, there are also differences in the data from that generated for this effort and that presented in Paragraph 1.11. Figure 43 presents the test results for 5/8 inch (15.9 mm) diameter bolts coated with graphite grease. The new data show an advantage for the bolts tested in this study. Although this initially was of concern, it was realized that there is one major difference in the two sets of fastener systems that were tested. The new fastener systems had a dry film lubricant on the nuts whereas the previous fastener systems did not. This, of course, indicates that an advantage in clamp-up force can be realized by use of a dry film lubricant in conjunction with a grease. Although not shown, the same trend is apparent for a similar comparison of the Moly-D data sets with the dry film lubricant in addition to the grease causing an increase in the induced tension in the fasteners.

1.13 COMPARISON OF MANUALLY AND MACHINE DEVELOPED TORQUE/TENSION DATA

Torque versus tension characteristics of high strength threaded fasteners have been documented in Paragraphs 1.12 and 1.13. In both efforts two greases were studied and torquing of the fasteners was done manually using digital torque wrenches. This method of applying torque may be suspect because of the possibility of human variables affecting the results. In addition, during some of the testing reported previously, the

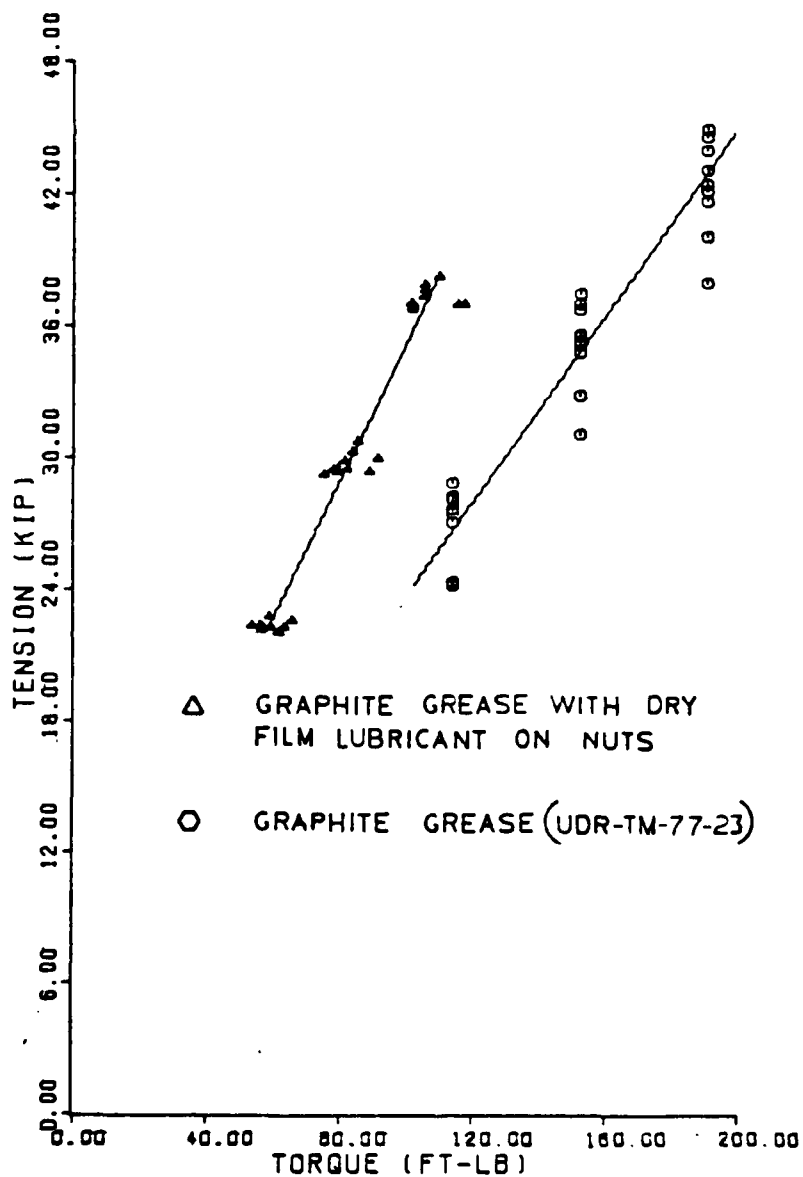


Figure 43. Comparison of Torque/Tension Characteristics for 5/8 Inch (15.9 mm) Diameter Fasteners With and Without Dry Film Lubricant on the Nuts.

operator detected what appeared to be an effect of turning rate of the wrench or twisting rate on the resultant torque.

In order to investigate any variations in the torque/tension relationships caused by torquing by hand as opposed to an automated method, the fastener was tested in a closed loop hydraulic test stand that could apply both torsional and axial loads.[18] Various twisting rates were used and the results were analyzed to determine if any variation in the data could be observed.

The fastener used in this evaluation was a high strength 5/8 inch (15.9 mm) bolt/nut combination that was previously tested. The nut had been supplied with a dry film lubricant on it. The same washers that were used in the previous tests were employed for this study and the lubricant, again the same, was molybdenum disulfide/petrolatum grease. This same fastener system had previously been loaded (torqued) five times to an axial load of 37 KIP (164 KN).

Torquing of the bolt was accomplished using an MTS hydraulic test machine which has both an axial and rotary actuator. The clamp-up force induced in the bolt was measured by a Lebow Force Washer. Torque was monitored by the torque/tension load cell in the MTS frame. The machine was run in rotary displacement control and a ramp rate was programmed into the controller to give a constant rotational rate of degrees per unit time. During the tests the axial actuator was set to load control with a small compressive force [<25 lb (111 N)] set in as a constant.

The test configuration was such that it correlated with the one previously used. The nut was turned relative to the bolt and transducer. This configuration makes rotational slip, excluding that of the threads, occur between the nut/washer interface and/or the washer/test rig interfaces. Between each run all threads and the washer under the nut were relubricated.

Two series of tests were run. In the first a pretorque of 10 ft-lb (13.6 N-m) was applied to the bolt with a torque

wrench before the sample was engaged in the machine grips and torqued under machine control. This procedure was used in order to obtain loads (and torques) that were relatively high on the torque/tension curve. Rotation displacement limitations of the test machine dictated this method. In the second series of tests no pretorque was applied to the fastener. The nut was tightened until a small load was observed and then the nut was backed off until zero load was again obtained. The bolt/nut was then engaged in the grips.

Fifteen runs were performed on the first series of tests with the preload. Three twisting rates were used: 8, 16, and 80 degrees per second. Each rate was tested sequentially, i.e., 8 degrees per second for run numbers 1, 4, 7, etc., 16 degrees per second for run numbers 2, 5, 8, etc., and 80 degrees per second for run numbers 3, 6, 9, etc. This test schedule was used so that any "wearing" of the fastener system would affect the average results in a uniform manner.

Eighteen test runs of the fastener system were performed using the second test condition (no pretorque). Twisting rates were 8, 16, and 32 degrees per second. Again each rate was applied sequentially: 8 degrees per second for runs 1, 4...16; 16 degrees per second for runs 2, 5, etc.

Tabulated results from the first series of tests are presented in Table 36. Torquing and loading rates were calculated at the load value shown in the last column. These values correspond to either: (1) the maximum induced torques and forces in the bolt at the time rotation was stopped; or (2) the last linear portion of the curve. A slight rounding of the very top of the curve existed for those bolts that were tested at 80 degrees per second and the linear portion previous to the rounding was used for calculating the rates. It should be noted that each of the three sets of data in Table 36 do not vary in a systematic manner, either increasing or decreasing, indicating that there was no apparent "wearing" of the fastener.

TABLE 36
TEST RESULTS FOR A 5/8 INCH (15.9 mm) BOLT LUBRICATED
WITH MOLY-D AND TESTED AT CONSTANT
ROTATIONAL RATE

Run No.	Rotation Rate	Torque Rate		Load Rate		Load	
	°/sec	ft-lb/sec	N-m/sec	KIP/sec	KN/sec	KIP	KN
1	8	8.16	11.06	1.89	8.41	29.0	129.0
4	8	7.22	9.79	1.93	8.58	34.7	154.3
7	8	7.66	10.39	2.00	8.90	34.7	154.3
10	8	7.48	10.14	1.98	8.81	34.7	154.3
13	8	7.06	9.57	1.95	8.67	34.6	153.9
2	16	15.0	20.34	3.85	17.12	36.2	161.0
5	16	15.7	21.29	3.80	16.90	34.8	154.8
8	16	15.0	20.34	3.92	17.44	34.7	154.3
11	16	14.9	20.20	3.92	17.44	34.2	152.1
14	16	15.6	21.15	3.90	17.35	34.5	153.4
3	80	76.2	103.33	18.9	84.07	34.0	151.2
6	80	67.1	90.98	20.3	90.29	35.5	157.9
9	80	71.2	96.55	19.0	84.51	32.8	145.9
12	80	73.7	99.94	20.2	89.85	34.3	152.5
15	80	79.2	107.39	19.3	85.85	34.2	152.1

Average values of torque and load rates are shown in Table 37 along with torque per degree rotation and load per degree rotation. The average torque per degree values are very close and the load per degree values are identical (for the significant places shown). The small variation in torque per degree does not change in an increasing or decreasing way with rotation rate which indicates the variation shown is normal data scatter and not the result of some phenomena associated with twisting rate. The conclusion can be drawn that there is no effect of rotation rates on the test data which indicates there is no effect of twisting rate on the resultant torque/tension relationships for fasteners (for the rates tested). Note that the slowest and fastest twisting rates are probably below and above, respectively, those of normal "hand" applied rates.

TABLE 37
AVERAGE VALUES OF TEST RESULTS FOR 5/8 INCH (15.9 mm) BOLT

Rotation Rate	Torque Rate		Torque per Degree Rotation		Load Rate		Load per Degree Rotation	
°/sec	ft-lb/sec	N-M/sec	ft-lb/°	N-M/°	KIP/sec	KN/sec	KIP/°	KN/°
8	7.52	10.20	0.94	1.27	1.95	8.67	0.24	1.08
16	15.24	20.66	0.95	1.29	3.88	17.26	0.24	1.08
80	73.50	99.67	0.92	1.25	19.50	86.74	0.24	1.08

The slowest rate would require approximately 11 seconds for a quarter turn of a nut and the highest would require approximately one second for the same quarter turn.

The test data from the second series of tests, those without pretorque, were evaluated for torque and load values at the point where the twisting was stopped. These data are presented in Figures 44, 45, and 46. The curve in these figures is the best fit curve for the data developed in Paragraph 1.12 on the same bolt/nut/washer/lubricant combination but for "hand" applied torques. In that program torquing was done using digital torque wrenches and the torquing was stopped at specific load values which were 20, 40, 60, 80, and 100 percent of the allowable design load for the particular fastener system. The data from Paragraph 1.12 was analyzed for the 60, 80, and 100 percent load values since the 20 and 40 percent values have no application for the particular high strength fasteners investigated. Since the torque/tension data developed in this evaluation were at the low end of the data presented in Paragraph 1.12, the 40 percent data from the previous effort were combined with the 60 and 80 percent data in order to develop a curve for comparing results from the two programs. The 40, 60, and 80 percent data are shown in Figure 47 along with the least squares fit polynomial. This curve is the same one shown in Figures 44, 45, and 46. All three data sets from the "machine" developed

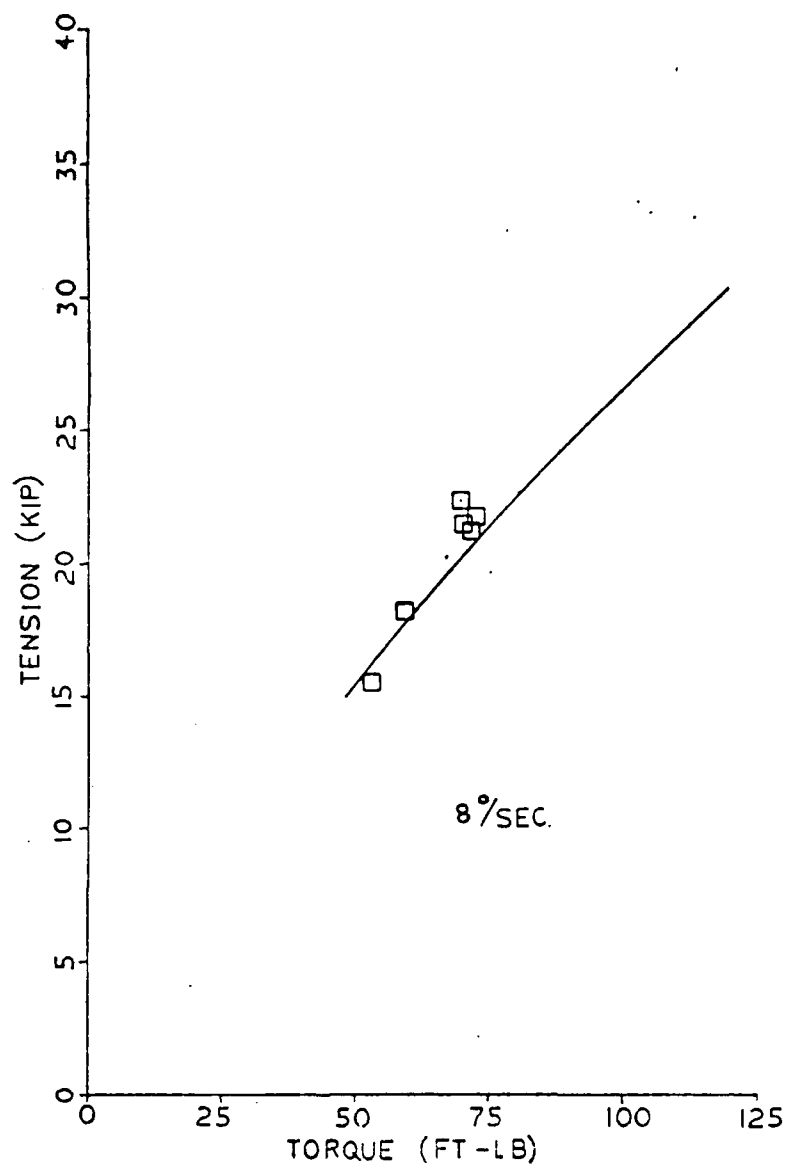


Figure 44. Comparison of Machine Developed (data points) and Manually Developed (solid curve) Torque/Tension Data.

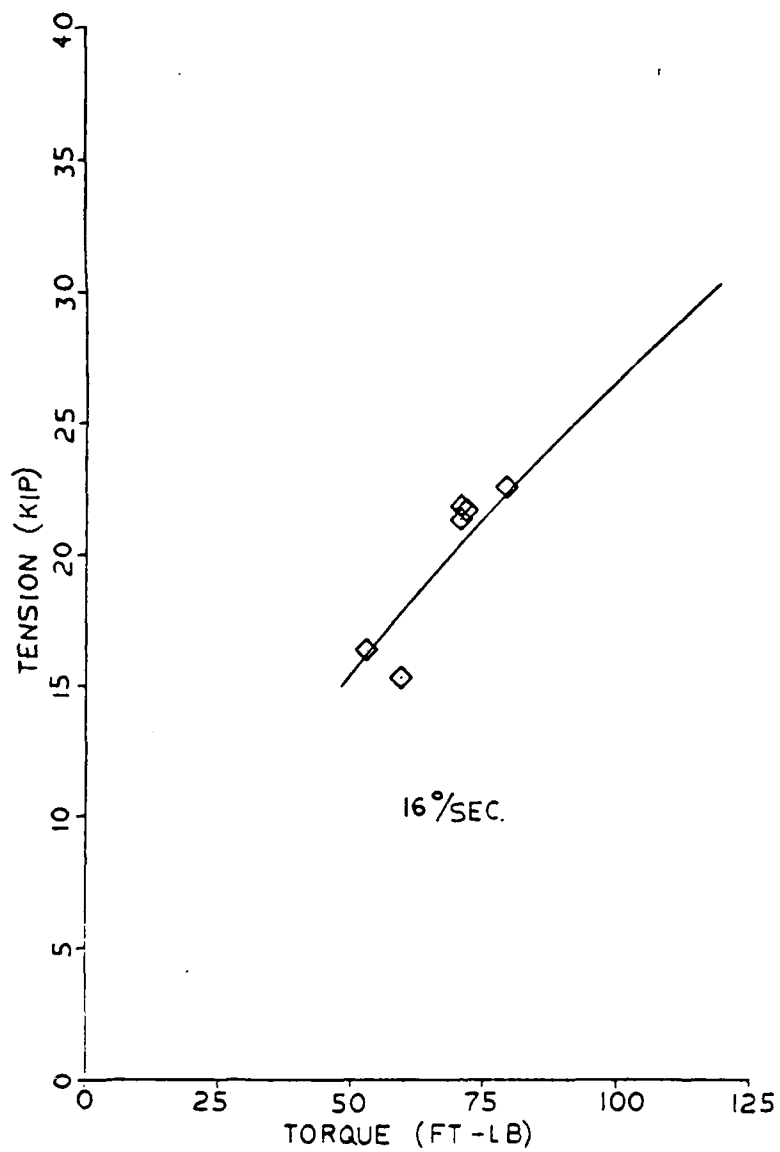


Figure 45. Comparison of Machine Developed (data points) and Manually Developed (solid curve) Torque/Tension Data.

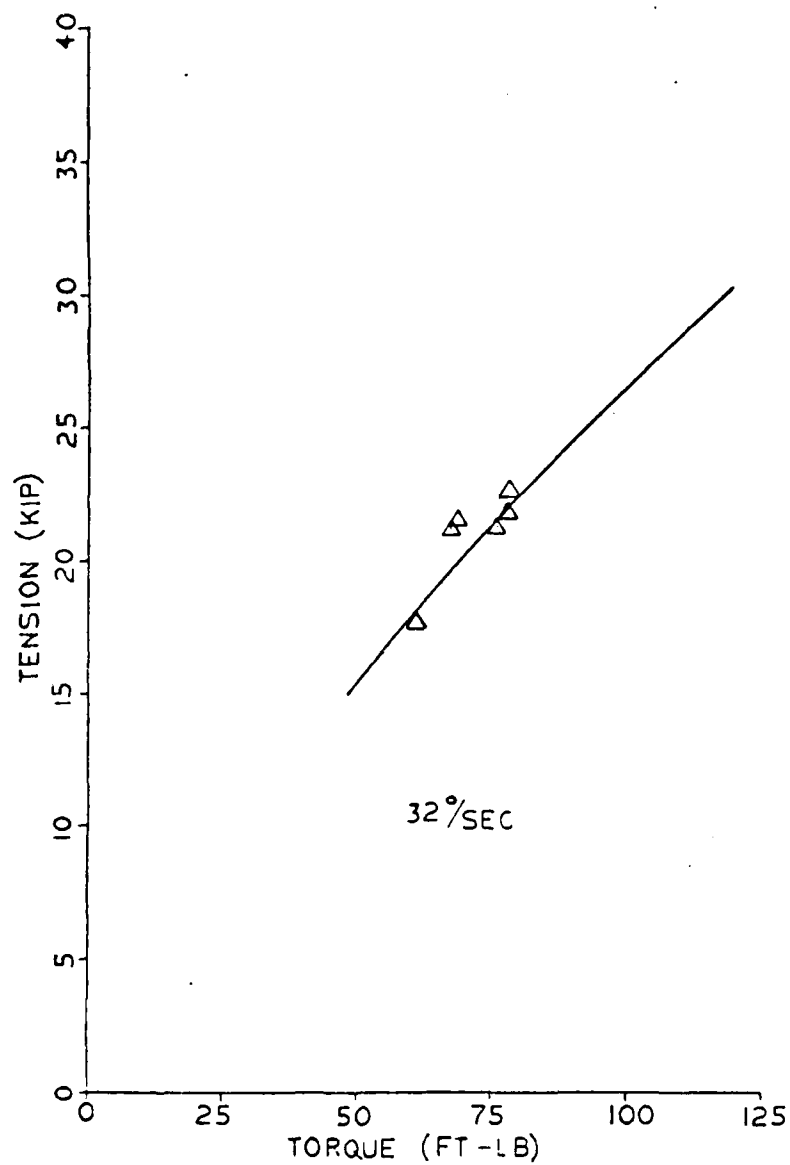


Figure 46. Comparison of Machine Developed (data points) and Manually Developed (solid curve) Torque/Tension Data.

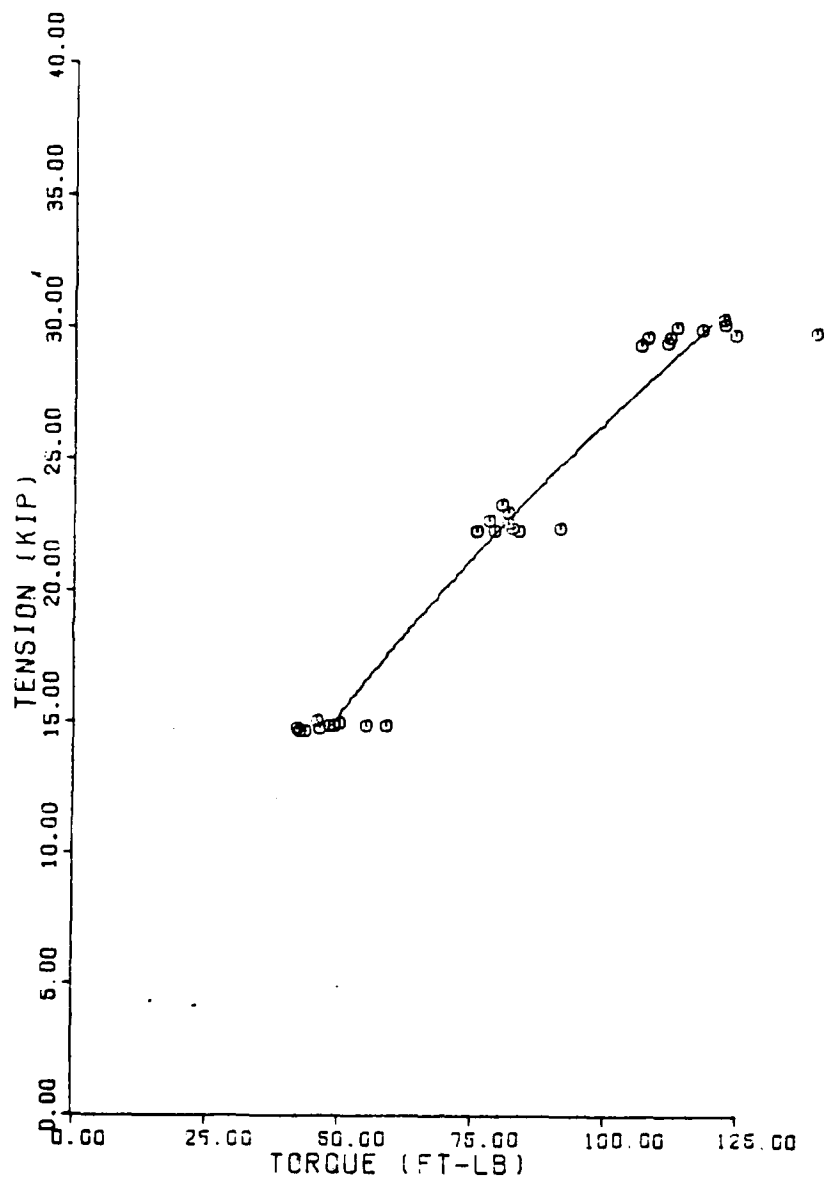


Figure 47. Individual Data Points and Best Fit Curve for Manually Developed Torque/Tension Data for 5/8 Inch (15.9 mm) Bolts Lubricated with Moly-D.

data closely match the "hand" developed best fit curve and the three data sets are all very close. The conclusion can be reached that "machine" generated data and "hand" developed data are the same and that rotational rates do not have any effect on the test results.

An important conclusion can be reached by combining the results from these lubricant evaluations. Two things common to all three programs were 5/8 inch (15.9 mm) diameter fasteners and Moly-D grease. In Paragraph 1.11, the nuts used in the fastener systems were bare prior to application of the lubricant. In Paragraph 1.12, the nuts were supplied and tested with a dry film lubricant on them. This film was left on the nuts and the Moly-D applied over it. Results from the two efforts showed that the dry film lubricant in conjunction with the Moly-D possessed better lubricating characteristics, i.e., high clamp-up force for a given torque. The data indicate the dry film effects will not wear away or diminish after repeated loosening and tightening of the nut. In Paragraph 1.12, the bolt/nut/washer was tested five times to 100 percent design load. In this effort, it was tested 15 times during the tests with pretorque and another 18 times while testing without pretorque for a total of 33 tests. As shown in the figures, the data from the last tests correlate with that from the first five tests indicating that the lubricating effect of the dry film is retained.

1.14 SOME TORQUE/TENSION DATA FOR THREADED FASTENERS

The performance and integrity of structures are often determined by the methodology of design and manufacturing. For systems that use threaded fasteners the performance is many times dependent on characteristics imparted to the system by the fastener. In the case of highly stressed fatigue loaded structures the "life" of the system can be enhanced by the use of interference fit fasteners. Similarly, for some loading conditions and structural configurations, a designer uses the clamp-up force developed by a fastener to impart beneficial

stresses/forces to the components in order to again insure the integrity of the system. In both cases the physical quantity ultimately introduced into the material surrounding the fastener hole is stress, whether permanent (residual) or temporary. For the first case cited, that of interference fit, the stress induced around the hole is inferred from the amount of expansion caused by insertion of an oversized bolt while for the second case, that of stresses caused by clamp-up forces, the stresses are inferred from the torque applied to the bolt/nut. As is quite often true in design and manufacturing, the quantity of interest is not measured but is deduced from some other easily measuring quantity through either analytical or empirical relationships.

Clamp-up force induced in a bolt by tightening the nut is in itself dependent on a number of variables such as the type of lubricant, the pitch of the thread, the torque, surface condition of the parts being fastened together, etc. However, for a given fastener type and size with washers used under the head of the bolt and under the nut, the relationship between torque and induced tension in the bolt then becomes fairly predictable for any one type of lubricant.

Torque/tension relationships for a number of high strength threaded fasteners lubricated with graphite grease and molybdenum disulfide (Moly-D) grease were documented in Paragraphs 1.11, 1.12, and 1.13. As a continuation of that effort, this evaluation^[19] was initiated to develop the same type of data for conditions where: (1) all threads and mating surfaces were bare (unlubricated), and (2) where all threads and mating surfaces had a dry film lubricant on them.

The work detailed employed the same equipment, technique, and fastener systems used in Paragraph 1.12. The only difference was the lubricants (or lack of lubricants). Dry film lubricant, procured per MIL-N-8984, was on the nuts as-supplied by the manufacturer. The stainless steel washers did not initially contain dry film lubricant. Dry film, developed by AFML,

was applied to the washers. The AFML-developed dry film is identified as AFSL-41.

In the work reported in Paragraph 1.12, the fastener systems were torqued until specific load values were reached. At each of the loads, which were 20, 40, 60, 80, and 100 percent of maximum design load for the fasteners, the torquing was stopped for a short period of time before the load was incremented to the next level. For the conditions of this evaluation using either bare fasteners or dry film lubricant, it was not possible or practical to load (torque) the bolts to the higher values because of the excessive torque requirements. Therefore, the data are much more limited. Also, because of the limited number of samples available, only one bolt/nut/washer combination was tested at each of the conditions although each was load cycled five times.

Only one sample from each of the three sizes of bolts was available for these tests. The same bolts were used for both conditions with the dry film lubricant tested first. After the dry film tests the bolts and new bare stainless steel washers and new bare nuts were cleaned in a hot vapor degreaser before the unlubricated condition was tested.

Because of the limited number of data points generated in this effort it was felt it would be impractical to perform a curve fitting routine on the data. Instead, a procedure similar to that employed in Paragraph 1.11 was used in which the raw torque data were linearly interpolated to coincide with the concomitant fixed (target) force values. These resultant values are presented in Tables 38 through 43 and the average and range values are plotted in Figures 48 through 50 along with the results from Paragraph 1.12.

It is apparent from an inspection of the three figures that the test results for the "unlubricated" and "dry film" conditions are significantly inferior to the previous results for the Moly-D and graphite greases. For the two conditions the test results for the unlubricated condition is the most inferior.

TABLE 38
TORQUE/TENSION VALUES FOR 5/8 INCH (15.9 mm) BOLTS
DRY FILM LUBRICANT

Run No.	1		2		3		4		5		Avg.	
	kip	kN	ft-lb	Nm	ft-lb	Nm	ft-lb	Nm	ft-lb	Nm	ft-lb	Nm
7.4	32.9		66.0	89.5	---	---	77.7	105.4	78.7	106.7	76.8	104.1
14.7	65.4		123.5	167.5	138.1	187.3	143.1	194.0	147.9	200.5	141.8	192.3
22.1	98.3		176.8	239.7	192.8	261.4	200.7	272.1	201.1	272.7	196.8	266.9
29.5	131.2		228.3	309.6	242.4	328.7	249.9	338.9	245.8	333.3	243.6	330.3

TABLE 39
TORQUE/TENSION VALUES FOR 3/4 INCH (19.0 mm) BOLTS
DRY FILM LUBRICANT

Run No.	1		2		3		4		5		Avg.	
	kip	kN	ft-lb	Nm	ft-lb	Nm	ft-lb	Nm	ft-lb	Nm	ft-lb	Nm
10.8	48.0		109.9	149.0	---	---	139.7	189.4	144.9	196.5	140.0	189.8
21.6	96.1		228.0	309.2	249.9	338.9	261.0	353.9	255.3	346.2	262.2	355.5
32.4	144.1		349.3	473.6	358.1	485.6	369.4	500.9	373.2	506.1	376.6	510.7

TABLE 40
TORQUE/TENSION VALUES FOR 7/8 INCH (22.2 mm) BOLTS
DRY FILM LUBRICANT

Run No.	1		2		3		4		5		Avg.	
	kip	kN	ft-lb	Nm	ft-lb	Nm	ft-lb	Nm	ft-lb	Nm	ft-lb	Nm
14.7	65.4	221.0	299.7	288.1	205.6	278.8	201.0	272.5	189.8	257.4	206.0	279.3
29.5	131.2	405.5	549.8	373.5	354.2	480.3	335.0	454.3	325.0	440.7	358.6	486.3

TABLE 41
TORQUE/TENSION VALUES FOR 5/8 INCH (15.9 mm) BOLTS
NO LUBRICANT

Run No.	1		2		3		4		5		Avg.	
	kip	kN	ft-lb	Nm	ft-lb	Nm	ft-lb	Nm	ft-lb	Nm	ft-lb	Nm
7.4	32.9	103.2	139.9	189.2	151.8	205.8	149.0	202.0	162.8	220.7	141.3	191.6
14.7	65.4	210.0	284.8	369.8	294.0	398.7	266.6	361.5	337.9	458.2	276.2	374.5

TABLE 42
TORQUE/TENSION VALUES FOR 3/4 INCH (19.0 mm) BOLTS
NO LUBRICANT

Run No.	1		2		3		4		5		Avg.	
	kip	Load kN	ft-lb	Nm	ft-lb	Nm	ft-lb	Nm	ft-lb	Nm	ft-lb	Nm
10.8	48.0	177.9	241.2	206.4	279.9	290.3	208.8	283.1	213.2	289.1	204.1	276.7
21.6	96.1	357.7	485.0	403.4	547.0	574.8	415.6	563.5	425.3	576.7	405.2	549.4

TABLE 43
TORQUE/TENSION VALUES FOR 7/8 INCH (22.2 mm) BOLTS
NO LUBRICANT

Run No.	1		2		3		4		5		Avg.	
	kip	Load kN	ft-lb	Nm	ft-lb	Nm	ft-lb	Nm	ft-lb	Nm	ft-lb	Nm
14.7	65.4	246.9	334.8	337.7	457.9	500.1	424.7	575.9	432.1	585.9	361.9	490.7
29.5	131.2	515.3	698.7	---	---	995.3	850.2	1152.9	---	---	699.8	948.9

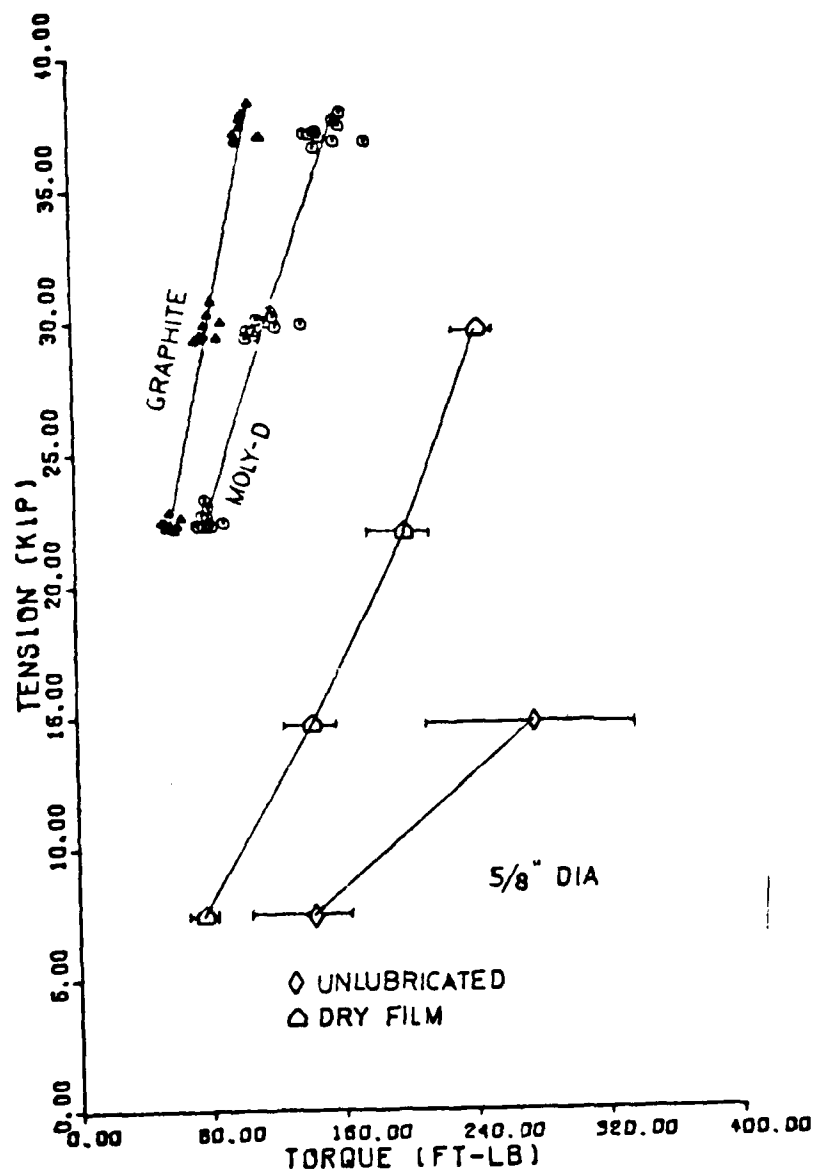


Figure 48. Torque/Tension Results for 5/8 Inch (15.9 mm) Bolts.

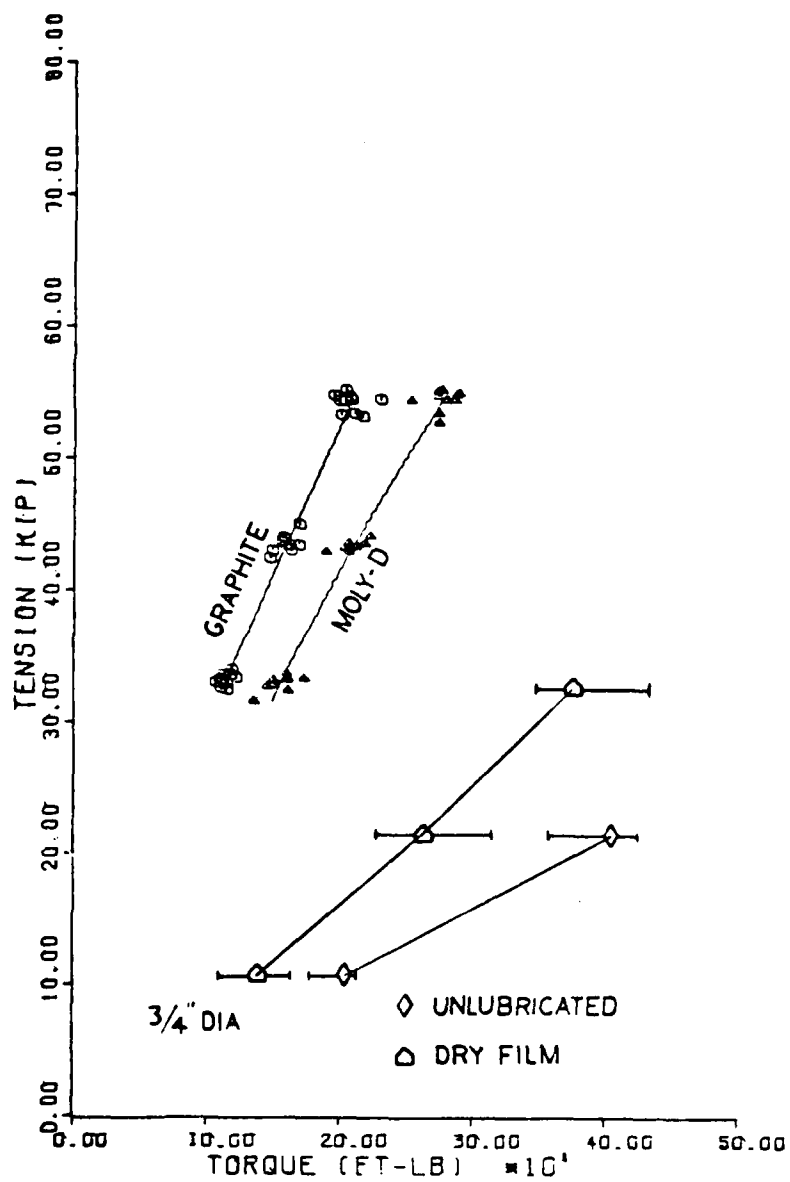


Figure 49. Torque/Tension Results for 3/4 Inch (19.0 mm) Bolts.

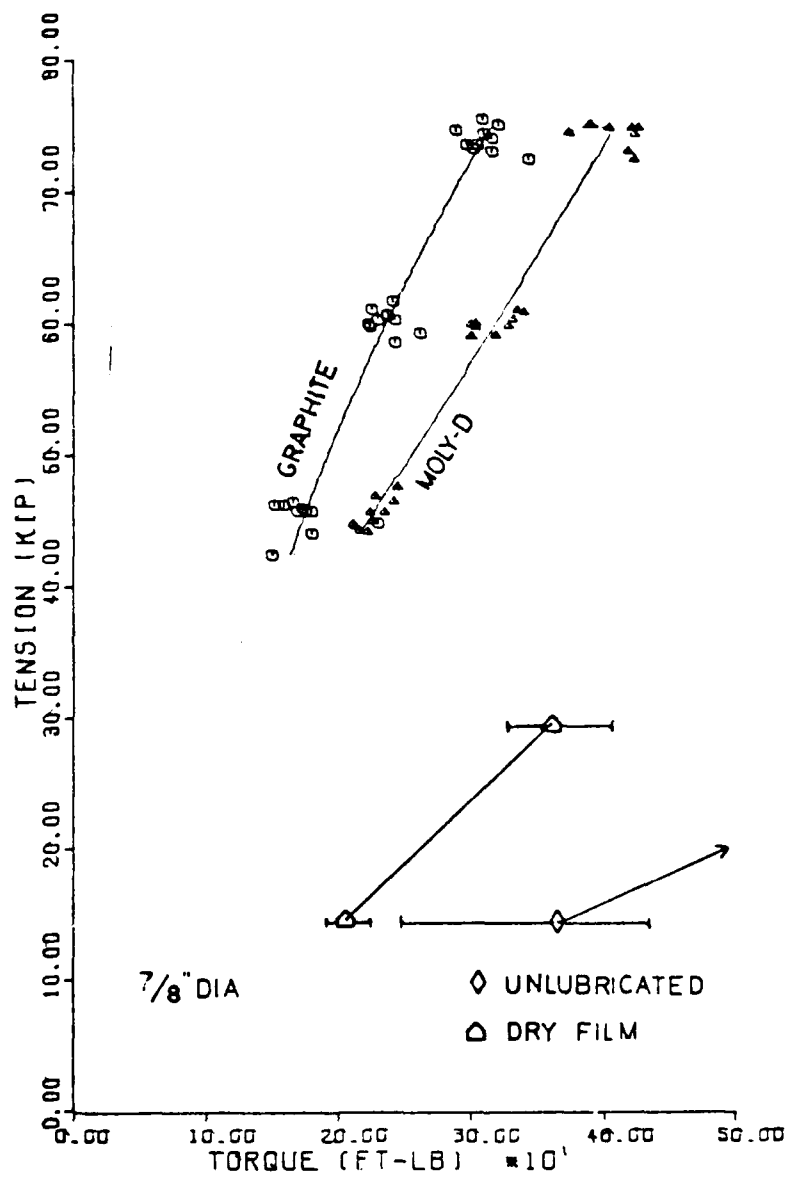


Figure 50. Torque/Tension Results for 7/8 Inch (22.2 mm) Bolts.

1.15 DETERMINATION OF TEST TECHNIQUE ON K_{ISCC} VALUES FOR ALUMINUM 7075-T651 IN A 3.5 PERCENT NaCl ENVIRONMENT

Corrosion is a problem that all materials are plagued with if placed in the proper environment. Gold, for example, a seemingly insensitive material under most conditions, will corrode rapidly when placed in a mercury environment, while iron begins to corrode or "rust" immediately upon exposure to a typical air atmosphere. Many materials, when exposed to the joint interaction of a tensile stress and a corrosive medium, undergo the phenomenon of stress corrosion cracking. For aircraft operating in a seacoast atmosphere, stress corrosion cracking has been found to significantly reduce the service life of many structural components. Examples of corrosion cracking problems experienced in aircraft have historically been associated with such components as landing gear where sustained loading and continuous environmental exposure have been known to produce catastrophic failures on quiescent aircraft. Because of the ever-increasing usage of new materials in the aerospace industry, it is necessary to thoroughly document these materials' susceptibility to stress corrosion cracking.

The use of linear-elastic fracture mechanics principles to categorize materials as to sensitivity to corrosion cracking has met with considerable success and is reported extensively in recent technical literature. These concepts have involved stressing a precracked specimen in some environment and determining a threshold stress intensity value, K_{ISCC} , below which stress corrosion cracking will not occur. Since there exists no standard test method yet which employs these fracture mechanics principles, specimen configuration and test methods vary for each laboratory. The American Society for Testing and Materials Committee on Fracture Testing, Subcommittee on Subcritical Crack Growth (ASTM-E24-04), has recently conducted a test program on 4340 steel investigating both the specimen geometry and test technique influence on the value of K_{ISCC} (results unpublished at this time). The purpose of this program was to

similarly study stress corrosion cracking testing methodology but for a different material and different testing conditions.

The material employed in this investigation was aluminum alloy 7075.[20] A T651 heat treatment was used because of its relatively high susceptibility to stress corrosion cracking. Two variations of loading an ASTM standard 3/4-inch (19 mm) compact type (CT) specimen were examined: a constant load, increasing stress intensity technique which models real life situations for most cases, and a constant displacement, decreasing stress intensity technique, achieved by wedging open a precracked CT specimen by means of properly torquing a bolt in one arm of the specimen. For both techniques a continuous exposure in a 3.5 percent by weight sodium chloride solution was employed.

Fracture toughness testing was accomplished with a Baldwin-Weidemann testing machine following guidelines set forth in ASTM Standard E399, Plane Strain Fracture Toughness on Metallic Materials. Fatigue precracking was performed on an MTS closed-loop, electrohydraulic fatigue testing machine. All specimens were precracked to a crack-length-to-specimen-width ratio (a/W) of approximately 0.5. Final maximum stress intensity used during precracking operations was limited to $6.5 \text{ KSI}\sqrt{\text{in}}$ ($7.4 \text{ MPa}\sqrt{\text{m}}$) to avoid any retardation effects on the stress corrosion testing.

The test solution employed for the stress corrosion testing was a 3.5 percent by weight sodium chloride (NaCl) solution with an initial pH reading of approximately 6.5. The two methods of loading investigated in this program are outlined in the following paragraphs.

Precracked compact type specimens were loaded via a clevis and pin-type arrangement in a vertical loading Satec stress-rupture testing machine which applied load to the specimen with dead weights acting through a lever arm. Clevises and pins were machined from aluminum to minimize any galvanic coupling effects. An environmental chamber was fashioned from a one-gallon plastic container which enclosed the specimen. The specimen was then

completely submerged in the test solution and the test load applied. Lab air was bubbled through the solution for the duration of the test to prevent any solute from precipitating out, as well as to supply oxygen to the corrosive medium. Periodically distilled water was added to replenish the water lost to evaporation. After 1,000 hours of test the entire solution was drained out and a fresh solution added.

Upon failure, defined as complete separation of the specimen, the specimens were removed and the initial stress-intensity recorded along with time to failure. If no failure was experienced after 2,000 hours, the test was terminated, the specimen broken apart, the fracture face examined for crack growth, and the initial stress intensity accurately determined.

The constant displacement or bolt-loaded test method employs a bolt of the same material as the test specimen (again to avoid galvanic corrosion effects) to apply an initial stress intensity. After initial stressing the specimens were submerged in the test environment for a 2,000-hour test duration. Upon completion of the exposure period the specimen was removed and the final stress intensity, after crack extension, was computed. Since this is a crack arrest method, the final stress intensity computed is the assumed threshold value for stress corrosion cracking.

Before the specimens were preloaded the necessary compliance data were obtained. A fatigue crack was grown to various lengths and at each length a trace of specimen crack opening displacement (COD) versus load was obtained. Typical traces of COD versus load obtained from a single specimen are presented in Figure 51. The data derived in this manner were then rearranged in the form of a series of curves as illustrated in Figure 52. Utilizing this compliance data, an initial stress intensity was applied by wedging open the crack with the bolt.

Precracked compact type specimens with a standard clip-on gage in place were initially loaded to stress intensities equal

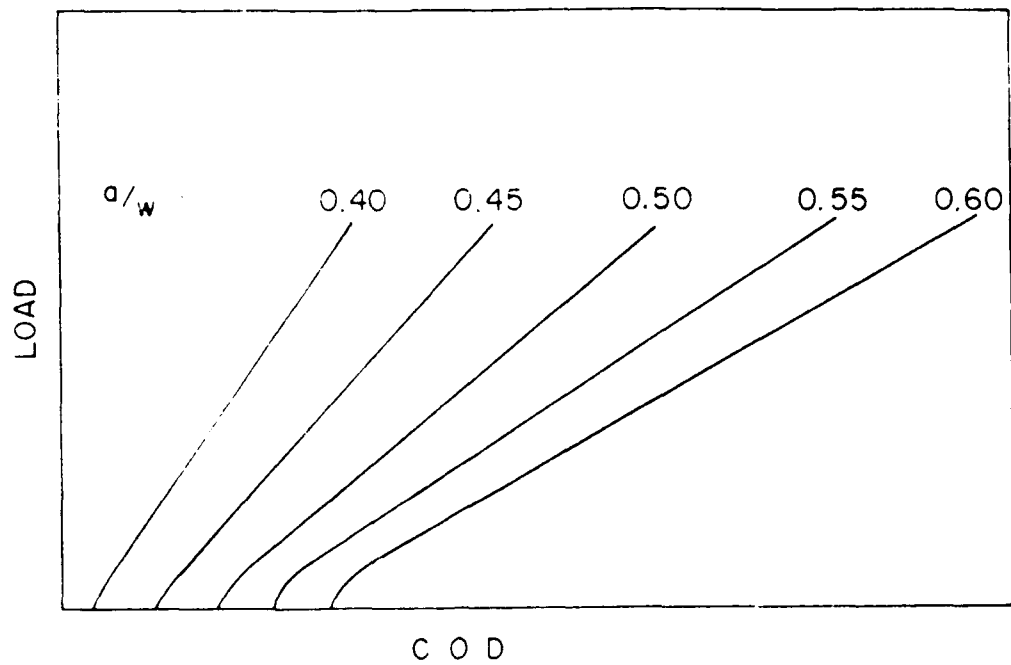


Figure 51. Typical Load Versus Crack Opening Displacement Traces.

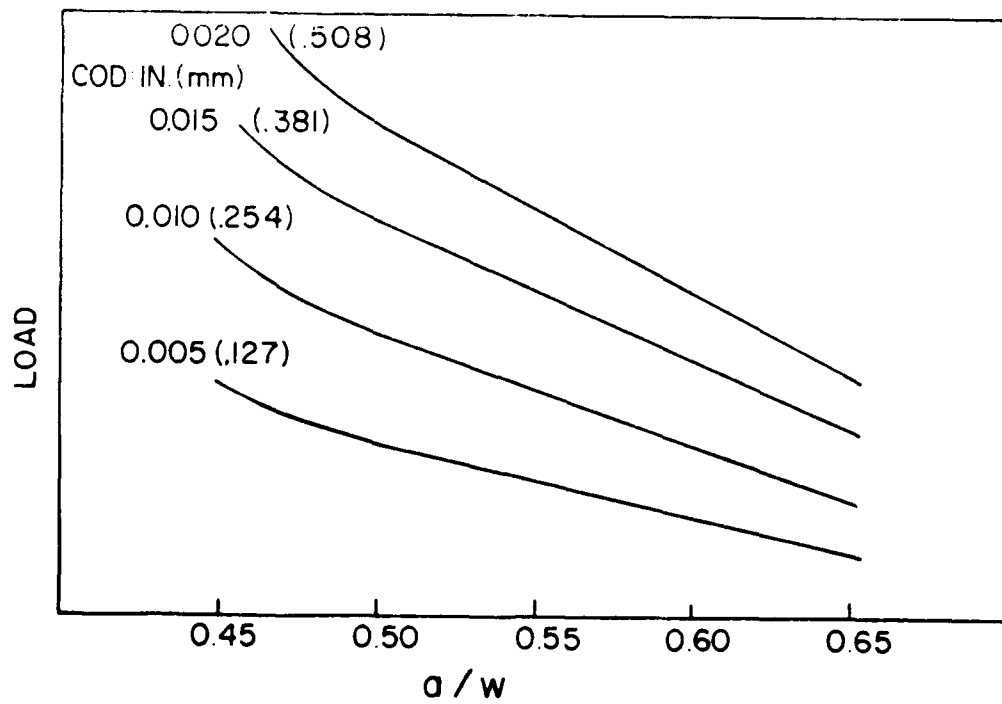


Figure 52. Compliance Curve Obtained for Bolt-Loaded Specimen.

to approximately 85 percent of the plane strain fracture toughness value by properly torquing the bolt until the desired COD, corresponding to the desired stress condition, was reached. The bolt tip was machined to a gentle radius to achieve point loading. Before and during torquing, a few drops of the test solution were placed at the crack tip so that the solution would be drawn into the crack as it opened. After the proper COD was reached, as indicated by the clip gage, the gage was removed and COD verified with a toolmaker's microscope. The specimen was then placed in an environmental chamber. The portion of the specimen containing the bolt was coated with paraffin to avoid any contact of the bolt tip with the solution as any corrosion build-up at the bolt tip could possibly wedge the specimen open further than desired. As with the previously mentioned constant load technique, air was bubbled through the solution, and the chamber drained and refilled with a fresh solution after 1,000 hours of test.

After the 2,000-hour exposure period the specimens were removed and the COD again measured. The bolt was then carefully removed and the specimen loaded in a Tinius-Olsen tensile test machine with the clip gage in place. A trace of load versus COD was obtained until complete specimen fracture, quite similar to the test procedure for fracture toughness testing. Afterwards, the load corresponding to the COD value created by the bolt at the conclusion of the corrosion test and the final crack length were determined and used to calculate the final stress intensity at crack arrest. This value for stress intensity is defined as the threshold for stress corrosion cracking in a decreasing stress intensity field.

Fracture toughness test results for short transverse-longitudinal (S-L) oriented specimens yielded an average toughness value of $18.4 \text{ KSI}\sqrt{\text{in}}$ ($20.2 \text{ MPa}\sqrt{\text{m}}$). These results are in good agreement with reference literature. [21,22]

The stress corrosion cracking results obtained for both test methods are illustrated in the computer-prepared curve

presented in Figure 53. The data points corresponding to the bolt-loaded test results represent the arrest stress intensities calculated after 2,000 hours in test solution. Since the crack lengths for these specimens were not monitored throughout the test, it is not known whether these threshold stress intensity values actually represent a condition of absolute crack arrest. Therefore, the results obtained for this technique, and similarly for the K-increasing technique, must be qualified as results obtained for a test duration of 2,000 hours. However, for the test period investigated, results for the two methods differ greatly. The bolt-loaded, decreasing stress intensity technique yielded an average threshold value of $13.4 \text{ KSI}\sqrt{\text{in}}$ ($14.7 \text{ MPa}\sqrt{\text{m}}$), while the constant load, increasing stress intensity technique yielded a threshold stress intensity value of approximately $9.0 \text{ KSI}\sqrt{\text{in}}$ ($9.89 \text{ MPa}\sqrt{\text{m}}$). Upon removal of the bolts for the constant displacement technique, the specimen COD did not return to the initial zero displacement as determined prior to beginning the test [0.0095 inch (0.241 mm) loading versus 0.006 inch (0.152 mm) unloading], indicating a possibility of corrosion product build-up on the fracture faces. The effect of such a corrosion build-up may result in an increase in specimen stress intensity and therefore an increase in crack extension; thus these threshold results might be yet higher if corrosion wedging had not taken place since the crack extension would be less. For the constant load specimen which did not fail after 2,400 hours (indicated by the runout arrow) when loaded at an initial stress intensity of $9.0 \text{ KSI}\sqrt{\text{in}}$ ($9.89 \text{ MPa}\sqrt{\text{m}}$), there was evidence of considerable crack extension. When the test was terminated, the calculated final stress intensity was approximately $14.5 \text{ KSI}\sqrt{\text{in}}$ ($15.9 \text{ MPa}\sqrt{\text{m}}$) indicating failure was inevitable. Thus, it appears that prolonging the test period would also yield a lower threshold value for this type of loading. Reference literature^[23] estimates a threshold stress intensity for this material under similar loading conditions of approximately $7 \text{ KSI}\sqrt{\text{in}}$ ($7.7 \text{ MPa}\sqrt{\text{m}}$).

7075-T651, KISCC

$K_{IC} = 18.4 \text{ KSI}\sqrt{\text{IN}} \text{ (} 20.2 \text{ MPa}\sqrt{\text{m}} \text{)}$

3.5% NaCl ENVIRONMENT

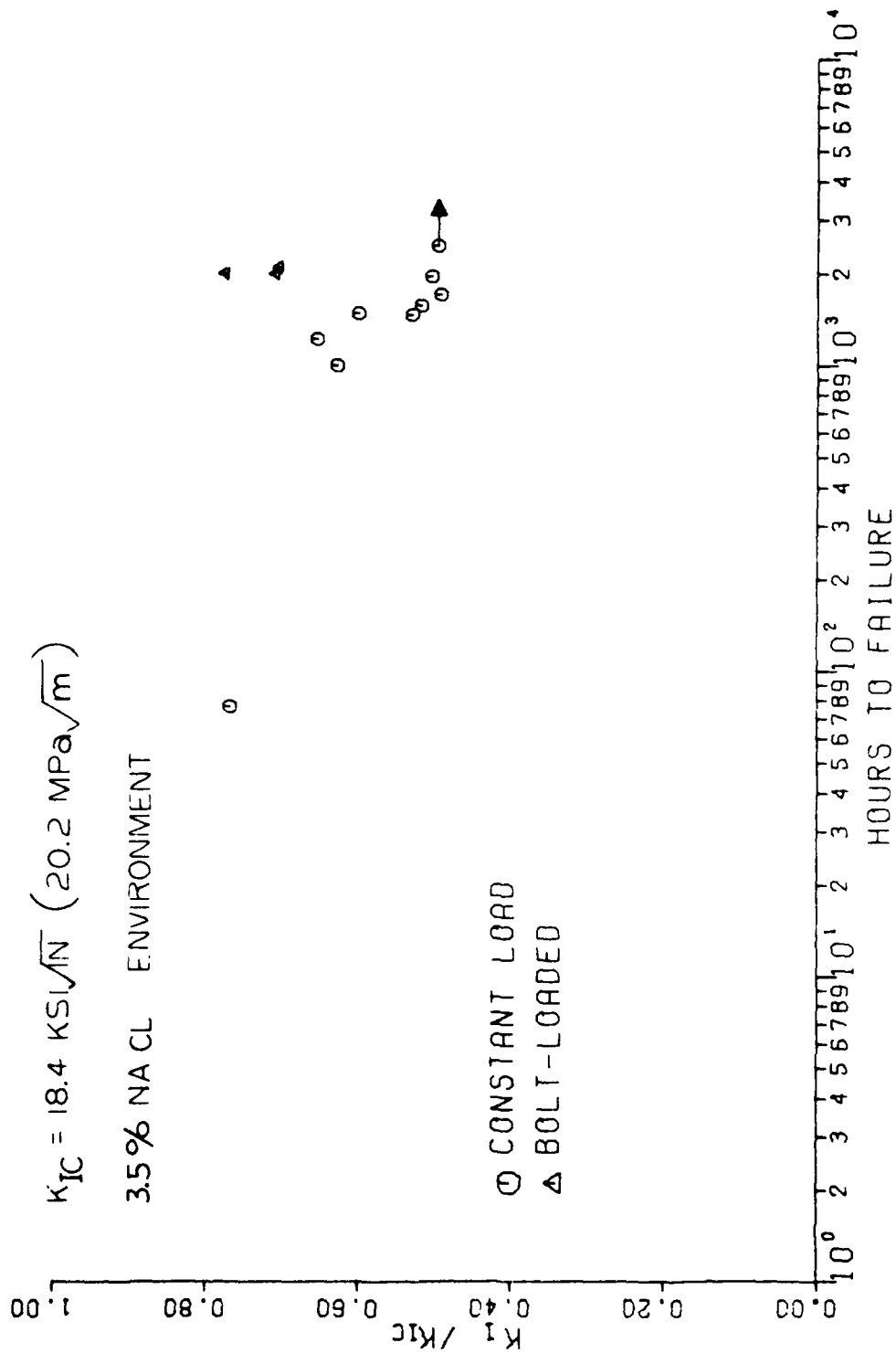


Figure 53. Stress Corrosion Cracking Results for Aluminum Alloy 7075-T651.

The bolt-loaded technique clearly offers advantages over the constant load technique in that it is a simple, low-cost, portable design which lends itself to large volume testing. Since this specimen is self-loading, it can be placed in practically any environment, without typing up any equipment. Although beyond the scope of this test program, the self-loaded specimen offers a more convenient means to obtain stress corrosion cracking rate characteristics, since it can be removed from the test environment and the crack tip observed rather easily. However, this technique yields nonconservative results for this material when compared to the more cumbersome and costlier constant load technique. Deviations for the two techniques might be explained under the following two hypotheses. Although the precracked specimens were prepared in similar manners, the initial loading conditions differed. For the bolt-loaded specimens the initial stress intensity applied was approximately 85 percent of the material's fracture toughness, while for the constant load specimens the initial stress intensities were in general lower. Due to the difference in the level of initial stress conditions, it is possible the crack incubation periods might likewise differ, i.e., the time spent for the crack in the specimen to change from a transgranular (fatigue) mode to an intergranular (corrosion cracking) mode and progress through the crack tip plastic zone. This phenomenon would cause differences in results if the tests were terminated prematurely.

Secondly, since the bolt-loaded technique is a decreasing stress intensity condition and if crack tip velocity is proportional to stress intensity, the crack growth rate will decrease with increasing crack extension. For some materials crack extension may continue indefinitely. Thus for this material, a 2,000-hour time period may not have been sufficient to produce a crack arrest or near-arrest condition. Test periods of 10,000 hours or more might yield a better (or worse) correlation between methods if time would permit; however, for the time period investigated, the constant displacement technique applied to this material must be labeled as yielding nonconservative results.

The test program was conducted on a single 2 inch (51 mm) thick plate of aluminum alloy 7075-T651. All stress corrosion testing was conducted in a constant immersion, 3.5 percent by weight solution of NaCl, with test time limited to 2,000 hours. The following conclusions were obtained:

1. The threshold stress intensity for stress corrosion cracking for this material was $13.4 \text{ KSI}\sqrt{\text{in}}$ ($14.7 \text{ MPa}\sqrt{\text{m}}$), employing a constant displacement, decreasing stress intensity testing method. For a constant load, increasing stress intensity technique, the threshold determined was less than $9 \text{ KSI}\sqrt{\text{in}}$ ($9.9 \text{ MPa}\sqrt{\text{m}}$).

2. For the given test period, the constant displacement technique yields a nonconservative estimation of this material's sensitivity to corrosion cracking relative to the constant load technique.

3. The constant displacement technique is a convenient and inexpensive test method which lends itself to portability and large scale testing. However, results obtained are sensitive to such parameters as test time period and corrosion product wedging, which can yield erroneous results if not taken into consideration.

SECTION 2

ELECTRONIC FAILURE ANALYSIS

The Air Force in 1961 adopted a methodology which has become known as Physics of Failure. This methodology was introduced to reduce failures and increase reliability in complex military equipment. Complex electronic systems, often in revolution, are commonly referred to as an exploding technology. Without time for orderly evolution of systems, applications of electronic materials and processes suffer the most from unreliability. Reliability is a problem at all levels of electronics from materials to operating systems, because materials go to make up parts, parts compose assemblies, and assemblies are combined into systems in ever increasing levels of sophistication. The performance of such systems places exacting demands on the individual materials, parts, and assemblies. Some systems, for example, are required to operate ten days continuously; each component, therefore, must have an average life expectancy of several thousand hours.

The University of Dayton Research Institute has been aiding the Air Force in the testing and failure analysis of electrical and electronic components. A wide variety of problems have been investigated such as stepper motors, mini-switches, variable resistors, and dielectric material measurements. A brief discussion of these investigations is included in this section.

2.1 VARIABLE RELUCTANCE STEPPER MOTOR

The variable reluctance stepper motor is an integral part of the Unified Fuel Control System of an F-100 jet engine. The stepper motor is part of a servo-loop in which it receives commands from an electronic fuel control and thereby regulates fuel flow to the engine. The motors are required to operate in a severe environment of a high temperature and pressure while being immersed in jet fuel.

The stepper motors have been the subject of physics of failure analyses for several years. In the past there have been two distinctive failure modes, either open or shorted stator windings. The open stator windings were due to either fuel corrosion or workmanship. The shorted stator windings were due to cracks in the insulation leading to insulation failure between the magnet wires.

Two stepper motors, manufactured by Singer Kearfott, were received for examination. A visual, mechanical, and electrical inspection of both stepper motors was done upon arrival. A visual inspection did not reveal any anomalies; however, two problem areas were identified during the mechanical and electrical inspection. One stepper motor (sample number 1) had an open stator winding and the other motor (sample number 2) had a frozen motor shaft.

To locate the open stator coil and the cause of the frozen motor shaft both stepper motors were carefully disassembled. This procedure first required unscrewing the tandem mounted geartrain casing from the motor casing. The motor casing was next split in half using a Dremel "moto-tool". This procedure exposed the stator coils of sample number 1 and armature and geartrain bearings of sample number 2.

Upon examining sample number 1, one lead-in wire was observed to be no longer attached to the magnet wire of one of the stator coils. Examining the break under high magnification the cross-sectional area of the wire appeared to be reduced. Crimps or twists in the wire that are associated with mechanical damage during assembly were not observed. Nevertheless, the reduced cross-sectional area of the wire in the vicinity of the break could have been caused by failure in tension or chemical attack. Although the specific failure mode could not be identified, once the wire cross-sectional area had been reduced it could easily be overstressed by localized heating, vibration, or differential expansion between the wire and potting compounds.

In sample number 2, the two armature bearings were found not to spin freely. The geartrain bearings were also removed for examination and the bearings did not spin freely. Examining both sets of bearings at 50X with an optical microscope revealed small particles of resin lodged in the bearings. In an effort to positively identify the foreign material a sample of potting compound (coating applied to stator windings for increased fuel resistance), a rotor and geartrain bearing were examined using Electron Spectroscopy for Chemical Analysis (ESCA). The carbon photoelectron peaks for the potting compound and bearings were each deconvoluted on a curve resolver. The peak intensities and binding energies of these components were all extremely close; however, this test procedure is subject to interpretation. For further identification of the foreign material, the potting compounds and bearings were submitted for examination with Infrared (IR). The transmittance spectrum for the potting compound and bearings were each very similar. Their spectra closely resembled that of an epoxy indicating the potting compound was flaking off due to low fuel resistance and was jamming the stepper motors' bearings.

2.2 SENSITIVE PUSH-BUTTON SWITCH

Mini-switches are a part of a push-to-talk microphone on an emergency radio transmitter set used by the Air Force. The switch failure mode has been reported as intermittent operation due to solder flux residues on the switch inner contact surfaces. Operation of the microphone switch is critical since the transmitter set apparently does not have a modulation indicator to inform the pilot of transmission.

Eight switches were received for examination. Six of the switches had been removed from field use and two were received new in their original unopened packages. The first test was to measure the contact resistance of each pair of normally open and closed contacts. The contact resistances for all switches were well within acceptable limits. The

measurements, however, were erratic enough to indicate that some residual material may still be present. The normally open contacts gave the most erratic results. It was also noticed that lateral pressure on the push-button would give erratic contact resistances with both the normally open and closed contacts.

According to a Product Evaluation Report prepared by Licon, the manufacturer, solder flux residues were found on the switch inner contact surfaces. It was, therefore, decided to determine whether flux residues were present in the switches submitted for evaluation. As an aid in detection, a determination was made as to whether solder flux fluoresces under ultraviolet illumination. Accordingly, some solder flux was melted and splashed onto a microscope slide. Examination of the residue revealed that the flux is fluorescent when exposed to light in the 385 to 420 nanometer range. In light of this finding several switches were opened and the contact members were examined. The eyelets of the solder lug blade were found to be fluorescent, however, no fluorescent particles were found on the switch contact surfaces.

In an attempt to identify the insulative film suspected of causing the continuity problem the contact surfaces were examined with Scanning Auger Mass Spectroscopy (SAMS). Large concentrations of carbon and oxygen were the predominant elements found, possibly indicating the presence of an organic film. The contacts were next examined using Chemical Ionization Mass Spectroscopy (CIMS). The contacts exhibited spectral peaks representing molecular weights of 258 and 285. Contacts from one of the new and used switches were also examined using this technique. A peak representing a molecular weight of 258 was obtained. In light of finding coinciding spectral peaks in both the new and used contacts, the plastic case was examined. The plastic case material was heated and a milky white substance, which exuded from the plastic was analyzed by CIMS. Spectral peaks representing molecular weights of 149, 258, 267, and 285

were obtained. Since two of the peaks from the plastic case match peaks from the contact surfaces the insulative film may very well have come from the plastic case.

An infrared spectral analysis was conducted on the contacts in an effort to determine the composition or the organic material present. Analysis indicates that the residue appears to be an aliphatic compound containing carbonyl groups; as ester, such as dibutyl adipate is a possible candidate.

Experimental evidence indicates the erratic switch behavior is due to an organic residue on contact surfaces. Exact identification of the contaminant was not possible; it is believed, however, the residue may have come from the plastic or from some other material associated with the manufacture of the switch. Attention should be focused on the molding operation and the molding materials such as thermoplastics, fillers, extenders, release agents, etc.

2.3 PRECISION VARIABLE RESISTORS

The precision multi-section variable resistors submitted for examination are intended for use in electronic and communication type equipment. They are qualified to the requirements of MIL-R-39023 and Drawing Number 577R900. These specifications cover requirements for precision variable resistors whose electrical output is either linear or nonlinear with respect to the angular position of the operating shaft. The reported problem from the field was excessive output noise.

Two variable resistors manufactured by New England Instrument Company were received for examination. Two electrical parameter tests, Total Cup Resistance and Output Smoothness, were chosen to determine the condition of the variable resistors. One variable resistor, sample number 1, had five cups which were out-of-tolerance. One cup was found to be an open circuit and four cups had output smoothnesses which were greater than the specified maximum. In sample number 2, two cups were found to

be out-of-tolerance. One cup failed to meet both the cup resistance and output smoothness tolerances. The second cup's output smoothness was greater than the specified maximum.

The predominant failure mode of the variable resistors was their inability to meet the Output Smoothness tolerances. Of the five cups that failed the test, all exhibited abrasions of their resistive coatings. The abrasions could be classified as grooving or pitting of the resistive coating. Although the grooving or pitting can be attributed to the friction of the spring wiper arm it is believed that the resistive coating is the prime factor in reducing the life expectancy of the two variable resistors. Factors which may affect surface hardness or cause gas to become trapped beneath the surface during manufacturing processes are the following: non-homogeneous resistive coatings mix, solvent concentration in the coating mix, incorrect temperature and rate of curing, hygroscopic material in the mix, outgassing plastic substrate during curing, and particle contamination of the work area.

2.4 THE DETERMINATION OF THE DIELECTRIC CONSTANT AND DISSIPATION FACTOR OF TWO DIELECTRIC MATERIALS

One investigation conducted during the period of the contract involved the determination of the dielectric constant of two materials. One of the materials under investigation consisted of a mixture of cyanoethylated cellulose (CNEC) in cyanoethylated phthalate (CNEP). The other was a slurry of barium titanate (BaTiO_3) in a binder. Both materials were supplied as rather high viscosity liquids of unknown concentrations. In order to optimize the effect of these materials in the electrical device for which they are intended, it was necessary to determine the dielectric constants and loss tangents for these substances as accurately as possible.

The test apparatus was a micrometer-capacitor (General Radio 1690A) type of dielectric sample holder. Such holders

are recommended in ASTM Specifications D-150 for use in the frequency range of 20 Hz and 50 Mhz. The test procedure first requires the test sample thickness to be measured with a machinist's micrometer. The sample is then inserted in the holder and the top electrode advanced until it is in firm contact with the dielectric material. The measuring bridge (General Radio 1650B Impedance Bridge) is subsequently balanced and its capacitance and loss tangent readings are recorded. Next, the sample is carefully removed and the bridge is re-balanced by readjusting the top electrode and loss tangent dial. The capacitance dial on the bridge is not touched. The electrode spacing and new loss tangent factor are recorded. The relative dielectric constants of the two test materials may be calculated as the ratio of the equivalent parallel capacitance of a capacitor in which one of the materials (CNEC/CNEP or BaTiO₃) is the dielectric, to the capacitance of the same capacitor with air as the dielectric.

Various deposition techniques for the preparation of two-inch dielectric disks were experimented with; the best films, however, were obtained by using a spin-casting technique. The materials were poured into rotating petri dishes. After allowing them to stand on a levelled table overnight, the dishes were placed in an oven to drive off the remaining solvent. The films were then peeled out the dishes. A number of films of each type of material were cast so that they could be stacked to build up the total thickness of the sample being measured.

The disc-shaped samples of each type of material were measured separately and stacked together in various combinations to give a variety of thicknesses. Due to electrical considerations, it was determined that greater sample thicknesses would produce more accurate measurements. Accordingly, enough samples were prepared to build up a total thickness for each type of over 100 mils. Results indicated that the samples of greater effective thickness gave higher dielectric constant values when

measured in the sample holder. As expected, dielectric constants calculated for the barium titanate films were of higher value but not significantly higher than those obtained for the cyanoethylated cellulose and cyanoethylated phthalate mixture. The dielectric constant value for the CNEC/CNEP material averaged approximately 12, and the barium titanate films averaged approximately 18.

The test procedure can cause errors to some extent for a number of reasons. It is extremely difficult to prepare discs of uniform thickness and exact size. Any irregularities present would have caused air gaps which would influence any measurements taken. Preparing thicker samples would have probably resulted in greater accuracy. All loss tangent information was lost due to the limitations of the measuring bridge.

SECTION 3 ELASTOMERS

It is highly desirable to accurately predict or determine the performance and useful life of the elastomeric seals and sealants which see widespread use in current U.S. Air Force aircraft and missile weapons systems. Safe performance and efficient maintenance and refurbishment of these systems is dependent on the ability to predict component life. The UDRI has provided many quick-response evaluations for the AFML to obtain physical and dynamic properties of elastomers to enhance the solutions to aircraft elastomeric component problems.

Materials performance and useful life criteria are determined through simulated or artificial aging of the seals and sealants. These criteria are also dependent on material compatibility with the various fuels and additives in use or being considered for use by the Air Force.

Although the major laboratory effort is contained in evaluating performance criteria and useful life determinations of seal and sealant materials, operational aircraft component problems occur which require rapid response solutions and analyses. In most instances, results of these laboratory evaluations were provided directly to the AFML project engineer and subsequently reported in bimonthly contract reports. Major tasks involving the development and performance of various seal and sealant materials are covered in this section.

3.1 FLUOROSILICONE O-RING SEALS

A major effort was initiated to determine useful life criteria for fluorosilicone O-ring seals. Fluorosilicone O-rings from different aircraft engines all having different hours of operation were evaluated for tensile strength and elongation. All of the rings were cut and tested as single strand specimens at room temperature with no additional conditioning. One group

included 30 packets of O-rings with three different sizes per packet. The largest O-ring, approximately 0.75 inch (19 mm) in diameter, was evaluated for tensile strength and elongation. The remainder of the rings were evaluated only for difference in stiffness by hand flexing.

Another group of fluorosilicone O-rings included three different part numbers. Half of the O-rings were used and half were new. The third set of O-rings were from aircraft engines with 539, 653, 1,120, and 1,237 operational hours. The data, presented in Tables 44, 45, and 46, respectively, for all of the above tests, however, were inconclusive.

3.2 DYNAMIC EVALUATION OF MIL-P-83461 O-RINGS

Three MIL-P-83461 O-ring compounds, Parker N756-75, Houghton 10V75-440, and Parco 4367-70, were evaluated for their dynamic properties on a rod seal test frame. The test fluid was MIL-H-5606C with test parameters of 1500 psi (10.3 MPa), 275°F (135°C), and a four-inch rod stroke at 30 cycles per minute. The test rods had a roughness of 10-20 RHR. The Parker N756-75 O-rings ranged from 84,500 to 170,500 cycles, the Houghton 10V75-440 O-rings ranged from 83,000 to 113,000 cycles, and the Parco 4367-70 O-rings ranged from 98,000 to 156,000 cycles. Tables 47, 48, and 49 present the results.

3.3 VOLUME CHANGE OF MIL-P-83461 O-RINGS IN TOLUENE

Seven O-ring compounds previously tested to the dynamic portion of MIL-P-83461 were evaluated for change in volume after being conditioned for 24 hours, 48 hours, and 120 hours in toluene at room temperature. These rings were evaluated to determine any relationship between the volume change of O-rings that show good dynamic performance compared to O-rings with low dynamic values. A 50 percent increase in volume change was determined between O-rings which failed at approximately 2,000 cycles and O-rings which exceeded 50,000 cycles in dynamic

TABLE 44
FLUOROSILICONE O-RINGS

Tensile Strength and Elongation

Engine S/N	Total Operating Hours	Tensile Str. (psi) (MPa)		Elongation (%)
P634256	??	610	4.20	60
F622763	?	610	4.20	70
P606497	?	460	3.17	50
P634312	?	410	2.83	50
P631135	?	330	2.28	40
P631899	??	520	3.58	68
F606287	???	360	2.48	56
P606081	??	---	---	---
P623379	???	550	3.79	60
P628162	35.5	470	3.24	40
P629398	147.4	340	2.34	44
P634132	167.7	350	2.41	40
F617841	189.3	---	---	--
P630060	217.4	240	1.65	32
P631642	275.6	250	1.72	40
P630794	287.0	340	2.34	40
F615100	3279.4	520	3.58	56
? #7 Eng.	316.4	630	4.34	60
F617967	333.1	310	2.14	28
P631087	342.9	530	3.65	50
P629600	364.0	630	4.34	80
P631052	374.4	350	2.41	40
F623000	424.7	250	1.72	30
P634103	474.4	550	3.79	90
F622737	494.6	400	2.76	40
P633204	517.1	510	3.52	46
F622896	524.2	590	4.07	56
P626420	565.2	450	3.10	58
F623138	906.0	370	2.55	60
F617853	1052.0	390	2.69	30

TABLE 45
FLUOROSILICONE O-RINGS

Flexibility

Ring A - 3/10 inch ID/ 4/10 inch OD

Ring B - 4/10 inch ID/ 6/10 inch OD

<u>Engine S/N</u>	<u>Hand Flex</u>
P634256	Ring A - Flexible Ring B - (Red) - Flexible (White) - Very flexible
F622763	Ring A - Flexible Ring B - (White) - Flexible
P606497	Ring A - Very slight flex loss Ring B - (White) - Very flexible
P634312	Ring A - Very slight flex loss Ring B - (Red) - Very slight flex loss
P631135	Ring A - Very slight flex loss Ring B - (Red) - Flexible
P631899	Ring A - Very slight flex loss Ring B - (Red) - Slight flex loss (White) - Very flexible
F606287	Ring A - Flexible Ring B - (Red) - Flexible
P606081	Ring A - Very slight flex loss Ring B - (Red) - Very slight flex loss
P623379	Ring A - Very slight flex loss Ring B - (Red) - Flexible
P628162	Ring A - Very slight flex loss Ring B - (White) - Very flexible
P629398	Ring A - Slight flex loss Ring B - (Red) - Slight flex loss
P634132	Ring A - Slight flex loss Ring B - (Red) - Flexible

TABLE 45 (Continued)
FLUOROSILICONE O-RINGS

<u>Engine S/N</u>	<u>Flexibility</u>	
	<u>Hand Flex</u>	
F617841	Ring A - Very slight flex loss	Ring B - (White) - Flexible
P630060	Ring A - Slight flex loss	Ring B - (Red) - Slight flex loss
P631642	Ring A - Very slight flex loss	Ring B - (Red) - Slight flex loss
P630794	Ring A - Very slight flex loss	Ring B - (Red) - Slight flex loss
F615100	Ring A - Slight flex loss	Ring B - (White) - Flexible
? #7	Ring A - Very slight flex loss	Ring B - (Red) - Flexible
F617967	Ring A - Slight flex loss	Ring B - (Red) - Slight flex loss
P631087	Ring A - Slight flex loss	Ring B - (Red) - Very slight flex loss
P629600	Ring A - Slight flex loss	Ring B - (White) - Flexible
P631052	Ring A - Very slight flex loss	Ring B - (Red) - Very slight flex loss
F623000	Ring A - Slight flex loss	Ring B - (Red) - Slight flex loss
F634103	Ring A - Very slight flex loss	Ring B - (Red) - Slight flex loss
F622737	Ring A - Slight flex loss	Ring B - (Red) - Very slight flex loss
P633204	Ring A - Very slight flex loss	Ring B - (Red) - Slight flex loss

TABLE 45 (Concluded)
FLUOROSILICONE O-RINGS

Flexibility	
<u>Engine S/N</u>	<u>Hand Flex</u>
F622896	Ring A - Slight flex loss Ring B - (Red) - Very slight flex loss
P626420	Ring A - Very slight flex loss Ring B - (Red) - Very slight flex loss
F623138	Ring A - Slight flex loss Ring B - (Red) - Slight flex loss
F617853	Ring A - Very slight flex loss Ring B - (Red) - Very slight flex loss

Rating: Very flexible
 Flexible
 Very slight flex loss
 Slight flex loss

TABLE 46
EVALUATION OF FLUROSILICONE O-RINGS

Specimen Number	Tensile Strength (psi) (MPa)		Elongation (%)
P/N 757435 - New			
1	730	5.03	50
2	510	3.52	40
3	660	4.55	60
4	700	4.83	60
P/N 757435 - Used			
1	230	1.59	40
2	610	4.21	60
3	610	4.21	40
P/N 767996 - New			
1	500	3.45	60
2	830	5.72	120
3	330	2.28	60
P/N 767996 - Used			
1	740	5.10	100
2	650	4.48	70
3	350	2.41	50
P/N 757436B - New			
1	880	6.07	110
P/N 757436B - Used			
1	800	5.52	90

TABLE 46 (Concluded)
EVALUATION OF FLUOROSILICONE O-RINGS

Specimen Number	Thickness (In.) (cm)		Tensile Strength (psi) (MPa)		Elongation (%)
From #58-010 Aircraft Engine #2 (S/N P632079) - 539.1 hrs.					
1	0.084	0.213	722	5.0	60
2	0.064	0.162	181	1.3	42
3	0.063	0.160	802	5.5	40
4	0.063	0.160	770	5.3	40
5	0.056	0.142	650	4.5	25
6	0.056	0.142	812	5.6	65
7	0.057	0.145	---	---	---
From #57-6497 Aircraft Engine #6 (S/N 627734) - 653.9 hrs.					
1	0.085	0.216	705	4.9	40
2	0.067	0.170	317	2.2	20
3	0.068	0.173	275	1.9	10
4	0.059	0.150	439	3.0	20
5	0.057	0.145	588	4.1	25
6	0.056	0.142	894	6.2	50
From #58-166 Aircraft Engine #1 (S/N P632620) - 1120.7 hrs.					
1	0.082	0.208	587	4.0	35
2	0.062	0.157	497	3.4	20
3	0.061	0.154	548	3.8	25
4	0.061	0.154	582	4.0	20
5	0.055	0.140	505	3.5	10
6	0.056	0.142	406	2.8	15
7	0.056	0.142	487	3.4	20
8	0.056	0.142	447	3.1	25
From #57-6499 Aircraft Engine -. (S/N P631394) - 1237.6 hrs.					
1	0.083	0.211	296	2.0	10
2	0.063	0.160	738	5.1	30
3	0.063	0.160	387	2.7	15
4	0.062	0.157	729	5.0	20
5	0.057	0.145	0	0	0
6	0.055	0.140	211	1.5	5
7	0.056	0.142	650	4.5	10
8	0.056	0.142	609	4.2	10

All #1 rings are the same diameter.
All #2, 3, and 4 rings are the same diameter.
All #5, 6, 7, and 8 rings are the same diameter.

TABLE 47
PARKER N756-75 DYNAMIC TESTS
TO MIL-P-83461

Position	Cycles to Failure	Leakage Rate	Total Leakage
Left	124,116	0.037 cc/min	70 cc
Right	---	0.022 cc/min	50 cc
Left	---	0.030 cc/min	60 cc
Right	84,600	0.038 cc/min	70 cc
Left	119,805	0.026 cc/min	70 cc
Right	---	---	0
Left	171,543	0.015 cc/min	70 cc
Right	---	0.013 cc/min	57 cc
Left	134,724	0.018 cc/min	70 cc
Right	---	---	0
Left	---	0.004 cc/min	10 cc
Right	122,670	0.021 cc/min	70 cc

Test Conditions: Rate - 30 cpm
Pressure - 1500 psi
Temperature - 275°F (135°C)
Stroke - 4"
Test Fluid - MIL-H-5606C

For the dynamic tests, the O-rings are tested in pairs left and right. Because one ring fails first, the remaining ring is not tested to failure, therefore, it will have no cycles to failure value.

TABLE 48
HOUGHTON 10V75-440 DYNAMIC TESTS
TO MIL-P-83461

Position	Cycles to Failure	Leakage Rate	Total Leakage
Left	---	0.026 cc/min	29.5 cc
Right	93,060	0.031 cc/min	70 cc
Left	---	0.013 cc/min	21.4 cc
Right	82,908	0.035 cc/min	70 cc
Left	90,130	0.033 cc/min	70 cc
Right	---	---	0
Left	---	0.021 cc/min	64.4 cc
Right	113,147	0.030 cc/min	70 cc
Left	---	---	0
Right	91,597	0.044 cc/min	70 cc
Left	---	0.028 cc/min	20.2 cc
Right	91,000	0.042 cc/min	70 cc

Test Conditions: Rate - 30 cpm
Pressure - 1500 psi
Temperature - 275°F (135°C)
Stroke - 4"
Test Fluid - MIL-H-5606C

For the dynamic tests, the O-rings are tested in pairs left and right. Because one ring fails first, the remaining ring is not tested to failure, therefore, it will have no cycles to failure value.

TABLE 49
PARCO 4367-70 DYNAMIC TESTS
TO MIL-P-83461

Position	Cycles to Failure	Leakage Rate	Total Leakage
Left	123,316	0.022 cc/min	70 cc
Right	---	---	0
Left	112,800	0.020 cc/min	70 cc
Right	---	---	0
Left	136,080	0.022 cc/min	70 cc
Right	---	---	0
Left	132,840	0.026 cc/min	70 cc
Right	---	---	0
Left	98,136	0.031 cc/min	70 cc
Right	---	---	0
Left	156,000	0.017 cc/min	70 cc
Right	---	0.015 cc/min	23.5 cc

Test Conditions: ate - 30 cpm
 Pressure - 1500 psi
 Temperature - 275°F (135°C)
 Stroke - 4"
 Test Fluid - MIL-H-5606C

For the dynamic tests, the O-rings are tested in pairs left and right. Because one ring fails first, the remaining ring is not tested to failure, therefore, it will have no cycles to failure value.

performance. No discernible differences in volume change, however, were noted for O-rings that had dynamic values greater than 50,000 cycles. These data are given in Table 50. Volume change determinations can be used to detect O-rings which will experience very early dynamic failure but cannot be used to determine which O-rings will pass the minimum dynamic requirements specified in MIL-P-83461.

3.4 EVALUATION OF O-RING KITS

Two O-ring kits, National Seal OK 311 and Aerocustom ACOK 311, were evaluated for tensile strength and elongation, Shore A hardness, TR-10, corrosion and adhesion, volume change, and compression set. These tests were conducted before and after conditioning for seven days at 158°F (71°C) in MIL-H-5606C, 70 hours at 275°F (135°C) in MIL-H-5606C, 72 hours at 75°F (24°C) in TT-S-735 Type I, 72 hours at 75°F (24°C) in TT-S-735 Type III, 72 hours at 75°F (24°C) in JP-4, 70 hours at 257°F (125°C) in Stauffer's Blend 7700, and 70 hours at 257°F (125°C) in air. The O-rings used for these tests were to be size 214. Since the kits did not have enough rings of the 214 size, a variety of O-ring sizes were used. The original properties evaluated were tensile strength, elongation, Shore A hardness, TR-10, and adhesion and corrosion using MIL-P-83461 metals. After conditioning for seven days at 158°F (71°C) in MIL-H-5606C, the O-rings were evaluated for tensile strength, elongation, Shore A hardness, TR-10, and volume change. After conditioning for 70 hours at 275°F (135°C) in MIL-H-5606C, the O-rings were evaluated for tensile strength, elongation, Shore A hardness, TR-10, volume change, and compression set. The O-rings were also evaluated for tensile strength, elongation, and volume change after being conditioned in Type I, Type III, and JP-4 as per Paragraph 4.7.4.3 of MIL-P-5315B. After conditioning for 70 hours at 257°F (125°C) in Stauffer's Blend 7700, the O-rings were evaluated for tensile strength, elongation, Shore A hardness, volume change, TR-10, and compression set as per Paragraphs 4.6.3 and 4.6.4 of MIL-R-7362D.

TABLE 50
VOLUME SWELL OF 83461 O-RINGS
IN TOLUENE FOR 24 HOURS

Initial Air	Initial H ₂ O	Final Air	Final H ₂ O	% Volume Swell
4367-70				
1.0177	0.1766	1.0180	0.0121	139
1.0079	0.1809	1.0080	0.0135	141
1.0180	0.1836	1.0180	0.0180	141
1.0300	0.1869	1.0340	0.0119	141
1.0096	0.1837	1.0090	0.0117	139
Avg.				140.7 80,000
A5566				
1.0654	0.2113	2.0980	0.0104	135
1.0712	0.2131	2.0450	0.0336	127
1.0672	0.2193	2.0540	0.0309	130
1.0675	0.2198	2.0420	0.0330	136
1.0722	0.2166	2.0480	0.0343	135
Avg.				133.7 110,000
SR8014-75 (New Varox)				
1.1897	0.2713	2.1440	0.0968	124
1.0902	0.1980	2.0001	0.0508	116
1.0894	0.1985	1.9722	0.0556	113
1.1696	0.2719	2.1390	0.0979	127
1.1744	0.2699	2.1540	0.0903	128
Avg.				122.7 125,000
SR8014-75 (Old Varox)				
1.1275	0.2067	2.0880	0.0496	121
1.1339	0.2083	2.1160	0.0463	124
1.1291	0.2075	2.0780	0.0531	120
1.1243	0.2059	2.0140	0.0435	115
1.1342	0.2085	2.1220	-0.0061	130
Avg.				122.7 76,000

TABLE 50 (Concluded)
VOLUME SWELL OF 83461 O-RINGS
IN TOLUENE FOR 24 HOURS

Initial Air	Initial H ₂ O	Final Air	Final H ₂ O	% Volume Swell
N75-440				
1.0447	0.1947	2.0430	0.0309	137
0.9989	0.1883	1.9120	0.0427	131
1.0405	0.1955	1.9920	0.0444	130
1.0373	0.1936	2.0280	0.0402	136
1.0461	0.1984	2.0000	0.0450	<u>131</u>
Avg.				133/ 50,000
N756-75				
1.0609	0.1930	1.9600	0.0525	120
1.0660	0.1948	2.0020	0.0489	124
1.0722	0.1961	1.9350	0.0570	114
1.0639	0.1933	1.9410	0.0581	116
1.0727	0.1938	2.0210	0.0468	<u>125</u>
Avg.				120/ 95,000
H14379				
1.0857	0.1919	2.5950	-0.0463	196
1.0618	0.1893	2.4120	-0.0366	181
1.1051	0.1966	2.6000	-0.0484	192
1.0890	0.1939	2.7550	-0.0766	216
1.0660	0.1914	2.4330	-0.0304	<u>182</u>
Avg.				193/ 2,000

The O-rings were evaluated for tensile strength, elongation, and Shore A hardness after conditioning in air for 70 hours at 257°F (125°C). Both National kit OK311 and Aerocustom kit ACOK311 failed TR-10 requirements for MIL-P-25732 and MIL-P-83461. The TR-10 results, incidentally, also did not satisfy the original property requirements for MIL-P-5315B and MIL-R-7362D. Both kits also failed volume change requirements of MIL-P-25732, MIL-P-83461, and MIL-R-7362D. Aerocustom kit ACOK311 additionally failed the hardness requirements of MIL-R-7362D. The data are given in Tables 51 and 52.

3.5 ELASTOMERS/JP-9 COMPATIBILITY EVALUATION

A materials evaluation program was initiated to determine the compatibility of various elastomeric materials with the JP-9 fuel system. Materials evaluated include O-rings, polysulfide sealants, sheet materials, and bladder materials.

O-rings evaluated include Parker N602-70 and N824-70 (MIL-P-5315, Buna-N), Parker N756-75 (MIL-P-83461, peroxide curing system), Parker L677-70 and L737-65 (MIL-R-25988, Type I, fluorosilicone), and Parker V747-75 (MIL-R-83248, fluoro-elastomer). In addition, VS-157 (MIL-R-83485, Type I, low-temperature fluoroelastomer) O-rings fabricated at Wright-Patterson Air Force Base were also evaluated.

The polysulfide sealants (MIL-S-8802D) tested include Pro Seal PS890 B-2 and Products Research Corporation PR-1422 B-2. Sheet materials evaluated were teflon and nylon, and bladder materials were Goodyear 52904, FT-99, and Uniroyal US566RL.

All materials were evaluated in their original condition and after conditioning in JP-9 for seven days at 75°F (25°C), six months at 75°F (25°C), seven days at 140°F (60°C), one month at 140°F (60°C), three months at 140°F (60°C), six months at 140°F (60°C), nine months at 140°F (60°C), and 12 months at 140°F (60°C).

TABLE 51
NATIONAL KIT OK 311

Condition	Tensile Str. (psi) (MPa)	Elongation (%)	Vol. Swell (%)	Hardness (Shore A)	TR-10* (°C) (°F)	Comp. Set (%)	Ring Size
Controls	1940 13.37	280		75	-32 -35.6		215 Hard-325
70 hrs. @ R.T. in 5606C			2.0				217
72 hrs. @ R.T. in JP-4	1210 8.34	200	9.1				218
72 hrs. @ R.T. in Type III	890 6.14	175	27.3				218
72 hrs. @ R.T. in Type I	1630 11.24	225	1.6				211
7 days @ 160°F (71°C) in 5606C	1580 10.89	228	13.3	71	-32 -35.6		216 Hard-325
70 hrs. @ 257°F (125°C) in air	1990 13.72	180		77			Hard-325 217
70 hrs. @ 275°F (135°C) in 5606C	1810 12.48	246	15.9	69	-32 -35.6	24.0	215 C.S.-213 Hard-325
70 hrs. @ 257°F (125°C) in Stauffer's 7700	1820 12.55	250	27.1	65	-43 -45.0	45.9	216 C.S.-213 VS- 211

Corrosion - very slight corrosion of 4130 steel - 213.

*TR-10 - All rings used were 214.

TABLE 52
AEROCUSTOM KIT ACOK 311

Condition	Tensile Str. (psi)	Tensile Str. (MPa)	Elongation (%)	Vol. Swell (%)	Hardness (Shore A)	TR-10* (°C) (°F)	Comp. Set (%)	Ring Size
Controls	2550	17.58	355		75	-22 -30		6227-23 TR-10-6227-19 Hard-6227-28
70 hrs. @ R.T. in 5606C				0.2				6227-18
72 hrs. @ R.T. in JP-4	1800	12.41	280	9.1				6227-14
72 hrs. @ R.T. in Type I	2460	16.96	350	0.6				6227-25
72 hrs. @ R.T. in Type III	1260	8.68	250	31.1				6227-24
7 days @ 160°F (71°C) in 5606C	1920	13.24	270	7.5	72	-19 -28.8 -31 -35.0		6227-22 TR-10-6227-20 Hard-6227-28
70 hrs. @ 257°F (121°C) in air	2300	15.86	174		70			6227-26 Hard-6227-29
70 hrs. @ 275°F (135°C) in 5606C	2090	14.41	199	1.9	69	-19 -28.8	56	6227-71 TR-10-6227-19 C.S.-6227-20 Hard-6227-28
72 hrs. @ 257°F (121°C) in Stauffer's 7700	1210	8.34	150	16.5	55	-26 -32.2	12.5	6227-25 VS-6227-14 Hard-6227-29 C.S.-6227-20

Corrosion - slight corrosion of 4130 steel - 6227-15

O-rings were evaluated for tensile strength, percent elongation, hardness (Shore A₂), volume change, temperature retraction (TR-10), and percent compression set per ASTM D395, Method B. The polysulfide sealants were evaluated for tensile strength, percent elongation, hardness (Shore A₂), volume change, and peel strength. The sheet materials were evaluated for tensile strength and percent elongation. The unbonded Goodyear 52904 bladder material was tested for tensile strength and percent elongation only, while the bonded FT-99 was tested for seam adhesion and permeability only. The Uniroyal US566RL bladder material, supplied in both unbonded and bonded form, was evaluated for tensile strength, percent elongation, seam adhesion, and permeability.

Test results of the N602-70 O-rings showed a slight decrease in tensile strength from the original condition but remained consistent throughout the aged conditions. Elongation showed little, if any, decrease.

The N824-70 O-rings showed a considerable drop in tensile strength after one week conditioning, and retained less than half of the original strength after one year. There was also a drop in elongation, although not as severe as the decrease in tensile strength.

The N756-75 and L677-70 O-rings dropped moderately in tensile strength, but only slightly or not at all in elongation. Both tensile strength and elongation were only slightly affected on the L737-65, V747-75, and VS-157 O-rings.

Tensile strength and elongation measurements for all O-rings aged at 140°F (60°C) were consistently lower than the tensile strength and elongation for the O-rings aged at 75°F (25°C), although the differences were slight.

The N602-70, N824-70, and N756-75 O-rings all showed a slight decrease in hardness from the original values in all conditions, but remained relatively consistent throughout these conditions. Hardness values on the L677-70, L737-65,

V747-75, and VS-157 did not appear to be significantly affected by aging, showing only minor variations.

The major effect of aging on volume change determinations appeared to be between the seven days at 140°F (60°C) in JP-9 and the seven days at 75°F (25°C) in JP-9 conditions on the N602-70, N824-70, and N756-75 O-rings. A large change was noted on the N602-70 O-rings between six months at 140°F (60°C) in JP-9 and six months at 75°F (25°C) in JP-9. Differences in volume change values at the two temperatures on all other specimens were slight at both seven days and six months. Differences between aging times at the same temperature showed no significant effect on volume change.

The TR-10 values for aged specimens were consistently lower than those for original specimens, but there was generally no significant difference between either aging times or temperatures. No results were obtained on the N824-70 O-rings at seven days at 140°F (60°C) or on the N756-75 rings at seven days at room temperature, seven days at 140°F (60°C), one month at 140°F (60°C), or nine months at 140°F (60°C), as these specimens broke in the test grips before they were able to be tested. All specimens but the nine months at 140°F (60°C) on the N756-75 O-rings were retested, but still failed.

There was a steady increase in percent compression set with both time and temperature in all materials except the fluoro-elastomer O-rings, which showed no significant change due to aging. Compression set values for these materials, however, were significantly higher at room temperature than at elevated temperature. The N602-70, N824-70, and N756-75 O-rings, which had a high percentage of volume swell, showed a negative compression set under short term aging. The L737-65 O-rings showed no set at all until three months. Complete data on all O-ring tests are shown in Table 53.

Tensile strength and elongation on the PS890 B-2 sealant appeared to be only slightly affected in all conditions, while

TABLE 53
ELASTOMERS/JP-9 COMPATIBILITY EVALUATION
O-RINGS

Material	Condition	Tensile Strength (psi)	Elongation (%)	Hardness (Pts. Shore A ₂)	Vol. Change (%)	TR-10 (Temp. °F)	Comp. Set (% Set)
N1L-P-5315	Original	1500	355	64	---	-54	---
	7 days @ R.T. in JP-9	1300	355	54	30.78	-61.6	-8.57
	7 days @ 140°F(60°C) in JP-9	1210	331	44	42.54	-65	-2.86
	1 mo. @ 140°F(60°C) in JP-9	1370	360	49	42.83	-67	5.71
	3 mo. @ 140°F(60°C) in JP-9	1330	347	42	39.68	-61.6	11.43
	6 mo. @ R.T. in JP-9	1350	356	54	31.4	-60	2.86
	6 mo. @ 140°F(60°C) in JP-9	1220	313	54	40.2	-60	22.86
	9 mo. @ 140°F(60°C) in JP-9	1280	325	45	42.1	-58	24.28
	12 mo. @ 140°F(60°C) in JP-9	1320	323	47	42.8	-58	34.29
	Original	1970	315	67	---	-50.8	---
	7 days @ R.T. in JP-9	1030	226	55	42.37	-63.4	-14.28
	7 days @ 140°F(60°C) in JP-9	910	205	47	53.10	*	-25.70
N824-70	1 mo. @ 140°F(60°C) in JP-9	890	212	---	50.40	-66	-18.5
	3 mo. @ 140°F(60°C) in JP-9	920	222	52	49.2	-69	-17.14
	6 mo. @ R.T. in JP-9	1120	240	56	43.4	-62	-14.3
	6 mo. @ 140°F(60°C) in JP-9	980	230	53	43.4	-62	-8.6
	9 mo. @ 140°F(60°C) in JP-9	1180	251	49	47.4	-81	4.3
	12 mo. @ 140°F(60°C) in JP-9	920	217	57	44.6	-83	0

* Broke in grips
--- N/A

TABLE 53 (Continued)
ELASTOMERS/JP-9 COMPATIBILITY EVALUATION
O-RINGS

Material	Condition	Tensile Strength (psi)	Tensile Strength (MPa)	Elongation (%)	Hardness (Pts. Shore A ₂)	Vol. Change (%)	TR-10 (Temp. °F)	Comp. Set (% Set)
ML-P-83461 N756-75	Original	1460	10.1	134	76	---	-54	---
	7 days @ R.T. in JP-9	980	6.76	119	63	24.65	*	-5.88
	7 days @ 140°F (60°C) in JP-9	850	5.86	116	61	34.08	*	-5.88
	1 mo. @ 140°F (60°C) in JP-9	770	5.31	110	60	31.72	*	2.9
	3 mo. @ 140°F (60°C) in JP-9	860	5.93	113	63	29.42	-87	5.88
	6 mo. @ R.T. in JP-9	1000	6.9	120	67	25.1	-85	-1.4
	6 mo. @ 140°F (60°C) in JP-9	960	6.6	120	66	27.1	-80	11.4
	9 mo. @ 140°F (60°C) in JP-9	1120	7.7	124	62	30.4	*	12.8
	12 mo. @ 140°F (60°C) in JP-9	990	6.8	129	68	27.7	-78	12.8
	Original	1030	7.10	179	73	---	-76	---
	7 days @ R.T. in JP-9	960	6.62	199	66	7.55	-85	7.14
	7 days @ 140°F (60°C) in JP-9	940	6.48	179	57	8.91	-90	5.71
ML-P-25988 Type I, Class I L677-70	1 mo. @ 140°F (60°C) in JP-9	990	6.83	181	73	8.86	-92	11.4
	3 mo. @ 140°F (60°C) in JP-9	940	6.48	193	64	12.09	-90	20.0
	6 mo. @ R.T. in JP-9	890	6.14	163	64	4.3	-85	10.0
	6 mo. @ 140°F (60°C) in JP-9	680	4.69	128	67	7.0	-93	32.86
	9 mo. @ 140°F (60°C) in JP-9	970	6.69	176	68	10.9	-94	42.86
	12 mo. @ 140°F (60°C) in JP-9	730	5.0	143	71	6.9	-78	45.71

* Broke in grips

--- N/A

TABLE 53 (Continued)
ELASTOMERS/JP-9 COMPATIBILITY EVALUATION
O-RINGS

Material	Condition	Tensile Strength (psi)	Tensile Strength (MPa)	Elongation (%)	Hardness (Pts. Shore A ₂)	Vol. Change (%)	IR-10 (Temp. °F)	Comp. Set (% Set)
MIL-P-25988 Type I, Class III L737-65	Original	880	6.07	230	50	---	-83	---
	7 days @ R.T. in JP-9	800	5.51	220	55	9.89	-89	0
	7 days @ 140°F (60°C) in JP-9	780	5.38	207	44	11.66	-87	0
	1 mo. @ 140°F (60°C) in JP-9	720	4.96	213	40	7.28	-90	0
	3 mo. @ 140°F (60°C) in JP-9	730	5.03	251	58	8.69	-94	5.88
	6 mo. @ R.T. in JP-9	900	6.2	250	53	10.0	-94	2.94
	6 mo. @ 140°F (60°C) in JP-9	780	5.4	220	50	9.6	-94	8.82
	9 mo. @ 140°F (60°C) in JP-9	820	5.65	216	52	9.2	-90	19.12
	12 mo. @ 140°F (60°C) in JP-9	760	5.2	216	49	8.1	-87	17.65
	Original	1640	11.3	193	78	---	3.2	---
	7 days @ R.T. in JP-9	1430	9.86	181	73	1.72	1.4	20.59
	7 days @ 140°F (60°C) in JP-9	1290	8.89	171	70	5.50	1.4	11.76
MIL-N-83248 Type I, Class I V747-75	1 mo. @ 140°F (60°C) in JP-9	1500	10.3	184	77	2.14	1.4	17.10
	3 mo. @ 140°F (60°C) in JP-9	1530	10.5	200	73	3.96	-4.0	14.71
	6 mo. @ R.T. in JP-9	1710	11.79	214	73	0.11	-4.0	14.71
	6 mo. @ 140°F (60°C) in JP-9	1640	11.31	214	72	2.0	-4.0	14.71
	9 mo. @ 140°F (60°C) in JP-9	1530	10.55	191	75	3.7	-0.4	17.65
	12 mo. @ 140°F (60°C) in JP-9	1590	11.0	200	76	1.8	-14.8	13.24

* Broke in grips

--- N/A

TABLE 53 (Concluded)
ELASTOMERS/JP-9 COMPATIBILITY EVALUATION
O-RINGS

Material	Condition	Tensile Strength (psi)	Tensile Strength (N/A)	Elongation (%)	Hardness (Pts. Shore A ₂)	Vol. Change (%)	TR-10 (Temp., °F)	Comp. Set (% Set)
MIL-R-83485 Type I VS-157	Original	1940	13.3	156	77	---	-23.8	---
	7 days @ R.T. in JP-9	1970	13.6	162	74	1.09	-23.8	22.2
	7 days @ 140°F (60°C) in JP-9	1650	11.4	154	68	5.60	-25.6	12.5
	1 mo. @ 140°F (60°C) in JP-9	1800	12.4	145	76	2.67	-22.0	16.7
	3 mo. @ 140°F (60°C) in JP-9	1580	10.9	143	74	5.59	-29.2	16.7
	6 mo. @ R.T. in JP-9	2000	13.79	160	75	0.79	-29.0	20.83
	6 mo. @ 140°F (60°C) in JP-9	1750	12.06	146	73	4.4	-33.0	13.89
	9 mo. @ 140°F (60°C) in JP-9	1690	11.65	146	76	3.9	-29.0	13.83
	12 mo. @ 140°F (60°C) in JP-9	1760	12.1	145	76	3.5	-29.0	11.43

* Broke in grips

--- N/A

a more significant change was noted with the PR-1422 B-2. This material showed a moderate decrease in tensile strength. Elongation increased slightly at both seven day conditions, but then decreased slightly during continued aging. Aging temperature also seemed to have more of an effect on the PR-1422 B-2, whereas these differences were negligible on the PS890 B-2.

The PS890 B-2 sealant showed only a minor drop in peel strength, while the PR-1422 B-2 sealant showed higher strengths in most aged conditions than in the original condition. The PR-1422 B-2 peels at seven days at room temperature in JP-9 showed very low values in comparison with the other conditions, so were retested. The second set of panels showed comparable data to all other aged PR-1422 B-2 panels. The low values initially obtained were possibly due to inadequate panel surface preparation.

Hardness test data showed no significant change in any condition on either the PS890 B-2 or the PR-1422 B-2 sealant materials.

Volume change measurements were approximately the same for both materials in the less severe conditions. The PR-1422 B-2, however, showed a more rapid decrease than the PS890 B-2, having a negative volume change (shrinkage) in the three months at 140°F (60°C) through the 12 months at 140°F (60°C) conditions. Complete data for the sealants are shown in Table 54.

The Goodyear 52904 Buna-N material dropped considerably in both tensile strength and elongation from the original condition, but did not seem to have a significant difference between aging times until the 12-month condition, where there was a noticeable decrease. There was also a noticeable difference between the 140°F (60°C) and room temperature conditions done at the same aging time.

Tensile strength on the nylon material increased as the severity of conditioning increased. Elongation decreased drastically in most conditions, retaining only about 15 percent

TABLE 54
ELASTOMERS/JP-9 COMPATIBILITY EVALUATIONS
POLYSULFIDE SEALANTS

Material	Condition	Tensile Strength (psi)	Tensile Strength (MPa)	Elongation (%)	Peel Strength (P.I.W.) (N/cm)	Peel Strength (% Coh.Fail.)	Hardness (Shore A ₂)	Volume Change (%)
MIL-S-8802D PS 890 B-2	Original	385	2.7	370	43.5	76.2	46	---
	7 days @ R.T. in JP-9	347	2.4	365	31.0	54.3	45	2.9
	7 days @ 140°F(60°C) in JP-9	345	2.4	370	38.7	67.8	43	4.1
	1 mo. @ 140°F(60°C) in JP-9	415	2.9	280	34.0	59.5	42	2.1
	3 mo. @ 140°F(60°C) in JP-9	380	2.6	300	40.7	71.3	47	1.6
	6 mo. @ R.T. in JP-9	354	2.4	333	35.0	61.3	49	0.15
	6 mo. @ 140°F(60°C) in JP-9	342	2.4	325	37.8	66.2	45	0.84
	9 mo. @ 140°F(60°C) in JP-9	360	2.5	341	32.9	57.6	43	0.80
	12 mo. @ 140°F(60°C) in JP-9	350	2.4	293	30.1	52.7	43	0.15
	Original	437	3.0	174	28.2	49.4	68	---
	7 days @ R.T. in JP-9	382	2.6	209	27.1	47.5	62	3.0
	7 days @ 140°F(60°C) in JP-9	307	2.1	192	29.4	51.5	56	2.3
MIL-S-8802D PR-1422 B-2	1 mo. @ 140°F(60°C) in JP-9	231	1.6	159	33.8	59.2	57	2.4
	3 mo. @ 140°F(60°C) in JP-9	246	1.7	96	39.5	69.2	63	-6.7
	6 mo. @ R.T. in JP-9	313	2.2	162	31.7	55.5	56	3.8
	6 mo. @ 140°F(60°C) in JP-9	245	1.7	81	29.4	51.5	62	-11.0
	9 mo. @ 140°F(60°C) in JP-9	317	2.2	84	33.0	57.8	68	-10.0
	12 mo. @ 140°F(60°C) in JP-9	280	1.9	69	22.6	37.8	67	-9.8

of its original at the nine and 12-month conditions. The seven days at 140°F (60°C), seven days at room temperature, and six months at room temperature condition, however, showed a significant increase in elongation, having three to four times the original values.

The nylon material was not significantly affected in tensile strength by any of the conditions, but showed a noticeable decrease in elongation. The Uniroyal US566RL bladder material showed no change in tensile strength and only slight to moderate changes in elongation.

Neither the Uniroyal US566RL bladder material nor the FT-99 (a Buna-N material) showed any significant change in any of the aging conditions. The failure mode was almost totally adhesive for all specimens, with the original specimens of the FT-99 material showing only five percent cohesive failure. Data from the above tests are shown in Table 55.

Permeability tests were run on FT-99, US566RL (complete construction) and US566RL (liner/barrier only) according to MIL-T-6396C using two different sealing materials, PLIC and nylon. All specimens had less than the maximum allowable diffusion rate of 0.025 fl.oz./sq.ft. (8 ml/m²) per 24 hours. The only noticeable effect on any specimens was in that the FT-99 material had a slightly higher diffusion rate with the nylon than with the PLIC. Permeability data are presented in Table 56.

3.6 CHALKING OF MIL-S-83430 FUEL TANK SEALANTS

Chalking of MIL-S-83430 fuel tank sealants in military aircraft was investigated. Tests to determine the causative factors in chalking were conducted on four different sealants in various fuel mixtures. The four sealants evaluated were Pro Seal 899, Pro Seal 890, Products Research PR-1750, and PR-1422. The fuel mixtures used Jet Reference Fluid blended by UDRI, Jet Reference Fluid blended by Phillips Industries, and JP-4 aircraft fuel with various controlled concentrations of mercaptan.

AD-A085 859

DAYTON UNIV OH RESEARCH INST

F78 11/4

QUICK REACTION EVALUATION OF MATERIALS FOR SYSTEMS APPLICATIONS--ETC (11)

APR 80 D R ASKINS, R R CERVAY, D L HART

F33615-78-C-5002

UNCLASSIFIED

UDR-TR-80-12

AFMIL-TR-80-4025

NL

3 of 4

ALL INFORMATION CONTAINED HEREIN IS UNCLASSIFIED

DATE 11-11-80 BY 1045

1045

TABLE 55
ELASTOMERS/JP-9 COMPATIBILITY EVALUATION
SHEET MATERIALS

Tensiles				
Material	Condition	Tensile Str. (psi)	(MPa)	Elongation (%)
Goodyear 52904 Buna-N	Original	1219	8.4	664
	7 days @ R.T. in JP-9	852	5.9	443
	7 days @ 140°F(60°C) in JP-9	722	5.0	359
	1 mo. @ 140°F(60°C) in JP-9	783	5.4	452
	3 mo. @ 140°F(60°C) in JP-9	703	4.8	453
	6 mo. @ R.T. in JP-9	827	5.7	536
	6 mo. @ 140°F(60°C) in JP-9	751	5.2	421
	9 mo. @ 140°F(60°C) in JP-9	803	5.5	410
	12 mo. @ 140°F(60°C) in JP-9	690	4.8	321
Nylon	Original	9788	67.5	78
	7 days @ R.T. in JP-9	9792	67.5	341
	7 days @ 140°F(60°C) in JP-9	9613	66.3	288
	1 mo. @ 140°F(60°C) in JP-9	10464	72.1	49
	3 mo. @ 140°F(60°C) in JP-9	10381	71.6	34
	6 mo. @ R.T. in JP-9	9472	65.3	259
	6 mo. @ 140°F(60°C) in JP-9	12444	85.8	32
	9 mo. @ 140°F(60°C) in JP-9	12250	84.5	11
	12 mo. @ 140°F(60°C) in JP-9	12310	84.9	13
Teflon	Original	1843	12.7	409
	7 days @ R.T. in JP-9	1965	13.5	242
	7 days @ 140°F(60°C) in JP-9	1862	12.8	268
	1 mo. @ 140°F(60°C) in JP-9	1783	12.3	336
	3 mo. @ 140°F(60°C) in JP-9	1826	12.6	303
	6 mo. @ R.T. in JP-9	1915	13.2	288
	6 mo. @ 140°F(60°C) in JP-9	1875	12.9	265
	9 mo. @ 140°F(60°C) in JP-9	1927	13.3	261
	12 mo. @ 140°F(60°C) in JP-9	1670	11.5	261
Uniroyal Bladder Mtl. US566RL	Original	11567	79.7	41
	7 days @ R.T. in JP-9	10711	73.8	31
	7 days @ 140°F(60°C) in JP-9	10613	73.2	21
	1 mo. @ 140°F(60°C) in JP-9	10470	72.2	44
	3 mo. @ 140°F(60°C) in JP-9	11174	77.0	48
	6 mo. @ R.T. in JP-9	11001	75.8	36
	6 mo. @ 140°F(60°C) in JP-9	10249	70.7	31
	9 mo. @ 140°F(60°C) in JP-9	10769	74.2	29
	12 mo. @ 140°F(60°C) in JP-9	10723	73.9	37

TABLE 55 (Concluded)
ELASTOMERS/JP-9 COMPATIBILITY EVALUATION
SHEET MATERIALS

Seam Adhesion				
Material	Condition	Peel Strength (P.I.W.)(N/cm)		Fail.Mode (% Coh.)
Uniroyal Bladder Mtl. US566RL	Original	13.1	22.9	0
	7 days @ R.T. in JP-9	10.7	18.7	0
	7 days @ 140°F(60°C) in JP-9	8.7	15.2	0
	1 mo. @ 140°F(60°C) in JP-9	13.4	23.5	0
	3 mo. @ 140°F(60°C) in JP-9	12.9	22.6	0
	6 mo. @ R.T. in JP-9	14.3	25.0	0
	6 mo. @ 140°F(60°C) in JP-9	14.3	25.0	0
	9 mo. @ 140°F(60°C) in JP-9	12.2	21.4	0
	12 mo. @ 140°F(60°C) in JP-9	10.8	18.9	0
Buna-N FT-99	Original	13.5	23.6	5
	7 days @ R.T. in JP-9	11.2	19.6	0
	7 days @ 140°F(60°C) in JP-9	11.9	20.8	0
	1 mo. @ 140°F(60°C) in JP-9	11.7	20.5	0
	3 mo. @ 140°F(60°C) in JP-9	13.0	22.8	0
	6 mo. @ R.T. in JP-9	12.3	21.5	0
	6 mo. @ 140°F(60°C) in JP-9	12.1	21.2	0
	9 mo. @ 140°F(60°C) in JP-9	11.1	19.4	0
	12 mo. @ 140°F(60°C) in JP-9	10.8	18.9	0

TABLE 56
ELASTOMERS/JP-9 COMPATIBILITY
PERMEABILITY EVALUATIONS

Material	Seal	Diffusion Rate (Fl.Oz./ft ² /24 hrs)
FT-99	PLIC	0.0062
		0.0111
	Nylon	0.0233
		0.0095
US 566 RL Complete Construction	PLIC	0.0074
		0.0079
	Nylon	0.0038
		0.0136
US 566 RL Liner/Barrier	PLIC	0.0071
		0.0066
	Nylon	0.0057
		0.0049

The initial tests were run in JRF and JRF/SW solutions in both Phillips' and University of Dayton's JRF. The Phillips' JRF was two years old and University of Dayton JRF was freshly mixed. All sealants and fluids are listed in Table 57. None of the Pro Seal sealants showed any chalking in the JRF blended by the University of Dayton. In the Phillips' JRF the PS-890 B-2, accelerated cure, started chalking in the JRF and JRF/SW solutions on the second day and the PS-890 B-2 cured for 14 days started chalking in the JRF and JRF/SW solutions on the fourth day. PR-1422 B-2, accelerated cure, did not chalk in JRF or JRF/SW; PR-1750 B-2, batch #C25041, accelerated cure, had no chalking in the JRF, but in the JRF/SW solution it had some very light spots. PR-1750 B-2, batch #C95027, accelerated cure and 14-day cure, showed some very light white spots in the JRF and JRF/SW solutions. PR-1750 and PR-1422 were aged in University of Dayton JRF only. The tests were run for nine days at 140°F (60°C) with six fluid changes. The data are given in Table 58.

In the second phase of testing, cadmium plated fasteners (QQ-P-416, Class 2, Type II) were added to the JRF blended by the University of Dayton and the JP-4 fuels with mercaptan levels of 0.000 percent, 0.001 percent, 0.003 percent, and 0.005 percent. The only sealant evaluated was Pro Seal 899 B-2. The initial chalking tests were started on September 23, 1978. The fluids were changed every day for one month and no chalking was observed. After 30 days another set of specimens was started and both sets were run with no change of fluid. After eight days very slight chalking was noticed on seven of the specimens. Of the original seven specimens that had shown slight chalking, five of the specimens showed increasing amounts of chalking, while two specimens did not exhibit any increase in chalking. The two specimens showing no increase were JP-4, Cad/0.001 percent started September 25, 1978 and JP-4/rivet/0.003 percent started October 23, 1978. Six more specimens started to chalk after November 10, 1978. Of the 13 specimens that chalked, all the fluids except two contained cadmium fasteners with varying percentages of mercaptan. The two fluids which didn't contain cadmium were JRF and JP-4 with 0.001 percent mercaptan.

TABLE 57
SEALANT CHALKING TESTS

Sealants

PR-1422 B-2	- Accelerated cure
PR-1750 B-2, Batch C95027	- Accelerated cure
PR-1750 B-2, Batch C95027	- 14 day cure
PR-1750 B-2, Batch C25041	- Accelerated cure
PS-890 B-2, Batch C85253	- Accelerated cure
PS-890 B-2, Batch C85253	- Accelerated cure (Phillips JRF)
PS-899 B-2, Batch S607R	- Available specimens
PS-899 B-2, Batch C732205	- Available specimens
PS-899 B-2, Batch C848223	- Accelerated cure
PS-899 B-2, Batch C848223	- 14 day cure
PS-899 B-2, Batch C848223	- 14 day cure (JRF/Cadmium)
PS-899 B-2, Batch C848223	- 14 day cure (JP-4/Cadmium)
PS-899 B-6, Batch 1098	- Available specimens
F-16 Fuel Tank Sealant	(Lo temp flex)

Fluids

Jet Reference Fluid formulated by UDRI
 Jet Reference Fluid formulated by Phillips Industries
 JP-4 fuel
 JP-4 fuel with 0.001% mercaptan
 JP-4 fuel with 0.003% mercaptan
 JP-4 fuel with 0.005% mercaptan
 Jet Reference Fluid/salt water

Hardware

Aircraft bolts and nuts, cadmium plated per QQ-P-416,
 Class 2, Type II

Chalking Tests

Chalking tests are conducted by immersing sealant specimens in fluid or fluid/hardware combinations for a minimum of nine days at 140°F (60°C) in original fluid plus six fluid changes.

TABLE 58
RESULTS OF CHALKING TESTS

Fluid	Date Chalking Noted
JRF/Cad.	No change (29 days) 11/2/78 (9 days)
JRF/Cad.	11/2/78 (10 days)
JP-4/Cad.	No change (29 days)
0.003% merc.	11/2/78 (9 days)
JP-4/Cad.	No change (29 days)
0.005% merc.	11/2/78 (9 days)
JP-4/Cad. Rivet 0.005% merc.	11/2/78 (10 days)
JP-4/Cad. Rivet 0.003% merc.	11/3/78 (11 days)
JP-4/Cad. 0.001% merc.	11/10/78 (17 days)
JRF	No change (29 days) 11/15/78 (22 days)
JP-4/Cad. 0.005% merc.	11/15/78 (22 days)
JP-4/Cad. 0.003% merc.	11/15/78 (22 days)
JP-4/Cad. 0.001% merc.	11/17/78 (24 days)
JP-4/Cad.	No change (29 days) 12/15/78 (52 days)
JP-4 0.001% merc.	12/15/78 (53 days)

Three specimens showed more rapid chalking than the remaining 10 of 13 specimens that exhibited chalking. These three specimens were in JP-4/Cad/0.005 percent, started September 25, 1978; JP-4/Cad/0.001 percent, started October 23, 1978; and JP-4/Cad/0.003 percent, started October 23, 1978.

The fluids containing chalking specimens were checked for mercaptan content on December 1, 1978. All fluids were low in mercaptan. All JP-4 containers were topped with fresh JP-4 containing 0.005 percent mercaptan. Sealant specimens that had chalked but showed no increase in chalking in the original JP-4, underwent increased chalking after the addition of JP-4/0.005 percent mercaptan. Specimens in JRF/Cadmium fluids also showed increased chalking after the addition of fresh JRF to the containers.

3.7 CHALKING OF SEALANTS IN TURBINE FUELS CONTAINING ANTI-STATIC ADDITIVES

Two MIL-S-8802D sealants, PS-890 B-2 and PR-1422 B-2, and one MIL-S-83430 sealant, PS-899 B-2, were evaluated for chalking in a number of fluid blends: (1) JP-4, (2) JP-4 with 2 ppm ASA-3, (3) JP-4 with 2 ppm Stadis 450, (4) equal portions of #2 and #3 fluids, (5) JP-8, (6) JP-8 with 2 ppm ASA-3, (7) JP-8 with 2 ppm Stadis 450, and (8) Equal portions of #6 and #7 fluids.

The chalking specimens were 1/8 inch by 1/8 inch by 5 inches (3 mm by 3 mm by 127 mm) in size with four specimens per 900 ml of fluid. There are two quarts of each fluid being run per sealant with one quart being changed every seven days and the other quart having the same fluid for the duration of test. The specimens were aged for 84 days at 140°F (60°C) and checked for chalking every seven days. After 84 days, there was no evidence of chalking on either of the MIL-S-8802D sealants or on the MIL-S-83430 sealant.

3.8 MIL-S-83430C SEALANT EVALUATION ON MIL-C-27725 and MIL-P-23377 COATINGS

Two MIL-S-83430C sealants, Pro Seal 899 and Product Research 1750, were evaluated for their peel strength and adhesion properties to MIL-C-27725 (urethane), MIL-P-23377 (epoxy) (standard cure), and MIL-P-23377 (two hours at 200°F (93°C) cure) coatings.

The MIL-S-83430 sealant panels were cured for 48 hours at standard conditions and 24 hours at 140°F (60°C). After curing the peel panel test specimens, the MIL-C-27725 coated panels were conditioned for seven and 70 days at 140°F (60°C) in Jet Reference Fluid (JRF) and JRF/salt water (SW) and the MIL-P-23377 coated panels were conditioned for seven days at 140°F (60°C) in salt water.

Seven batches of PS-899 B-2 C848223, C847084, C847104, C84926, C84891, C85432, and C85251; three batches of PS-899 B-6 C84839, C84848, and C85374; two batches of PS-899 A-12, C84874 and C846982; and one batch each of PS-899 B-1/2, C849223, PS-899 A-2, C745162, and PR-1750 B-2, C25041.

All the sealants had no difficulty in bonding to the MIL-C-27725 coating after conditioning for seven days and 70 days in JRF and JRF/SW. On the MIL-P-23377 standard cure and 200°F (93°C) cure panels all of the sealants had various degrees of difficulty in adhering to the surface. To determine if the problem was inherent in the sealants or in the coating, MIL-P-23377, panels were obtained from different manufacturers; Kappers Company, Inc., Atlas Paint and Varnish Company, Products/Techniques, Inc., Deft Chemical Coatings, Lemar, Inc., Dexter Corporation-Midland Division, and Advanced Coatings and Chemicals. Peel panels were prepared using Pro Seal 899B-2, Batch C848223/C848323, and were cured for 14 days at 78°F (25.6°C) and 50 percent relative humidity. After curing, the panels were conditioned for seven days at 140°F (60°C) in a three percent saltwater solution. All panels exhibited 100 percent cohesive failure with the exception of one panel having the Deft Chemical MIL-P-23377D coating which was 95 percent cohesive. Results are shown in Tables 59 and 60.

TABLE 59
EVALUATION OF MIL-P-23377D PANELS

Panel	Coating Manufacturer	Conditioning	Load		Failure Mode (% Cohesive)
P-3	Koppers Company, Inc.	7 days @ 140°F (60°C) in saltwater	54.5 <u>54.3</u> 54.4	95.4 <u>95.1</u> 95.2	100 100
P-5	Atlas Paint & Varnish Co.	7 days @ 140°F (60°C) in saltwater	53.7 <u>56.2</u> 55.0	94.0 <u>98.4</u> 96.2	100 100
P-7	Products/Techniques, Inc.	7 days @ 140°F (60°C) in saltwater	49.6 <u>52.6</u> 51.1	86.9 <u>92.1</u> 89.5	100 100
P-10	Deft Chemical Coatings	7 days @ 140°F (60°C) in saltwater	57.6 <u>63.0</u> 60.3	100.9 <u>110.3</u> 105.6	100 95
P-15	Lemmar, Inc.	7 days @ 140°F (60°C) in saltwater	59.2 <u>56.5</u> 57.9	103.7 <u>98.9</u> 101.4	100 100
P-16	Dextar Corporation- Midland Division	7 days @ 140°F (60°C) in saltwater	64.3 <u>59.5</u> 61.9	112.6 <u>104.2</u> 108.4	100 100
P-20	Advanced Coatings and Chemicals	7 days @ 140°F (60°C) in saltwater	59.4 <u>62.9</u> 61.2	104.0 <u>110.2</u> 107.1	100 100

TABLE 60
MIL-S-83430 SEALANT EVALUATION
ON MIL-C-27725 AND MIL-P-23377 COATING

Sealant	Conditioning	Panel Coating	Peel Strength (P.I.W.) (N/cm)		Failure Mode (% Coh.)
PS-899 B-2 #C848223	7 days @ 140°F (60°C)/SW	MIL-P-23377 (GD) (Std)	59.0	103.3	100
PR-1750 B-2 #C25041	7 days @ 140°F (60°C)/SW	MIL-P-23377 (GD) (Std)	58.0	101.5	100*
PS-899 B-2 #C84926	7 days @ 140°F (60°C)/JRF	MIL-C-27725	29.9	52.4	100
PS-899 B-2 #C84926	7 days @ 140°F (60°C)/JRF/SW	MIL-C-27725	39.0	68.3-JRF	100
			45.7	80.0-SW	100
PS-899 B-2 #C84926	7 days @ 140°F (60°C)/SW	MIL-P-23377 [200°F (93°C) cure]	60.7	106.3	100
PS-899 B-2 #C84926	7 days @ 140°F (60°C)/SW	MIL-P-23377 (Std. cure)	8.3	14.5	0
PS-899 B-2 #C847104	7 days @ 140°F (60°C)/JRF	MIL-C-27725	26.1	45.7	90
PS-899 B-2 #C847104	7 days @ 140°F (60°C)/JRF/SW	MIL-C-27725	36.3	63.6-JRF	100
			45.9	80.4-SW	100
PS-899 B-2 #C847104	7 days @ 140°F (60°C)/SW	MIL-P-23377 (Std. cure)	5.7	10.0	0
PS-899 B-2 #C847104	7 days @ 140°F (60°C)/SW	MIL-P-23377 [200°F (93°C) cure]	59.6	104.4	90
PS-899 B-2 #C847084	7 days @ 140°F (60°C)/JRF	MIL-C-27725	23.0	40.3	95
PS-899 B-2 #C847084	7 days @ 140°F (60°C)/JRF/SW	MIL-C-27725	34.5	60.4-JRF	100
			35.9	62.9-SW	100
PS-899 B-2 #C847084	7 days @ 140°F (60°C)/SW	MIL-P-23377 [200°F (93°C) cure]	48.9	85.6	80
PS-899 B-2 #C847084	7 days @ 140°F (60°C)/SW	MIL-P-23377 (Std. cure)	2.5	4.4	0

*MIL-C-23377 coating pulled from panel ~20%.

TABLE 60 (Continued)
MIL-S-83430 SEALANT EVALUATION
ON MIL-C-27725 AND MIL-P-23377 COATING

Sealant	Conditioning	Panel Coating	Peel Strength (P.I.W.) (N/cm)		Failure Mode (% Coh.)
PS-899 A-12 #C84874	7 days @ 140°F (60°C)/JRF	MIL-C-27725	22.6	39.6	100
PS-899 A-12 #C84874	7 days @ 140°F (60°C)/JRF/SW	MIL-C-27725	31.1 35.4	54.4-JRF 62.0-SW	100 100
PS-899 A-12 #C84874	7 days @ 140°F (60°C)/SW	MIL-P-23377 (Std. cure)	30.3	53.1	80
PS-899 A-12 #C84874	7 days @ 140°F (60°C)/SW	MIL-P-23377 [200°F(93°C) cure]	32.2	56.4	100
PS-899 B-2 #C848223	7 days @ 140°F (60°C)/JRF	MIL-C-27725	23.1	40.4	100
PS-899 B-2 #C848223	7 days @ 140°F (60°C)/JRF/SW	MIL-C-27725	40.1 40.1	70.2-JRF 70.2-SW	100 100
PS-899 B-2 #C848223	7 days @ 140°F (60°C)/SW	MIL-P-23377 [200°F(93°C) cure]	50.2	87.9	100
PS-899 B-2 #C848223	7 days @ 140°F (60°C)/SW	MIL-P-23377 (Std. cure)	3.0	5.3	0
PS-899 B-2 #C848223	7 days @ 140°F (60°C)/JRF	MIL-C-27725	43.0	75.3	100
PS-899 B-2 #C848223	7 days @ 140°F (60°C)/JRF/SW	MIL-C-27725	39.4 41.1	69.0-JRF 72.0-SW	100 100
PS-899 B-2 #C848223	7 days @ 140°F (60°C)/SW	MIL-P-23377 (Std. cure)	4.4	7.7	0
PS-899 B-2 #C848223	7 days @ 140°F (60°C)/SW	MIL-P-23377 [200°F(93°C) cure]	11.4	20.0	10
PR-1750 B-2 #C25041	7 days @ 140°F (60°C)/JRF	MIL-C-27725	23.8	41.7	100
PR-1750 B-2 #C25041	7 days @ 140°F (60°C)/JRF/SW	MIL-C-27725	20.6 19.3	36.1-JRF 33.8-SW	100 75

TABLE 60 (Continued)
MIL-S-83430 SEALANT EVALUATION
ON MIL-C-27725 AND MIL-P-23377 COATING

Sealant	Conditioning	Panel Coating	Peel Strength (P.I.W.) (N/cm)		Failure Mode (% Coh.)
PR-1750 B-2 #C25041	7 days @ 140°F (60°C)/SW	MIL-P-23377 (R.T. cure)	42.0	73.5	75
PR-1750 B-2 #C25041	7 days @ 140°F (60°C)/SW	MIL-P-23377 [200°F(93°C) cure]	39.4	69.0	67
PS-899 A-2 #C745162	7 days @ 140°F (60°C)/JRF	MIL-C-27725	13.6	23.8	100
PS-899 A-2 #C745162	7 days @ 140°F (60°C)/JRF/SW	MIL-C-27725	18.6	32.6-JRF	100
			24.6	43.1-SW	100
PS-899 A-2 #C745162	7 days @ 140°F (60°C)/SW	MIL-P-23377 (Std. cure)	32.7	57.3	85
PS-899 A-2 #C745162	7 days @ 140°F (60°C)/SW	MIL-P-23377 [200°F(93°C) cure]	39.8	69.7	100
PS-899 A-12 #C846982	7 days @ 140°F (60°C)/JRF	MIL-C-27725	18.4	32.2	100
PS-899 A-12 #C846982	7 days @ 140°F (60°C)/JRF/SW	MIL-C-27725	38.0	66.5-JRF	100
			39.0	68.3-SW	100
PS-899 A-12 #C846982	7 days @ 140°F (60°C)/SW	MIL-P-23377 (Std. cure)	5.0*	8.8	15
PS-899 A-12 #C846982	7 days @ 140°F (60°C)/SW	MIL-P-23377 [200°F(93°C) cure]	39.7	69.5	100
PS-899 B-1/2 #C849223	7 days @ 140°F (60°C)/JRF	MIL-C-27725	24.2	42.4	100
PS-899 B-1/2 #C849223	7 days @ 140°F (60°C)/JRF/SW	MIL-C-27725	42.1	73.7-JRF	100
			43.1	75.5-SW	100
PS-899 B-1/2 #C849223	7 days @ 140°F (60°C)/SW	MIL-P-23377 (Std. cure)	1.0	1.8	0
PS-899 B-1/2 #C849223	7 days @ 140°F (60°C)/SW	MIL-P-23377 [200°F(93°C) cure]	2.0	3.5	0

*Had one peak load of 37.0 lbs. - dropped from average.

TABLE 60 (Continued)
MIL-S-83430 SEALANT EVALUATION
ON MIL-C-27725 AND MIL-P-23377 COATING

Sealant	Conditioning	Panel Coating	Peel Strength (P.I.W.) (N/cm)		Failure Mode (% Coh.)
PS-899 B-2 #C84891	7 days @ 140°F (60°C)/JRF	MIL-C-27725	14.4	25.2	100
PS-899 B-2 #C84891	7 days @ 140°F (60°C)/JRF/SW	MIL-C-27725	25.5	44.6-JRF	100
			27.1	47.4-SW	100
PS-899 B-2 #C84891	7 days @ 140°F (60°C)/SW	MIL-P-23377 (Std. cure)	20.8	36.4	100
PS-899 B-2 #C84891	7 days @ 140°F (60°C)/SW	MIL-P-23377 (Std. cure)	37.2	65.1	100
PS-899 B-6 #C84839	7 days @ 140°F (60°C)/JRF	MIL-C-27725	36.0	63.0	100
PS-899 B-6 #C84839	7 days @ 140°F (60°C)/JRF/SW	MIL-C-27725	23.1	40.4-JRF	100
			37.1	65.0-SW	100
PS-899 B-6 #C84839	7 days @ 140°F (60°C)/SW	MIL-P-23377 (Std. cure)	6.8	11.9	5
PS-899 B-6 #C84839	7 days @ 140°F (60°C)/SW	MIL-P-23377 [200°F(93°C) cure]	25.5	44.6	85
PS-899 B-6 #C84848	7 days @ 140°F (60°C)/JRF	MIL-C-27725	24.9	43.6	100
PS-899 B-6 #C84848	7 days @ 140°F (60°C)/JRF/SW	MIL-C-27725	29.3	51.3-JRF	100
			36.9	64.6-SW	100
PS-899 B-6 #C84848	7 days @ 140°F (60°C)/SW	MIL-P-23377 (GD) (Std)	54.0	94.6	100
PS-899 B-6 #C84848	7 days @ 140°F (60°C)/SW	MIL-P-23377 [200°F(93°C) cure]	49.2	86.1	100
PS-899 B-6 #C85374	7 days @ 140°F (60°C)/JRF	MIL-C-27725	20.5	36.9	100
PS-899 B-6 #C85374	7 days @ 140°F (60°C)/JRF/SW	MIL-C-27725	25.1	44.0-JRF	100
			29.0	50.8-SW	100

TABLE 60 (Concluded)
MIL-S-83430 SEALANT EVALUATION
ON MIL-C-27725 AND MIL-P-23377 COATING

Sealant	Conditioning	Panel Coating	Peel Strength (P.I.W.) (N/cm)		Failure Mode (% Coh.)
PS-899 B-2 #C85251	7 days @ 140°F (60°C)/JRF	MIL-C-27725	27.6	48.3	100
PS-899 B-2 #C85251	7 days @ 140°F (60°C)/JRF/SW	MIL-C-27725	27.7 39.2	48.3-JRF 68.6-SW	100 100
PS-899 B-2 #C85432	7 days @ 140°F (60°C)/JRF	MIL-C-27725	25.2	44.1	100
PS-899 B-2 #C85432	7 days @ 140°F (60°C)/JRF/SW	MIL-C-27725	29.0 38.3	50.8-JRF 67.1-SW	100 100
PR-1750 B-2 #C25041	70 days @ 140°F (60°C)/JRF	MIL-C-27725	24.4	42.7	100
PR-1750 B-2 #C25041	70 days @ 140°F (60°C)/JRF/SW	MIL-C-27725	29.4 27.0	51.5-JRF 47.7-SW	100 100
PS-899 B-2 #C848223	70 days @ 140°F (60°C)/JRF	MIL-C-27725	21.0	36.8	100
PS-899 B-2 #C848223	70 days @ 140°F (60°C)/JRF/SW	MIL-C-27725	31.8 27.2	55.7-JRF 47.6-SW	100 100

3.9 PURGING FLUIDS

The volume change characteristics of elastomeric materials were evaluated in three purging fluids, JP-5, JP-5 with 10 percent MIL-L-6082 grade 1065 oil, and Soltrol 220. The elastomeric materials evaluated were Pro Seal 890 B-2 (MIL-S-8802D) and Product Research PR-1221 B-2 (MIL-S-7502) sealants, Precision 7866 (MIL-P-5315, Buna-N) and Precision 11647 (MIL-R-25988, fluorosilicone) O-rings; Products Research PR-703 and Dow Corning 94-031 channel sealants, CL-1 GR60 PMP, AMS 3227 PMP, KK-125 PMP, and 17466 Kirkill marmon clamps.

The elastomeric materials were immersed in JP-4 for seven days at 77°F (25°C), after which their volume changes were measured. The materials were then immersed in one each of the purging fluids for eight hours at 77°F (25°C), and their volume changes were again measured. The materials were then held in air at 77°F (25°C) and 50 percent relative humidity and their volume changes measured after one, seven, 30, and 60 days. After 60 days the materials were reimmersed in JP-4 for seven days at 77°F (25°C) and their volume changes again measured.

In the JP-5 and JP-5/oil purging fluid all materials showed a decrease in swell except the PR-703 channel sealant after eight hours. After drying for 60 days at 77°F (25°C) all the materials had a negative swell except the PR-703 channel sealant in the JP-5 purging fluid. After reimmersion in JP-4 for an additional week, all the materials' volume swells returned to their original swell except the MIL-S-8802D and MIL-S-7502 fuel tank sealants. These two materials still had negative volume swells.

In the Soltrol 220 purging fluid all the materials had a decrease in volume swell. After air drying for 60 days at 77°F (25°C) all the materials had a negative volume swell; however, after reimmersion in JP-4 for seven days at 77°F (25°C) all the materials regained their original volume swell except the MIL-S-8802D and MIL-S-7052 sealants. These two materials still had negative volume swells. Results are presented in Tables 61 and 62.

TABLE 61
EVALUATION OF ELASTOMERIC MATERIALS IN JP-4/SOLTROL 220

Material	After JP-4	Soltrol- Init.	Volume Swell - %				60 day Post	Addit. JP-4
			1 day Post	1 wk Post	30 day Post			
94-031 Groove Sealant	2.7	0.2	-2.8	-3.3	-3.3	-3.9	1.9	
PR-703 Groove Sealant	4.0	3.4	0.7	-2.4	-2.2	-2.5	3.0	
PR-1221 B-2 MIL-S-7502 Sealant	1.5	0.5	-0.7	-2.9	-4.1	-4.8	-2.2	
PS-890 B-2 MIL-S-8802D Sealant	0.8	0.4	-0.7	-2.3	-3.5	-3.8	-1.4	
Precision 7866 MIL-P-5315 O-ring	15.0	2.6	-6.0	-10.7	-13.1	-14.8	11.7	
Precision 11647 MIL-R-25988 O-ring	7.7	4.5	0.9	-0.7	-0.9	-0.3	7.2	
KK-125 Marmon clamp	106.0	44.0	28.0	12.9	-2.4	-9.3	107.1	

Conditioning Cycle: 7 Days @ R.T. in JP-4 + 8 Hrs. @ R.T. in Soltrol 220
+ 60 Days Air-Dry @ R.T. + 7 Days @ R.T. in JP-4

TABLE 62
VOLUME CHANGE DETERMINATION ON ELASTOMERS IN JP-5

Material	Condition	% Vol. Swell After JP-4	% Vol. Swell After 8 hrs.	% Vol. Swell 1 day post	% Vol. Swell 1 week post	% Vol. Swell 30 day post	% Vol. Swell 60 day post	% Vol. Swell Addtl. 1 wk./JP-4
PR-1221 B-2 MIL-S-7502 sealant	7 days in JP-4 @ R.T. + 8 hrs. in JP-5 @ R.T.	-0.64	-1.35	-3.40	-5.76	-7.63	-8.46	-12.27
	7 days in JP-4 @ R.T. + 8 hrs. in 90% JP-5/10% MIL-L-6082 oil @ R.T.	-0.84	-1.28	-3.25	-5.58	-7.39	-8.25	-5.49
	7 days in JP-4 @ R.T. + 8 hrs. in JP-5 @ R.T.	0.93	0.82	-0.47	-2.12	-3.44	-4.00	-1.71
	7 days in JP-4 @ R.T. + 8 hrs. in 90% JP-5/10% MIL-L-6082 oil @ R.T.	1.23	0.71	-0.38	-2.01	-3.48	-4.02	-1.54
94-031 P-15 fuel tank sealant	7 days in JP-4 @ R.T. + 8 hrs. in JP-5 @ R.T.	5.51	2.08	*	-2.60	-2.34	-3.35	3.04
	7 days in JP-4 @ R.T. + 8 hrs. in 90% JP-5/10% MIL-L-6082 oil @ R.T.	5.43	2.50	-1.44	-2.74	-2.14	-3.29	3.41
	7 days in JP-4 @ R.T. + 8 hrs. in JP-5 @ R.T.	2.88	3.25	*	-1.13	-2.11	-2.17	2.37
	7 days in JP-4 @ R.T. + 8 hrs. in 90% JP-5/10% MIL-L-6082 oil @ R.T.	3.43	3.52	1.02	-2.12	-2.22	-1.90	2.60
KK-125 PMP maroon clamp	7 days in JP-4 @ R.T. + 8 hrs. in JP-5 @ R.T.	93.00	87.35	50.29	1.67	-13.08	-14.80	91.40
	7 days in JP-4 @ R.T. + 8 hrs. in 90% JP-5/10% MIL-L-6082 oil @ R.T.	92.19	79.17	45.74	10.45	-5.88	-10.13	90.67

* Wide scatter - probable weighing error.

TABLE 62 (Concluded)
VOLUME CHANGE DETERMINATION ON ELASTOMERS IN JP-5

Material	Condition	% Vol. Swell After JP-4	% Vol. Swell After 8 hrs.	% Vol. Swell 1 day post	% Vol. Swell 1 wk post	% Vol. Swell 30 day post	% Vol. Swell 60 day post	% Vol. Swell Addtl. 1 wk./JP-4
17466 Kirkhill marmon clamp	7 days in JP-4 @ R.T. + 8 hrs. in JP-5 @ R.T.	11.31	9.66	5.96	0.60	- 5.01	- 6.28	8.33
	7 days in JP-4 @ R.T. + 8 hrs. in 90% JP-5/10% MIL-L-6082 oil @ R.T.	12.57	9.97	5.38	-0.12	- 4.40	- 5.80	8.60
	7 days in JP-4 @ R.T. + 8 hrs. in JP-5 @ R.T.	14.14	11.81	6.84	-0.54	- 6.73	- 7.32	11.16
CL-1 GR60 PMP marmon clamp	7 days in JP-4 @ R.T. + 8 hrs. in 90% JP-5/10% MIL-L-6082 oil @ R.T.	14.69	11.18	5.84	-1.46	- 6.04	- 7.74	11.03
	7 days in JP-4 @ R.T. + 8 hrs. in JP-5 @ R.T.	12.96	11.24	7.59	1.25	- 3.74	- 5.48	9.32
	7 days in JP-4 @ R.T. + 8 hrs. in 90% JP-5/10% MIL-L-6082 oil @ R.T.	12.29	11.08	7.10	1.20	- 3.84	- 5.59	9.08
Precision 7866 O-rings MIL-P-5315	7 days in JP-4 @ R.T. + 8 hrs. in JP-5 @ R.T.	12.29	5.82	-4.39	-11.56	-14.89	-15.35	10.59
	7 days in JP-4 @ R.T. + 8 hrs. in 90% JP-5/10% MIL-L-6082 oil @ R.T.	11.84	4.98	-5.39	-11.76	-15.12	-15.26	10.45
	7 days in JP-4 @ R.T. + 8 hrs. in JP-5 @ R.T.	8.75	5.80	1.96	0.17	-0.0026	0.24	8.40
Precision 11647 MIL-R-25988	7 days in JP-4 @ R.T. + 8 hrs. in 90% JP-5/10% MIL-L-6082 oil @ R.T.	8.94	5.62	1.92	0.22	-0.0027	- 0.50	8.48

3.10 EVALUATION OF ALIPHATIC NAPHTHA IN MIL-C-38736 CLEANER

Because of environmental considerations, the replacement of aromatic naphtha, TT-N-97, Type I, with aliphatic naphtha, TT-N-95, Type II, in MIL-C-38736 cleaner had been proposed. To compare the adhesion of sealant on panels cleaned with a solvent mixture containing either aliphatic naphtha or aromatic naphtha, three different coatings were cleaned with each mixture. The three coatings were MIL-C-27725 (urethane), C-130 with old MIL-C-27725 and MIL-P-23377 (epoxy) coated panels cured two hours at 200°F (93°C). The peel panels were fabricated using both MIL-S-8802D (PR1422) and MIL-S-83430 (PS899) sealants. Eight panels of each type coating were cleaned with each MIL-C-38736 cleaner with four panels of each type coating being wiped dry and four panels of each type coating being allowed to evaporate. The peel panels were cured for 48 hours at standard conditions plus 24 hours at 140°F (60°C). After curing, half of the MIL-C-27725 coated panels and half of the C-130 panels were aged for seven days at 140°F (60°C) in Jet Reference Fluid. The remaining MIL-C-27725 and C-130 panels were aged for seven days at 140°F (60°C) in JRF/three percent SW. The MIL-P-23377 coated panels were aged for seven days at 140°F (60°C) in a three percent saltwater solution. The results, shown in Table 63, indicate that aliphatic naphtha is comparable to aromatic naphtha when used with PR1422 sealant on MIL-C-27725 coatings and with both PR1422 and PS899 sealants on MIL-C-23377 coatings. Aliphatic naphtha, however, is not comparable to aromatic naphtha on aged MIL-C-23377 coatings when used with a manganese dioxide cure sealant such as PS899.

3.11 CHANNEL SEALANTS

An extensive program was undertaken to evaluate six channel sealants under a variety of test conditions for the purpose of updating the military specification for channel sealants. Channel sealants used were General Electric G651 and G250; Dow Corning 94-011, 94-031, and X4-2805; and Products Research

TABLE 63
EVALUATION OF ALIPHATIC NAPHTHA IN
MIL-C-38736 CLEANER

MIL-C-27725 Panels
7 days @ 140°F (60°C) in JRF/S.W.

Material	Panel Cleaner	Peel Strength				Failure Mode (% Coh.)	
		(lbs/in width) JRF	(lbs/in width) S.W.	(N/cm width) JRF	(N/cm width) S.W.	JRF	S.W.
MIL-S-83430 PS899	Aliphatic Naptha (unwiped)	34.0	46.0	59.5	80.5	75	100
		38.0	37.0	66.5	64.8	75	100
		Avg 36.0	42.0	63.0	73.5		
	Aliphatic Naptha (wiped)	36.5	41.5	63.9	72.7	100	100
		33.5	43.5	58.7	76.2	100	100
		Avg 35.0	42.0	61.3	73.5		
	MIL-C-38736 (unwiped)	37.0	38.5	64.8	67.4	100	100
		34.0	42.0	59.5	73.5	100	100
		Avg 35.5	40.5	62.2	70.9		
	MIL-C-38736 (wiped)	36.0	37.7	63.0	66.0	100	100
		26.0	33.5	45.5	58.7	100	100
		Avg 31.0	33.6	54.3	58.8		
MIL-S-8802 PR1422	Aliphatic Naptha (unwiped)	21.0	23.0	36.8	40.3	100	100
		20.5	20.5	35.9	35.9	100	100
		Avg 20.7	21.7	36.2	38.0		
	Aliphatic Naptha (wiped)	22.5	25.0	39.4	43.8	100	100
		23.0	22.2	40.3	38.9	100	100
		Avg 22.7	23.6	39.7	41.3		
	MIL-C-38736 (unwiped)	21.5	22.3	37.6	39.0	100	100
		21.5	22.3	37.6	39.0	100	100
		Avg 21.5	22.3	37.6	39.0		
	MIL-C-38736 (wiped)	20.2	24.3	35.4	42.5	100	100
		20.5	22.8	35.9	39.9	100	100
		Avg 20.3	23.6	35.5	41.3		

TABLE 63 (Continued)
EVALUATION OF ALIPHATIC NAPHTHA IN
MIL-C-38736 CLEANER

C-130 panels (dark green)
7 days @ 140°F(60°C) in JRF/S.W.

Material	Panel Cleaner	Peel Strength				Failure Mode	
		(lbs/in width)		(N/cm width)		(% Coh.)	
		JRF	S.W.	JRF	S.W.	JRF	S.W.
MIL-S-83430 PS899	Aliphatic Naptha	0	0	0	0	0	0
	(unwiped)	<u>0</u>	<u>0</u>	<u>0</u>	<u>0</u>	0	0
	Avg	0	0	0	0		
	Aliphatic Naptha	0	0	0	0	0	0
	(wiped)	<u>0</u>	<u>0</u>	<u>0</u>	<u>0</u>	<u>0</u>	<u>0</u>
	Avg	0	0	0	0		
	MIL-C-38736	27.5	25.7	48.2	45.0	100	100
	(unwiped)	<u>30.3</u>	<u>25.0</u>	<u>53.1</u>	<u>43.8</u>	100	100
	Avg	28.9	25.4	50.6	44.5		
	MIL-C-38736	31.0	33.0	54.3	57.8	100	100
MIL-S-8802 PR1422	(wiped)	<u>32.0</u>	<u>28.5</u>	<u>56.0</u>	<u>49.9</u>	100	100
	Avg	31.5	30.7	55.2	53.8		
	Aliphatic Naptha	16.7	16.2	29.2	28.4	100	90
	(unwiped)	<u>19.0</u>	<u>20.0</u>	<u>33.3</u>	<u>35.0</u>	100	100
	Avg	17.9	18.1	31.3	31.7		
	Aliphatic Naptha	15.0	16.0	26.3	28.0	100	100
	(wiped)	<u>16.9</u>	<u>18.3</u>	<u>29.6</u>	<u>32.0</u>	100	100
	Avg	16.0	17.2	28.0	30.1		
	MIL-C-38736	24.0	24.5	42.0	42.9	100	100
	(unwiped)	<u>23.0</u>	<u>25.0</u>	<u>40.3</u>	<u>43.8</u>	100	100
	Avg	23.5	24.7	41.1	43.2		
	MIL-C-38736	20.0	22.0	35.0	38.5	100	100
	(wiped)	<u>23.0</u>	<u>24.3</u>	<u>40.3</u>	<u>42.5</u>	100	100
	Avg	21.5	23.2	37.6	40.6		

TABLE 63 (Concluded)
EVALUATION OF ALIPHATIC NAPHTHA IN
MIL-C-38736 CLEANER

MIL-P-23377 Panels
7 days @ 140°F(60°C) in S.W.

Material	Panel Cleaner	Peel Strength		Failure Mode (% Coh.) S.W.
		(lbs/in width) S.W.	(N/cm width) S.W.	
MIL-S-83430 PS899	Aliphatic Naptha (unwiped)	19.0 <u>39.3</u>	33.3 <u>68.8</u>	5 50
	Avg	29.2	51.1	
	Aliphatic Naptha (wiped)	59.3 <u>42.5</u>	103.8 <u>74.4</u>	100 100
	Avg	50.9	89.1	
	MIL-C-38736 (unwiped)	49.3 <u>53.8</u>	86.3 <u>94.2</u>	100 100
	Avg	51.6	90.4	
	MIL-C-38736 (wiped)	53.0 <u>48.3</u>	92.8 <u>84.6</u>	100 100
	Avg	50.6	88.6	
	Aliphatic Naptha (unwiped)	22.6 <u>25.1</u>	39.6 <u>44.0</u>	90 100
	Avg	23.8	41.7	
	Aliphatic Naptha (wiped)	19.7 <u>19.3</u>	34.5 <u>33.8</u>	100 100
	Avg	19.5	34.1	
MIL-S-8802 PR1422	MIL-C-38736 (unwiped)	17.0 <u>17.5</u>	29.8 <u>30.6</u>	100 100
	Avg	17.3	30.3	
	MIL-C-38736 (wiped)	17.4 <u>18.5</u>	30.5 <u>32.4</u>	100 100
	Avg	18.0	31.5	

Corporation PR-702. Tests included volume change, density, weight loss, flatwise tension, low temperature flexibility, pressure rupture, corrosion, nonvolatile content, thermal extrusion, and extrusion rate.

Volume change, density, and weight loss evaluations were all done on the same specimens, which were 0.060 inch by 1 inch by 2.5 inch (1.5 mm by 25.4 mm by 63.5 mm) sections of sealant applied to a 1 inch by 2.75 inch (25.4 mm by 70 mm) panel. Panels used were 6Al-4V titanium, 7075 Alclad Aluminum (QQ-A-250/13), MIL-C-27725, MIL-A-8625, and MIL-C-5541. The PR-702 and X4-2805 materials, received late in the program were evaluated on the MIL-C-5541 coating only. Agings were done in both JRF and Type I (Iso-octane) fluid at room temperature and at elevated temperatures (see Table 64). The G651 sealant was not tested in Type I fluid at the elevated temperature because it fell off the panels while aging. Complete data are presented in Table 65.

Flatwise tension specimens were fabricated using MIL-C-5541, 6Al-4V titanium, MIL-A-8625, 7075-T6 Al (QQ-A-250/13), and MIL-C-27725 panels. The X4-2805 material and combinations of the other sealants which were mixed to determine compatibility of the mixed materials were applied to MIL-C-27725 panels only. The mixtures of sealant were 50 percent each of two materials. The most noticeable drop in strength from the original to the aged specimens was shown on the 94-031, 94-011, and G250, while the most noticeable drop in failure mode (percent Coh) was on the G651 and the mixtures of G651 and G250 with other materials. The mixture of G651 and G250 showed no ill effects after aging. Results are shown in Table 66.

Low temperature flexibility tests were done on MIL-C-5541, 7075-T6 Al (QQ-A-250/13), MIL-A-8625, titanium and MIL-C-27725 panels. All materials passed in the original condition. The G250, 94-011, and 94-031 materials all passed the aged condition, although the G250 and 94-011 showed some bubbling. The G651

TABLE 64
CHANNEL SEALANTS
VOLUME CHANGE, DENSITY
AND WEIGHT LOSS

Conditions

- (1) 7 days @ R.T. in JRF
- (2) 7 days @ R.T. in Type I
- (3) 25 days @ 140°F (60°C) in Type I +
72 hrs @ 160°F (71°C) in Type I +
6 hrs @ 180°F (82°C) in Type I +
7 days @ 160°F (71°C) air-dry
- (4) 25 days @ 140°F (60°C) in JRF +
72 hrs @ 160°F (71°C) in JRF +
6 hrs @ 180°F (82°C) in JRF +
24 hrs @ 200°F (93°C) air-dry
- (5) 25 days @ 140°F (60°C) in JRF +
72 hrs @ 160°F (71°C) in JRF +
6 hrs @ 180°F (82°C) in JRF +
7 days @ 160°F (71°C) air-dry

TABLE 65
CHANNEL SEALANTS
VOLUME CHANGE, DENSITY, AND WEIGHT LOSS

Channel Sealant	Panel	Condition	Spec.	Density	Vol. Change(%)		Wt. Loss(%)
					After Fuel	After air-dry	After air-dry
G651	5541	(1)	1	1.48	18.6		
			2	1.44	20.2		
			3	1.46	16.2		
			4	1.47	16.7		
			5	1.48	16.6		
			Avg.	1.47	17.7		
	5541	(2)	1	1.48	4.1		
			2	1.48	5.3		
			3	1.48	4.8		
			4	1.47	4.2		
			5	1.48	3.5		
			Avg.	1.48	4.4		
	5541	(3)	1	1.49			
			2	1.49			
			3	1.49	*		
			4	1.48			
			5	1.49			
			Avg.	1.49			
	5541	(4)	1	1.50	20.1	3.0	-5.5
			2	1.49	19.5	6.0	-5.2
			3	1.48	19.5	1.9	-5.1
			Avg.	1.49	19.7	3.6	-5.3
	Titanium	(4)	1	1.49	21.6	1.5	-4.8
			2	1.45	21.3	0.8	-5.1
			3	1.46	20.1	6.2	-5.5
			Avg.	1.47	21.0	2.9	-5.1
	7075	(4)	1	1.49	20.1	2.8	-5.2
			2	1.48	20.0	0.6	-5.5
			3	1.49	19.3	1.1	-5.4
			Avg.	1.49	19.8	0.8	-5.3
	27725	(4)	1	1.48	18.7	5.6	-5.4
			2	1.45	18.3	0.3	-6.0
			3	1.42	13.5	0.2	-5.7
			Avg.	1.45	16.7	2.0	-5.7
	8625	(4)	1	1.44	20.5	1.0	-5.6
			2	1.47	18.9	3.1	-5.5
			3	1.47	21.2	3.2	-4.6
			Avg.	1.46	20.2	2.4	-5.3

* Sealant fell off panel during aging.

TABLE 65(Continued)

CHANNEL SEALANTS
VOLUME CHANGE, DENSITY, AND WEIGHT LOSS

Channel Sealant	Panel	Condition	Spec.	Density	Vol. Change(%)		Wt. Loss(%)
					After Fuel	After air-dry	
G250	5541	(1)	1	1.58	4.2		
			2	1.58	5.3		
			3	1.58	5.0		
			4	1.58	5.0		
			5	1.61	6.4		
			Avg.	1.59	5.2		
	5541	(2)	1	1.55	3.0		
			2	1.57	0.5		
			3	1.56	0.9		
			4	1.57	4.0		
			5	1.56	-0.8		
			Avg.	1.56	1.5		
	5541	(3)	1	1.56	0.5	7.2*	-2.5
			2	1.57	0.7	-3.0	-2.3
			3	1.56	0.04	-4.1	-2.1
			4	1.55	-0.5	-4.4	-2.1
			5	1.59	1.4	-2.9	-1.8
			Avg.	1.57	0.4	-3.6	-2.2
	5541	(4)	1	1.60	3.8	1.0	-4.0
			2	1.59	4.2	-0.4	-4.0
			3	1.59	5.6	2.4	-4.5
			Avg.	1.59	4.5	1.0	-4.2
	Titanium	(4)	1	1.60	7.3	4.5	-3.9
			2	1.51	6.1	3.1	-4.0
			3	1.56	4.6	2.1	-3.8
			Avg.	1.56	6.0	3.2	-3.9
	7075	(4)	1	1.60	6.8	1.0	-4.4
			2	1.57	4.4	2.9	-4.2
			3	1.58	5.2	1.2	-3.7
			Avg.	1.58	5.5	1.7	-4.1
	27725	(4)	1	1.58	3.8	-0.11	-4.6
			2	1.59	3.7	0.03	-4.9
			Avg.	1.59	3.8	-0.04	-4.8
	8625	(4)	1	1.58	4.9	1.3	-3.9
			2	1.57	4.7	-0.2	-4.1
			3	1.59	4.7	-0.3	-4.2
			Avg.	1.58	4.8	0.3	-4.1

* Not in Average

TABLE 65(Continued)
CHANNEL SEALANTS
VOLUME CHANGE, DENSITY, AND WEIGHT LOSS

Channel Sealant	Panel	Condition	Spec.	Density	Vol. Change(%)		Wt. Loss(%)
					After Fuel	After air-dry	After air-dry
94-011	5541	(1)	1	1.63	11.2		
			2	1.64	11.4		
			3	1.63	11.1		
			4	1.63	11.2		
			5	1.64	11.8		
			Avg.	1.63	11.3		
	5541	(2)	1	1.64	6.8		
			2	1.63	6.9		
			3	1.63	6.5		
			4	1.56	1.8*		
			5	1.62	6.5		
			Avg.	1.62	6.7		
	5541	(3)	1	1.64	12.4	-3.1	-2.4
			2	1.62	12.6	-3.0	-2.4
			3	1.65	13.1	-2.5	-2.4
			4	1.63	11.9	-2.8	-2.4
			5	1.77	14.2	-3.1	-2.4
			Avg.	1.66	12.8	-2.9	-2.4
	5541	(4)	1	1.64	16.9	6.1	-2.4
			2	1.64	16.0	-1.3	-2.3
			3	1.63	15.0	-1.3	-2.4
			Avg.	1.64	16.0	1.2	-2.4
	Titanium	(4)	1	1.63	16.0	5.9	-2.4
			2	1.70	14.2	-1.7	-2.2
			3	1.64	15.0	4.7	-3.0
			Avg.	1.66	15.1	3.0	-2.5
	7075	(4)	1	1.62	14.6	1.8	-2.4
			2	1.65	15.6	-2.3	-2.5
			3	1.63	15.7	4.0	-2.5
			Avg.	1.63	15.3	1.2	-2.5
	27725	(4)	1	1.62	14.4	-0.7	-2.2
			2	1.62	16.1	-2.7	-2.7
			3	1.63	15.6	-2.8	-2.4
			Avg.	1.62	15.4	-2.1	-2.4
	8625	(4)	1	1.59	13.3	5.4	-2.5
			2	1.61	14.1	0.7	-2.4
			3	1.57	11.4	0.7	-2.5
			Avg.	1.59	13.0	2.3	-2.5

* Not in Average

TABLE 65 (Continued)

CHANNEL SEALANTS
VOLUME CHANGE, DENSITY, AND WEIGHT LOSS

Channel Sealant	Panel	Condition	Spec.	Density	Vol. Change(%)		Wt. Loss(%)
					After Fuel	After air-dry	After air-dry
94-031	5541	(1)	1	1.50	13.9		
			2	1.49	13.4		
			3	1.50	13.2		
			4	1.49	12.1		
			5	1.50	12.9		
			Avg.	1.50	13.1		
	5541	(2)	1	1.45	4.9		
			2	1.50	6.1		
			3	1.51	5.4		
			4	1.50	5.9		
			5	1.49	6.1		
			Avg.	1.49	5.7		
	5541	(3)	1	1.50	11.4	-1.4	-2.0
			2	1.49	11.2	-3.0	-2.0
			3	1.50	11.0	-2.6	-2.0
			4	1.50	11.0	-1.7	-2.0
			5	1.51	12.0	-0.8	-1.6
			Avg.	1.50	11.3	-1.9	-1.9
	5541	(4)	1	1.50	29.1	26.3	-1.6
			2	1.51	26.4	20.7	-1.3
			3	1.51	25.8	26.0	-1.5
			Avg.	1.51	27.1	24.5	-1.5
	Titanium	(4)	1	1.53	24.3	25.4	-1.2
			2	1.42	19.0	15.3	-1.6
			3	1.45	25.7	26.9	-1.5
			Avg.	1.47	23.3	22.5	-1.4
	7075	(4)	1	1.51	25.8	26.7	-1.5
			2	1.49	29.7	24.9	-1.7
			3	1.50	26.4	27.1	-1.3
			Avg.	1.50	27.3	26.2	-1.5
	27725	(4)	1	1.50	27.0	28.4	-1.3
			2	1.50	26.2	27.7	-1.5
			3	1.50	26.7	30.2	-1.1
			Avg.	1.50	26.6	28.8	-1.3
	8625	(4)	1	1.51	26.2	27.7	-1.6
			2	1.48	26.3	30.9	-1.5
			3	1.14	22.5	17.5	-1.4
			Avg.	1.38	25.0	25.4	-1.5

TABLE 65 (Concluded)
CHANNEL SEALANTS
VOLUME CHANGE, DENSITY, AND WEIGHT LOSS

Channel Sealant	Panel	Condition	Spec.	Density	Vol. Change(%)		Wt. Loss(%)
					After Fuel	After air-dry	After air-dry
X4-2805	5541	(1)	1	1.37	26.1		
			2	1.40	27.7		
			3	1.39	26.7		
			4	1.39	26.4		
			5	1.39	24.8		
			Avg.	1.39	26.3		
	5541	(2)	1	1.40	15.3		
			2	1.41	24.1		
			3	1.40	15.2		
			4	1.39	18.1		
			5	1.39	17.2		
			Avg.	1.40	18.0		
	5541	(3)	1	1.41	29.5	9.7	-3.7
			2	1.40	28.9	6.8	-3.8
			3	1.39	29.5	-0.5*	-3.7
			4	1.39	28.7	8.3	-3.8
			5	1.37	24.9	16.6*	-3.7
			Avg.	1.39	28.3	8.3	-3.7
	5541	(5)	1	1.39	50.5	58.3	-0.6
			2	1.39	49.4	45.5	-1.7
			3	1.40	52.6	64.9	-0.1
			4	1.37	48.4	43.0	-0.9
			5	1.40	51.5	38.2	-0.7
			Avg.	1.39	50.5	50.0	-0.5
PR-702	5541	(1)	1	1.64	11.9		
			2	1.63	12.7		
			3	1.62	10.5		
			4	1.64	12.4		
			5	1.64	11.3		
			Avg.	1.63	11.8		
	5541	(2)	1	1.64	-0.9		
			2	1.63	-0.9		
			3	1.62	-1.1		
			4	1.61	-1.3		
			5	1.63	-1.4		
			Avg.	1.63	-1.1		
	5541	(3)	1	1.61	-1.0	15.3	-2.0
			2	1.68	-2.2	14.5	-1.6
			3	1.62	-2.0	12.6	-1.9
			4	1.63	-1.4	14.2	-1.6
			5	1.62	-1.0	15.9	-1.7
			Avg.	1.63	-1.5	14.5	-1.8

* Not in Average

TABLE 66
CHANNEL SEALANTS
FLATWISE TENSION

Material	Panel	Condition	Spec.	Ult. Str. (psi) (MPa)		Failure Mode (% Coh)
G651	MIL-C-5541	Control	1	12.7	(0.09)	100
			2	12.4	(0.09)	100
			3	12.0	(0.08)	100
			Avg.	12.4	(0.09)	
		Aged(1)	1	8.5	(0.06)	80
			2	9.0	(0.06)	70
			3	9.8	(0.07)	70
			Avg.	9.1	(0.06)	
	Titanium 6Al-4V	Control	1	12.7	(0.08)	100
			2	14.0	(0.10)	100
			3	13.2	(0.09)	100
			Avg.	13.3	(0.09)	
		Aged(1)	1	12.0	(0.08)	60
			2	11.3	(0.08)	60
			3	6.3	(0.04)	60
			Avg.	9.9	(0.07)	
	MIL-A-8625	Control	1	10.3	(0.07)	100
			2	11.2	(0.08)	100
			3	11.0	(0.08)	100
			Avg.	10.8	(0.07)	
		Aged(1)	1	8.8	(0.06)	50
			2	4.2	(0.03)	60
			3	8.6	(0.06)	50
			Avg.	7.2	(0.05)	
	7075-T6 Al QQ-A-250/13	Control	1	10.7	(0.07)	100
			2	10.6	(0.07)	100
			3	10.3	(0.07)	100
			Avg.	10.5	(0.07)	
		Aged(1)	1	7.5	(0.05)	70
			2	5.5	(0.04)	70
			3	7.0	(0.05)	70
			Avg.	6.7	(0.05)	
	MIL-C-27725	Control	1	14.0	(0.10)	100
			2	11.7	(0.08)	100
			3	11.6	(0.08)	100
			Avg.	12.4	(0.09)	
		Aged(1)	1	7.2	(0.05)	50
			2	7.2	(0.05)	60
			3	6.2	(0.04)	70
			Avg.	6.9	(0.05)	

TABLE 66 (Continued)

CHANNEL SEALANTS
FLATWISE TENSION

Material	Panel	Condition	Spec.	Ult. Str. (psi) (MPa)		Failure Mode (% Coh)
94-031	MIL-C-5541	Control	1	21.1	(0.15)	60
			2	20.2	(0.14)	50
			3	30.7	(0.21)	40
			Avg.	24.0	(0.17)	
		Aged(1)	1	14.3	(0.10)	60
			2	13.7	(0.09)	80
			3	19.5	(0.13)	60
			Avg.	15.8	(0.11)	
	Titanium 6Al-4V	Control	1	30.8	(0.21)	50
			2	32.4	(0.22)	60
			3	29.9	(0.21)	80
			Avg.	31.0	(0.21)	
		Aged(1)	1*	---	---	90
			2	12.3	(0.08)	90
			3	13.4	(0.09)	70
			Avg.	12.9	(0.09)	
	MIL-A-8625	Control	1	28.6	(0.20)	40
			2	26.1	(0.18)	80
			3	29.2	(0.20)	90
			Avg.	28.0	(0.19)	
		Aged(1)	1	12.4	(0.09)	80
			2	12.0	(0.08)	80
			3	10.0	(0.07)	90
			Avg.	11.5	(0.08)	
	7075-T6 Al QQ-A-250/13	Control	1	24.1	(0.17)	60
			2	23.5	(0.16)	60
			3	24.3	(0.17)	70
			Avg.	24.0	(0.17)	
		Aged(1)	1*	---	---	90
			2*	---	---	100
			3*	---	---	95
			Avg.			
	MIL-C-27725	Control	1	27.4	(0.19)	50
			2	29.2	(0.20)	50
			3	29.2	(0.20)	50
			Avg.	28.6	(0.20)	
		Aged(1)	1	11.7	(0.08)	100
			2	13.0	(0.09)	90
			3	14.8	(0.10)	80
			Avg.	13.2	(0.09)	

* Pin not in grip.

TABLE 66 (Continued)

CHANNEL SEALANTS
FLATWISE TENSION

Material	Panel	Condition	Spec.	Ult. Str. (psi) (MPa)		Failure Mode (% Coh)
G250	MIL-C-5541	Control	1	25.5	(0.17)	100
			2	24.0	(0.17)	100
			3	22.7	(0.16)	100
			Avg.	24.1	(0.17)	
		Aged(1)	1	13.1	(0.09)	90
			2	12.0	(0.08)	95
			3	8.2	(0.06)	100
			Avg.	11.1	(0.08)	
	Titanium 6Al-4V	Control	1	23.1	(0.16)	100
			2	24.3	(0.17)	100
			3	22.3	(0.15)	100
			Avg.	23.2	(0.16)	
		Aged(1)	1	15.1	(0.10)	80
			2	13.5	(0.09)	95
			3	13.8	(0.10)	95
			Avg.	14.1	(0.10)	
	MIL-A-8625	Control	1	26.5	(0.18)	100
			2	25.8	(0.18)	100
			3	25.1	(0.17)	100
			Avg.	25.8	(0.18)	
		Aged(1)	1	13.0	(0.09)	90
			2	10.2	(0.07)	90
			3	12.0	(0.08)	90
			Avg.	11.7	(0.08)	
	7075-T6 Al QQ-A-250/13	Control	1	19.1	(0.13)	100
			2	18.4	(0.13)	100
			3	19.3	(0.13)	100
			Avg.	18.9	(0.13)	
		Aged(1)	1	13.3	(0.09)	95
			2	8.7	(0.06)	95
			3	5.6	(0.04)	90
			Avg.	9.2	(0.06)	
	MIL-C-27725	Control	1	22.1	(0.15)	100
			2	21.3	(0.15)	100
			3	26.3	(0.18)	100
			Avg.	23.2	(0.16)	
		Aged(1)	1	11.8	(0.08)	90
			2	12.1	(0.08)	90
			3	6.4	(0.04)	95
			Avg.	10.1	(0.07)	

TABLE 66 (Continued)

CHANNEL SEALANTS
FLATWISE TENSION

Material	Panel	Condition	Spec.	Ult. Str. (psi) (MPa)	Failure Mode (% Coh)
94-011	MIL-C-5541	Control	1	31.0 (0.21)	30
			2	33.5 (0.23)	30
			3	31.8 (0.22)	90
			Avg.	32.1 (0.22)	
		Aged(1)	1	10.2 (0.07)	100
			2	16.3 (0.11)	50
			3	10.7 (0.07)	90
			Avg.	12.4 (0.09)	
	Titanium 6Al-4V	Control	1	35.1 (0.24)	30
			2	34.1 (0.24)	30
			3	38.3 (0.26)	20
			Avg.	35.8 (0.25)	
		Aged(1)	1	10.4 (0.07)	100
			2	6.4 (0.04)	100
			3	13.2 (0.09)	90
			Avg.	10.0 (0.07)	
	MIL-A-8625	Control	1	28.5 (0.19)	95
			2	31.3 (0.22)	80
			3	30.5 (0.21)	70
			Avg.	30.1 (0.21)	
		Aged(1)	1	7.2 (0.05)	75
			2	6.6 (0.05)	100
			3	14.6 (0.10)	100
			Avg.	9.5 (0.07)	
	7075-T6 Al QQ-A-250/13	Control	1	30.9 (0.21)	30
			2	32.0 (0.22)	30
			3	30.7 (0.21)	30
			Avg.	31.2 (0.22)	
		Aged(1)	1	6.2 (0.04)	100
			2	14.8 (0.10)	40
			3	8.8 (0.06)	90
			Avg.	9.9 (0.07)	
	MIL-C-27725	Control	1	32.0 (0.22)	70
			2	36.3 (0.25)	70
			3	34.6 (0.24)	50
			Avg.	34.3 (0.25)	
		Aged(1)	1	9.9 (0.07)	90
			2	11.5 (0.08)	90
			3	17.8 (0.12)	75
			Avg.	13.1 (0.09)	

TABLE 66 (Continued)

CHANNEL SEALANTS
FLATWISE TENSION

Material	Panel	Condition	Spec.	Ult. Str. (psi) (MPa)	Failure Mode (% Coh)
X4-2085	MIL-C-27725	Control	1	20.0 (0.14)	50
			2	23.2 (0.16)	90
			3	20.9 (0.14)	40
			4	22.8 (0.16)	85
			5	25.6 (0.18)	40
			Avg.	22.5 (0.16)	
		Aged (2)	1	13.5 (0.09)	40
			2	20.0 (0.14)	50
			3	14.8 (0.10)	80
			4	18.4 (0.13)	25
			5	17.6 (0.12)	50
			Avg.	16.9 (0.12)	
94-031 + X4-2805 (50/50 Mixture)	MIL-C-27725	Control	1	10.8 (0.07)	100
			2	16.7 (0.12)	100
			3	14.8 (0.10)	100
			Avg.	14.1 (0.10)	
		Aged (3)	1	7.5 (0.05)	100
			2	6.8 (0.05)	100
			3	9.7 (0.07)	100
			Avg.	8.0 (0.06)	
94-031 + G250 (50/50 Mixture)	MIL-C-27725	Control	1	18.4 (0.13)	50
			2	18.4 (0.13)	50
			3	24.6 (0.17)	25
			Avg.	20.5 (0.14)	
		Aged (3)	1	9.9 (0.07)	5
			2	11.8 (0.08)	0
			3	9.1 (0.06)	0
			Avg.	10.3 (0.07)	
94-031 + G651 (50/50 Mixture)	MIL-C-27725	Control	1	12.3 (0.08)	50
			2	12.2 (0.08)	40
			3	12.9 (0.09)	35
			Avg.	12.5 (0.09)	
		Aged (3)	1	5.0 (0.03)	0
			2	12.5 (0.09)	0
			3	11.9 (0.08)	0
			Avg.	9.8 (0.07)	

TABLE 66 (Continued)

CHANNEL SEALANTS
FLATWISE TENSION

Material	Panel	Condition	Spec.	Ult. Str. (psi) (MPa)		Failure Mode (% Coh)
X4-2805+ G250 (50/50 Mixture)	MIL-C-27725	Control	1	16.8	(0.12)	100
			2	15.8	(0.11)	100
			3	14.7	(0.10)	100
			Avg.	15.8	(0.11)	
		Aged(3)	1	11.7	(0.08)	10
			2	10.8	(0.07)	15
			3	11.8	(0.08)	20
			Avg.	11.3	(0.08)	
X4-2805+ G651 (50/50 Mixture)	MIL-C-27725	Control	1	13.5	(0.09)	90
			2	13.6	(0.09)	85
			3	13.4	(0.09)	95
			Avg.	13.5	(0.09)	
		Aged(3)	1	4.7	(0.03)	0
			2	8.5	(0.06)	0
			3	11.5	(0.08)	0
			Avg.	8.2	(0.06)	
G250 + G651 (50/50 Mixture)	MIL-C-27725	Control	1	11.3	(0.08)	100
			2	12.1	(0.08)	100
			3	12.1	(0.08)	100
			Avg.	11.8	(0.08)	
		Aged(3)	1	11.3	(0.08)	100
			2	9.5	(0.07)	100
			3	11.4	(0.08)	100
			Avg.	10.7	(0.07)	
94-031 + PR-702 (50/50 Mixture)	MIL-C-27725	Control	1	22.4	(0.15)	100
			2	24.8	(0.17)	100
			3	23.2	(0.16)	100
			Avg.	23.5	(0.16)	
		Aged(3)	1	19.6	(0.14)	90
			2	12.5	(0.09)	80
			3	16.3	(0.11)	90
			Avg.	16.1	(0.11)	
X4-2805+ PR-702 (50/50 Mixture)	MIL-C-27725	Control	1	19.5	(0.13)	100
			2	23.3	(0.16)	100
			3	22.5	(0.16)	100
			Avg.	21.8	(0.15)	
		Aged(3)	1	7.6	(0.05)	80
			2	15.0	(0.10)	90
			3	18.9	(0.13)	90
			Avg.	13.8	(0.10)	

TABLE 66 (Concluded)

CHANNEL SEALANTS
FLATWISE TENSION

Material	Panel	Condition	Spec.	Ult. Str. (psi) (MPa)		Failure Mode (% Coh)		
G250 + PR-702 (50/50 Mixture)	MIL-C-27725	Control	1	26.8	(0.18)	100		
			2	23.7	(0.16)	100		
			3	25.1	(0.17)	100		
			Avg.	25.2	(0.17)			
		Aged (3)	1	20.5	(0.14)	95		
			2	16.6	(0.11)	95		
			3	17.5	(0.12)	95		
			Avg.	18.2	(0.13)			
		G651 + PR-702	MIL-C-27725	Control	1	18.8	(0.13)	100
					2*	---	---	
3	18.7				(0.13)			
Avg.	18.8				(0.13)			
Aged (3)	1			12.8	(0.09)	100		
	2			13.8	(0.10)	95		
	3			12.1	(0.08)	95		
	Avg.			12.9	(0.09)			

* Block to Panel Failure.

Agings:

- (1) 96 hrs. @ 120°F(49°C) in JRF +
16 hrs. @ 160°F(71°C) in JRF +
1 hr. @ 180°F(82°C) in JRF +
24 hrs. @ 225°F(107°C)/air +
16 hrs. @ 310°F(154°C)/air +
8 hrs. @ 350°F(177°C)/air
- (2) 96 hrs. @ 140°F(60°C) in JRF +
16 hrs. @ 160°F(71°C) in JRF +
1 hr. @ 180°F(82°C) in JRF +
24 hrs. @ 225°F(107°C)/air +
16 hrs. @ 310°F(154°C)/air +
8 hrs. @ 350°F(177°C)/air
- (3) 96 hrs. @ 140°F(60°C) in JRF +
16 hrs. @ 160°F(71°C) in JRF +
1 hr. @ 180°F(82°C) in JRF +
24 hrs. @ 225°F(107°C)/air +
16 hrs. @ 310°F(154°C)/air +
1 hr. @ 350°F(177°C)/air

sealant failed the aged condition, developing cracks on all panels. The G651 fell off one of the MIL-A-8625 panels while in the 180°F (82°C)/JRF condition. Data on the low temperature flexibility tests are given in Table 67.

G651 sealant was the only material significantly affected by aging in the pressure rupture tests, dropping to less than one-third of its original values. The other materials showed either a slight drop or an increase. The G651 sealant also had the lowest original values. Pressure rupture results are presented in Table 68.

Corrosion tests were done on 7075 bare (QQ-A-250/12) aluminum. Portions of the panel not covered with channel sealant were sealed with a Class "A" polysulfide sealant to insure that whatever corrosion took place was through the channel sealant. Results are in Table 69.

Data for the nonvolatile content, thermal extrusion, and extrusion rate tests are presented in Tables 70 through 72.

After the initial test phase, all the original materials plus three additional materials, two separate batches of X4-2805 (E-3331-37 and E-3453-130) and 94-011 with the addition of fluorosilicone crumbs, were rerun to different aging conditions and tests. The tests include volume change, weight change, and specific gravity, adhesion (flatwise tension), pressure rupture, and seal efficiency.

Conditions of the volume change specimens are controls, seven days at room temperature in JRF, seven days at room temperature in Type I fluid (Iso-octane), 25 days at 140°F (60°C) in JRF + 72 hours at 160°F (71°C) in JRF + six hours at 180°F (82°C) in JRF + seven days at 160°F (71°C) air-dry, and 25 days at 140°F (60°C) in Type I + 72 hours at 160°F (71°C) in Type I + six hours at 180°F (82°C) in Type I + seven days at 160°F (71°C) air-dry. The PR-702 and 94-031 materials were tested at the elevated temperature in JRF only; the G651 was tested at the elevated temperature in both JRF and Type I; the two

TABLE 67
CHANNEL SEALANTS
LOW TEMP. FLEX

Channel Sealant	Metal Coating	Condition	Results
G-651	MIL-C-5541	Control	Passed Passed
		Conditioned	Cracked Cracked
	QQ-A-250/13 7075 Clad	Control	Passed Passed
		Conditioned	Cracked Cracked
	MIL-A-8625 (Dichromate Sealed)	Control	Passed Passed
		Conditioned	Cracked Sealant fell off @ 180°F(82°C)/JRF
	MIL-T-9046 Titanium	Control	Passed Passed
		Conditioned	Cracked Cracked
	MIL-C-27725	Control	Passed Passed
		Conditioned	Cracked Cracked

Conditioning: 96 hrs. @ 120°F(49°C) in JRF +
16 hrs. @ 160°F(71°C) in JRF +
1 hr. @ 180°F(82°C) in JRF +
24 hrs. @ 225°F(107°C) dry +
16 hrs. @ 310°F(154°C) dry +
8 hrs. @ 350°F(177°C) dry

TABLE 67 (Continued)

CHANNEL SEALANTS
LOW TEMP. FLEX

Channel Sealant	Metal Coating	Condition	Results
G-250	MIL-C-5541	Original	Passed Passed
		Conditioned	Passed (Bubbled) Passed (Bubbled)
	QQ-A-250/13 7075 Clad	Control	Passed Passed
		Conditioned	Passed (Bubbled) Passed (Bubbled)
	MIL-A-8625 (Water sealed)	Control	Passed Passed
		Conditioned	Passed (Bubbled) Passed (Bubbled)
	MIL-T-9046 Titanium	Control	Passed Passed
		Conditioned	Passed (Bubbled) Passed (Bubbled)
	MIL-C-27725	Control	Passed Passed
		Conditioned	Passed (Bubbled) Passed (Bubbled)

Conditioning: 96 hrs. @ 120°F(49°C) in JRF +
 16 hrs. @ 160°F(71°C) in JRF +
 1 hr. @ 180°F(82°C) in JRF +
 24 hrs. @ 225°F(107°C) dry +
 16 hrs. @ 310°F(154°C) dry +
 8 hrs. @ 350°F(177°C) dry

TABLE 67 (Continued)

CHANNEL SEALANTS
LOW TEMP. FLEX

Channel Sealant	Metal Coating	Condition	Results
94-011	MIL-C-5541	Control	Passed Passed
		Conditioned	Passed (50% Bubble) Passed (Slight bubbling)
	QQ-A-250/13 7075 Clad	Control	Passed Passed
		Conditioned	Passed (Slight bubbling) Passed (Slight bubbling)
	MIL-A-8625 (Dichromate sealed)	Control	Passed Passed
		Conditioned	Passed (Slight bubbling) Passed (Slight bubbling)
	MIL-T-9046 Titanium	Control	Passed Passed
		Conditioned	Passed (Slight bubbling) Passed (Slight bubbling)
	MIL-C-27725	Control	Passed Passed
		Conditioned	Passed (Slight bubbling) Passed (Slight bubbling)
	MIL-A-8625 (water sealed)	Control	Passed Passed
		Conditioned	Passed (Slight bubbling) Passed (Slight bubbling)

Conditioning: 96 hrs. @ 120°F(49°C) in JRF +
 16 hrs. @ 160°F(71°C) in JRF +
 1 hr. @ 180°F(82°C) in JRF +
 24 hrs. @ 225°F(107°C) dry +
 16 hrs. @ 310°F(154°C) dry +
 8 hrs. @ 350°F(177°C) dry

TABLE 67 (Concluded)

CHANNEL SEALANTS
LOW TEMP. FLEX

Channel Sealant	Metal Coating	Condition	Results
94-031	MIL-C-5541	Control	Passed Passed
		Conditioned	Passed Passed
	QQ-A-250/13 7075 Clad	Control	Passed Passed
		Conditioned	Passed Passed
	MIL-A-8625 (Dichromate sealed)	Control	Passed Passed
		Conditioned	Passed Passed
	MIL-T-9046 Titanium	Control	Passed Passed
		Conditioned	Passed Passed
	MIL-C-27725	Control	Passed Passed
		Conditioned	Passed Passed

Conditioning: 96 hrs. @ 120°F(49°C) in JRF +
 16 hrs. @ 160°F(71°C) in JRF +
 1 hr. @ 180°F(82°C) in JRF +
 24 hrs. @ 225°F(107°C) dry +
 16 hrs. @ 310°F(154°C) dry +
 8 hrs. @ 350°F(177°C) dry

TABLE 68
CHANNEL SEALANTS
PRESSURE RUPTURE

Channel Sealant	Condition	Pressure at Failure	
		(In. Hg)	(Cm Hg)
94-011	Original	20.25	51.44
		21.50	54.61
		<u>20.00</u>	<u>50.80</u>
		20.58	52.28
	Conditioned	17.50	44.45
		29.50	74.93
		<u>30.25</u>	<u>76.84</u>
		25.75	65.41
94-031	Original	27.75	70.49
		28.50	72.39
		<u>26.00</u>	<u>66.04</u>
		27.42	69.64
	Conditioned	22.00	55.88
		14.00	35.56
		<u>25.00</u>	<u>63.50</u>
		20.33	51.65
X4-2805	Original	15.75	40.01
		16.00	40.64
		<u>16.25</u>	<u>41.28</u>
		16.00	40.64
	Conditioned	22.00	55.88
		10.00	25.40
		<u>10.00</u>	<u>25.40</u>
		14.00	35.56
G-250	Original	17.00	43.18
		23.50	59.69
		<u>20.25</u>	<u>51.44</u>
		20.25	51.44
	Conditioned	34.00	86.36
		5.00	12.70
		<u>25.00</u>	<u>63.50</u>
		21.33	54.19

TABLE 68 (Concluded)

CHANNEL SEALANTS
PRESSURE RUPTURE

Channel Sealant	Condition	Pressure at Failure	
		(In. Hg)	(Cm Hg)
G-651	Original	13.00	33.02
		12.50	31.75
		<u>12.00</u>	<u>30.48</u>
		12.50	31.75
	Conditioned	5.00	12.70
		4.00	10.16
		<u>2.00</u>	<u>5.08</u>
		3.67	9.31

Conditioning: 96 hrs. @ 140°F(60°C) in JRF +
 16 hrs. @ 160°F(71°C) in JRF +
 1 hr. @ 180°F(82°C) in JRF +
 24 hrs. @ 225°F(107°C) dry +
 16 hrs. @ 310°F(154°C) dry +
 8 hrs. @ 350°F(177°C) dry

TABLE 69
CHANNEL SEALANTS
CORROSION

Material	Results
94-031	No corrosion
94-011	No corrosion
XR-2805	Very slight pitting throughout
G-250	Severely discolored - Saltwater section only
G-651	Moderate to severe discolora- tion on saltwater section, very slight discoloration on JRF and vapors section
PR-702	Very slight discoloration throughout

TABLE 70
CHANNEL SEALANTS
NON-VOLATILE CONTENT

Channel Sealant	% Non-Volatile Content
94-031	99.65
	<u>99.65</u>
	99.65
94-011	99.65
	<u>99.65</u>
	99.65
G-250	99.78
	<u>99.77</u>
	99.78
G-651	99.52
	<u>99.41</u>
	99.47
X4-2805	99.49
	<u>99.55</u>
	99.52

Conditioning: 7 days @ 160°F(71°C)/Air

TABLE 71
CHANNEL SEALANTS
THERMAL EXTRUSION

Channel Sealant	Vol. of Sealant Ext. (cc)		% Volume Extruded
	Ends	Center	
94-011	0.1085	0.1268	21.20
	0.0962	0.1421	21.47
	0.1122	0.1569	24.29
	0.1152	0.1477	23.68
	<u>0.1198</u>	<u>0.1397</u>	<u>23.38</u>
	0.1105	0.1427	22.80
94-031	0.1529	0.1943	31.28
	0.1429	0.1893	29.93
	0.1270	0.1850	28.11
	0.1452	0.1876	29.98
	<u>0.1331</u>	<u>0.1771</u>	<u>29.95</u>
	0.1402	0.1867	29.85
G-250	0.0698	0.2190	17.91
	0.0775	0.1537	20.83
	0.0722	0.1275	17.99
	0.0671	0.1460	19.20
	<u>0.0667</u>	<u>0.1214</u>	<u>16.95</u>
	0.0707	0.1355	18.58
G-651	0.1069	0.1262	21.00
	0.0930	0.1297	20.14
	0.1077	0.1537	23.55
	0.1059	0.1378	21.95
	<u>0.1058</u>	<u>0.1233</u>	<u>20.64</u>
	0.1040	0.1341	21.46
X4-2805	0.1213	0.1554	24.93
	0.1427	0.1512	26.48
	0.1305	0.1684	26.93
	0.1383	0.1401	25.08
	<u>0.1412</u>	<u>0.1431</u>	<u>25.61</u>
	0.1348	0.1516	25.81

Conditioned: 1 hr. @ 350°F (177°C)

$$\text{Volume of Sealant Extruded} = \frac{\text{Weight of Sealant}}{\text{Specific Gravity}}$$

$$\% \text{ Volume Extruded} = 100 - \left(\frac{\text{Vol}_{\text{init}} - \text{Vol}_{\text{ext}}}{\text{Vol}_{\text{init}}} \times 100 \right)$$

TABLE 72
CHANNEL SEALANTS
EXTRUSION RATE

Channel Sealant	Spec.	Extrusion Rate	
		(lbs)	(N)
94-031	1	258	1148
	2	299	1331
	Avg.	279	1242
94-011	1	234	1041
	2	238	1059
	Avg.	236	1050
G-250	1	233	1037
	2	243	1081
	Avg.	238	1059
G-651	1	163	725
	2	176	783
	Avg.	170	757
X4-2805	1	248	1104
	2	264	1175
	Avg.	256	1139
PR-702	1	986	4388
	2	959	4268
	Avg.	973	4330

new batches of X4-2805 and the 94-011 with fluorosilicone crumbs were tested at all conditions. Volume change, weight change, and specific gravity data are presented in Table 73.

Conditions on the adhesion specimens are controls and 96 hours at 140°F (60°C) in JRF + two hours at 180°F (82°C) in JRF + four hours at 260°F (127°C) in air + 40 min. at 320°F (160°C) in air + 60 min. at 360°F (182°C) in air. All materials except PR-702 were tested for adhesion. Data are in Table 74.

The two other tests under this program, pressure rupture and seal efficiency, have not yet been completed. The three new materials will be added to seal efficiency tests presently being run. The aging cycle on this test is 96 hours at 140°F (60°C) in JRF + two hours at 180°F (82°C) in JRF + four hours at 260°F (127°C) in air + 40 min. at 320°F (160°C) in air + 60 min. at 360°F (182°C) in air, and is repeated six times. The pressure rupture specimens are also tested after one of these cycles, in addition to controls, after 96 hours at 140°F (60°C) in JRF, and after 120 days at 160°F (71°C)/95 percent R.H.

3.12 HYDROLYTIC STABILITY TESTS OF F-15 FUEL TANK FOAMS

Four polyester foams are being evaluated for hydrolytic stability after being conditioned at 120°F (49°C) in 95 percent relative humidity. Two test samples are being tested every two weeks for tensile strength and elongation. The four foams being evaluated are: W901P (15-4), TMP baseline, with red pigment; W258R, non-TMP, with red and orange pigments; S/N 74-126 red foam from the upper wing skin (PN 2022) after two years service; and S/N 72-114 red foam from the upper wing skin (PN 2001) after five years service. S/N 72-114 red foam had deteriorated after 28 weeks in humidity and testing was terminated. The test results up to and including the 36-week data are given in Table 75.

W258R red foam is undergoing additional testing to obtain tensile strength and elongation under both wet and dry test conditions. Data for the first 20 weeks are shown in Table 76.

TABLE 73
CHANNEL SEALANTS
VOLUME CHANGE, WEIGHT CHANGE,
AND SPECIFIC GRAVITY

Material	Condition	% Volume Change		% Wt. Chg.	Specific Gravity
		After Fuel Soak	After Air-Dry	After Air-Dry	
PR-702	25 days @ 140°F(60°C)	23.77	-6.74	-4.42	1.65
	in JRF + 72 hrs @ 160°F	23.94	-6.30	-4.52	1.66
	(71°C) in JRF + 6 hrs	23.70	-2.73	-4.13	1.63
	@ 180°F(82°C) in JRF +	26.58	1.99*	-3.80	1.67
	7 days @ 160°F(71°C)	<u>25.49</u>	<u>-3.19</u>	<u>-4.03</u>	<u>1.66</u>
	air-dry				
	Avg	24.70	-4.74	-4.18	1.65
94-031	25 days @ 140°F(60°C)	26.88	-0.17	-1.62	1.52
	in JRF + 72 hrs @ 160°F	26.10	0.10	-1.30	1.51
	(71°C) in JRF + 6 hrs	26.62	1.24	-1.30	1.52
	@ 180°F(82°C) in JRF +	26.34	4.13	-1.01	1.51
	7 days @ 160°F(71°C)	<u>25.51</u>	<u>1.52</u>	<u>-1.40</u>	<u>1.51</u>
	air-dry				
	Avg	26.29	1.36	-1.33	1.51
G651	25 days @ 140°F(60°C)	20.02	-4.92	-5.08	1.49
	in JRF + 72 hrs @ 160°F	18.17	-6.93	-6.73	1.47
	(71°C) in JRF + 6 hrs	20.42	-5.21	-5.21	1.48
	@ 180°F(82°C) in JRF +	18.95	-5.84	-6.04	1.48
	7 days @ 160°F(71°C)	<u>19.76</u>	<u>-5.21</u>	<u>-4.93</u>	<u>1.47</u>
	air-dry				
	Avg	19.46	-5.62	-5.60	1.48
G651	25 days @ 140°F(60°C) in Type I + 72 hrs @ 160°F(71°C) in Type I + 6 hrs @ 180°F(82°C) in Type I + 7 days @ 160°F(71°C) air-dry	Sealant fell off panels during 140°F(60°C) aging.			
X4-2805 E-3331- 37	7 days @ R.T. in JRF	15.31			1.38
		12.03			1.39
		7.80*			1.36
		12.68			1.37
		<u>13.33</u>			<u>1.40</u>
	Avg	13.34			1.38

* Not in average

TABLE 73 (Continued)
CHANNEL SEALANTS
VOLUME CHANGE, WEIGHT CHANGE,
AND SPECIFIC GRAVITY

Material	Condition	% Volume Change		% Wt.Chg. After Air-Dry	Specific Gravity
		After Fuel Soak	After Air-Dry		
X4-2805 E-3331- 37	7 days @ R.T. in Type I	11.37			1.40
		9.31			1.41
		6.80			1.38
		23.09*			1.40
		8.09			<u>1.38</u>
		Avg 8.89			1.39
X4-2805 E-3331- 37	25 days @ 140°F(60°C) in JRF + 72 hrs @ 160°F (71°C) in JRF + 6 hrs @ 180°F(82°C) in JRF + 7 days @ 160°F(71°C) air-dry	30.88	1.98	-3.31	1.38
		33.17	-2.26	-2.50	1.40
		30.37	2.79	-2.67	1.37
		31.00	-5.73	-2.34	1.40
		<u>29.56</u>	<u>-7.95</u>	<u>-3.34</u>	<u>1.41</u>
		Avg 31.00	-2.23	-2.83	1.39
X4-2805 E-3331- 37	25 days @ 140°F(60°C) in Type I + 72 hrs @ 160°F(71°C) in Type I + 6 hrs @ 180°F(82°C) in Type I + 7 days @ 160°F(71°C) air-dry	12.17	-5.22	-3.70	1.38
		11.47	-4.85	-3.47	1.38
		12.38	-4.10	-3.67	1.39
		14.97	-1.54	-2.72	1.42
		<u>11.79</u>	<u>-4.78</u>	<u>-3.74</u>	<u>1.39</u>
		Avg 12.56	-4.10	-3.46	1.39
X4-2805 E-3453- 130	7 days @ R.T. in JRF	15.91			1.44
		18.57			1.41
		16.39			1.39
		17.18			1.43
		<u>16.53</u>			<u>1.42</u>
		Avg 16.92			1.42
X4-2805 E-3453- 130	7 days @ R.T. in Type I	10.01			1.41
		11.62			1.43
		8.11			1.39
		11.22			1.42
		<u>11.52</u>			<u>1.43</u>
		Avg 10.50			1.42
X4-2805 E-3453- 130	25 days @ 140°F(60°C) in JRF + 72 hrs @ 160°F (71°C) in JRF + 6 hrs @ 180°F(82°C) in JRF + 7 days @ 160°F (71°C) air-dry	32.35	7.31	-2.39	1.39
		32.84	5.98	-2.69	1.41
		32.83	3.23	-2.50	1.40
		31.70	5.72	-2.83	1.37
		<u>31.93</u>	<u>5.31</u>	<u>-2.76</u>	<u>1.41</u>
		Avg 32.33	5.51	-2.63	1.40

* Not in average.

TABLE 73 (Concluded)
CHANNEL SEALANTS
VOLUME CHANGE, WEIGHT CHANGE,
AND SPECIFIC GRAVITY

Material	Condition	% Volume Change		% Wt.Chg.	Specific Gravity
		After Fuel Soak	After Air-Dry	After Air-Dry	
X4-2805	25 days @ 140°F(60°C)	15.51	-1.88	-3.14	1.44
E-3453-	in Type I + 72 hrs @	13.88	-1.34	-3.60	1.42
130	160°F(71°C) in Type I +	13.19	-3.62	-3.53	1.41
	6 hrs @ 180°F(82°C) in	16.17	-0.97	-3.01	1.42
	Type I + 7 days @ 160°F	14.07	-2.96	-3.41	1.42
	(71°C) air-dry Avg	14.56	-2.15	-3.34	1.42
94-011	7 days @ R.T. in JRF	15.93			1.44
with		15.93			1.41
fluoro-		12.93			1.39
silicone		15.66			1.43
crumbs		15.49			1.42
	Avg	15.19			1.42
94-011	7 days @ R.T. in	10.50			1.44
with	Type I	11.89			1.42
fluoro-		11.37			1.46
silicone		12.82			1.43
crumbs		10.94			1.42
	Avg	11.50			1.43
94-011	25 days @ 140°F(60°C)	19.32	-1.70	-2.07	1.39
with	in JRF + 72 hrs @ 160°F	19.91	-1.57	-2.32	1.42
fluoro-	(71°C) in JRF + 6 hrs	20.10	-1.64	-2.41	1.43
silicone	@ 180°F(82°C) in JRF +	19.83	-1.72	-2.35	1.43
crumbs	7 days @ 160°F(71°C)	20.54	-0.90	-2.47	1.44
	air-dry Avg	19.94	-1.51	-2.32	1.42
94-011	25 days @ 140°F(60°C)	16.81	-0.53	-2.22	1.45
with	in Type I + 72 hrs @	15.10	-1.69	-1.94	1.38
fluoro-	160°F(71°C) in Type I	15.58	-1.17	-2.34	1.43
silicone	+ 6 hrs @ 180°F(82°C)	14.88	-1.32	-2.46	1.41
crumbs	in Type I + 7 days @	15.68	-0.85	-2.43	1.42
	160°F(71°C) air-dry Avg	15.61	-1.11	-2.28	1.42

TABLE 74
CHANNEL SEALANTS
FLATWISE TENSION

Material	Condition	Specimen No.	Ult. Strength psi (MPa)	Failure Mode (% Coh.)
X4-2805 E-3453-130	Original	1	15.0 (0.10)	100
		2	16.4 (0.11)	100
		3	15.3 (0.11)	95
		4	16.6 (0.11)	95
		5	15.7 (0.11)	95
		Avg	15.8 (0.11)	
X4-2805 E-3453-130	Aged	1	11.1 (0.08)	85
		2	7.9 (0.05)	90
		3	7.1 (0.05)	95
		4	8.4 (0.06)	90
		5	6.8 (0.05)	85
		Avg	8.3 (0.06)	
X4-2805 E-3331-37	Original	1	14.5 (0.10)	85
		2	15.5 (0.11)	100
		3	13.3 (0.09)	95
		4	12.5 (0.09)	80
		5	16.0 (0.11)	80
		Avg	14.4 (0.10)	
X4-2805 E-3331-37	Aged	1	8.0 (0.06)	25
		2	9.3 (0.06)	10
		3	9.6 (0.07)	20
		4	6.0 (0.04)	0
		5	8.3 (0.06)	10
		Avg	8.2 (0.06)	
94-011 with fluoro- silicone crumbs	Original	1	18.1 (0.12)	10
		2	13.7 (0.09)	5
		3	14.4 (0.10)	5
		4	13.5 (0.09)	5
		5	16.7 (0.12)	10
		Avg	15.3 (0.11)	
94-011 with fluoro- silicone crumbs	Aged	1	2.7 (0.02)	0
		2	*	0
		3	2.6 (0.02)	0
		4	2.5 (0.02)	0
		5	*	0
		Avg	2.6 (0.02)	

*Specimen failed while loading.

TABLE 74 (Concluded)

CHANNEL SEALANTS
FLATWISE TENSION

Material	Condition	Specimen No.	Ult. Strength psi (MPa)	Failure Mode (% Coh.)
94-031	Original	1	**	
		2	**	
		3	18.4 (0.13)	60
		4	20.3 (0.14)	50
		5	22.0 (0.15)	40
		Avg	20.2 (0.14)	
94-031	Aged	1	10.9 (0.08)	100
		2	11.2 (0.08)	100
		3	11.5 (0.08)	100
		4	10.2 (0.07)	100
		5	10.4 (0.07)	100
		Avg	10.8 (0.08)	
G651	Original	1	15.5 (0.11)	100
		2	13.3 (0.09)	100
		3	14.7 (0.10)	100
		4	14.3 (0.10)	100
		5	16.9 (0.12)	100
		Avg	14.9 (0.10)	
G651	Aged	1	12.7 (0.09)	60
		2	12.4 (0.09)	40
		3	14.5 (0.10)	50
		4	9.8 (0.07)	80
		5	13.3 (0.09)	50
		Avg	12.5 (0.09)	
X4-2805 E-2349-137	Original	1	19.8 (0.14)	90
		2	18.2 (0.13)	90
		3	13.3 (0.09)	90
		4	14.9 (0.10)	80
		5	16.8 (0.12)	80
		Avg	16.6 (0.11)	
X4-2805 E-2349-137	Aged	1	8.5 (0.06)	60
		2	8.2 (0.06)	40
		3	6.7 (0.05)	40
		4	8.7 (0.06)	70
		5	8.5 (0.06)	80
		Avg	8.1 (0.06)	

Aging: 96 hrs @ 140°F(60°C) in JRF + 2 hrs @ 180°F(82°C) in JRF +
4 hrs @ 260°F(127°C) in air + 40 min @ 320°F(160°C) in air
+ 60 min @ 360°F(182°C) in air

** Failed at panel/block bond

TABLE 75
HYDROLYTIC STABILITY OF FOAMS
W901P RED FOAM
120°F (49°C) + 95% R.H.

Time (Hours)	Condition	Height (in.)	Volume (cc)	Weight (g)
0	Wet	29.2	(0.17)	371
1	Wet	31.4	(0.17)	34
		30.1	(0.17)	34
		Avg 30.6	(0.17)	34
2	Wet	30.1	(0.17)	367
		29.5	(0.17)	346
		Avg 30.0	(0.17)	348
4	Wet	30.2	(0.17)	373
		30.3	(0.17)	441
		Avg 30.3	(0.17)	382
6	Wet	28.1	(0.16)	347
		28.0	(0.16)	347
		Avg 28.0	(0.16)	347
8	Wet	24.8	(0.17)	387
		26.2	(0.18)	365
		Avg 25.5	(0.18)	376
10	Wet	26.6	(0.18)	373
		27.1	(0.19)	376
		Avg 26.9	(0.18)	375
12	Wet	25.4	(0.18)	316
		23.2	(0.17)	297
		Avg 24.4	(0.17)	305
14	Wet	23.4	(0.16)	323
		20.7	(0.14)	316
		Avg 22.1	(0.15)	319
16	Wet	26.9	(0.19)	310
		21.4*	(0.15)	315*
		Avg 24.2	(0.18)	347
18	Wet	25.6	(0.18)	329
		26.5	(0.18)	350
		Avg 26.5	(0.18)	341
20	Wet	24.6	(0.17)	440
		21.6	(0.15)	390
		Avg 23.1	(0.16)	415
22	Wet	23.7	(0.16)	292
		22.0	(0.15)	320
		Avg 22.9	(0.16)	306
24	Wet	22.8	(0.16)	381
		21.8	(0.15)	368
		Avg 22.3	(0.15)	374
26	Wet	21.2	(0.15)	388
		23.2	(0.16)	335
		Avg 22.2	(0.15)	362
28	Wet	20.9	(0.14)	351
		18.6	(0.13)	333
		Avg 19.7	(0.14)	342
30	Wet	13.6	(0.09)	284
		16.1	(0.11)	297
		Avg 14.9	(0.10)	291
32	Wet	14.9	(0.10)	250
		13.6	(0.09)	270
		Avg 14.2	(0.10)	260
34	Wet	8.7	(0.06)	173
		9.0	(0.06)	176
		Avg 8.8	(0.06)	175
36	Wet	8.0	(0.06)	113
		8.3	(0.06)	106
		Avg 8.1	(0.06)	110

* Not in average

TABLE 75 (Continued)
HYDROLYTIC STABILITY OF FOAMS
W258R (1-1) RED FOAM
120°F (49°C) + 95% R.H.

Weeks in Corrosion	Test Condition	Tensile Strength Psi (Mpa)		Elongation (%)
None (Controls)	---	31.6	(0.22)	280
		39.0	(0.27)	370
		32.7	(0.23)	340
		Avg 34.4	(0.24)	330
2	Wet	21.6	(0.15)	342
		29.6	(0.20)	344
		27.7	(0.19)	420
		Avg 26.3	(0.18)	369
4	Wet	35.0	(0.24)	363
		34.7	(0.24)	416
		Avg 34.9	(0.24)	390
6	Wet	26.4	(0.18)	292
		32.8	(0.23)	408
		28.6	(0.20)	380
		Avg 29.3	(0.20)	360
8	Wet	22.3	(0.15)	231
		23.4	(0.16)	315
		Avg 22.9	(0.16)	273
10	Wet	29.5	(0.20)	295
		21.8	(0.15)	278
		Avg 25.7	(0.18)	287
12	Wet	19.09*	(0.13)*	202*
		31.11	(0.21)	317
		33.31	(0.23)	320
		Avg 32.21	(0.22)	319
14	Wet	30.91	(0.21)	373
		30.56	(0.21)	384
		Avg 30.73	(0.21)	378
16	Wet	34.90	(0.24)	310
		35.37	(0.24)	345
		Avg 35.14	(0.24)	328
18	Wet	30.92	(0.21)	339
		29.49	(0.20)	439
		Avg 30.21	(0.21)	389
20	Wet	21.5	(0.15)	252
		29.5	(0.20)	325
		27.4	(0.19)	295
		Avg 26.2	(0.18)	291
22	Wet	25.7	(0.18)	315
		25.6	(0.18)	334
		Avg 25.6	(0.18)	324
24	Wet	32.4	(0.22)	325
		27.7	(0.19)	320
		Avg 30.0	(0.21)	323
26	Wet	27.7	(0.19)	289
		29.5	(0.20)	367
		Avg 28.6	(0.20)	378
28	Wet	21.4	(0.15)	390
		22.3	(0.15)	372
		Avg 21.9	(0.15)	381
30	Wet	29.1	(0.20)	395
		28.2	(0.19)	355
		Avg 28.7	(0.20)	375
32	Wet	21.2	(0.15)	278
		18.6	(0.13)	228
		Avg 19.9	(0.14)	253
34	Wet	15.9	(0.11)	260
		18.1	(0.12)	265
		Avg 17.0	(0.12)	263

TABLE 75 (Continued)
HYDROLYTIC STABILITY OF FOAMS
74-126 RED FOAMS
120°F (49°C) + 95% R.H.

Weeks in Condition	Test Condition	Tensile Strength		Elongation (%)
		psi	(MPa)	
None (Controls)	---	23.8	(0.16)	280
		24.7	(0.17)	320
		Avg 24.0	(0.17)	300
2	Wet	25.0	(0.17)	290
		26.1	(0.18)	290
		Avg 25.6	(0.18)	290
4	Wet	20.4	(0.14)	283
		23.4	(0.16)	280
		Avg 21.9	(0.15)	282
6	Wet	22.5	(0.16)	259
		20.6	(0.14)	276
		Avg 21.6	(0.15)	268
8	Wet	20.3	(0.14)	312
		20.6	(0.14)	310
		Avg 20.5	(0.14)	311
10	Wet	19.0	(0.13)	325
		18.7	(0.13)	238
		Avg 18.9	(0.13)	282
12	Wet	18.4	(0.13)	288
		20.2	(0.14)	272
		Avg 19.3	(0.13)	280
14	Wet	14.8	(0.10)	234
		16.0	(0.11)	270
		Avg 15.4	(0.11)	252
16	Wet	15.8	(0.11)	270
		15.8	(0.11)	306
		Avg 15.8	(0.11)	288
18	Wet	13.2	(0.09)	241
		17.8	(0.12)	255
		Avg 15.0	(0.10)	319
20	Wet	15.3	(0.11)	272
		12.5	(0.09)	281
		Avg 10.9	(0.08)	277
22	Wet	11.7	(0.08)	279
		8.1	(0.06)	155
		Avg 10.2	(0.07)	200
24	Wet	9.2	(0.06)	178
		7.1	(0.05)	113
		Avg 8.0	(0.06)	137
26	Wet	7.5	(0.05)	125
		5.8	(0.04)	75
		Avg 6.0	(0.04)	93
28	Wet	5.9	(0.04)	84
		4.5	(0.03)	65
		Avg 5.3	(0.04)	72
30	Wet	4.9	(0.03)	69
		2.7	(0.02)	53
		Avg 3.7	(0.03)	71
32	Wet	3.2	(0.02)	62
		4.3	(0.03)	45
		Avg 5.2	(0.04)	50
34	Wet	4.8	(0.03)	48
		Deteriorated		

TABLE 75 (Concluded)
HYDROLYTIC STABILITY OF FOAMS
72-114 RED FOAM
120°F (49°C) + 95% R.H.

Weeks in Condition	Test Condition	Tensile Strength psi (MPa)		Elongation (%)
None (Controls)	----	25.9	(0.18)	370
		25.5	(0.18)	320
	Avg	25.7	(0.18)	345
2	Wet	21.9	(0.15)	310
		27.3	(0.19)	340
		23.5	(0.16)	340
	Avg	24.2	(0.17)	330
4	Wet	20.3	(0.14)	300
		17.1	(0.12)	322
		18.7	(0.13)	311
	Avg			
6	Wet	19.4	(0.13)	311
		21.4	(0.15)	304
		20.4	(0.14)	308
	Avg			
8	Wet	14.7	(0.10)	328
		17.9	(0.12)	364
		16.3	(0.11)	346
	Avg			
10	Wet	16.0	(0.11)	340
		18.3	(0.13)	400
		17.2	(0.12)	370
	Avg			
12	Wet	16.4	(0.11)	334
		14.5	(0.10)	314
		15.5	(0.11)	324
	Avg			
14	Wet	12.3	(0.08)	270
		13.4	(0.09)	280
		12.9	(0.09)	275
	Avg			
16	Wet	12.7	(0.09)	317
		10.8	(0.07)	303
		11.7	(0.08)	310
	Avg			
18	Wet	7.9	(0.05)	215
		9.5	(0.07)	203
		8.8	(0.06)	209
	Avg			
20	Wet	7.4	(0.05)	200
		5.9	(0.04)	143
		6.6	(0.05)	171
	Avg			
22	Wet	3.9	(0.03)	80
		4.9	(0.03)	87
		4.4	(0.03)	84
	Avg			
24	Wet	2.2	(0.02)	18
		3.2	(0.02)	40
		2.7	(0.02)	29
	Avg			
26	Wet	3.8	(0.03)	53
		1.7	(0.01)	19
		2.7	(0.02)	36
	Avg			
28		Deteriorated		

TABLE 76
HYDROLYTIC STABILITY OF FOAMS
W258R (1-1) RED FOAM RE-TEST
120°F (49°C) + 95% R.H.

Weeks in Condition	Test Condition	Tensile Strength		Elongation (%)
		psi	(MPa)	
2	Wet	35.6	(0.25)	362
		38.6	(0.27)	356
		Avg 37.1	(0.26)	359
2	Dry	35.3	(0.24)	295
		34.3	(0.24)	324
		Avg 34.8	(0.24)	310
4	Wet	33.2	(0.23)	363
		29.6	(0.20)	376
		Avg 31.4	(0.22)	370
4	Dry	35.7	(0.25)	370
		32.5	(0.22)	304
		Avg 34.1	(0.24)	337
6	Wet	30.9	(0.21)	309
		28.7	(0.20)	321
		Avg 29.8	(0.21)	315
6	Dry	27.0	(0.19)	289
		29.8	(0.21)	238
		Avg 28.4	(0.20)	264
8	Wet	35.1	(0.24)	277
		23.9	(0.16)	330
		Avg 29.5	(0.20)	304
8	Dry	23.0	(0.16)	355
		28.1	(0.19)	357
		Avg 25.6	(0.18)	356
10	Wet	32.6	(0.22)	331
		33.0	(0.23)	363
		Avg 32.8	(0.23)	347
10	Dry	30.2	(0.21)	305
		37.4	(0.26)	308
		Avg 33.8	(0.23)	307
12	Wet	25.7	(0.18)	348
		34.8	(0.24)	406
		Avg 30.2	(0.21)	377
12	Dry	36.5	(0.25)	310
		31.7	(0.23)	334
		Avg 34.1	(0.24)	322

TABLE 76 (Concluded)
 HYDROLYTIC STABILITY OF FOAMS
 W258R (1-1) RED FOAM RE-TEST
 120°F (49°C) + 95% R.H.

Weeks in Condition	Test Condition	Tensile Strength		Elongation (%)
		psi	(MPa)	
14	Wet	25.7	(0.18)	348
		34.8	(0.24)	406
		Avg 30.2	(0.21)	377
14	Dry	36.5	(0.25)	310
		31.7	(0.22)	334
		Avg 34.1	(0.24)	322
16	Wet	30.8	(0.21)	280
		29.3	(0.20)	290
		Avg 30.0	(0.21)	285
16	Dry	27.3	(0.19)	380
		35.2	(0.24)	340
		Avg 31.3	(0.22)	360
18	Wet	28.9	(0.20)	302
		21.9	(0.15)	200
		28.3	(0.20)	294
		Avg 26.4	(0.18)	265
18	Dry	24.6	(0.17)	211
		21.9	(0.15)	258
		Avg 23.3	(0.16)	235
20	Wet	30.3	(0.21)	303
		28.8	(0.20)	300
		Avg 29.6	(0.20)	302
20	Dry	22.4	(0.15)	200
		28.8	(0.20)	210
		30.6	(0.21)	297
		Avg 27.3	(0.19)	236

W901P, TMP baseline with orange pigment, and W258R, non-TMP with orange pigment are also being evaluated for hydrolytic stability. The 14-week data are presented in Table 77.

3.13 COMPATIBILITY OF RETICULATED FOAMS WITH TURBINE FUELS CONTAINING ANTI-STATIC ADDITIVES

Tests of the first group of reticulated foam specimens in a program to evaluate the effects of anti-static additives on the life of reticulated foams in a turbine fuel environment have been completed. All specimens were conditioned at 160°F (71°C) in the various test fluids listed below and tested at four-week intervals to a total of 24 weeks, with the fluids being changed at the four-week intervals:

- Fluid No. 1 - JP-4 (no additives);
- Fluid No. 2 - JP-5 (no additives);
- Fluid No. 3 - JP-4 with 5 ppm ASA-3 and 5 ppm Stadis 450;
- Fluid No. 4 - JP-4 with 2 ppm ASA-3 and 2 ppm Stadis 450;
- Fluid No. 5 - JP-5 with 2 ppm ASA-3 and 2 ppm Stadis 450;
- Fluid No. 6 - JP-4 with 2 ppm ASA-3;
- Fluid No. 7 - JP-4 with 2 ppm Stadis 450;
- Fluid No. 8 - JP-5 with 2 ppm ASA-3;
- Fluid No. 9 - JP-5 with 2 ppm Stadis 450;
- Fluid No. 10 - JP-4 with 2 ppm ASA-3, 2 ppm Stadis 450, 1 ppm CI (corrosion inhibitor), 1 ppm AO (anti-oxidant), 1 ppm MDI (metal deactivator), and 1 ppm FSII (fuel system icing inhibitor); and
- Fluid No. 11 - JP-5 with 2 ppm ASA-3, 2 ppm Stadis 450, 1 ppm CI, 1 ppm AO, 1 ppm MDI, and 1 ppm FSII.

Materials evaluated were W236R Batch (19-1) and W236R Batch (3-1) blue polyether fine pore foam per MIL-B-83054B (Type V) and two red polyester fine pore foams per MIL-B-83054B (Type III). The two red foams were a non-TMP material identified as run W258R (1-1) and a TMP material identified as run W901P (15-4). The TMP material was run in JP-4 with all additives. All foams underwent testing for tensile strength and elongation after rinsing with petroleum ether followed by air drying for 30 minutes.

TABLE 77
HYDROLYTIC STABILITY OF FOAMS
W547R ORANGE FOAMS (Non-TMP)
120°F (49°C) + 95% R.H.

Weeks in Condition	Test Condition	Tensile Strength (psi) (MPa)		Elongation (%)
None (controls)	Dry	17.6	(0.12)	220
		17.0	(0.12)	238
		18.2	(0.13)	229
		16.0	(0.11)	205
		<u>16.4</u>	<u>(0.11)</u>	<u>200</u>
		Avg	17.0 (0.12)	218
2	Wet	15.9	(0.11)	270
		<u>12.1</u>	<u>(0.08)</u>	<u>330</u>
		Avg	14.0 (0.10)	300
4	Wet	10.9	(0.08)	286
		<u>11.6</u>	<u>(0.08)</u>	<u>290</u>
		Avg	11.3 (0.08)	288
6	Wet	10.2	(0.07)	235
		<u>10.6</u>	<u>(0.07)</u>	<u>222</u>
		Avg	10.4 (0.07)	229
8	Wet	14.6	(0.10)	415
		<u>15.5</u>	<u>(0.11)</u>	<u>413</u>
		Avg	15.1 (0.10)	414
10	Wet	11.3	(0.08)	380
		<u>15.1</u>	<u>(0.10)</u>	<u>320</u>
		Avg	13.2 (0.09)	350
12	Wet	14.2	(0.10)	350
		<u>11.3</u>	<u>(0.08)</u>	<u>332</u>
		Avg	12.7 (0.09)	341
14	Wet	13.0	(0.09)	311
		<u>12.3</u>	<u>(0.08)</u>	<u>276</u>
		Avg	12.6 (0.09)	294

TABLE 77 (Continued)
 HYDROLYTIC STABILITY OF FOAMS
 W593R ORANGE FOAM (TMP)
 120°F (49°C) + 95% R.H.

Weeks in Condition	Test Condition	Tensile Strength		Elongation
		(psi)	(MPa)	(%)
None (controls)	Dry	22.4	(0.15)	284
		21.0	(0.14)	263
		22.4	(0.15)	230
		23.7	(0.16)	226
		<u>21.6</u>	<u>(0.15)</u>	<u>218</u>
		Avg	22.2 (0.15)	244
2	Wet	15.4	(0.11)	330
		<u>17.3</u>	<u>(0.12)</u>	<u>377</u>
		Avg	16.3 (0.11)	353
4	Wet	18.8	(0.13)	333
		<u>16.9</u>	<u>(0.12)</u>	<u>433</u>
		Avg	17.8 (0.12)	383
6	Wet	19.7	(0.14)	387
		<u>14.3</u>	<u>(0.10)</u>	<u>347</u>
		Avg	17.0 (0.12)	367
8	Wet	17.0	(0.12)	397
		<u>18.1</u>	<u>(0.12)</u>	<u>378</u>
		Avg	17.6 (0.12)	388
10	Wet	17.9	(0.12)	360
		<u>15.0</u>	<u>(0.10)</u>	<u>390</u>
		Avg	16.5 (0.11)	375
12	Wet	11.4	(0.08)	266
		<u>15.4</u>	<u>(0.11)</u>	<u>315</u>
		Avg	13.4 (0.09)	291
14	Wet	17.6	(0.12)	339
		<u>16.5</u>	<u>(0.11)</u>	<u>340</u>
		Avg	17.1 (0.12)	340

TABLE 77 (Concluded)
HYDROLYTIC STABILITY OF FOAMS
ORANGE FOAM
120°F (49°C) + 95% R.H.

Weeks in Condition	Test Condition	Tensile Strength		Elongation
		(psi)	(MPa)	(%)
W901P (TMP)				
2	Wet	15.4	(0.11)	330
		<u>17.3</u>	<u>(0.12)</u>	<u>377</u>
		Avg 16.3	(0.11)	353
4	Wet	19.7	(0.14)	387
		<u>14.3</u>	<u>(0.10)</u>	<u>347</u>
		Avg 17.0	(0.12)	367
W258R (Non-TMP)				
2	Wet	15.9	(0.11)	270
		<u>12.1</u>	<u>(0.08)</u>	<u>330</u>
		Avg 14.0	(0.10)	300
4	Wet	10.2	(0.07)	235
		<u>10.5</u>	<u>(0.07)</u>	<u>222</u>
		Avg 10.4	(0.07)	229

W236R Blue Foam was tested in both a fuel wet and dry condition. Blue foam data are presented in Table 78. Data for W258R (1-1) Red Foam are presented in Table 79. The red non-TMP polyester reverted in Fluids 4, 5, 8, 9, and 10. Red TMP polyester (W901P) reverted in Fluid No. 10 after 16 weeks as indicated in Table 80.

Three special polyether foams were evaluated in JP-4 turbine fuel No. 10 at 160°F (71°C). These polyether foams are designated W402-2 containing 1.1 parts standard PDI Blue Pigment, W403-2 containing 1.6 parts of experimental orange pigment No. 4602, and W404-2 containing 1.6 parts of experimental red pigment X13623-4. Data are given in Tables 81, 82, and 83.

Since the W258R, non-TMP, and W901P, TMP, foams all deteriorated after 20 weeks a second test phase has been initiated. The new materials being evaluated are compound production runs W593R-31-1, TMP, and W547R-26-1, non-TMP, and are from current production orange (Type I) foam. These foams are being evaluated under the same conditions and aging times as Phase I, except the concentration of the additives in the fuels have been lowered and the water removed from the fuels. The new fuel blends are:

- Fluid No. 22 - JP-5 (no additives);
- Fluid No. 31 - JP-5 (1 ppm ASA-3, 1 ppm Stadis 450, 1 ppm CI, 1 ppm AO, 1 ppm MDI, and 1 ppm FSII);
- Fluid No. 32 - JP-5 (1 ppm ASA-3, 1 ppm Stadis 450, 1 ppm CI, and 1 ppm FSII);
- Fluid No. 21 - JP-4 (no additives);
- Fluid No. 23 - JP-4 (5 ppm ASA-3, 5 ppm Stadis 450);
- Fluid No. 24 - JP-4 (1 ppm ASA-3, 1 ppm Stadis 450);
- Fluid No. 30 - JP-4 (1 ppm ASA-3, 1 ppm Stadis 450, 1 ppm CI, 1 ppm AO, 1 ppm MDI, 1 ppm FSII);
- Fluid No. 33 - JP-4 (1 ppm ASA-3, 1 ppm Stadis 450, 1 ppm CI, and 1 ppm FSII);
- Fluid No. 34 - JP-4 (1 ppm CI, 1 ppm FSII); and
- Fluid No. 10 - JP-4 (10 ml water, 1 ppm ASA-3, 1 ppm Stadis 450, 1 ppm CI, 1 ppm AO, 1 ppm MDI, and 1 ppm FSII).

TABLE 78
COMPATIBILITY OF RETICULATED FOAMS IN FUELS
W236R BLUE FOAM

Time (weeks)	Test Condition	Tensile Strength									
		Fluid No. 1	Fluid No. 3	Fluid No. 4	Fluid No. 6	Fluid No. 7	Fluid No. 10				
		psi (MPa)	psi (MPa)	psi (MPa)	psi (MPa)	psi (MPa)	psi (MPa)	psi (MPa)	psi (MPa)	psi (MPa)	psi (MPa)
4	Dry	15.7 (0.11)	16.5 (0.11)	15.3 (0.10)	15.3 (0.11)	16.0 (0.11)	15.3 (0.10)	15.3 (0.10)	15.3 (0.10)	15.3 (0.10)	15.3 (0.10)
		15.4 (0.11)	16.4 (0.11)	18.4 (0.13)	16.6 (0.11)	16.1 (0.11)	15.8 (0.11)	15.8 (0.11)	15.8 (0.11)	15.8 (0.11)	15.8 (0.11)
	Avg	15.1 (0.10)	21.0 (0.14)	17.8 (0.12)	17.9 (0.12)	15.3 (0.11)	16.1 (0.11)	16.1 (0.11)	16.1 (0.11)	16.1 (0.11)	16.1 (0.11)
8		15.4 (0.11)	18.0 (0.12)	17.2 (0.12)	16.6 (0.11)	15.8 (0.11)	15.7 (0.11)	15.7 (0.11)	15.7 (0.11)	15.7 (0.11)	15.7 (0.11)
	Dry	16.3 (0.11)	20.7 (0.14)	14.6 (0.10)	18.0 (0.12)	15.5 (0.11)	15.0 (0.10)	15.0 (0.10)	15.0 (0.10)	15.0 (0.10)	15.0 (0.10)
		16.2 (0.11)	17.3 (0.12)	17.5 (0.12)	18.6 (0.13)	16.7 (0.12)	17.7 (0.12)	17.7 (0.12)	17.7 (0.12)	17.7 (0.12)	17.7 (0.12)
12		18.1 (0.12)	16.4 (0.11)	16.5 (0.11)	15.4 (0.11)	15.8 (0.11)	17.9 (0.12)	17.9 (0.12)	17.9 (0.12)	17.9 (0.12)	17.9 (0.12)
	Avg	16.9 (0.12)	18.1 (0.12)	16.2 (0.11)	17.4 (0.12)	15.7 (0.11)	16.8 (0.12)	16.8 (0.12)	16.8 (0.12)	16.8 (0.12)	16.8 (0.12)
	Dry	13.8 (0.10)	14.6 (0.10)	14.8 (0.10)	16.8 (0.12)	16.7 (0.12)	16.6 (0.11)	16.6 (0.11)	16.6 (0.11)	16.6 (0.11)	16.6 (0.11)
16		15.3 (0.11)	16.3 (0.11)	14.9 (0.10)	15.6 (0.11)	15.6 (0.11)	16.9 (0.12)	16.9 (0.12)	16.9 (0.12)	16.9 (0.12)	16.9 (0.12)
	Avg	13.3 (0.09)	15.2 (0.10)	14.5 (0.10)	15.7 (0.11)	19.9 (0.14)	17.1 (0.12)	17.1 (0.12)	17.1 (0.12)	17.1 (0.12)	17.1 (0.12)
		14.1 (0.10)	15.4 (0.11)	14.7 (0.10)	16.0 (0.11)	17.4 (0.12)	16.9 (0.12)	16.9 (0.12)	16.9 (0.12)	16.9 (0.12)	16.9 (0.12)
20	Dry	12.3 (0.08)	12.8 (0.09)	11.7 (0.08)	14.1 (0.10)	13.2 (0.09)	11.9 (0.08)	11.9 (0.08)	11.9 (0.08)	11.9 (0.08)	11.9 (0.08)
		13.2 (0.09)	10.9 (0.08)	12.6 (0.09)	13.8 (0.10)	13.7 (0.09)	12.7 (0.09)	12.7 (0.09)	12.7 (0.09)	12.7 (0.09)	12.7 (0.09)
	Avg	12.8 (0.09)	14.5 (0.10)	15.1 (0.10)	13.8 (0.10)	12.7 (0.09)	12.4 (0.09)	12.4 (0.09)	12.4 (0.09)	12.4 (0.09)	12.4 (0.09)
24		12.7 (0.09)	12.7 (0.09)	13.2 (0.09)	13.9 (0.10)	13.2 (0.09)	12.3 (0.09)	12.3 (0.09)	12.3 (0.09)	12.3 (0.09)	12.3 (0.09)
	Dry	15.0 (0.10)	14.8 (0.10)	17.4 (0.12)	14.4 (0.10)	15.6 (0.11)	14.3 (0.10)	14.3 (0.10)	14.3 (0.10)	14.3 (0.10)	14.3 (0.10)
		14.8 (0.10)	14.3 (0.10)	15.1 (0.10)	14.8 (0.10)	16.1 (0.11)	17.3 (0.12)	17.3 (0.12)	17.3 (0.12)	17.3 (0.12)	17.3 (0.12)
24		13.9 (0.10)	14.3 (0.10)	19.4 (0.13)	14.9 (0.10)	14.6 (0.10)	15.9 (0.11)	15.9 (0.11)	15.9 (0.11)	15.9 (0.11)	15.9 (0.11)
	Avg	14.6 (0.10)	14.5 (0.10)	17.3 (0.12)	14.7 (0.10)	15.4 (0.11)	15.8 (0.11)	15.8 (0.11)	15.8 (0.11)	15.8 (0.11)	15.8 (0.11)
	Dry	14.7 (0.10)	15.0 (0.10)	14.7 (0.10)	15.2 (0.10)	14.6 (0.10)	16.6 (0.11)	16.6 (0.11)	16.6 (0.11)	16.6 (0.11)	16.6 (0.11)
24		17.2 (0.12)	14.9 (0.10)	14.8 (0.10)	10.5 (0.07)	17.3 (0.12)	15.3 (0.11)	15.3 (0.11)	15.3 (0.11)	15.3 (0.11)	15.3 (0.11)
	Avg	14.3 (0.10)	14.7 (0.10)	16.1 (0.11)	15.0 (0.10)	19.4 (0.13)	11.7 (0.08)	11.7 (0.08)	11.7 (0.08)	11.7 (0.08)	11.7 (0.08)
		15.4 (0.11)	14.9 (0.10)	15.2 (0.10)	13.6 (0.09)	17.1 (0.12)	14.5 (0.10)	14.5 (0.10)	14.5 (0.10)	14.5 (0.10)	14.5 (0.10)

TABLE 78 (Continued)
COMPATIBILITY OF RETICULATED FOAMS IN FUELS
W236R BLUE FOAM

Time (weeks)	Test Condition	Tensile Strength							
		Fluid No. 1 psi (MPa)	Fluid No. 3 psi (MPa)	Fluid No. 4 psi (MPa)	Fluid No. 6 psi (MPa)	Fluid No. 7 psi (MPa)	Fluid No. 10 psi (MPa)		
4	Wet	9.3 (0.06)	8.8 (0.06)	9.1 (0.06)	8.8 (0.06)	10.7 (0.07)	9.7 (0.07)		
		8.3 (0.06)	9.9 (0.07)	8.6 (0.06)	10.2 (0.07)	9.0 (0.06)	8.2 (0.06)		
	Avg	8.9 (0.06)	8.7 (0.06)	8.8 (0.06)	8.6 (0.06)	10.6 (0.07)	11.1 (0.08)		
8	Wet	8.8 (0.06)	9.1 (0.06)	8.8 (0.06)	9.2 (0.06)	10.1 (0.07)	9.7 (0.07)		
		9.2 (0.06)	10.7 (0.07)	7.9 (0.05)	8.5 (0.06)	11.3 (0.08)	9.5 (0.07)		
	Avg	7.9 (0.05)	9.1 (0.06)	9.2 (0.06)	9.0 (0.06)	8.7 (0.06)	8.5 (0.06)		
12	Wet	9.6 (0.07)	8.7 (0.06)	8.7 (0.06)	8.9 (0.06)	9.4 (0.06)	10.4 (0.07)		
		8.9 (0.06)	9.5 (0.06)	8.6 (0.06)	8.8 (0.06)	9.8 (0.07)	9.5 (0.07)		
	Avg	8.2 (0.06)	7.9 (0.05)	7.5 (0.05)	7.9 (0.05)	8.9 (0.06)	8.6 (0.06)		
16	Wet	7.9 (0.05)	7.6 (0.05)	8.8 (0.06)	10.2 (0.07)	8.1 (0.06)	8.6 (0.06)		
		9.9 (0.07)	8.0 (0.06)	7.1 (0.05)	8.6 (0.06)	8.2 (0.06)	8.4 (0.06)		
	Avg	8.7 (0.06)	7.8 (0.05)	7.7 (0.05)	8.9 (0.06)	8.4 (0.06)	8.5 (0.06)		
20	Wet	7.5 (0.05)	7.7 (0.05)	8.3 (0.06)	8.2 (0.06)	8.4 (0.06)	6.9 (0.05)		
		7.0 (0.05)	9.1 (0.06)	8.2 (0.06)	7.8 (0.05)	7.5 (0.05)	7.9 (0.05)		
	Avg	7.8 (0.05)	7.9 (0.05)	7.4 (0.05)	8.4 (0.06)	7.9 (0.05)	7.8 (0.05)		
24	Wet	7.5 (0.05)	8.3 (0.06)	8.0 (0.06)	8.1 (0.06)	7.9 (0.05)	7.5 (0.05)		
		8.7 (0.06)	9.0 (0.06)	7.9 (0.05)	8.6 (0.06)	7.5 (0.05)	7.0 (0.05)		
	Avg	7.9 (0.05)	8.2 (0.06)	8.8 (0.06)	8.7 (0.06)	8.4 (0.06)	8.7 (0.06)		
24	Wet	8.1 (0.06)	8.9 (0.06)	7.5 (0.05)	8.1 (0.06)	7.9 (0.05)	7.4 (0.05)		
		8.2 (0.06)	8.7 (0.06)	8.0 (0.06)	8.5 (0.06)	7.9 (0.05)	7.7 (0.05)		
	Avg	7.8 (0.05)	5.9 (0.04)	6.1 (0.04)	7.8 (0.05)	7.9 (0.05)	6.8 (0.05)		
24	Wet	6.5 (0.04)	7.7 (0.05)	7.2 (0.05)	8.4 (0.06)	8.0 (0.06)	7.8 (0.05)		
		6.7 (0.05)	6.9 (0.05)	7.4 (0.05)	7.2 (0.05)	7.6 (0.05)	7.8 (0.05)		
	Avg	7.0 (0.05)	6.8 (0.05)	6.9 (0.05)	7.8 (0.05)	7.8 (0.05)	7.5 (0.05)		

TABLE 78 (Continued)
COMPATIBILITY OF RETICULATED FOAMS IN FUELS
W236R BLUE FOAM

Time (weeks)	Test Condition	Elongation							
		Fluid No. 1 (percent)	Fluid No. 3 (percent)	Fluid No. 4 (percent)	Fluid No. 6 (percent)	Fluid No. 7 (percent)	Fluid No. 10 (percent)		
4	Dry	203	180	189	189	153	155		
		176	155	190	173	167	188		
		172	200	182	172	178	179		
		Avg 184	178	187	178	166	174		
8	Dry	150	140	160	147	132	155		
		112	128	145	115	115	164		
		120	125	157	113	126	147		
		Avg 127	131	154	125	124	155		
12	Dry	99	105	100	104	117	162		
		106	132	100	110	134	141		
		114	128	115	120	138	129		
		Avg 106	122	105	111	130	144		
16	Dry	173	138	128	145	146	139		
		142	149	95	130	127	149		
		156	149	153	122	157	153		
		Avg 157	145	125	132	143	147		
20	Dry	124	159	87	132	123	114		
		132	185	200	131	196	162		
		115	171	175	130	182	137		
		Avg 124	172	154	131	167	138		
24	Dry	123	82	84	92	123	125		
		120	89	113	88	113	102		
		122	103	90	122	121	105		
		Avg 122	91	96	101	119	111		

TABLE 78 (Continued)
COMPATIBILITY OF RETICULATED FOAMS IN FUELS
W236R BLUE FOAM

Time (weeks)	Test Condition	Elongation							
		Fluid No. 1 (percent)	Fluid No. 3 (percent)	Fluid No. 4 (percent)	Fluid No. 6 (percent)	Fluid No. 7 (percent)	Fluid No. 10 (percent)		
4	Wet	112	96	72	96	80	87		
		112	113	77	90	91	109		
		76	101	98	106	92	106		
		Avg 100	103	82	97	88	101		
8	Wet	69	70	74	84	80	87		
		85	66	77	88	66	74		
		74	76	75	65	92	67		
		Avg 76	71	75	79	79	76		
12	Wet	76	104	73	76	58	98		
		100	90	109	53	63	78		
		80	95	100	89	60	82		
		Avg 85	96	94	73	60	86		
16	Wet	78	100	93	98	95	78		
		93	77	88	75	101	65		
		75	79	77	121	107	96		
		Avg 82	85	86	98	101	80		
20	Wet	58	52	61	73	85	68		
		59	40	65	74	76	77		
		83	54	60	67	64	90		
		Avg 66	49	62	71	75	78		
24	Wet	56	66	69	74	69	70		
		41	67	60	63	45	84		
		43	68	68	62	73	72		
		Avg 47	67	66	66	62	75		

TABLE 78 (Continued)
COMPATIBILITY OF RETICULATED FOAMS IN FUELS
W236R BLUE FOAM

Time (weeks)	Test Condition	Tensile Strength									
		Fluid No. 2	Fluid No. 5	Fluid No. 8	Fluid No. 9	Fluid No. 11	Fluid No. 2	Fluid No. 5	Fluid No. 8	Fluid No. 9	Fluid No. 11
		psi (MPa)	psi (MPa)	psi (MPa)	psi (MPa)	psi (MPa)	psi (MPa)	psi (MPa)	psi (MPa)	psi (MPa)	psi (MPa)
4	Dry	13.5 (0.09)	16.4 (0.11)	15.6 (0.11)	14.8 (0.10)	16.1 (0.11)	13.5 (0.09)	16.4 (0.11)	15.6 (0.11)	14.8 (0.10)	16.1 (0.11)
	Avg	17.0 (0.12)	15.7 (0.11)	16.3 (0.11)	15.4 (0.11)	15.7 (0.11)	17.0 (0.12)	15.7 (0.11)	16.3 (0.11)	15.4 (0.11)	15.7 (0.11)
8	Dry	16.8 (0.12)	15.0 (0.10)	14.2 (0.10)	13.8 (0.10)	13.1 (0.09)	16.8 (0.12)	15.0 (0.10)	14.2 (0.10)	13.8 (0.10)	13.1 (0.09)
	Avg	15.8 (0.11)	15.7 (0.11)	15.3 (0.11)	14.7 (0.10)	15.0 (0.10)	15.8 (0.11)	15.7 (0.11)	15.3 (0.11)	14.7 (0.10)	15.0 (0.10)
12	Dry	13.9 (0.10)	17.8 (0.12)	14.2 (0.10)	15.5 (0.11)	14.2 (0.10)	13.9 (0.10)	17.8 (0.12)	14.2 (0.10)	15.5 (0.11)	14.2 (0.10)
	Avg	17.5 (0.12)	17.7 (0.12)	13.9 (0.10)	16.3 (0.11)	13.9 (0.10)	17.5 (0.12)	17.7 (0.12)	13.9 (0.10)	16.3 (0.11)	13.9 (0.10)
16	Dry	11.6 (0.08)	15.4 (0.11)	15.0 (0.10)	15.3 (0.11)	14.2 (0.10)	11.6 (0.08)	15.4 (0.11)	15.0 (0.10)	15.3 (0.11)	14.2 (0.10)
	Avg	14.3 (0.10)	16.9 (0.12)	14.4 (0.10)	15.7 (0.11)	14.1 (0.10)	14.3 (0.10)	16.9 (0.12)	14.4 (0.10)	15.7 (0.11)	14.1 (0.10)
20	Dry	11.5 (0.08)	15.4 (0.11)	10.6 (0.07)	14.7 (0.10)	11.5 (0.08)	11.5 (0.08)	15.4 (0.11)	10.6 (0.07)	14.7 (0.10)	11.5 (0.08)
	Avg	11.8 (0.08)	17.1 (0.12)	12.3 (0.08)	15.3 (0.11)	17.0 (0.12)	11.8 (0.08)	17.1 (0.12)	12.3 (0.08)	15.3 (0.11)	17.0 (0.12)
24	Dry	11.7 (0.08)	16.1 (0.11)	11.3 (0.08)	14.0 (0.10)	13.7 (0.09)	11.7 (0.08)	16.1 (0.11)	11.3 (0.08)	14.0 (0.10)	13.7 (0.09)
	Avg	11.7 (0.08)	16.2 (0.11)	11.4 (0.08)	14.7 (0.10)	14.1 (0.10)	11.7 (0.08)	16.2 (0.11)	11.4 (0.08)	14.7 (0.10)	14.1 (0.10)
28	Dry	15.1 (0.10)	13.7 (0.09)	14.5 (0.10)	14.9 (0.10)	13.5 (0.09)	15.1 (0.10)	13.7 (0.09)	14.5 (0.10)	14.9 (0.10)	13.5 (0.09)
	Avg	13.2 (0.09)	12.5 (0.09)	17.5 (0.12)	14.9 (0.10)	15.1 (0.10)	13.2 (0.09)	12.5 (0.09)	17.5 (0.12)	14.9 (0.10)	15.1 (0.10)
32	Dry	13.7 (0.09)	14.2 (0.10)	17.6 (0.12)	15.3 (0.11)	14.7 (0.10)	13.7 (0.09)	14.2 (0.10)	17.6 (0.12)	15.3 (0.11)	14.7 (0.10)
	Avg	14.0 (0.10)	13.5 (0.09)	16.5 (0.11)	15.0 (0.10)	14.4 (0.10)	14.0 (0.10)	13.5 (0.09)	16.5 (0.11)	15.0 (0.10)	14.4 (0.10)
36	Dry	15.9 (0.11)	17.4 (0.12)	14.4 (0.10)	15.6 (0.11)	15.3 (0.11)	15.9 (0.11)	17.4 (0.12)	14.4 (0.10)	15.6 (0.11)	15.3 (0.11)
	Avg	13.8 (0.10)	15.1 (0.10)	14.8 (0.10)	15.5 (0.11)	15.9 (0.11)	13.8 (0.10)	15.1 (0.10)	14.8 (0.10)	15.5 (0.11)	15.9 (0.11)
40	Dry	16.2 (0.11)	19.4 (0.13)	14.9 (0.10)	14.9 (0.10)	15.9 (0.11)	16.2 (0.11)	19.4 (0.13)	14.9 (0.10)	14.9 (0.10)	15.9 (0.11)
	Avg	15.3 (0.11)	17.3 (0.12)	14.7 (0.10)	15.3 (0.11)	15.7 (0.11)	15.3 (0.11)	17.3 (0.12)	14.7 (0.10)	15.3 (0.11)	15.7 (0.11)
44	Dry	14.7 (0.10)	15.7 (0.11)	15.2 (0.10)	14.9 (0.10)	15.3 (0.11)	14.7 (0.10)	15.7 (0.11)	15.2 (0.10)	14.9 (0.10)	15.3 (0.11)
	Avg	15.1 (0.10)	17.4 (0.12)	15.4 (0.11)	17.4 (0.12)	13.6 (0.09)	15.1 (0.10)	17.4 (0.12)	15.4 (0.11)	17.4 (0.12)	13.6 (0.09)
48	Dry	16.7 (0.12)	13.6 (0.09)	14.2 (0.10)	15.8 (0.11)	15.0 (0.10)	16.7 (0.12)	13.6 (0.09)	14.2 (0.10)	15.8 (0.11)	15.0 (0.10)
	Avg	15.5 (0.11)	15.6 (0.11)	14.9 (0.10)	16.1 (0.11)	14.6 (0.10)	15.5 (0.11)	15.6 (0.11)	14.9 (0.10)	16.1 (0.11)	14.6 (0.10)

TABLE 78 (Continued)
COMPATIBILITY OF RETICULATED FOAMS IN FUELS
W236R BLUE FOAM

Tensile Strength											
Time (weeks)	Test Condition	Fluid No. 2 psi	Fluid No. 2 (MPa)	Fluid No. 5 psi	Fluid No. 5 (MPa)	Fluid No. 8 psi	Fluid No. 8 (MPa)	Fluid No. 9 psi	Fluid No. 9 (MPa)	Fluid No. 11 psi	Fluid No. 11 (MPa)
4	Wet	9.1	(0.06)	8.3	(0.06)	11.3	(0.08)	10.8	(0.07)	8.4	(0.06)
		8.8	(0.06)	9.6	(0.07)	11.6	(0.08)	8.4	(0.06)	9.1	(0.06)
	Avg	9.3	(0.06)	8.2	(0.06)	8.8	(0.06)	8.1	(0.06)	8.2	(0.06)
		9.1	(0.06)	8.7	(0.06)	10.6	(0.07)	9.1	(0.06)	8.7	(0.06)
8	Wet	9.9	(0.07)	10.1	(0.07)	8.5	(0.06)	9.6	(0.07)	10.4	(0.07)
		9.0	(0.06)	10.9	(0.08)	9.0	(0.06)	8.6	(0.06)	8.9	(0.06)
	Avg	9.5	(0.07)	9.9	(0.07)	8.9	(0.06)	7.9	(0.05)	9.9	(0.07)
		9.4	(0.06)	10.3	(0.07)	8.8	(0.06)	8.7	(0.06)	9.8	(0.07)
12	Wet	8.4	(0.06)	8.2	(0.06)	7.9	(0.05)	8.4	(0.06)	8.4	(0.06)
		7.5	(0.05)	8.0	(0.06)	9.2	(0.06)	9.1	(0.06)	8.6	(0.06)
	Avg	9.8	(0.07)	9.1	(0.06)	8.9	(0.06)	11.2	(0.08)	9.2	(0.06)
		8.5	(0.06)	8.4	(0.06)	8.7	(0.06)	9.6	(0.07)	8.7	(0.06)
16	Wet	7.9	(0.05)	7.5	(0.05)	9.2	(0.06)	9.4	(0.06)	8.3	(0.06)
		8.8	(0.06)	8.4	(0.06)	8.4	(0.06)	8.0	(0.06)	7.5	(0.05)
	Avg	8.3	(0.06)	8.3	(0.06)	7.7	(0.05)	9.9	(0.07)	7.9	(0.05)
		8.3	(0.06)	8.1	(0.06)	8.4	(0.06)	9.1	(0.06)	7.9	(0.05)
20	Wet	7.4	(0.05)	8.3	(0.06)	9.5	(0.07)	7.3	(0.05)	7.3	(0.05)
		7.5	(0.05)	9.3	(0.06)	9.5	(0.07)	7.9	(0.05)	7.5	(0.05)
	Avg	9.1	(0.06)	8.2	(0.06)	8.6	(0.06)	7.5	(0.05)	7.2	(0.05)
		8.0	(0.06)	8.6	(0.06)	9.2	(0.06)	7.6	(0.05)	7.4	(0.05)
24	Wet	7.7	(0.05)	9.1	(0.06)	8.1	(0.06)	7.5	(0.05)	6.9	(0.05)
		7.6	(0.05)	9.7	(0.07)	10.6	(0.07)	7.9	(0.05)	7.4	(0.05)
	Avg	7.9	(0.05)	9.0	(0.06)	8.6	(0.06)	8.0	(0.06)	7.0	(0.05)
		7.8	(0.05)	9.2	(0.06)	9.1	(0.06)	7.8	(0.05)	7.1	(0.05)

TABLE 78 (Continued)
COMPATIBILITY OF RETICULATED FOAMS IN FUELS
W236R BLUE FOAM

Elongation						
Time (weeks)	Test Condition	Fluid No. 2 (percent)	Fluid No. 5 (percent)	Fluid No. 8 (percent)	Fluid No. 9 (percent)	Fluid No. 11 (percent)
4	Dry	194	156	172	86	188
		172	190	168	149	170
		182	153	154	179	136
		Avg 183	166	165	138	165
8	Dry	94	147	123	124	135
		115	144	115	110	95
		75	144	117	133	124
		Avg 95	145	118	122	118
12	Dry	80	87	75	119	82
		80	95	85	110	124
		75	116	108	86	123
		Avg 78	99	89	105	109
16	Dry	162	170	153	167	142
		146	134	164	167	146
		149	148	136	135	136
		Avg 152	151	151	156	141
20	Dry	152	87	132	158	146
		150	200	131	141	144
		125	175	130	143	125
		Avg 142	154	131	147	138
24	Dry	114	104	115	133	116
		137	101	95	135	134
		167	80	100	130	140
		Avg 137	95	103	133	130

TABLE 78 (Concluded)
COMPATIBILITY OF RETICULATED FOAMS IN FUELS
W236R BLUE FOAM

Time (weeks)	Test Condition	Elongation				
		Fluid No. 2 (percent)	Fluid No. 5 (percent)	Fluid No. 8 (percent)	Fluid No. 9 (percent)	Fluid No. 11 (percent)
4	Wet	103	113	110	94	109
		75	101	103	114	108
		111	132	112	115	108
		Avg 96	115	108	108	107
8	Wet	96	82	84	66	69
		93	---	88	84	85
		76	68	65	63	74
		Avg 88	75	79	71	76
12	Wet	40	55	78	51	63
		43	49	60	58	78
		49	42	47	57	30
		Avg 44	49	62	55	57
16	Wet	103	91	78	97	74
		91	91	94	77	100
		108	106	102	91	98
		Avg 101	96	91	88	91
20	Wet	52	68	68	48	63
		63	56	47	67	64
		50	52	67	66	60
		Avg 55	59	61	60	62
24	Wet	60	40	54	50	42
		58	50	53	55	72
		46	35	45	39	51
		Avg 55	42	51	48	55

TABLE 79
COMPATIBILITY OF RETICULATED FOAMS IN FUELS
W258R (1-1) RED FOAM

Time (weeks)	Test Condition	Tensile Strength							
		Fluid No. 1 psi (MPa)	Fluid No. 3 psi (MPa)	Fluid No. 4 psi (MPa)	Fluid No. 6 psi (MPa)	Fluid No. 7 psi (MPa)	Fluid No. 10 psi (MPa)		
4	Dry	36.75 (0.25)	35.51 (0.24)	30.64 (0.21)	27.80 (0.19)	26.57 (0.18)	32.59 (0.22)		
		32.29 (0.22)	29.18 (0.21)	30.83 (0.21)	28.70 (0.20)	34.35 (0.24)	17.30* (0.12)*		
		29.22 (0.20)	21.71* (0.15)*	18.79* (0.13)*	23.83 (0.16)	30.30 (0.21)	35.73 (0.25)		
8	Dry	Avg. 32.74 (0.23)	32.35 (0.22)	30.74 (0.21)	26.79 (0.18)	30.31 (0.21)	34.16 (0.24)		
		29.32 (0.20)	25.49 (0.18)	4.49 (0.03)	19.40 (0.13)	27.59 (0.19)	12.79 (0.09)		
		30.55 (0.21)	33.57 (0.23)	5.09 (0.04)	23.69 (0.16)	27.61 (0.19)	14.47 (0.10)		
12	Dry	28.38 (0.20)	30.01 (0.21)	5.21 (0.04)	26.33 (0.18)	27.28 (0.19)	14.47 (0.10)		
		Avg. 29.42 (0.20)	29.69 (0.20)	4.93 (0.03)	23.14 (0.16)	27.49 (0.19)	13.91 (0.10)		
		22.71 (0.16)	20.68 (0.14)	Deteriorated	14.81 (0.10)	22.52 (0.16)	8.31 (0.06)		
16	Dry	25.14 (0.17)	18.86 (0.13)		14.90 (0.10)	13.14 (0.09)	6.87 (0.05)		
		23.24 (0.16)	23.06 (0.16)		13.53 (0.09)	18.18 (0.13)	7.33 (0.05)		
		Avg. 23.70 (0.16)	20.87 (0.14)		14.41 (0.10)	17.95 (0.12)	7.50 (0.05)		
20	Dry	0.79 (0.005)	Deteriorated	10.38 (0.07)	0.80 (0.01)	4.74 (0.03)	Deteriorated		
		3.10 (0.021)		15.07 (0.10)	4.50 (0.03)	4.32 (0.03)			
		4.15 (0.029)		11.27 (0.08)	2.23 (0.02)	3.04 (0.02)			
	Avg.	2.68 (0.018)		12.24 (0.08)	2.51 (0.02)	4.03 (0.03)			
	Dry	Deteriorated		Deteriorated	Deteriorated	Deteriorated			

*Not included in average.

TABLE 79 (Continued)
COMPATIBILITY OF RETICULATED FOAMS IN FUELS
W258R (1-1) RED FOAM

Time (weeks)	Test Condition	Elongation							
		Fluid No. 1 (percent)	Fluid No. 3 (percent)	Fluid No. 4 (percent)	Fluid No. 6 (percent)	Fluid No. 7 (percent)	Fluid No. 10 (percent)		
4	Dry	351	365	286	382	280	350		
		380	304	338	404	385	178*		
		<u>364</u>	*	*	<u>301</u>	<u>394</u>	<u>390</u>		
		Avg. 365	335	312	362	353	370		
8	Dry	318	209	30	189	274	200		
		282	321	37	300	308	168		
		<u>329</u>	<u>242</u>	<u>55</u>	<u>297</u>	<u>279</u>	<u>200</u>		
		Avg. 310	257	41	262	287	189		
12	Dry	240	217	Deteriorated	95	255	81		
		252	236		160	232	63		
		<u>243</u>	<u>234</u>		<u>182</u>	<u>224</u>	<u>46</u>		
		Avg. 245	229		146	237	63		
16	Dry	22	Deteriorated	171	3	38	Deteriorated		
		13		238	28	72			
		<u>36</u>		<u>205</u>	<u>33</u>	<u>35</u>			
		Avg. 24		205	21	48			
20	Dry	Deteriorated		Deteriorated	Deteriorated	Deteriorated			

*Not included in average.

TABLE 79 (Continued)
COMPATIBILITY OF RETICULATED FOAMS IN FUELS
W258R (11-1) RED FOAM

Time (weeks)	Test Condition	Tensile Strength				
		Fluid No. 2 psi (MPa)	Fluid No. 5 psi (MPa)	Fluid No. 8 psi (MPa)	Fluid No. 9 psi (MPa)	Fluid No. 11 psi (MPa)
4	Dry	32.75 (0.23)	29.18 (0.20)	29.49 (0.20)	35.48 (0.24)	32.92 (0.23)
		34.31 (0.24)	29.85 (0.21)	28.14 (0.19)	36.44 (0.25)	32.46 (0.22)
		29.15 (0.20)	35.57 (0.18)	23.84 (0.16)	30.09 (0.21)	29.31 (0.20)
	Avg	32.07 (0.22)	31.53 (0.22)	27.16 (0.19)	34.00 (0.23)	31.56 (0.22)
8	Dry	34.37 (0.24)	24.52 (0.17)	---	26.07 (0.18)	12.86 (0.09)
		25.73 (0.18)	21.80 (0.15)	8.51 (0.06)	20.44 (0.14)	18.39 (0.13)
		29.78 (0.21)	27.31 (0.19)	7.22 (0.05)	24.74 (0.17)	17.76 (0.12)
	Avg	29.96 (0.21)	24.54 (0.17)	7.87 (0.05)	23.75 (0.16)	16.34 (0.11)
12	Dry	12.10 (0.08)	21.81 (0.15)	6.48 (0.04)	22.25 (0.15)	9.03 (0.06)
		9.32 (0.06)	27.95 (0.19)	5.98 (0.04)	14.64 (0.10)	6.74 (0.05)
		8.44 (0.06)	27.01 (0.19)	4.27 (0.03)	14.18 (0.10)	8.04 (0.06)
	Avg	9.95 (0.07)	25.59 (0.18)	5.58 (0.04)	17.02 (0.12)	7.94 (0.05)
16	Dry	4.93 (0.03)	Deteriorated	Deteriorated	Deteriorated	2.04 (0.01)
		6.83 (0.05)				* 2.84 (0.02)
		4.90 (0.03)				2.44 (0.02)
	Avg	5.55 (0.04)				2.44 (0.02)
20	Dry	Deteriorated				Deteriorated

*Fell apart

TABLE 79 (Concluded)
COMPATIBILITY OF RETICULATED FOAMS IN FUELS
W258R (1-1) RED FOAM

Time (weeks)	Test Condition	Elongation				
		Fluid No. 2 (percent)	Fluid No. 5 (percent)	Fluid No. 8 (percent)	Fluid No. 9 (percent)	Fluid No. 11 (percent)
4	Dry	333	364	315	350	371
		364	374	370	368	300
		326	361	402	252	330
		Avg. 341	366	362	323	334
8	Dry	298	280	86	261	238
		267	228	82	261	254
		260	263	90	275	228
		Avg. 275	257	86	266	240
12	Dry	175	224	42	104	115
		127	308	26	110	58
		95	308	45	120	79
		Avg. 132	280	38	111	84
16	Dry	31	Deteriorated	Deteriorated	Deteriorated	36
		53				*
		59				25
		Avg. 48				31
20	Dry	Deteriorated				Deteriorated

*Fell apart

TABLE 80
COMPATIBILITY OF RETICULATED FOAMS IN FUELS
W901P RED FOAM (Fluid No. 10)

Time (weeks)	Test Condition	Tensile Strength psi (MPa)		Elongation (%)
4	Dry	20.71	(0.14)	398
		21.14	(0.15)	439
		<u>24.45</u>	<u>(0.17)</u>	<u>426</u>
	Avg	22.10	(0.15)	421
8	Dry	19.16	(0.13)	303
		25.18	(0.17)	323
		<u>22.79</u>	<u>(0.16)</u>	<u>305</u>
	Avg	22.38	(0.15)	310
12	Dry	14.35	(0.10)	248
		13.41	(0.09)	247
		<u>11.61</u>	<u>(0.08)</u>	<u>232</u>
	Avg	13.12	(0.09)	242
16		DETERIORATED		

TABLE 81
COMPATIBILITY OF RETICULATED FOAMS IN FUELS
W402-2 BLUE FOAM (Fluid No. 10)

Time (weeks)	Test Condition	Tensile psi	Strength (MPa)	Elongation (%)
4	Wet	8.70	(0.06)	97
		9.11	(0.06)	115
		8.70	(0.06)	93
		Avg 8.84	(0.06)	102
4	Dry	15.61	(0.11)	115
		13.89	(0.10)	93
		16.71	(0.12)	133
		Avg 15.40	(0.11)	114
8	Wet	6.98	(0.05)	86
		8.62	(0.06)	82
		8.21	(0.06)	86
		Avg 7.94	(0.05)	85
8	Dry	12.21	(0.08)	167
		9.96	(0.07)	110
		12.57	(0.09)	118
		Avg 11.58	(0.08)	132
12	Wet	8.2	(0.06)	69
		7.4	(0.05)	39
		10.2	(0.07)	76
		Avg 8.6	(0.06)	61
12	Dry	15.4	(0.11)	140
		12.9	(0.09)	100
		11.1	(0.08)	95
		Avg 13.1	(0.09)	112
16	Wet	7.3	(0.05)	71
		8.1	(0.06)	56
		7.5	(0.05)	62
		Avg 7.6	(0.05)	63
16	Dry	13.3	(0.09)	63
		13.1	(0.09)	82
		15.0	(0.10)	113
		Avg 13.8	(0.10)	86
20	Wet	7.6	(0.05)	105
		8.3	(0.06)	115
		7.9	(0.05)	90
		Avg 8.0	(0.06)	103
20	Dry	15.2	(0.10)	140
		15.8	(0.11)	155
		15.6	(0.11)	145
		Avg 15.6	(0.11)	147
24	Wet	6.7	(0.05)	69
		7.4	(0.05)	56
		7.6	(0.05)	59
		Avg 7.2	(0.05)	61
24	Dry	14.7	(0.10)	112
		14.1	(0.10)	104
		12.7	(0.09)	92
		Avg 13.8	(0.10)	103

TABLE 82
COMPATIBILITY OF RETICULATED FOAMS IN FUELS
W403-2 ORANGE FOAM (Fluid No. 10)

Time (weeks)	Test Condition	Tensile Strength		Elongation (%)
		psi	(MPa)	
4	Wet	12.18	(0.08)	66
		11.00	(0.08)	70
		<u>10.61</u>	<u>(0.07)</u>	<u>80</u>
		Avg 11.26	(0.08)	72
4	Dry	17.31	(0.12)	137
		17.40	(0.12)	120
		<u>17.90</u>	<u>(0.12)</u>	<u>136</u>
		Avg 17.54	(0.12)	131
8	Wet	11.29	(0.08)	90
		8.87	(0.06)	76
		<u>9.68</u>	<u>(0.07)</u>	<u>84</u>
		Avg 9.95	(0.07)	83
8	Dry	15.19	(0.10)	120
		15.09	(0.10)	133
		<u>13.94</u>	<u>(0.10)</u>	<u>109</u>
		Avg 14.73	(0.10)	120
12	Wet	10.8	(0.07)	73
		10.8	(0.07)	70
		<u>10.4</u>	<u>(0.07)</u>	<u>60</u>
		Avg 10.6	(0.07)	68
12	Dry	18.1	(0.12)	122
		18.4	(0.13)	139
		<u>18.1</u>	<u>(0.12)</u>	<u>137</u>
		Avg 18.2	(0.13)	133
16	Wet	9.6	(0.07)	73
		9.4	(0.06)	56
		<u>9.6</u>	<u>(0.07)</u>	<u>57</u>
		Avg 9.5	(0.07)	62
16	Dry	17.8	(0.12)	110
		17.4	(0.12)	135
		<u>16.5</u>	<u>(0.11)</u>	<u>110</u>
		Avg 17.2	(0.12)	118
20	Wet	9.8	(0.07)	105
		9.3	(0.06)	100
		<u>9.6</u>	<u>(0.07)</u>	<u>130</u>
		Avg 9.6	(0.07)	112
20	Dry	16.0	(0.11)	155
		16.4	(0.11)	190
		<u>17.8</u>	<u>(0.12)</u>	<u>135</u>
		Avg 16.7	(0.12)	160
24	Wet	9.0	(0.06)	80
		7.2	(0.05)	72
		<u>7.6</u>	<u>(0.05)</u>	<u>54</u>
		Avg 7.9	(0.05)	69
24	Dry	14.3	(0.10)	121
		16.2	(0.11)	123
		<u>20.1</u>	<u>(0.14)</u>	<u>121</u>
		Avg 16.9	(0.12)	122

TABLE 83
COMPATIBILITY OF RETICULATED FOAMS IN FUELS
W404-2 RED FOAM (Fluid No. 10)

Time (weeks)	Test Condition	Tensile Strength		Elongation
		psi	(MPa)	(%)
4	Wet	8.40	(0.06)	110
		8.40	(0.06)	97
		<u>8.80</u>	<u>(0.06)</u>	<u>102</u>
		Avg 8.53	(0.06)	103
4	Dry	15.17	(0.10)	115
		16.44	(0.11)	147
		<u>15.52</u>	<u>(0.11)</u>	<u>146</u>
		Avg 15.71	(0.11)	136
8	Wet	8.40	(0.06)	81
		9.60	(0.07)	77
		<u>8.80</u>	<u>(0.06)</u>	<u>82</u>
		Avg 8.90	(0.06)	80
8	Dry	10.91	(0.08)	113
		9.50	(0.07)	80
		<u>9.07</u>	<u>(0.06)</u>	<u>125</u>
		Avg 9.83	(0.07)	106
12	Wet	9.2	(0.06)	72
		7.6	(0.05)	57
		<u>8.8</u>	<u>(0.06)</u>	<u>61</u>
		Avg 8.5	(0.06)	63
12	Dry	13.7	(0.09)	106
		10.5	(0.07)	74
		<u>14.2</u>	<u>(0.10)</u>	<u>129</u>
		Avg 12.8	(0.09)	103
16	Wet	10.6	(0.07)	74
		9.4	(0.06)	91
		<u>9.6</u>	<u>(0.07)</u>	<u>97</u>
		Avg 9.9	(0.07)	87
16	Dry	13.2	(0.09)	100
		13.2	(0.09)	87
		<u>12.3</u>	<u>(0.08)</u>	<u>83</u>
		Avg 13.1	(0.09)	90
20	Wet	7.3	(0.05)	120
		7.6	(0.05)	145
		<u>7.3</u>	<u>(0.05)</u>	<u>85</u>
		Avg 7.4	(0.05)	117
20	Dry	15.0	(0.10)	120
		15.3	(0.11)	160
		<u>16.3</u>	<u>(0.11)</u>	<u>153</u>
		Avg 15.5	(0.11)	144
24	Wet	7.2	(0.05)	71
		7.1	(0.05)	77
		<u>7.3</u>	<u>(0.05)</u>	<u>92</u>
		Avg 7.2	(0.05)	80
24	Dry	13.9	(0.10)	133
		13.9	(0.10)	174
		<u>13.1</u>	<u>(0.09)</u>	<u>135</u>
		Avg 13.6	(0.09)	147

3.14 RTV-133

A one-part silicone sealant, RTV-133, was submitted by General Electric for evaluation to MIL-S-38249. This specification concerns firewall sealing compounds.

With the exception of low temperature flexibility and peel strength tests, all evaluations were conducted according to MIL-S-38249. These included specific gravity, non-volatile content, flow, tack-free time, curing rate, thermal rupture, oil resistance, and accelerated storage stability. Substrate materials, other than those specified in MIL-S-38249, were substituted in the low temperature flexibility, peel strength, and corrosion evaluations. For low temperature flexibility, aluminum QQ-A-250/13 T6 is replacing aluminum QQ-A-355. Aluminum QQ-A-250/12 and stainless steel MIL-S-5059 Comp 304 annealed, Finish 2B are replacing aluminum QQ-A-355 and stainless steel MIL-S-5059 Comp 302, Finish 2B, respectively, for corrosion evaluation. The peel test substrates are aluminum QQ-A-250/13, stainless steel MIL-S-5059 Comp 304 annealed, Finish 2B and titanium MIL-T-9046 Type III, Composition C. One-half of each type of peel panel was fabricated without a primer prior to sealant application. The other half was fabricated using SS-4004 primer on the substrate materials. The data are given in Table 84.

3.15 MIL-A-8625 ANODIZED ALUMINUM PANELS

PR-1422 A-1/2, Batch C26486 and PR-1422 B-2, Batch C28847 sealants were used to evaluate the bondability of both water-sealed and dichromate-sealed MIL-A-8625 anodized aluminum panels. Seven each water-sealed and seven each dichromate-sealed panels were prepared with each sealant and were cured for 48 hours at 78°F (25.6°C) plus 24 hours at 140°F (60°C).

Eight panels (four with PR-1422 A-1/2 and four with PR-1422 B-2 on both water-sealed and dichromate-sealed MIL-A-8625) were conditioned for seven days at 140°F (60°C) in JRF. Six similar

TABLE 84

RTV-133

Tack-Free Time - Passed in five hours. Material was soft underneath, but top film was tack free. After 21-1/2 hrs. the material beneath the skin had firmed up.

Flow - 0.1 inch

Standard Cure - Shore_A - 37 pts. @ 48 hrs.

Re_x - 45 pts. @ 48 hrs.

Non-Volatile Content - 95.44%

Thermal Rupture - 15 min. @ 2000°F (1093°C) - Passed

15 min. @ 400°F (204°C) - Passed

Flame Resistance - 2000°F (1093°C) for 15 min. - did not burn through to the panel

- 3500°F (1927°C) for 15 min. - burned through to the panel at small area. RTV-133 got red but did not flame.

- 3500°F (1927°C) for 15 min. - burned through to the panel at very small area. RTV-133 got red but did not flame.

Low Temp. Flex - Passed

Specific Gravity - 1.27, 1.28

After conditioning tube for 14 days @ 120°F (49°C)

Tack Free - 6 hrs. - skinned over but still soft beneath top film

Flow - Failed - material ran down fixture as a disk.

Adhesion Corrosion -

(a) had adhesion

(b) no corrosion beneath sealant

Oil Resistance - 3 days @ 140°F (60°C) in Stauffer's Blend 7700 (corrosion) Passed

TABLE 84 (Continued)

RTV-133

Panel	Conditioning	Load PIW (N/cm)		Failure Mode (% Coh)
7075 Clad SS-4004 Primer	Control	4.6	(8.1)	20
		4.4	(7.7)	
		Avg. 4.5	(7.9)	
7075 Clad No Primer	Control	1.7	(3.0)	5
		0.85	(1.5)	5
		Avg. 1.3	(2.3)	
7075 Clad SS-4004 Primer	72 hrs. @ 400°F (204°C)/Air	18.3	(32.0)	70
		15.5	(27.1)	70
		Avg. 16.9	(29.6)	
7075 Clad No Primer	72 hrs. @ 400°F (204°C)/Air	5.9	(10.3)	5
		4.5	(7.9)	5
		Avg. 5.2	(9.1)	
MIL-S-5059 Stainless steel SS-4004 Primer	Control	16.3	(28.5)	100 (adhesive to screen)
		11.3	(19.8)	100
		Avg. 13.8	(24.2)	(adhesive to screen)
MIL-S-5059 Stainless steel No Primer	Control	2.3	(4.0)	5
		4.2	(7.4)	5
		Avg. 3.3	(5.8)	
MIL-S-5059 Stainless steel SS-4004 Primer	72 hrs. @ 400°F (204°C)/Air	18.1	(31.7)	90
		18.6	(32.6)	95
		Avg. 18.3	(32.0)	
MIL-S-5059 Stainless steel No Primer	72 hrs. @ 400°F (204°C)/Air	17.9	(31.3)	100
		17.9	(31.3)	95
		Avg. 17.9	(31.3)	

TABLE 84 (Concluded)

RTV-133

Panel	Conditioning	Load		Failure Mode (% Coh)
		PIW	(N/cm)	
MIL-T-9046 Titanium SS-4004 Primer	Control	13.1	(22.9)	100 (sealant to screen)
		12.8	(22.4)	100
	Avg	13.0	(22.7)	(sealant to screen)
MIL-T-9046 Titanium No Primer	Control	0		0
		0.9	(1.6)	5
	Avg	0.45	(0.8)	
MIL-T-9046	72 hrs. @ 400°F	17.2	(30.1)	85
	(204°C)/Air	19.0	(33.3)	100
	Avg	18.1	(31.7)	
MIL-T-9046 Titanium No Primer	72 hrs. @ 400°F	6.9	(12.1)	15
	(204°C)/Air	7.7	(13.5)	10
	Avg	7.3	(12.8)	

panels were also conditioned for seven days at 140°F (60°C) in JRF/SW.

The peel panels fabricated with PR-1422 A-1/2, and conditioned in JRF, exhibited cohesive failures, with failure ultimately occurring at the cloth/sealant interface. The PR-1422 A-1/2 panels conditioned in JRF/SW failed cohesively with approximately 50 percent of the failure occurring at the cloth interface.

One water-sealed MIL-A-8625 panel fabricated with PR-1422 B-2 had 30 percent adhesive failure in JRF, and one had 100 percent adhesive failure in JRF/SW. The data are given in Table 85.

TABLE 85
PEEL STRENGTH

PR1422 A-1/2

Conditioning	Panel Type	Load		% Cohesive Failure	
7 days @ 140°F(60°C)/ JRF Avg.	8625 (Gray) ¹	10.1 9.2 9.7		* ³ * ³	
7 days @ 140°F(60°C)/ JRF Avg.	8625 (Green) ²	6.4 7.3 6.9		* ³ * ³	
7 days @ 140°F(60°C)/ JRF/SW Avg.	8625 (Gray) ¹	JRF SW 25.9 30.4 29.3 28.8 27.6 29.6		JRF ³ SW ³ 50 45 60 45	
7 days @ 140°F(60°C)/ JRF/SW Avg.	8625 (Green) ²	JRF SW 29.1 34.4 24.6 32.9 26.9 33.7		JRF ³ SW ³ 50 50 65 50	

NOTE: The peel panels did not have a top cap of 1/32 inch, thus causing the peel angle to increase and give lower loads.

¹Water-sealed

²Dichromate-sealed

³None of the failures were to the panel. All failures not cohesive were at the cloth.

TABLE 85 (Concluded)

PEEL STRENGTH

PR1422 B-2

Conditioning	Panel Type	Load	% Cohesive Failure
7 days @ 140°F (60°C) / JRF Avg.	8625 (Gray) ¹	22.9 17.4 <u>20.2</u>	100 70/30 ³
7 days @ 140°F (60°C) / JRF Avg.	8625 (Green) ²	20.9 21.3 <u>21.1</u>	100 100
7 days @ 140°F (60°C) / JRF/SW	8625 (Gray) ¹	JRF - 7.7 SW - 4.0	JRF - 5/95 ³ SW - 0
7 days @ 140°F (60°C) / JRF/SW	8625 (Green) ²	JRF - 27.8 SW - 16.0	JRF - 100 SW - 20 ⁴

¹Water-sealed²Dichromate-sealed³Adhesive to panel failure⁴80% of failure was at sealant cloth interface

SECTION 4

PLASTICS, ADHESIVES, AND COMPOSITES

The UDRI has been conducting engineering research and development work in the field of plastics, adhesives, and composites for aircraft systems for over 20 years. During the period reported here this work has involved conducting many types of mechanical tests and environmental characterizations with these types of materials. Plastics investigations have involved transparent materials, injection molded materials, and cast materials. Adhesive investigations have dealt with adhesives for use in portable tactical shelters, high temperature investigations, and aircraft structural applications and have also included studies of various surface preparation processes. Composite materials investigations have included evaluations of materials for high temperature applications. The major efforts in these various areas are discussed in detail in the following sections.

4.1 STRESS CRACKING OF POLYETHERSULFONE

The use of injection molded thermoplastics for rotating band applications on both small and large bore ammunition has been under investigation for several years. One of the materials currently being utilized in this regard on 20 mm projectile is polyethersulfone (PES). Bands made of this material possess many desirable features. One problem area which has been observed, however, involves solvent resistance. Molded bands have been observed to develop crazing when exposed to solvent (ethyl acetate) laden atmospheres. The presence of residual stresses resulting from thermal contraction during cool-down and melt stresses in the polymer on filling the cavity aggravate this stress cracking problem. The purpose of this investigation was to establish the magnitude of this residual molded-in stress level.

Tensile specimens of PES were subjected to solvent-induced stress-rupture tests and a relationship between applied stress and both time-to-craze and time-to-failure was developed. After this relationship between tensile stress and time-to-craze was established, actual projectiles with molded PES rotating bands were immersed in solvent and the time-to-craze recorded. Correlation of the projectile test results with the tensile specimen test results were then made to develop an estimate of the residual molded-in stress in the rotating bands.

Finally, a solvent resistant coating was applied to a number of tensile stress-rupture specimens in an effort to reduce the susceptibility of PES to solvent-induced stress cracking.

Two types of specimens were utilized in this investigation. The first was an injection-molded 8.5 inch (21.6 cm) long tensile specimen whose dimensions corresponded to that prescribed in ASTM D638, Type I. Overall specimen length was 8.5 inches (21.6 cm). Specimen thickness was 0.135 ± 0.005 inch (0.343 ± 0.013 cm). This specimen type was injection molded on a Newbury-Eldorado Model 3V-75RS injection molding machine. Prior to molding, the resin was dried overnight at 325°F (163°C). After molding, the specimens were annealed to relieve residual molded-in stresses. Specimens were annealed by placing them in a room temperature (R.T.) air circulating oven, raising the temperature to 380°F (193°C), holding this temperature for 18 hours, then turning off heat but allowing the air to circulate and cooling to 150°F (66°C) before removal. Examination of specimens under cross-polarized light indicated that annealing did reduce the residual stress levels, but also that even in the unannealed condition, the residual stresses in the tensile specimens were quite low to start with (on the order to a few hundred psi at most).

The second type of specimen was an actual rotating band molded onto a 20 mm projectile (Figure 54). These specimens were molded by AVCO* and provided to us for this investigation.

* AVCO Corporation, Wilmington, Massachusetts.



Figure 54 . Plastic Rotating Band Specimen. (Note imperfection at gate location where excess material was trimmed.)

The bands were injection molded with two tunnel or submarine gates diametrically opposed to each other. After molding, a roughened imperfection on the band surface was observed at the gating locations.

In the final phase of the investigation, in which the effect of a coating on solvent stress cracking behavior was examined, 6 inch (15.2 cm) long tensile specimens (ASTM D638, Type I) were molded and provided by ICI*. All of the dimensions of these specimens were identical to those of the longer specimen described above except for the length of the two gripping sections. These specimens were not annealed. Two coatings were evaluated, one blue and another yellow. Both the blue and yellow paints corresponded to TT-E-516, composition L (alternatively TT-E-515, composition L). The yellow was color number 33538 and the blue was color number 25109, both per Federal Standard 595. The coatings were applied by AVCO and to our knowledge differ only in pigment.

Specimens for tensile stress-rupture tests were sealed in a test tube with a slot cut into the bottom. The seal around the specimen passing through the slot was achieved with RTV 118 silicone rubber adhesive/sealant. After mounting of this specimen/tube assembly in a creep machine (Figure 55), taking care to insure accurate axial alignment, the specimen was loaded to the desired stress level. The solvent was then introduced as rapidly as possible into the test tube, taking care not to splash into the gripped area. When the tube had been filled (a process requiring about three seconds), the time-to-craze and time-to-failure counts were started.

Projectile rotating band specimens for solvent stress cracking tests were placed in a small beaker and brightly illuminated with several high intensity microscope light. Opposite sides of the rotating bands were observed through

* ICI United States, Inc., Wilmington, Delaware.

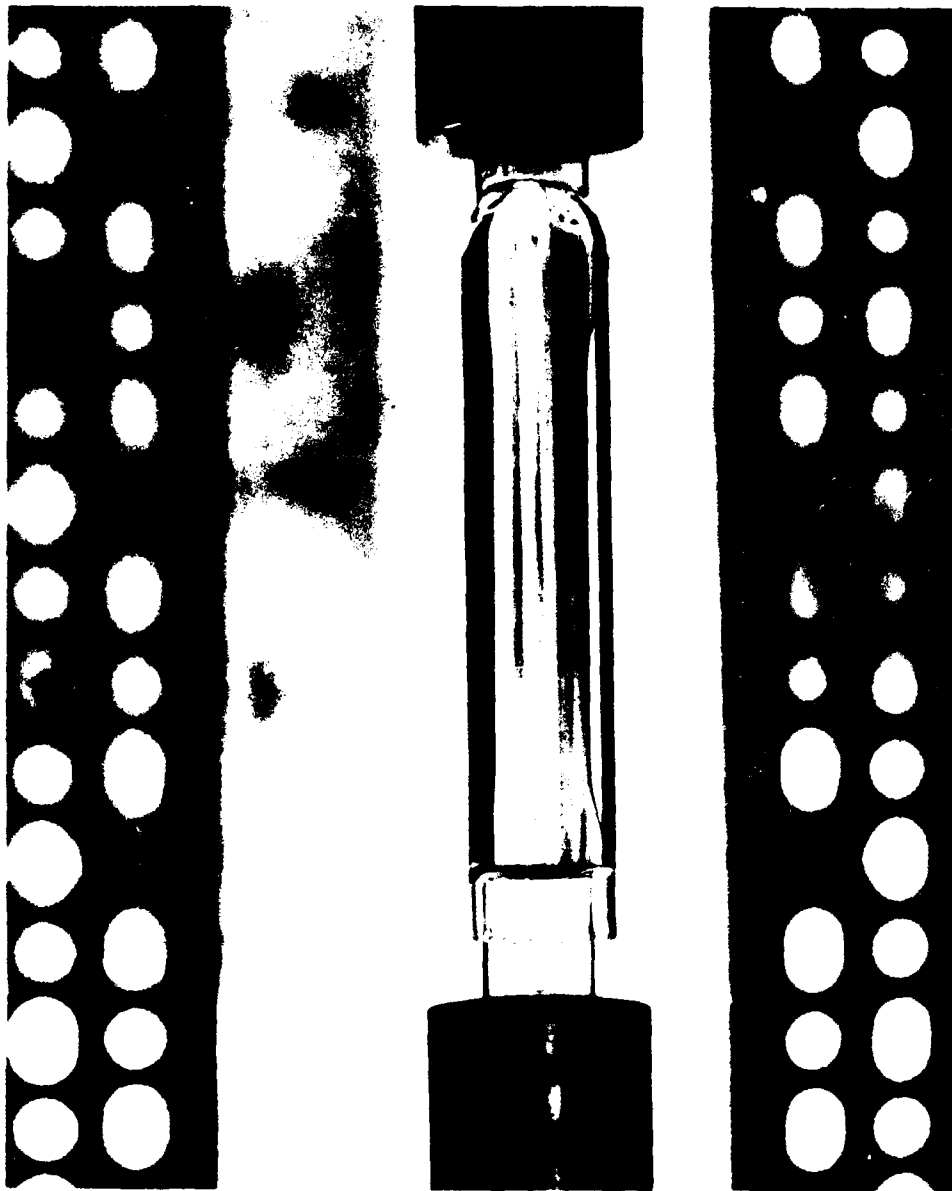


Figure 55. Tensile Stress-Rupture Specimen Immersed in Solvent and Under Load.

two telescopes. When the lighting was set and the telescopes focused on the band, the solvent was rapidly introduced into the beaker and the time count to the appearance of the first craze started. During this observation period, the projectile was slowly rotated by hand so that the two observers could continuously inspect the entire circumference.

For each tensile stress-rupture specimen described in the preceding paragraphs and illustrated in Figure 55, two times were recorded; (1) the time elapsed until the first craze appeared, and; (2) the time elapsed until total fracture. This information was desired over the stress range of 500 to 5,000 psi (3.45 to 34.45 MPa). The use of three different solvents was required in order to develop time-to-craze/fracture versus applied stress data over this entire stress region in convenient time periods. Methoxyethanol was used in the low stress region (500-2,500 psi or 3.45-17.23 MPa) acetic acid in the midrange (1,500-3,500 psi or 10.34-24.12 MPa), and isopropanol in the high stress region (3,000-5,000 psi or 20.67-34.45 MPa). Table 86 presents the results of these tests. Figures 56-61 present these data in graphical form.

Figure 62 illustrates typical crazes which occurred in the rotating band specimens tested as described in the preceding paragraphs. Only crazing could be observed on these rotating band specimens, not total failure as with the tensile specimens. Presumably, as crazing occurred, the hoop stresses were relieved and no stresses remained to cause complete fracture. In every case, the crazes which occurred on the rotating band specimens occurred at the two gating locations and also at the two "weld" lines located midway around the band between the two gates. Table 86 lists the observed time-to-craze for each of the projectile specimens tested.

In order to estimate the residual molded-in stress in the PES rotating bands, the time-to-craze for the bands was compared to the time-to-craze for the tensile specimens. These comparisons

TABLE 86
POLYETHERSULFONE TENSILE STRESS CRACKING BEHAVIOR

Stress		Time to Craze	Time to Fracture	Time to Craze	Time to Fracture	Time to Craze	Time to Fracture
Psi	MPa	Isopropanol		Acetic Acid		Methoxyethanol	
5000	34.45	1.4 M 0.5 M 0.4 M	<3.3 H 1 H 0.6 H				
4500	31.01	3.25 M 0.7 M 0.6 M	3.7 H 2.5 H 2 H	instant	45 s		
4000	27.56	5.5 M 9 M 4.5 M	13.9 H 16.2 H 8.4 H				
3500	24.12	0.5-1.0 H 44 M 42 M	97 H 70.1 H 73.5 H	7 s	0.09 H		
3000	20.67	72 H	>460 H	12 s	0.1 H		
2500	17.23	>150 H		40 s 45 s	0.24 H 0.23 H	5 s 3 s 2 s	15 s 18 s 20 s
2000	13.78	>76 H		45 s 60 s 65 s	0.3 H 0.36 H 0.75 H	5 s 15 s 7 s 6 s 3 s	25 s 45 s 45 s 20 s 29 s
1500	10.34	>76 H		60 s 306 s 60 s 65 s	2.7 H 2.43 H 0.78 H 2.32 H	10 s 20 s 10 s 7 s 5 s	75 s 70 s 20 s 20 s 22 s
1000	6.89	>485 H		50 s 6 M 60 s 9 M >189 H	3.94 H 15.5 H >428 H >236 H >189 H	80 s 60 s 15 s 20 s 190 s	465 s 213 s 20 s 25 s 255 s
900	6.20					115 s 80 s 630 s	230 s 288 s 666 s
750	5.17					540 s	1040 s
500	3.45					1040 s	3420 s
Projectile Bands		>30 H >30 H		75 s <120 s 18 s		21 s 10 s 9 s 21 s	

NOTE: Designations - H=hours; M=minutes; s=seconds;
>=greater than; <=less than.

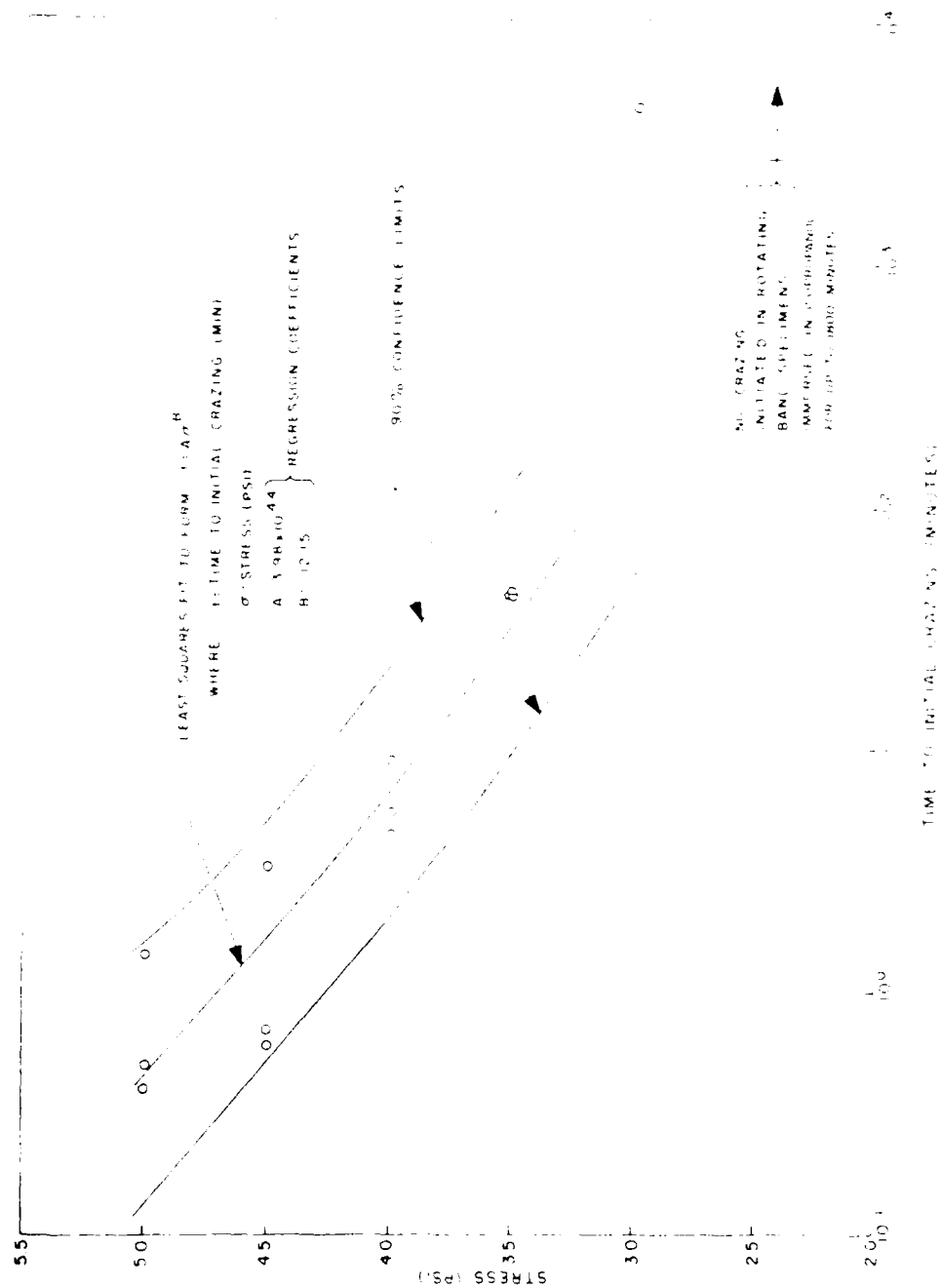


Figure 56. Effect of Stress on Stress Cracking Behavior of Polyethersulfone in Isopropanol.

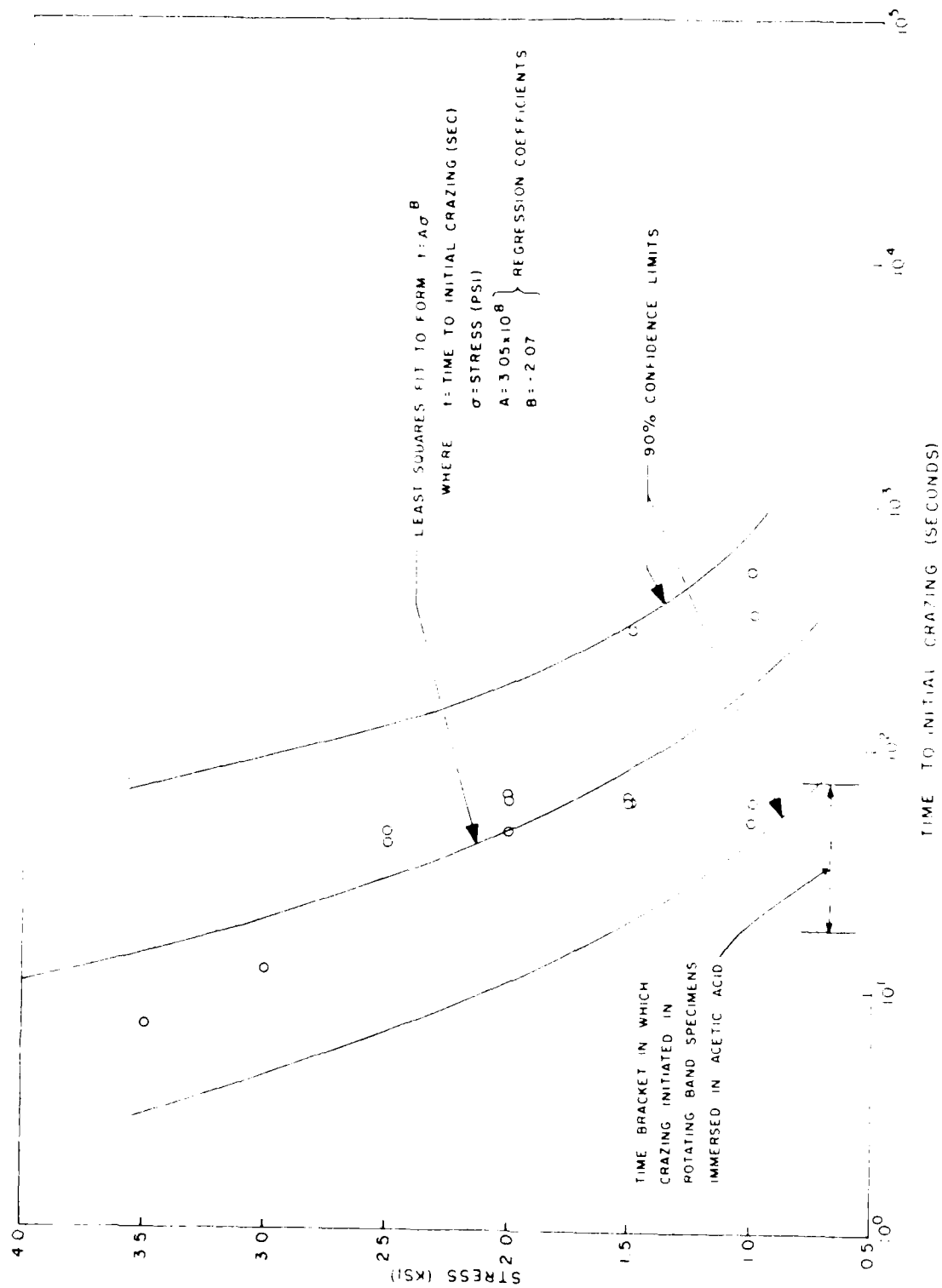


Figure 57. Effect of Stress on Stress-Crazing Behavior of Polyethersulfone in Acetic Acid.

AD-A085 859

DAYTON UNIV OH RESEARCH INST

F/O 11/4

QUICK REACTION EVALUATION OF MATERIALS FOR SYSTEMS APPLICATIONS--ETC(11)

APR 80 D R ASKINS, R R CERVAY, D L HART

F33615-78-C-5002

UNCLASSIFIED UOR-TR-80-12

AFWAL-TR-80-4025

ML

4-4

25

030-010

END

DATE

FILED

8-80

DTIC

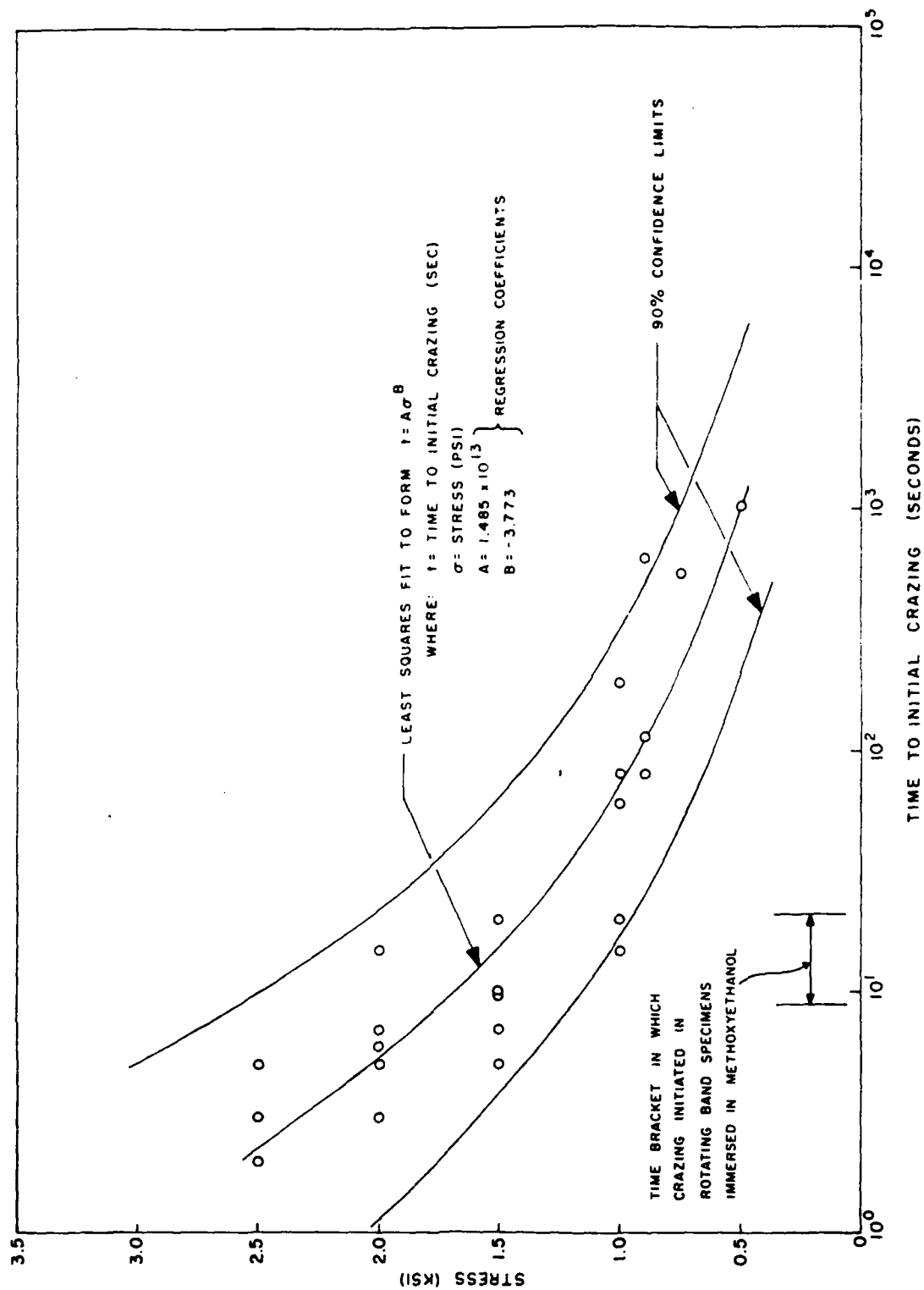


Figure 58. Effect of Stress on Stress Crazing Behavior of Polyethersulfone in Methoxyethanol.

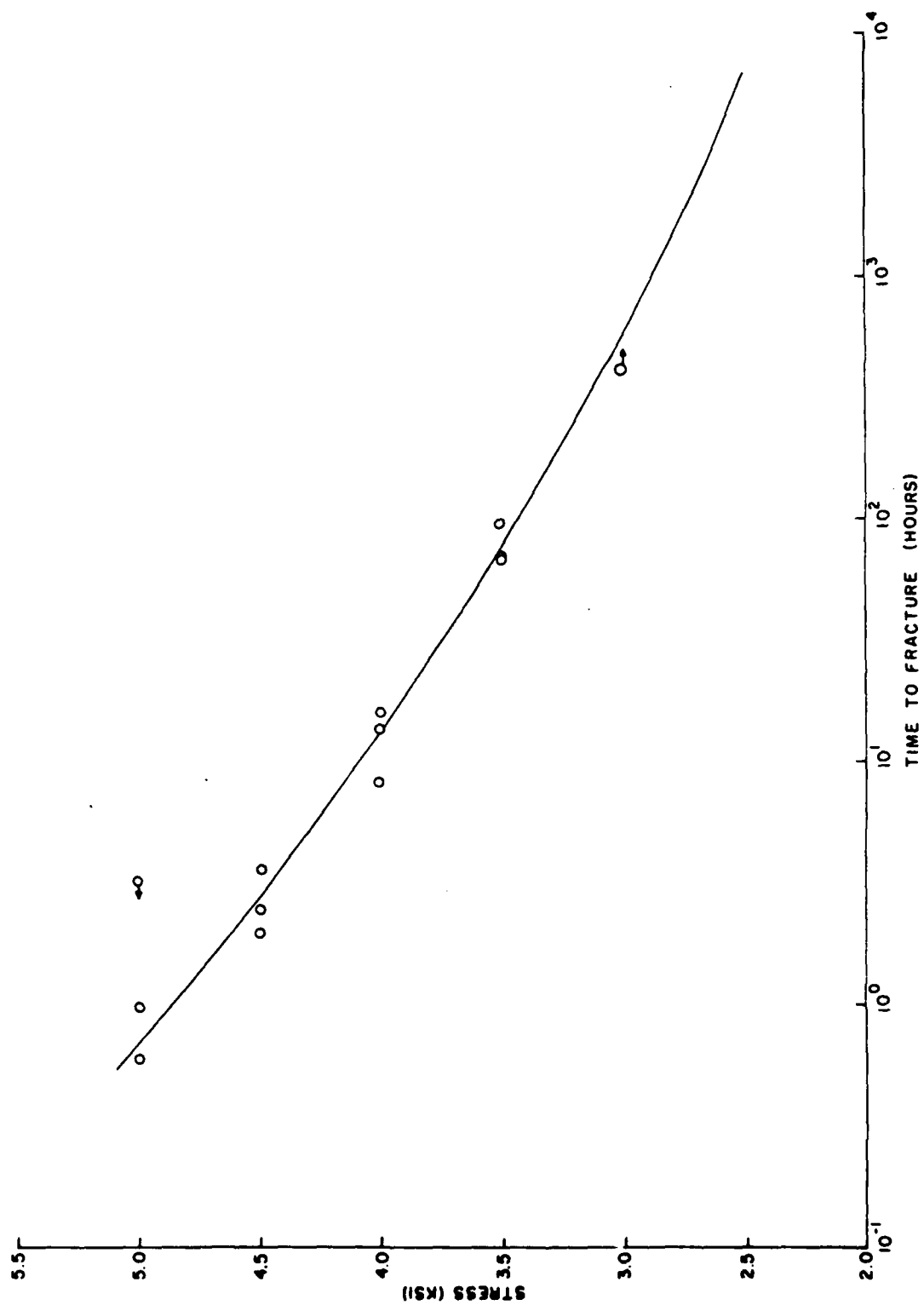


Figure 59. Effect of Stress on Stress Fracture Behavior of Polyethersulfone in Isopropanol.

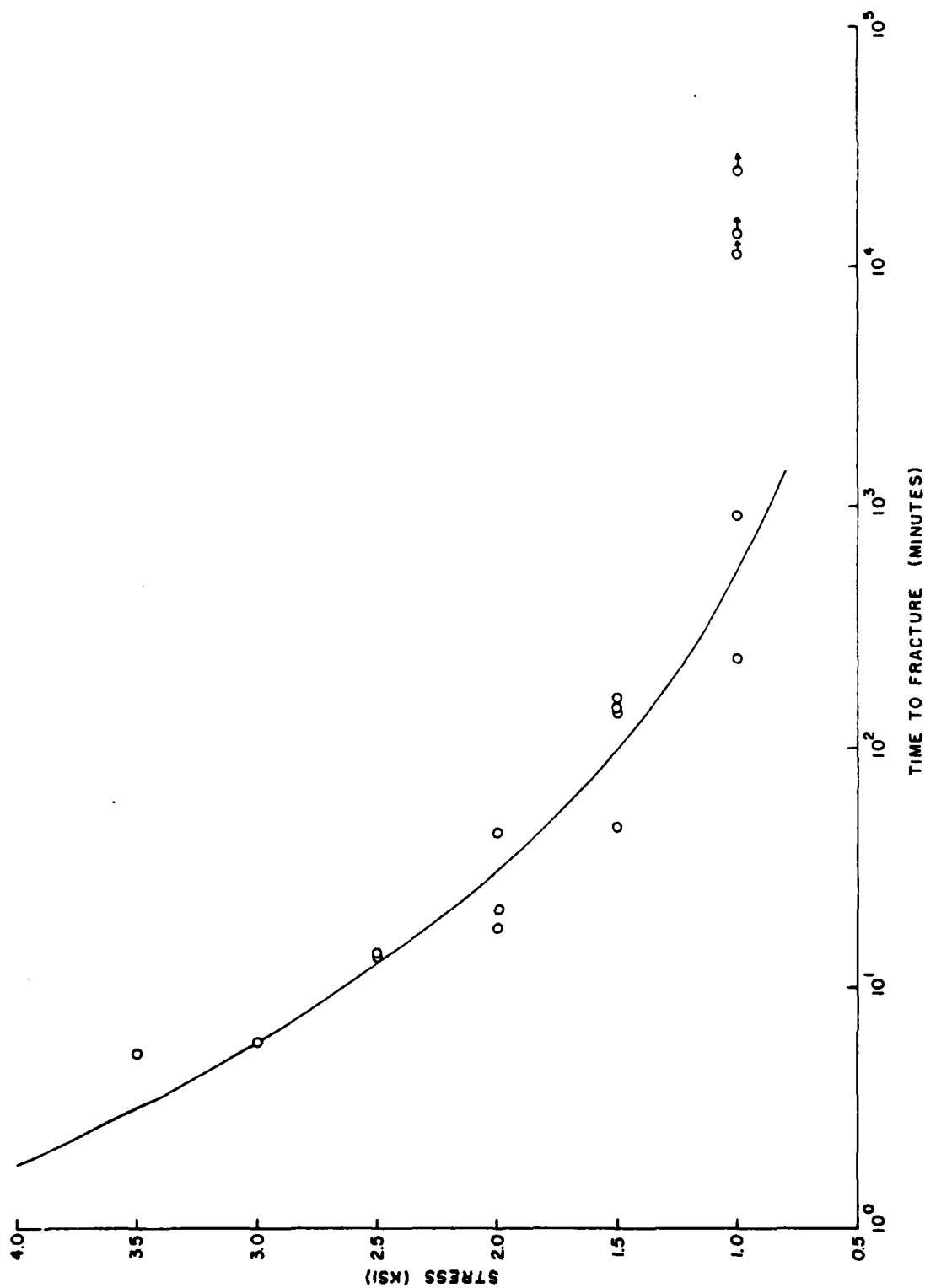


Figure 60. Effect of Stress on Stress Fracture Behavior of Polyethersulfone in Acetic Acid.

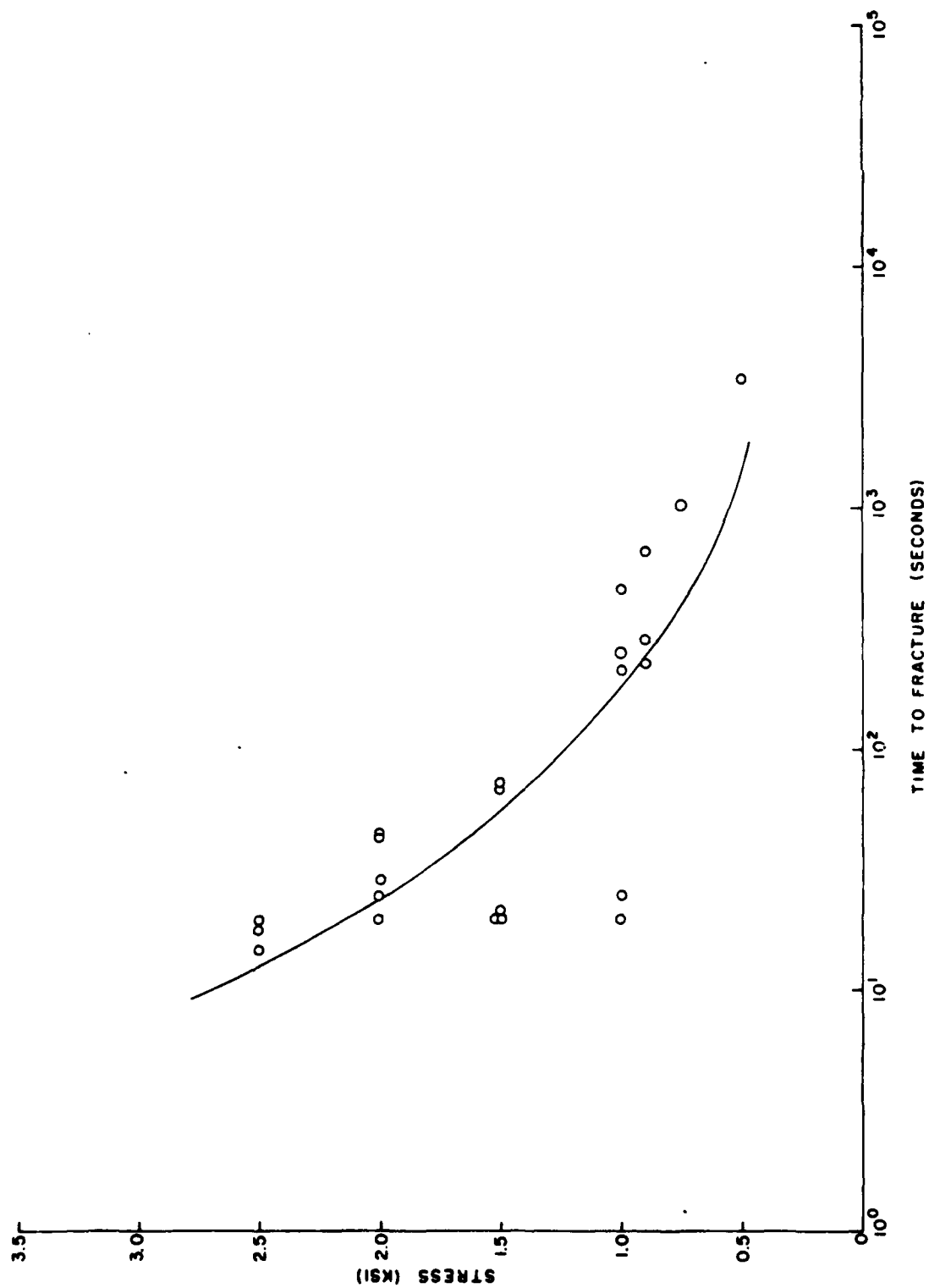


Figure 61. Effect of Stress on Stress Fracture Behavior of Polyethersulfone in Methoxyethanol.



Figure 62. Typical Crazing in PES Rotating Bands on 20 mm Projectiles.

are presented graphically in Figures 56-58. Since the rotating band specimens immersed in isopropanol had not crazed in 30 hours, it would appear, from Figure 56, that the residual stress is less than 2,850 psi (19.64 MPa). The scatter in the acetic acid crazing data makes it difficult to estimate the residual stress level from the data plotted in Figure 57, although on the low end one could conclude that it was greater than 750 psi (5.17 MPa). The methoxyethanol data, presented in Figure 58, indicates that the residual stress is in the 950-2,550 psi (6.55-17.57 MPa) region [$1,750 \pm 850$ psi (12.06 ± 5.51 MPa)] which is consistent with the isopropanol and acetic acid data, although still more statistically uncertain than one would like. Since the number of specimens, and particularly the rotating band specimens, was limited, it was impossible to obtain a larger statistical sampling and, presumably, a concomitant reduction in scatter and uncertainty.

The tests to determine the effectiveness of the painted coatings on solvent stress cracking behavior were conducted in the same manner as those previously described except that the shorter ICI molded specimens were used. Two different immersion solvents were used. The first was pure ethyl acetate and the second was a 50/50 mixture, by volume, of ethyl acetate and ethanol. In the pure ethyl acetate, painted and unpainted specimens were stressed to 1,000 psi (6.89 MPa) and 2,000 psi (13.78 MPa) and immersed in the solvent. In the 50/50 solvent mixture, painted and unpainted specimens were stressed to 4,000 psi (27.56 MPa) before immersion. Table 87 presents the results of these tests.

In the pure ethyl acetate, both the blue and yellow paint softened and wrinkled up on the specimens after only a few seconds and shortly thereafter developed multiple pinholes along the corners of the specimen cross section, with this deterioration occurring somewhat more rapidly on the blue paint than on the yellow. In the solvent mixture, the blue paint also started wrinkling almost immediately, while the yellow paint did not start wrinkling until ten minutes after immersion.

TABLE 87
EFFECT OF PAINT ON TENSILE STRESS CRACKING
BEHAVIOR OF POLYETHERSULFONE

Stress (psi) (MPa)		Solvent	Time to Fracture (minutes)		
			Unpainted	Blue	Yellow
1000	6.89	Ethyl Acetate ↓	3.0	8.5	22.0
			27.4	8.2	45.6
				18.3	
				1.1	
		Avg.	15.2	9.0	33.8
2000	13.78	Ethyl Acetate ↓	0.48	0.58	0.42
			0.80	0.63	0.65
					2.50
		Avg.	0.64	0.61	1.18
4000	27.56	50/50 Ethyl Acetate/Ethanol ↓	2.43	3.75	15.83
			2.57	4.83	21.67
				4.38	16.50
					16.08
		Avg.	2.50	4.32	17.52

The data in Table 87 indicate that the blue paint as applied to these tensile specimens offers little or no protection to PES in the presence of ethyl acetate. The yellow paint does offer some protection although its tendency to soften and wrinkle would indicate that it is also attacked rather severely by the ethyl acetate solvent.

Three conclusions could be drawn as a result of this investigation. These were: (1) the residual molded-in stress level in 20 mm polyethersulfone rotating bands is in the region of $1,750 \pm 800$ psi (12.06 ± 5.51 MPa); (2) the residual molded-in stresses are concentrated at the weld lines and gating points on the bands; and, (3) the yellow paint offers more protection to the PES tensile specimens in the environments tested than the blue paint, which provided little if any benefit over the unpainted PES. A complete description of this work and discussion

of the results has been published in an Air Force Materials Laboratory technical report, AFML-TR-78-185, "Experimental Determination of Residual Molded-In Stress Level in Plastic Rotating Bands."

4.2 EVALUATION OF "TUFFAK" POLYCARBONATE

Currently, many aircraft transparencies are being fabricated from polycarbonate. To date only one manufacturing source has been qualified. In order to determine whether other polycarbonate materials may offer hope for qualifying additional sources, some preliminary data on Tuffak polycarbonate have been generated at UDRI. The test methods and procedures used are those specified in MIL-P-83310, "Plastic Sheet, Polycarbonate, Transparent." The specification covers transparent flat polycarbonate plastic sheet material suitable for aerospace transparent enclosures requiring excellent optical properties. The properties obtained are shown in Tables 88-92.

4.3 THINWALL NYLON TENSILE TESTS

A 6/12 type nylon filled with 30 percent chopped glass fiber, used as a cartridge case material, was tested to determine the directionality of its mechanical properties. One of the requirements for this application is that the case material possess a minimum tensile strength of about 20 ksi (137.8 MPa). The sidewall of the cartridge case is injection molded and has a wall thickness of 0.045 inch (1.14 mm). Because of the thin section dimension, fiber orientation, caused by resin flow in the mold, was expected to be very anisotropic. In order to confirm that this results in highly directional strength properties (and if the weakest direction falls below 20 ksi (137.8 MPa), thin [0.045 inch (1.14 mm)] 4 inch (10.2 cm) diameter discs were injection molded). It was expected that the fiber orientation in these discs would be similar to that in the cartridge cases. Tensile specimens were cut from these discs in the longitudinal and transverse directions (with respect

TABLE 88
MECHANICAL AND THERMAL PROPERTIES OF
TUFFAK POLYCARBONATE

Test	Test Temperature		Test Result
	°F	(°C)	
Tensile Yield Strength	-65	(-54)	12,700 psi (87.6 MPa)
	0	(-18)	10,900 psi (75.2 MPa)
	72	(22)	9,600 psi (66.6 MPa)
	150	(66)	7,900 psi (54.5 MPa)
	260	(127)	4,700 psi (32.4 MPa)
Tensile Ult. Strength	-65	(-54)	10,700 psi (73.8 MPa)
	0	(-18)	8,700 psi (60.0 MPa)
	72	(22)	8,600 psi (59.3 MPa)
	150	(66)	6,600 psi (45.5 MPa)
	260	(127)	4,300 psi (29.7 MPa)
Tensile Elongation	-65	(-54)	17.6%
	0	(-18)	49.6%
	72	(22)	134%
	150	(66)	123%
	260	(127)	179%
Impact Strength	72	(22)	1.915 ft. lb/in (10.427Kg. meters/meter)
Deflection Temperature Under Load	---		---
Thermal Stability	---		1.14%
Tensile Yield	72	(22)	10,900 psi (75.2 MPa)
Tensile Ultimate	72	(22)	10,800 psi (74.5 MPa)
Tensile Elongation	72	(22)	6.5%
Impact Strength	72	(22)	1.462 ft. lb/in (7.961 Kg. meters/meter)
Coefficient of Thermal Expansion	---		---

TABLE 89

GENERAL DATA ON TUFFAK POLYCARBONATE

Test	Result
Length	----
Width	48.25 in. (122.6 cm)
Thickness	0.254 to 0.250 in. (0.622 to 0.635 cm)
Color	Water White
Specific Gravity	1.201
Luminous Transmittance	----

TABLE 90

OPTICAL QUALITY DATA ON TUFFAK POLYCARBONATE

Test	Result
Index of Refraction	1.5131
Luminous Transmittance	----
Haze	----
Angular Deviation (Arc Minutes)	2.15
Yellowness Index	----
Distortion	65 inches (165 cm)

TABLE 91

ENVIRONMENTAL DATA ON TUFFAK POLYCARBONATE

Test	Result
Flammability	----
Crazing	
Ethylene Glycol	No Effect
Acetone	Very Bad Crazing
MEK	Crazing
Naptha	No Effect
Isopropyl Alcohol	No Effect
Accelerated Weathering	
Luminous Transmittance	----
Haze	----

TABLE 92

COEFFICIENT OF THERMAL CONDUCTIVITY OF
TUFFAK POLYCARBONATE

Temperature (°C)	Coefficient of Thermal Conductivity (W/M°K)
20	0.230
30	0.233
40	0.236
50	0.240
60	0.243
70	0.247
80	0.250
90	0.254
100	0.258

to the predominant fiber orientation) and tested at 72°F (22°C) for strength and elastic modulus.

Three different glass filled materials were molded and tested in our investigation: (1) LNPOF1006, a polyphenylene sulfide; (2) Zytel 7010-33, a nylon; and, (3) Zytel 77G33, a nylon. Four inch (10.2 cm) discs of each of the three materials were molded. Half of the discs were used to cut tensile specimens parallel to the resin flow direction and half were used for tensile specimens perpendicular to the resin flow direction. The results of the tensile tests on these specimens are presented in Table 93. Since the chopped fiber in the resin would be expected to align preferentially along the direction of resin flow during the injection molding of these thin discs, one would expect the resultant longitudinal and transverse tensile properties to reflect this anisotropy. It can be seen in Table 93 that the strength in the longitudinal direction is about 50 percent higher than the strength in the transverse direction. The longitudinal modulus is also significantly higher than the transverse modulus, by 20 percent for the polyphenylene sulfide and 60 percent for the nylon.

The effect of loading rate was investigated on the third material by testing at three different speeds. The strength in both directions was observed to increase with increasing testing speed.

4.4 URALITE 3130-URETHANE CAST ELASTOMER

A two-part test request was received involving Uralite 3130, a castable urethane elastomer. The first part of the request was to conduct a reversion test. Four specimens were prepared using a 100/30 parts by weight mixture of the elastomer/catalyst. The cured specimens were aged at 200°F (93°C) and 95 percent R.H. Shore A and D hardness readings were taken on the original material and after one day, four days, and one week in aging. Table 94 presents the hardness readings taken from the four specimens.

TABLE 93

TENSILE PROPERTIES OF THINWALL NYLON

Material	Strength		Modulus		Fiber Direction	Remarks
	(psi)	(MPa)	(psi)	(MPa)		
LNP-OF1006	5572	38.42	1.04×10^6	7.17×10^3	Transverse	5 ea. @ 0.05 inch/min. (1.27 mm/min.)
LNP-OF1006	8297	57.21	1.22×10^6	8.41×10^3	Longitudinal	5 ea. @ 0.05 inch/min. (1.27 mm/min.)
Zytel-7010-33	10,526	72.57	0.64×10^6	4.41×10^3	Transverse	5 ea. @ 0.05 inch/min. (1.27 mm/min.)
Zytel-7010-33	16,149	111.34	1.04×10^6	7.17×10^3	Longitudinal	5 ea. @ 0.05 inch/min. (1.27 mm/min.)
Zytel-77G33	11,140	76.81	0.71×10^6	4.90×10^3	Transverse	10 ea. @ 0.05 inch/min. (1.27 mm/min.)
Zytel-77G33	11,971	82.54	0.76×10^6	5.24×10^3	Transverse	5 ea. @ 0.50 inch/min. (12.7 mm/min.)
Zytel-77G33	12,812	88.34	0.69×10^6	4.76×10^3	Transverse	5 ea. @ 2.00 inch/min. (50.8 mm/min.)
Zytel-77G33	17,063	117.64	1.16×10^6	8.00×10^3	Longitudinal	10 ea. @ 0.05 inch/min. (1.27 mm/min.)
Zytel-77G33	18,301	126.18	1.28×10^6	8.83×10^3	Longitudinal	5 ea. @ 0.50 inch/min. (12.7 mm/min.)
Zytel-77G33	19,833	136.74	1.46×10^6	10.07×10^3	Longitudinal	5 ea. @ 2.00 inch/min. (50.8 mm/min.)

TABLE 94
HARDNESS MEASUREMENTS

Specimen	Test	Orig.	1 Day	4 Days	7 Days
3130-1	Shore A	84	86	89	88
	Shore D	36	35	39	37
3130-2	Shore A	85	86	88	88
	Shore D	37	37	38	38
3130-3	Shore A	85	87	87	87
	Shore D	35	35	38	39
3130-4	Shore A	86	87	87	87
	Shore D	36	35	37	38

The second part of the request involved a mixing ratio sensitivity test. Five different elastomer/catalyst mixtures were prepared and the gel time for each was measured. The test was run in accordance with ASTM D2471. Table 95 lists the measured gel times.

4.5 CHARACTERIZATION OF RESIN MATRIX SYSTEMS

Three epoxy resin matrix systems were characterized for their mechanical properties. The characterization procedure was the same as that described in AFML-TR-70-305, Part II. Average stress strain curves were obtained and are presented in Figure 63.

4.6 DETERMINATION OF TEMPERATURE PROFILE IN POTTING COMPOUNDS

The objective of this investigation was to determine whether 180°F (82°C) is a realistic temperature to use for evaluating potting compounds for portable tactical shelter applications.

Specimens were prepared with two potting compounds, Fuller FE 6026 and Hysol EA 931. The specimens consisted of a 6.0 inch (15.24 cm) square honeycomb sandwich panel made with aluminum skin and a 2.0 inch (5.08 cm) thick paper honeycomb

TABLE 95
GEL TIMES OF VARIOUS URETHANE MIX RATIOS
AT 72°F (22°C)

Elastomer/Catalyst Mix Ratio (Parts by Wt.)	Gel Time (minutes)
(100/28)	25.10
(100/29)	24.05
(100/30)	22.05
(100/31)	20.10
(100/32)	18.40

NOTE: 12.5g samples were used.

core. The front face of this sandwich structure was painted olive drab. A 1.0 inch (2.54 cm) diameter hole was cut into the center of the back skin and a 2.0 inch (5.08 cm) diameter section of the core (concentric with the hole in the skin) was reamed out. This cavity was filled with potting compound. Six thermocouples were embedded in the slug of potting compound; three spaced evenly along the axis of the slug (one near front skin, one in center, and one near rear surface) and three spaced evenly, from front to rear, near the edge of the slug. These enable the measurement of a temperature profile, through the thickness, in the center and at the edge of the potting compound insert.

The two panels were exposed to solar heating in Dayton, Ohio during the month of September on several occasions. The panels were inclined to face the sun directly. Measured or recorded data included temperatures of the six embedded thermocouples in each panel, air temperature, wind velocity, cloud cover, and intensity of solar radiation. Maximum internal temperatures in excess of 150°F (66°C) were obtained. It would thus appear that in a more tropical climate and in mid-summer, a temperature of 180°F (82°C) would indeed be realistic.

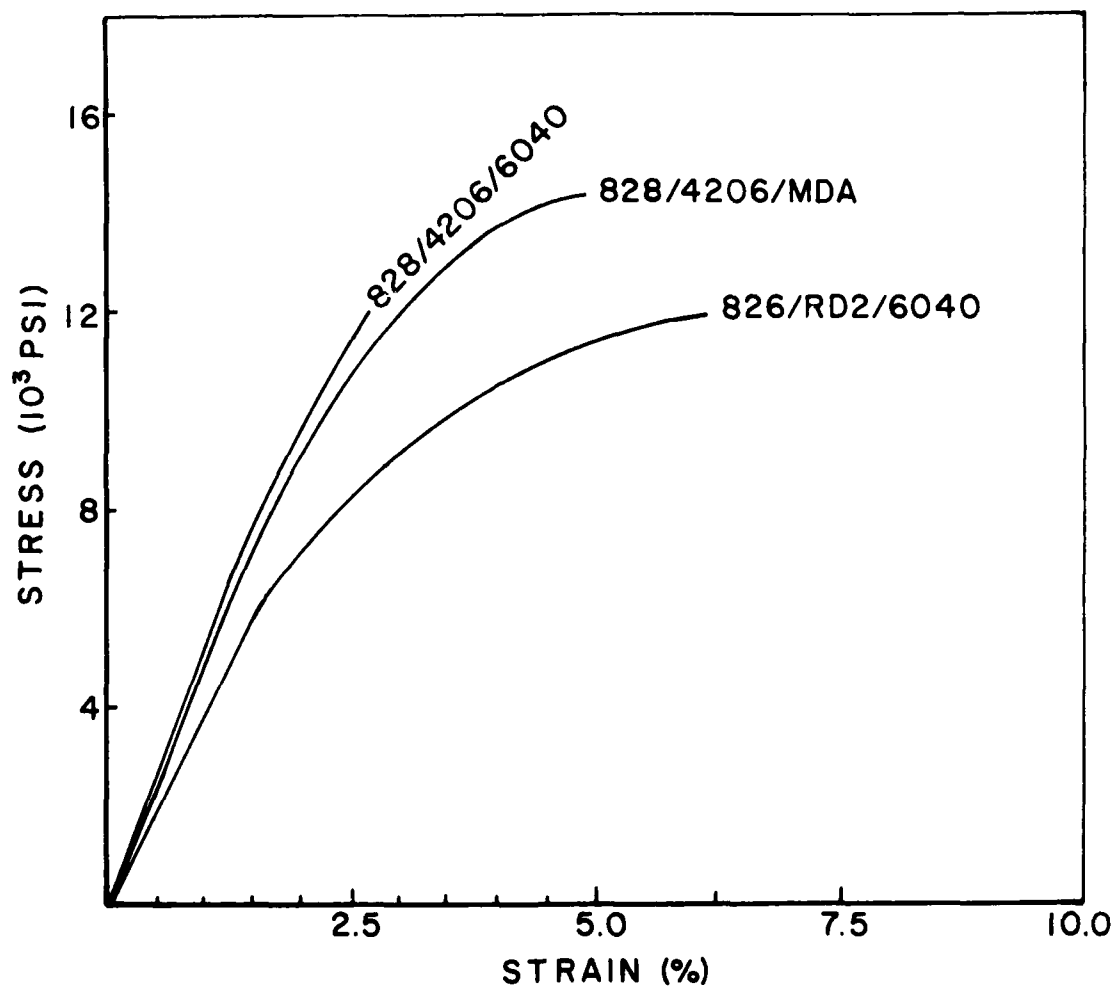


Figure 63. Tensile Stress-Strain Curves of Cast Resin Matrix Systems.

4.7 VESPEL (POLYIMIDE) COMPATIBILITY WITH JP-8 AND JP-4

The compatibility of Vespel SP-21 and SP-21D polyimide material with JP-8 and JP-4 fuels was determined by measuring change in volume in accordance with Method 6211 of Federal Test Method Standard No. 601. Vespel SP-21 was purchased in the form of a rod, 1.0 inch (25.4 mm) in diameter by 9.0 inches (228.6 mm) long. Specimens, with a length of 0.625 inch (15.875 mm), were machined from the rod. Vespel SP-21D was purchased in the form of slugs, 0.875 inch (22.225 mm) in diameter by 1.0 inch (25.4 mm) long. These slugs were tested as received. Three specimens of each material were exposed to each condition. Table 96 describes the exposure conditions and presents the test results.

4.8 CORE SPLICE EVALUATION

Two (2) core splice adhesives were tested on a tube shear type specimen at several different temperatures and after several pre-test aging conditions. The two adhesives were Plastilok 653 and Thermofoam 3057. In order to insure uniform results a special test jig was designed and utilized for this particular program. The results are shown in Table 97.

4.9 EVALUATION OF F-178 RESIN

Lap-shear adhesive specimens, comprised of F-178 spar wrap bonded to 2219 aluminum alloy with F-178 resin, were received for testing. The F-178 spar wrap adherend and glue line bond were co-cured. All the results obtained are given in Table 98.

4.10 COMPRESSIVE PROPERTIES OF SHELTER POTTING COMPOUND

Recently a program studying chronic problems plaguing the Electron Systems Division's field deployed portable tactical shelters was conducted. As a result of that study, an investigation of potting compounds used in these shelters was undertaken.

TABLE 96
EFFECT OF FUEL IMMERSION ON VESPEL POLYIMIDE

Material	Immersion Condition			Volume Change	
	Time	Temp.	Fluid	Avg. %	Std. Deviation
Vespel SP-21	7 days	140°F (60°C)	JP-4	+0.18	0.03
Vespel SP-21	7 days	140°F (60°C)	JP-8	-0.23	0.26
Vespel SP-21	7 days	140°F (60°C)	JP-4		
then	7 days	140°F (60°C)	JP-8	+0.11	0.19
Vespel SP-21D	7 days	140°F (60°C)	JP-4	-0.46	0.02
Vespel SP-21D	7 days	140°F (60°C)	JP-8	-0.34	0.28
Vespel SP-21D	7 days	140°F (60°C)	JP-4		
then	7 days	140 °F (60°C)	JP-8	+0.05	0.02

TABLE 97
TUBE SHEAR TEST RESULTS FOR CORE SPLICE ADHESIVES

Test Temperature (°F) (°C) (10 min. soak at test temperature)		Pretest Conditioning	Tube Shear Strength			
			Thermofoam 3057 (psi) (MPa)		Plastilok 653 (psi) (MPa)	
72	22	None	1937	13.35	1679	11.57
270	132	None	395	2.72	1159	7.99
350	177	None	504	3.47	1254	8.64
420	216	None	190	1.31	1211	8.34
-65	-54	None	1933	1.33	1622	11.18
420	216	10 hrs. @ 420°F (216°C)	419	2.89	1222	8.42
72	22	30 days @ 160°F (71°C) and 100% R.H.	1601	11.03	2070	14.26

TABLE 98
LAP-SHEAR TEST RESULTS OF F-178 RESIN

Test Temperature		Aging Condition	Lap Shear Strength	
°F	(°C)		psi	(MPa)
72	22	As Received	2010	13.86
72	22	1000 hrs. @ 420°F (216°C)	1415	9.76
420	216	1/2 hr. @ 420°F (216°C)	1725	11.89
72	22	30 days @ 120°F (49°C) / 95% R.H.	2010	13.86

Twelve potting compound materials were evaluated. The materials, test procedures, and environmental aging conditions were generally specified by the Nonmetallic Engineering Branch (MXE), Systems Support Division, Wright-Patterson Air Force Base, Ohio.

The test specimen and procedure used in the evaluation were from ASTM D695, "Compression Properties of Rigid Plastics." The standard test specimen for this procedure is a right cylinder whose length is twice the diameter, preferably 0.5 inch (12.7 mm) by 1 inch (25.4 mm). The specimens used in this program were machined from castings formed and cured in teflon tubes having an inside diameter of 0.5 inch (12.7 mm) and about 2-1/2 to 3 inches (62 to 76 mm) long. After curing, the specimens were removed from the Teflon tubes with the aid of a rod and a hand arbor press. Two (2) test specimens were machined from each cast rod. The cast rod was cut in half, and each half machined to ensure that the ends were parallel to each other and perpendicular to the axis of the cylinder.

The environmental conditions to which the specimens were exposed were 180°F (82°C) and 100 percent R.H. for two, four, and six weeks. Specimens were tested at three different temperatures[-65°F (-54°C), 72°F (22°C), and 180°F (82°C)].

Specimen deformation during testing was measured from crosshead travel, and the load-deformation curve was automatically plotted on a strip-chart recorder. Each test condition was run in triplicate. After the specimen was placed in the test fixture, the test chamber was permitted to return to the desired test temperature. The specimens were then "soaked" for ten minutes at the test temperature after the oven had returned to that temperature. The -65°F (-54°C) test condition was eliminated on four of the candidate materials at the request of MXE. The test results obtained in this program are presented in Table 99.

4.11 SHELTER ADHESIVE RETEST PROGRAM

The Air Force, as well as the other services, has been utilizing lightweight, air transportable shelters for a wide

TABLE 99
EFFECT OF ENVIRONMENTAL AGING ON THE COMPRESSIVE
STRENGTH OF POTTING COMPOUNDS

Potting Material	Test Temp.	As Cast		Aging Conditions									
				2 weeks @ 180°F/100% R.H.			4 weeks @ 180°F/100% R.H.			6 weeks @ 180°F/100% R.H.			
		Stress (psi)	Stress (MPa)	Compression (%)	Stress (psi)	Stress (MPa)	Compression (%)	Stress (psi)	Stress (MPa)	Compression (%)	Stress (psi)	Stress (MPa)	Compression (%)
Scotchcast XR5236	-65°F	18,500	127.5	9	14,200	97.9	10	14,500	100.0	17,200	118.6	9	17,200
	R.T.	5,400	37.2	40	1,600	11.0	40	2,000	13.8	4,700	32.4	40	4,700
	180°F	400	2.8	25	400	2.8	25	500	3.4	700	4.8	25	700
Scotchcast XR5240	-65°F	19,900	137.2	7	14,900	102.7	13	13,600	93.8	14,300	98.6	12	14,300
	R.T.	8,500	58.6	40	2,800	19.3	40	2,600	17.9	2,900	20.0	40	2,900
	180°F	1,300	9.0	25	1,100	7.6	25	900	6.2	800	5.5	25	800
Shur-Lok SLE3009	-65°F	22,000	151.7	9	15,700	108.2	15	17,200	118.6	14,100	97.2	10	14,100
	R.T.	11,600	80.0	5	6,700	46.2	15	6,700	46.2	6,300	43.4	15	6,300
	180°F	500	3.4	15	800	5.5	15	1,000	6.9	600	4.1	15	600
Epon 828(70 pts) Ver. 140(30 pts)	-65°F	22,800	157.2	9	21,400	147.5	15	22,600	155.8	22,600	155.8	15	22,600
	R.T.	12,200	84.1	5	10,600	73.1	9	9,700	66.9	9,800	67.4	15	9,800
	180°F	400	2.8	15	3,000	20.7	15	2,200	15.2	1,300	9.0	15	1,300
Epon 815(70 pts) Ver. 140(30 pts) HTS (15 pts)	-65°F	23,400	161.3	10	19,800	136.5	12	21,700	149.6	21,900	151.0	13	21,900
	R.T.	11,800	81.3	5	8,200	56.5	15	7,600	52.4	7,000	48.3	7	7,000
	180°F	400	2.8	15	800	5.5	15	700	4.8	700	4.8	15	700
Hysol EA934	-65°F	21,900	151.0	13	23,300	160.6	24	23,400	161.3	24,000	165.5	24	24,000
	R.T.	11,000	75.8	6	13,400	92.4	24	12,600	86.9	10,900	75.1	23	10,900
	180°F	7,600	52.4	25	7,400	51.0	24	7,300	50.3	5,600	38.6	20	5,600
Reliabond R-371	-65°F	10,800	74.5	8	9,600	66.2	11	10,500	72.4	9,900	68.3	11	9,900
	R.T.	4,200	29.0	40	3,200	22.1	40	3,800	26.2	3,200	22.1	40	3,200
	180°F	700	4.8	25	600	4.1	25	500	3.4	500	4.1	25	500
Reliabond R-380	-65°F	19,300	133.1	8	23,300	160.6	19	25,300	174.4	23,200	159.9	18	23,200
	R.T.	10,900	75.1	5	11,700	80.7	18	11,500	79.3	11,400	78.6	22	11,400
	180°F	7,400	51.0	25	5,800	40.0	20	6,400	44.1	6,600	45.5	21	6,600

NOTE: Results are an average of three tests.

TABLE 99 (Concluded)

EFFECT OF ENVIRONMENTAL AGING ON THE COMPRESSIVE
STRENGTH OF POTTING COMPOUNDS

Potting Material	Test Temp.	As Cast		Aging Conditions					
				2 weeks @ 180° F/100% R. H.			4 weeks @ 180° F/100% R. H.		
		Stress (psi)	Compress- ion (%)	Stress (psi)	Compress- ion (%)	Stress (psi)	Stress (psi)	Compress- ion (%)	Compress- ion (%)
Fuller FE 6024	R.T. 180°F	11,800	4.6	11,600	25	11,100	9,900	25	25
		6,500	25	3,000	25	2,200	2,100	25	25
Epon 828 (70 pts) Ver. 125 (30 pts)	R.T. 180°F	12,500	5.9	14,300	25	14,200	14,600	25	25
		1,100	25	6,000	25	6,000	5,400	25	25
Epon 828 (75 pts) Ver. 140 (25 pts)	R.T. 180°F	13,800	6.0	15,700	25	15,600	15,100	25	25
		1,100	25	8,800	25	7,400	6,700	25	25
Epon 828 (60 pts) Ver. 115 (40 pts)	R.T. 180°F	10,000	5.7	9,200	15	9,300	9,400	15	15
		300	15	2,000	15	1,800	1,400	15	15

variety of purposes for a number of years. Some of the many uses for these type shelters include the housing of personnel, hospital facilities, offices, and electronic instrument stations. The use of modular building concepts incorporating such features as sandwich wall construction and adhesive bonding are routinely used for these structures to reduce production costs. Walls can consist of honeycomb or foam cores between aluminum skins. Besides the skin-to-core bonding in the walls, adhesives are also used for metal-to-metal lap-type joints, and frequently serve both as a load bearing structural member as well as a joint sealant against environmental infiltration.

Shelters of this sort are used in many locations throughout the world and are consequently subjected to a wide variety of environmental exposure conditions. These range from subzero arctic temperatures to hot, dry desert climates as well as hot, humid tropical conditions. Besides exposure to these various climatic extremes, the periodic subjection of the shelters to abnormal stresses due to transport from one location to another exacerbate the demands made upon the structural members and bonded joints. The shelter design requirements which most heavily influence the type of adhesives selected for use in structural bonding are: (1) maximum and minimum exposure temperatures of -40°F (-40°C) to 200°F (93°C) with concomitant interior/exterior thermal gradients; (2) water resistance; (3) overall stress loads ranging from 300 to 1,200 psi (2.1 to 8.3 MPa); and (4) long-term durability of up to ten years in-the-field use.

Experience has demonstrated that the hot-humid environment is the most demanding and that the adhesively bonded joints in these structures are the sites most susceptible to failure as a result of exposure to the stresses and climatic conditions described above. The primary objective of this investigation was to identify commercially available adhesives which have the capability of retaining a substantial portion of their structural integrity after prolonged exposure to the combined effects of elevated temperature and high humidity. A secondary objective

was to evaluate the effect of selected surface preparation variables upon the interfacial durability of bonded joints. Some of the work undertaken was in direct response to the expressed concerns and desires of both the shelter manufacturers and adhesive vendors as well as that of the using services.

There are four major categories of materials and processes which were of interest to this investigation: (1) adherend alloy; (2) adherend surface preparation procedure; (3) adhesive surface primer; and (4) adhesive.

The two principle adherend materials were the bare aluminum alloys of 5052H34 and 6061T6. A third aluminum alloy, bare 2024T3 was used to a limited extent as a baseline during the program because of extensive prior experience with this alloy in adhesive bonding work. It is not generally used in shelter construction, however.

The primary surface preparation procedure used for the adhesive bonding work in this program was the optimized FPL etch treatment, although the nonoptimized FPL etch treatment (ASTM D2651, Method A) was used for some of the early work.

During the early part of this work, involving lap shear testing and the environmental aging of unstressed lap shear specimens, each combination of adherend alloy/surface preparation method/adhesive was used with both primed and unprimed adherend surfaces. Two corrosion inhibiting primers were used for the primed surfaces, for a total of three primer conditions.

Seven adhesives were evaluated. These, to the best of our knowledge, were all modified epoxies. Six of the adhesives were supplied in the form of a supported film while one was a low viscosity, two-part system applied as a thin film by hand after mixing.

Four types of tests were used for evaluation during this program: (1) lap shear, (2) floating roller peel, (3) stress-durability, and (4) thick adherend, Double-Cantilever-Beam (DCB)

crack extension. Lap shear tests were conducted to measure the effect of both elevated temperature and humidity aging upon adhesive properties. The environmental exposure conditions were selected to correspond to those measured in the field [200°F (93°C) and 95 to 100 percent R.H.]. Peel tests were conducted to characterize the toughness/brittleness of the adhesive at low temperatures. Stress-durability tests consisted of imposing a predetermined shear stress on a lap shear specimen which was subsequently exposed to an elevated temperature, high humidity environment until failure or until the exposure period reached a preselected maximum. At this point, the specimen was removed from aging, unloaded, and a residual strength determined. This test was aimed at providing additional data on the effect of environment upon adhesives. While not necessarily providing real-life design type data, it did provide a comparative ranking of adhesive resistance to environmental degradation. Crack extension tests were conducted to measure the influence of surface preparation variables upon the environmental degradation of a bonded joint.

Numerical data in the form of strengths, times-to-failure, or crack lengths were used in conjunction with observed failure modes to interpret the results of this investigation and to develop conclusions. In an adhesive joint one can encounter a variety of failure modes, such as; (a) cohesive failure, or failure entirely within the adhesive layer, (b) interfacial failure between the adhesive layer and the primer layer, (c) failure entirely within the primer layer, (d) interfacial failure between the primer layer and the adherend surface oxide, (e) failure within the adherend oxide layer, or, (f) a mixture of the above. It is very difficult, with the naked eye, to ascertain the exact failure mode unless it is type (a). Interfacial failure modes (types b or d) may appear obvious but one cannot be sure, short of resorting to expensive surface instrumental analysis, that a very thin layer of primer or adhesive has not remained adhered to an otherwise clean appearing surface.

Since the primer layer is so thin, the only evidence of its presence, to the eye, is generally color. In this investigation the only discriminations made regarding failure mode were those detectable by eye. Thus, failure modes of the types (a), (b), and (d) were the only ones recorded.

Lap shear tests were conducted in accordance with ASTM Method D1002 on specimens from both the standard (fully machined after bonding) and the preslotted (finger) types of test panel (see Figure 64). Specimens were used only if the applied primer thickness fell within the manufacturer's recommended limits [0.0002-0.0004 inches (0.0051-0.0102 mm) for BR127 and 0.0001-0.0003 inches (0.0025-0.0076 mm) for SC3950] and the cured glue-line thickness fell between 0.004 and 0.007 inch (0.102-0.178 mm). Tests were conducted at 72°F (22°C) on as-fabricated specimens, and at 200°F (93°C) on specimens which had been exposed to 200°F (93°C) and 95-100 percent R.H. for 14 days. There were a total of seven adhesives, two adherend alloys, two surface preparations, three primer conditions (unprimed and primers BR127 and XC3950), and two specimen types involved in the lap shear testing portion of this program. This produced a total of 168 combinations. Ten specimens were tested for each combination: five at 72°F (22°C) and five at 200°F (93°C) after the 14-day humidity aging.

Floating Roller Peel (frequently referred to as "Bell" peel) tests were conducted in accordance with ASTM Method D3167 (see Figure 65). Tests were conducted at both 72°F (22°C) and -65°F (-54°C). Seven adhesives, three adherend alloys, one surface preparation, and one primer were involved in the peel testing for a total of 21 combinations. Additionally, one of the adhesives was used without a primer, adding three more combinations for a total of 24. Four specimens of each combination were tested at each of the two test temperatures.

Stress-durability tests were conducted in accordance with ASTM Method D2919 (see Figure 66). Standard lap shear tests were conducted at 72°F (22°C) and 140°F (60°C) on dry unaged

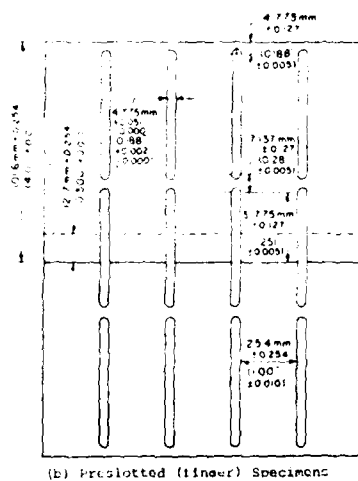
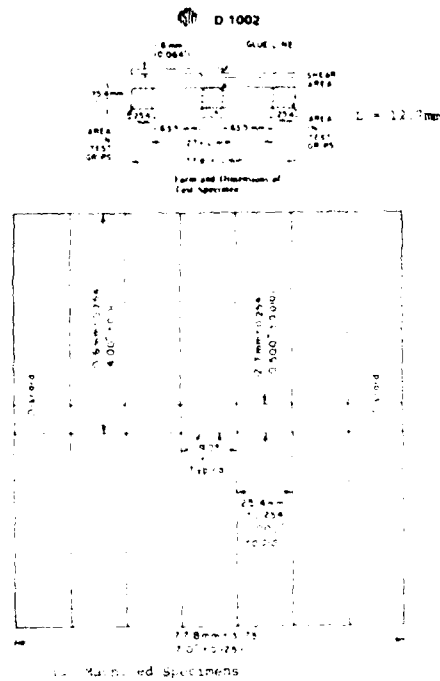


Figure 64. Lap Shear Specimens (from ASTM).

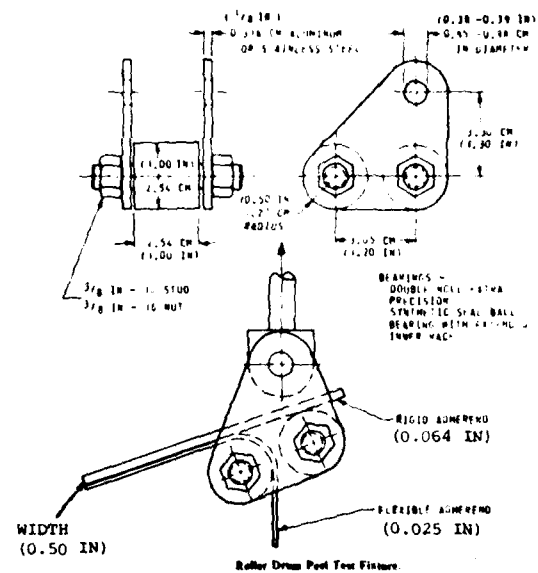
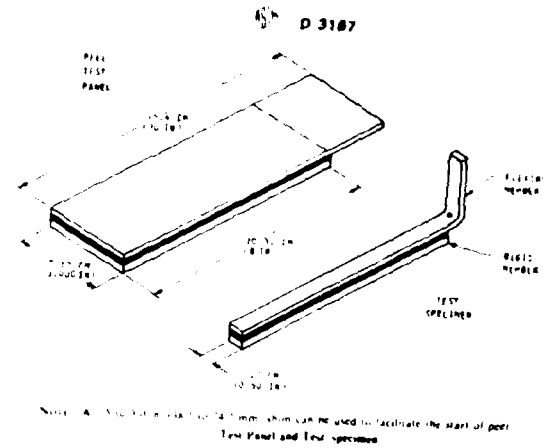


Figure 65. Floating Roller ("Bell") Peel Specimen and Fixture (from ASTM).

specimens to provide baseline data. Stress-durability tests were conducted in a 140°F (60°C) and 95 to 100 percent R.H. environment at two stress levels: (1) 40 percent of the 140°F (60°C) dry ultimate strength, and (2) 60 percent of the 140°F (60°C) dry ultimate strength. Times-to-failure were recorded and any specimens which had not failed within 1,000 hours were removed and tested for residual strength at 140°F (60°C). Seven adhesives, two adherend alloys, one surface preparation, and one primer were used for these tests; a total of 14 combinations. Additionally, as before, one of the adhesives was used without primer, bringing the total number of combinations to 16. Three specimens of each combination were tested at the two baseline conditions and five specimens of each combination were tested for durability at the two stress levels.

Crack extension tests were conducted with the thick adherend DCB specimen, and in accordance with the procedures described in AFML-TR-76-173. This specimen is illustrated in Figure 67. The tests were conducted in a 140°F (60°C), 95 to 100 percent R.H. environment and crack lengths were measured as a function of time. The crack propagation locus was also recorded (i.e., interfacial or within the adhesive layer).

The objective of this portion of the program was to examine the effect of surface preparation variables upon the bond between the metal-oxide and the surface primer. Only one adhesive (FM73) was used and was selected to maximize the probability of failure along the oxide/primer interface. Only one primer (BR127) was used. One exception to this work plan was the use of a second adhesive (LR100-172) without primer in a few tests.

One of the differences between the standard and optimized FPL etching solutions is that the optimized solution is "sweetened" with some dissolved 2024 aluminum before it is used for panel etching. This "sweetening" has been found to provide significantly improved bonding. One question which arose in the course of this investigation was whether the "sweetening" of

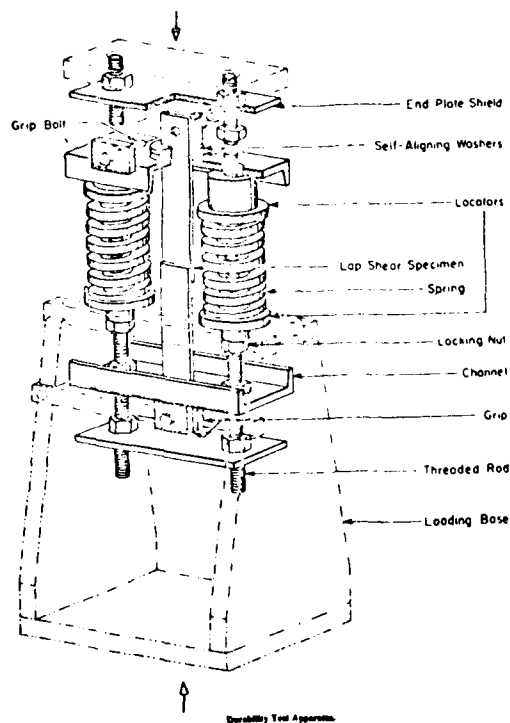
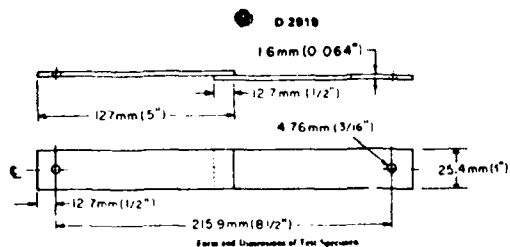


Figure 66. Lap Shear Specimen and Stress Durability Fixture (from ASTM).

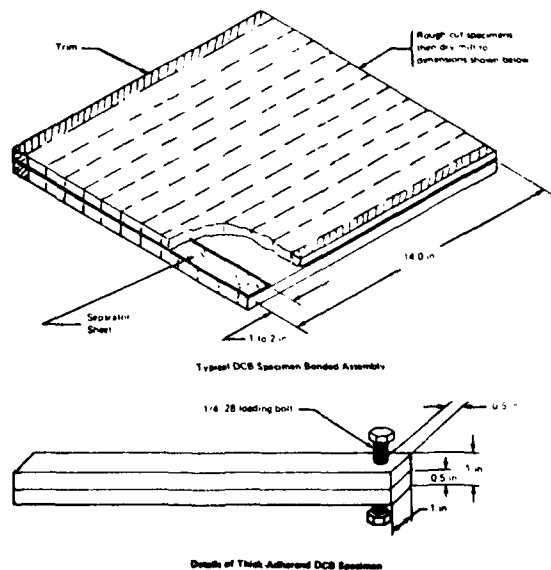


Figure 67. Thick Adherend Double Cantilever Beam (DCB) Crack Extension Specimen (from AFML-TR-76-173).

the initial etch solution should be accomplished by dissolving 2024 aluminum alloy (as the normal optimized FPL process calls for) in the etch solution regardless of the type of alloy to be treated, or whether the solution should be "sweetened" with the same alloy as that which is to be etched. Three different alloy "sweeteners" were consequently utilized in this portion of the program.

After etching, the adherends are rinsed before drying. This rinse can be done with either tap water or deionized water. Some question existed as to whether deionized water rinsing leads to significant bond improvement considering its considerably higher cost. This was also examined.

The data obtained from the testing of the lap shear specimens are presented in Tables 100-103. A cursory inspection indicates that, in general, the ranking of the adhesives, as far as their resistance to moisture degradation is concerned, is unaffected by the type of specimen used (machined versus pre-slotted).

In general, five adhesives [(1) LR100-172; (2) XA180; (3) LR100-252; (4) MA-429; and (5) R382-7] withstood moisture attack well, one (EA9601NW) was very susceptible to moisture degradation.

It is impossible to make an unequivocal general statement regarding the relative merit of one primer condition over another for these lap shear tests.

The optimized FPL etch produces consistently higher strength levels than the standard FPL etch on the machined lap shear specimens. On the preslotted type specimens, however, some adhesive/primer combinations exhibited higher strengths on the FPL etched surface than on the OFPL etched surface.

In general, specimens made with the 6061T6 alloy exhibit higher joint strengths than those made with the 5052H34 alloy. Since the 6061T6 has a higher yield stress than the 5052H34, the bending of the lap area is postponed until a higher load is

TABLE 100
ADHESIVE LAP SHEAR TEST RESULTS ON 6061T6
ADHERENDS WITH MACHINED SPECIMENS

Surface Prep. ¹	Primer	Adhesive	Lap Shear Strength ²			
			72°F (22°C)		200°F (93°C) after aging	
			psi	(MPa)	psi	(MPa)
FPL	None	LR100-172	3150	(21.7)	2940	(20.3)
		R7114	5550	(38.2)	270	(1.86)
		XA180	5040	(34.7)	1750	(12.1)
		LR100-252	N.A.		N.A.	
		MA-429	N.A.		N.A.	
		R382-7	2990	(20.6)	1460	(10.1)
		EA9601NW	4250	(29.3)	410	(2.82)
	BR127	LR100-172	3080	(21.2)	2170	(15.0)
		R7114	5000	(34.5)	510	(3.51)
		XA180	4720	(32.5)	2320	(16.0)
		LR100-252	N.A.		N.A.	
		MA-429	N.A.		N.A.	
		R382-7	3340	(23.0)	2130	(14.7)
		EA9601NW	4340	(29.9)	1110	(7.65)
	XC3950	LR100-172	3010	(20.7)	2170	(15.0)
		R7114	5600	(38.6)	1110	(7.65)
		XA180	4880	(33.6)	2000	(13.8)
		LR100-252	N.A.		N.A.	
		MA-429	N.A.		N.A.	
		R382-7	2950	(20.3)	1940	(13.4)
		EA9601NW	3540	(24.4)	500	(3.45)
OFPL	None	LR100-172	4880	(33.6)	2740	(18.9)
		R7114	5680	(39.1)	720	(4.96)
		XA180	5220	(36.0)	2680	(18.5)
		LR100-252	5000	(34.5)	2250	(15.5)
		MA-429	5260	(36.2)	550	(3.79)
		R382-7	4030	(27.8)	2180	(15.0)
		EA9601NW	4940	(34.0)	1110	(7.65)
	BR127	LR100-172	5280	(36.4)	3540	(24.4)
		R7114	5210	(36.0)	680	(4.69)
		XA180	4710	(32.5)	2290	(15.8)
		LR100-252	5120	(35.3)	2530	(17.4)
		MA-429	5270	(36.3)	960	(6.61)
		R382-7	3860	(26.6)	3500	(24.1)
		EA9601NW	5410	(37.3)	1130	(7.79)

TABLE 100 (Concluded)
ADHESIVE LAP SHEAR TEST RESULTS ON 6061T6
ADHERENDS WITH MACHINED SPECIMENS

Surface Prep. ¹	Primer	Adhesive	Lap Shear Strength ²			
			72°F(22°C)		200°F(93°C) after aging	
			psi	(MPa)	psi	(MPa)
OFPL	XC3950	LR100-172	5190	(35.8)	2970	(20.5)
		R7114	5410	(37.3)	730	(5.03)
		XA180	4960	(34.2)	2630	(18.1)
		LR100-252	5340	(36.8)	2760	(19.0)
		MA-429	5590	(38.5)	1350	(9.30)
		R382-7	3990	(27.5)	1970	(13.6)
		EA9601NW	5090	(35.1)	1930	(13.3)

NOTES: ¹FPL represents standard etch procedure. OFPL represents optimized etch procedure.

²Each value represents average of five specimens.

TABLE 101
ADHESIVE LAP SHEAR TEST RESULTS ON 5052H34
ADHERENDS WITH MACHINED SPECIMENS

Surface Prep. ¹	Primer	Adhesive	Lap Shear Strength ²			
			72°F (22°C)		200°F (93°C) after aging	
			psi	(MPa)	psi	(MPa)
FPL	None	LR100-172	3030	(20.9)	2510	(17.3)
		R7114	4260	(29.4)	420	(2.89)
		XA180	4420	(30.5)	2000	(13.7)
		LR100-252	N.A.		N.A.	
		MA-429	N.A.		N.A.	
		R382-7	2420	(16.7)	1340	(9.23)
		EA9601NW	3090	(21.3)	380	(2.61)
	BR127	LR100-172	3180	(21.9)	2550	(17.6)
		R7114	4170	(28.7)	760	(5.24)
		XA180	3320	(22.9)	2290	(15.8)
		LR100-252	3290	(22.7)	1790	(12.3)
		MA-429	N.A.		N.A.	
		R382-7	2280	(15.7)	2440	(16.8)
		EA9601NW	2950	(20.3)	700	(4.82)
	XC3950	LR100-172	2900	(20.0)	1980	(13.6)
		R7114	4550	(31.3)	870	(6.00)
		XA180	3760	(25.9)	1290	(8.89)
		LR100-252	N.A.		N.A.	
		MA-429	N.A.		N.A.	
		R382-7	2420	(16.7)	1610	(11.1)
		EA9601NW	3100	(21.4)	530	(3.65)
OFPL	None	LR100-172	4120	(28.4)	2880	(19.8)
		R7114	4670	(32.2)	890	(6.13)
		XA180	4660	(32.1)	2280	(15.7)
		LR100-252	4380	(30.2)	3320	(22.9)
		MA-429	4710	(32.5)	1350	(9.30)
		R382-7	3630	(25.0)	1830	(12.6)
		EA9601NW	4120	(28.4)	1010	(6.96)
	BR127	LR100-172	4180	(28.8)	2690	(18.5)
		R7114	4570	(31.5)	670	(4.61)
		XA180	3840	(26.5)	1140	(7.85)
		LR100-252	4520	(31.1)	2510	(17.3)
		MA-429	4490	(30.9)	2240	(15.4)
		R382-7	2750	(18.9)	1240	(8.54)
		EA9601NW	4430	(30.5)	1360	(9.37)

TABLE 101 (Concluded)
ADHESIVE LAP SHEAR TEST RESULTS ON 5052H34
ADHERENDS WITH MACHINED SPECIMENS

Surface Prep. ¹	Primer	Adhesive	Lap Shear Strength ²			
			72°F (22°C)		200°F (93°C) after aging	
			psi	(MPa)	psi	(MPa)
OFPL	XC3950	LR100-172	4400	(30.3)	2730	(18.8)
		R7114	4810	(33.1)	590	(4.07)
		XA180	3980	(27.4)	1370	(9.44)
		LR100-252	4630	(31.9)	3060	(21.1)
		MA-429	4520	(31.1)	2030	(13.9)
		R382-7	3160	(21.8)	1830	(12.6)
		EA9601NW	4070	(28.0)	760	(5.24)

NOTES: ¹FPL represents standard etch procedure. OFPL represents optimized etch procedure.

²Each value represents average of five specimens.

TABLE 102
ADHESIVE LAP SHEAR TEST RESULTS ON 6061T6
ADHERENDS WITH PRESLOTTED SPECIMENS

Surface Prep. ¹	Primer	Adhesive	Lap Shear Strength ²			
			72°F (22°C)		200°F (93°C) after aging	
			psi	(MPa)	psi	(MPa)
FPL	None	LR100-172	3790	(26.1)	3150	(21.7)
		R7114	5330	(36.7)	350	(2.41)
		XA180	4920	(33.9)	2180	(15.0)
		R382-7	3560	(24.5)	560	(3.86)
		EA9601NW	4770	(32.9)	390	(2.69)
	BR127	LR100-172	3890	(26.8)	3390	(23.4)
		R7114	5370	(37.0)	490	(3.38)
		XA180	4530	(31.2)	2190	(15.1)
		R382-7	4180	(28.8)	1550	(10.7)
		EA9601NW	5000	(34.5)	1650	(11.4)
	XC3950	LR100-172	4210	(29.0)	3060	(21.1)
		R7114	5770	(39.8)	700	(4.82)
		XA180	4820	(33.2)	2420	(16.7)
		R382-7	4440	(30.6)	1490	(10.3)
		EA9601NW	4930	(34.0)	1350	(9.30)
OFPL	None	LR100-172	4700	(32.4)	2880	(19.8)
		R7114	2400	(16.5)	90	(0.62)
		XA180	3100	(21.4)	1510	(10.4)
		R382-7	3710	(25.6)	1500	(10.3)
		EA9601NW	5050	(34.8)	490	(3.38)
	BR127	LR100-172	4230	(29.1)	3120	(21.5)
		R7114	3300	(22.7)	130	(0.89)
		XA180	2440	(16.8)	1130	(7.79)
		R382-7	3880	(26.7)	1450	(9.99)
		EA9601NW	5300	(36.5)	1270	(8.75)
	XC3950	LR100-172	4550	(31.3)	3080	(21.2)
		R7114	3070	(21.2)	100	(0.69)
		XA180	2860	(19.7)	1340	(9.23)
		R382-7	3890	(26.6)	1320	(9.09)
		EA9601NW	5030	(34.7)	1050	(7.23)

NOTES: ¹FPL represents standard etch procedure. OFPL represents optimized etch procedure.

²Each value represents average of five specimens.

TABLE 103

ADHESIVE LAP SHEAR TEST RESULTS ON 5052H34
ADHERENDS WITH PRESLOTTED SPECIMENS

Surface Prep. ¹	Primer	Adhesive	Lap Shear Strength ²			
			72°F (22°C)		200°F (93°C) after aging	
			psi	(MPa)	psi	(MPa)
FPL	None	LR100-172	2520	(17.4)	2590	(17.8)
		R7114	4130	(28.5)	200	(1.38)
		XA180	3490	(24.0)	1460	(10.1)
		R382-7	2570	(17.7)	300	(2.07)
		EA9601NW	3500	(24.1)	230	(1.58)
	BR127	LR100-172	2620	(18.1)	2750	(18.9)
		R7114	3700	(25.5)	620	(4.27)
		XA180	2880	(19.8)	1650	(11.4)
		R382-7	2680	(18.5)	950	(6.55)
		EA9601NW	3090	(21.3)	830	(5.72)
	XC3950	LR100-172	2400	(16.5)	2410	(16.6)
		R7114	3590	(24.7)	310	(2.14)
		XA180	3070	(21.2)	1390	(9.58)
		R382-7	2690	(18.5)	1270	(8.75)
		EA9601NW	3140	(21.6)	590	(4.07)
OFPL	None	LR100-172	3200	(22.0)	2790	(19.2)
		R7114	2960	(20.4)	80	(0.55)
		XA180	2140	(14.7)	1060	(7.30)
		R382-7	2920	(20.1)	580	(4.00)
		EA9601NW	N.A.		210	(1.45)
	BR127	LR100-172	3700	(25.5)	3040	(20.9)
		R7114	2900	(20.0)	100	(0.69)
		XA180	2240	(15.4)	1120	(7.72)
		R382-7	3270	(22.5)	960	(6.61)
		EA9601NW	N.A.		430	(2.96)
	XC3950	LR100-172	3320	(22.9)	2780	(19.2)
		R7114	3050	(21.0)	90	(0.62)
		XA180	2490	(17.2)	1320	(9.09)
		R382-7	3310	(22.8)	1610	(11.1)
		EA9601NW	N.A.		520	(3.58)

NOTES: ¹FPL represents standard etch procedure. OFPL represents optimized etch procedure.

²Each value represents average of five specimens.

reached during a lap shear test. This, in turn, postpones the introduction of peel stresses into the joint and leads to the higher joint strengths.

The data obtained from the testing of the peel specimens are presented in Table 104. Probably the most obvious feature of these data is the fact that the bond formed between BR127 primer and adhesive LR100-172 has very little resistance to peeling stresses. All of the specimens primed with BR127 and bonded with LR100-172 failed along the primer/adhesive interface. The peel properties of the unprimed specimens bonded with LR100-172 were significantly higher than those of the primed specimens bonded with this adhesive. Failures were predominantly along the metal/adhesive interface. In marked contrast to the LR100-172/BR127 adhesive/primer incompatibility manifested by the peel tests, the lap shear test results, discussed previously, and the lap shear stress-durability test results, discussed later, failed to provide any indication of this problem.

The data obtained from the stress-durability testing of lap shear specimens are presented in Table 105. Alongside the hours-to-failure exhibited by each adhesive, the stress level to which the specimens were subjected during exposure are noted. Since each adhesive system exhibits its own characteristic strength and since the exposure stress levels were set at a percentage of the adhesive's lap shear strength at 140°F (60°C), one must consider the stress during exposure as well as the time-to-failure and failure mode in assessing relative stress-durability of the various adhesives. One can see from the data that adhesives LR100-252, MA-425, and EA9601NW appear to be the most durable. One can also see that the use of a primer with LR100-172 appears to significantly improve its stress-durability. The unprimed LR100-172 specimens exhibit a change in failure mode from static to stress-durability testing, the failures being primarily within the adhesive layer in the static tests while in the durability tests the failures are predominantly along the adhesive/metal interface. On all of the primed specimens, the failure modes

TABLE 104
ADHESIVE FLOATING ROLLER PEEL TEST RESULTS

Substrate Alloy ¹	Primer	Adhesive	Peel Strength ²			
			72°F (22°C)		-65°F (-54°C)	
			(lb/in)	(N/cm)	(lb/in)	(N/cm)
2024T3	None	LR100-172	25.5	(44.6)	20.6	(36.1)
		BR127	4.0	(7.00)	4.7	(8.23)
	BR127	R7114	41.5	(72.7)	24.3	(42.5)
		XA180	38.7	(67.7)	21.7	(38.0)
		LR100-252	44.9	(78.6)	11.8	(20.7)
		MA-429	15.3	(26.8)	3.5	(6.13)
		R382-7	15.4	(27.0)	3.5	(6.13)
		EA9601NW	40.8	(71.4)	33.6	(58.9)
6061T6	None	LR100-172	11.6	(20.1)	14.4	(25.2)
		BR127	4.4	(7.70)	3.0	(5.25)
	BR127	R7114	37.2	(65.1)	17.6	(30.8)
		XA180	42.4	(74.2)	26.3	(46.1)
		LR100-252	29.8	(52.2)	7.9	(13.8)
		MA-429	24.0	(42.0)	6.7	(11.7)
		R382-7	22.5	(39.4)	6.7	(11.7)
		EA9601NW	52.0	(91.0)	30.6	(53.6)
5052H34	None	LR100-172	18.6	(32.6)	18.4	(32.2)
		BR127	3.0	(5.25)	3.4	(5.95)
	BR127	R7114	19.7	(34.5)	10.1	(17.7)
		XA180	21.3	(37.3)	21.1	(37.0)
		LR100-252	41.4	(72.5)	21.7	(38.0)
		MA-429	20.5	(35.9)	14.6	(25.6)
		R382-7	24.0	(42.0)	19.6	(34.3)
		EA9601NW	28.9	(50.6)	17.6	(30.8)

NOTES: ¹All specimens were prepared with an optimized FPL etch surface.

²All values represent average of four specimens.

TABLE 105
ADHESIVE STRESS-DURABILITY TEST RESULTS

Substrate Alloy ¹	Primer	Adhesive	Stress-Durability Time to Failure (hrs) ⁷					
			40% Stress Level ⁸			60% Stress Level ⁸		
			(Hrs. to Failure)	Exposure Stress (psi)	(MPa)	(Hrs. to Failure)	Exposure Stress (psi)	(MPa)
6061T6	None	LR100-172	33	1700	(11.7)	16	2550	(17.5)
		BR127	963 ²	2110	(14.5)	112	3170	(21.8)
		R7114	346	1940	(13.4)	19	2910	(20.0)
		XA180	1000+ ³	1660	(11.4)	87	2490	(17.2)
		LR100-252	1000+ ³	2030	(14.0)	181	3050	(21.0)
		MA-429	1000+ ³	2170	(15.0)	114	3260	(22.5)
		R382-7	309	1860	(12.8)	8	2790	(19.2)
		EA9601NW	856 ⁴	2060	(14.2)	197	3090	(21.3)
5052H34	None	LR100-172	766	1500	(10.3)	95 ⁵	2250	(15.5)
		BR127	575 ⁶	1700	(11.7)	48	2550	(17.6)
		R7114	48	1450	(10.0)	32	2180	(15.0)
		XA180	742	1180	(8.13)	310 ⁶	1780	(12.3)
		LR100-252	574	1610	(11.1)	898	2420	(16.7)
		MA-429	948 ¹⁰	1920	(13.2)	754	2890	(19.9)
		R382-7	362	1600	(11.0)	115	2400	(16.5)
		EA9601NW	262	1790	(12.3)	768	2680	(18.5)

NOTES: ¹All specimens were prepared with an optimized FPL etch surface.

²Four specimens survived for 1000 hours without failure, one failed at 815 hours.

³All specimens survived for 1000 hours without failure.

⁴Three specimens survived for 1000 hours without failure, two failed around 640 hours.

⁵Four specimens failed within first seven hours, one failed at 463 hours.

⁶Three specimens failed within first 50 hours, two failed at over 600 hours.

⁷All values represent average of five specimens.

⁸Based on baseline ultimate strength of dry unaged specimens tested at 140°F (60°C).

⁹One specimen survived for 1000 hours.

¹⁰Three specimens survived for 1000 hours, two failed at 869 hours.

of the respective adhesives, while varying from adhesive-to-adhesive, were the same in the durability tests as in the static tests.

The data obtained from the DCB crack extension testing are presented in Table 106. The principle conclusion of these results is that regardless of the aluminum alloy being etched, the etch bath should be sweetened with 2024 alloy for highest bond durability. The reason for this is generally felt to be the presence of copper in the 2024 alloy. In fact, some investigators believe that sweetening the bath with copper alone is sufficient. Examination of the failure modes for these tests corroborate the differences in interfacial bond quality obtained when the etch bath is sweetened with 2024 rather than a non-aluminum containing alloy. The baths sweetened with the copper containing 2024 alloy produced bonds which failed predominantly in the adhesive layer, while those sweetened with the non-copper alloys produced bonds which failed predominantly at the adherend-primer interface. An important implication of this result which relates to the processing of a large volume of aluminum for bonding is that when alloys are being etched which contain little or no copper, the etch bath must not only be "presweetened" but continually replenished with dissolved copper. If this is not done, the bath will become depleted in copper content and one will be etching with a bath similar to those sweetened with 5052 or 6061 alloy, a condition which produces bonding surfaces of dramatically reduced durability.

The use of a deionized rinse rather than a tap water rinse appears to be worthwhile. On a 2024 alloy adherend etched with a 2024 sweetened bath, a deionized rinse produced a more durable bond, the difference becoming relatively greater as the aging time increased. On a 6061 alloy adherend etched with a 6061 sweetened bath, however, the deionized rinse produced a less durable one. Since these latter two bonds were both poor due to the use of a non-copper containing sweetener, the relative

TABLE 106
DCB CRACK EXTENSION RESULTS

Adherend Alloy	OFPL Sweetening Alloy	Rinse Water Type	Adhesive: Primer	G_I $\frac{\text{in-lb.}}{\text{in}^2}$ $\left[\frac{\text{cm-N}}{\text{cm}^2} \right]$				
				t = 0 hr.	t = 1 hr.	t = 24 hrs.	t = 168 hrs.	t = 336 hrs.
2024T3	2024	TAP	FM73-BR127	(19.3) [33.8]	(15.2) [26.6]	(10.8) [18.9]	(6.2) [14.4]	(7.3) [12.8]
2024T3	2024	Deionized	FM73-BR127	(18.0) [31.5]	(15.8) [27.7]	(12.5) [22.1]	(10.6) [13.6]	(7.8) [17.2]
5052H34	2024	TAP	FM73-BR127	(30.0) [52.5]	(23.9) [41.8]	(20.0) [35.0]	(19.1) [33.4]	(18.3) [32.5]
5052H34	5052	TAP	FM73-BR127	(3.3) [5.79]	(0.13) [0.23]	(0.11) [0.19]	(0.11) [0.19]	(0.11) [0.19]
6061T6	2024	TAP	FM73-BR127	(16.2) [28.4]	(12.7) [22.2]	(11.2) [19.6]	(9.4) [16.5]	(9.7) [15.2]
6061T6	6061	Deionized	FM73-BR127	(13.8) [24.2]	(0.24) [0.42]	(0.15) [0.26]	(0.15) [0.26]	(0.14) [0.26]
6061T6	6061	TAP	FM73-BR127	(11.6) [20.3]	(3.7) [6.48]	(0.46) [0.81]	(0.47) [0.79]	(0.45) [0.79]
5052H34	2024	TAP	LR100-172: None	(5.2) [9.11]	(5.4) [9.46]	(5.4) [9.46]	(5.4) [9.46]	(5.2) [9.11]
6061T6	2024	TAP	LR100-172: None	(1.3) [2.28]	(1.3) [2.28]	(1.2) [2.10]	(1.2) [2.10]	(1.1) [1.93]

effects of the two rinse methods may have been obscured by the poor bonds.

The last observation available from these results is that the LR100-172 adhesive without primer is very inferior to the FM73/BR127 combination insofar as its initial (up to 504 hours and more) ability to withstand crack extension is concerned. The LR100-172 adhesive degraded much less during exposure than the FM73/BR127 system; however, and it is conceivable that had the exposures been extended to a long enough time (60-100 days) the LR100-172 may have proven the more durable. The fact that these LR100-172 bonded joints failed predominantly within the adhesive layer rather than at the adherend-adhesive interface indicates that this adhesive forms a bond directly to the bare etched metal which does not require a primer layer to impart environmental durability when loaded in a cleavage mode.

As a result of work done over the past several years with adhesives in general and shelter adhesives in particular, a testing scheme for evaluating candidate adhesives has been developed and generally accepted by the shelter industry. This includes agreement upon the types of tests, test conditions, and test specimens which will be utilized to evaluate candidate adhesives.

The work in this program has clearly demonstrated that the use of only one or two types of test is inadequate since some adhesives can display good property levels in one type test and poor property levels in another.

The use of carefully controlled environmental exposures to characterize candidate adhesives for shelter applications is required for adequate materials selection.

The use of the preslotted (finger) specimens for lap shear testing offer no advantages over machined specimens in the development of shear data since the adhesives evaluated were ranked in the same order of decreasing strength by both types of specimens. Since the finger specimens are more expensive, they will not be used in future lap shear evaluations.

The use of an FPL type etch solution for surface preparation of aluminum for adhesive bonding requires the presence of dissolved copper in order to obtain bonding surfaces resistant to humidity degradation.

4.12 SHELTER REPAIR ADHESIVE EVALUATION

During the evaluation of adhesives suitable for the manufacturing of the Air Force portable tactical shelters, it became apparent that adhesive requirements for shelter field repair work would have to be similar to those for production adhesives. Substantially different conditions exist between the production and field repair environments. These differences include the temperatures and pressure available for the curing of adhesive bonds. Because of this difference, adhesives used in field repair of shelters are, of necessity, described as room temperature curing, usually requiring minimal pressures. Another difference is in the degree of surface preparation which is attainable in the field on the bonding surfaces. Adhesives capable of being used in the field under the circumstances described above are available. However, available data on these materials have been limited to temperatures of 140°F (60°C) or less in most cases, while the shelter requirements go up to 200°F (93°C).

The objective of the investigation described here is to identify, test and evaluate adhesive candidates for use in the field repair of Air Force tactical shelters. The investigation is designed to rank the various "field repair" room temperature curing adhesive candidates currently available according to their best features while simultaneously identifying any troublesome deficiencies.

The materials involved in the investigation are listed below.

Five Adhesives: [All Are Two-Part Pastes]
EA 9320 A/B by Hysol
EA 9324 A/B by Hysol
EC 3501 B/A by 3M
EA 934 A/B by Hysol
Epibond 1524 A/B by Furane

Two Adherends: 5052-H34 bare aluminum
6061-T6 bare aluminum

One Primer: BR127 by American Cyanamid

The adherend surface preparation used was phosphoric acid anodization (ARP 1524). This surface preparation was selected to insure the best bonding surface possible. The program then would be evaluating the candidate adhesives only, rather than interfacial bonding characteristics.

All specimens used in this investigation of shelter repair adhesives were machined, single lap-shear tensile specimens prepared in accordance with ASTM D-1002-72 (Figure 68) and ASTM D-2919-71 (Figure 66) with the exception that the panels were 9.0 inches (22.8 mm) wide instead of 7.0 inches (17.7 mm), which made available seven lap-shear specimens per panel instead of five.

The test program was conducted in three phases. Phase I consisted of static tensile lap-shear tests. Phases II and III consisted of stress-durability testing in spring tension fixtures and were conducted simultaneously.

The test results for Phase I are reported in Tables 107 and 108. The test results obtained to date for Phase II are reported in Tables 109 and 110. The test results obtained to date for Phase III are reported in Tables 111 and 112.

4.13 EVALUATION OF SCAR SPECIMEN DESIGN

While doing the Shelter Adhesive Retest and the Shelter Adhesive Repair Programs it became apparent that a multi-joint adhesive specimen would be useful in developing stress-durability data at an accelerated rate. This program was undertaken to evaluate stress environmental durability data utilizing two types of specimens and two loading methods. The two different types of specimens were Stress-Continuous-Adhesive-Replicate (SCAR) specimens illustrated in Figure 69, and the standard single lap-shear specimen illustrated in Figure 70. The SCAR specimen

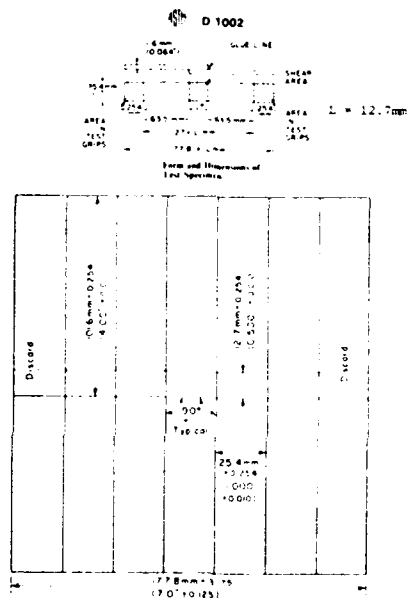


Figure 68. Lap Shear Specimens (from ASTM).

TABLE 107

SHELTER REPAIR PROGRAM
 PHASE I: BASELINE LAP-SHEAR DATA ON 5052-H34 ADHERENDS
 [0.063 Inch (1.59 mm)]

Adhesive	Room Temperature (psi) (MPa)	140°F (60°C) after 10 min. @ 140°F (60°C)	200°F (93°C) after 10 min. @ 200°F (93°C)	140°F (60°C) after 14 days @ 140°F (60°C)	200°F (93°C) after 14 days @ 200°F (93°C)	-65°F (-54°C) after 10 min. @ -65°F (-54°C)
		(psi) (MPa)	(psi) (MPa)	(psi) (MPa)	(psi) (MPa)	(psi) (MPa)
EA9320 A/B Average	4320 30.0	3420 24.0	1670 12.0	3720 26.0	1130 8.0	4120 28.3
EA9324 A/B Average	3540 24.3	3270 23.0	2560 18.0	3420 24.0	2360 16.2	2170 15.0
EC3501 B/A Average	2230 15.4	1310 9.0	580 4.0	560 4.0	400 3.0	270 2.0
EA934 A/B Average	3370 23.2	3280 23.0	2530 17.4	3370 23.2	2410 17.0	2330 16.0
1524 A/B Average	3990 27.4	3350 23.0	3160 22.0	3500 24.1	3140 22.0	2680 18.4

TABLE 108
SHELTER REPAIR PROGRAM
PHASE I: BASELINE LAP-SHEAR DATA ON 6061-T6 ADHERENDS
[0.063 Inch (1.59 mm)]

Adhesive	Room Temperature		140°F (60°C) after 10 min. @ 140°F (60°C)		200°F (93°C) after 10 min. @ 200°F (93°C)		140°F (60°C) after 14 days @ 140°F (60°C)		200°F (93°C) after 14 days @ 200°F (93°C)		-65°F (-54°C) after 10 min. @ -65°F (-54°C)	
	(psi)	(MPa)	(psi)	(MPa)	(psi)	(MPa)	(psi)	(MPa)	(psi)	(MPa)	(psi)	(MPa)
EA9320 A/B Average	4930	34.0	4180	28.8	2300	16.0	3950	27.2	1430	10.0	4810	33.1
EA9324 A/B Average	3710	25.6	34.0	24.0	2240	15.4	3820	26.3	2934	20.2	2530	17.4
EC3501 B/A Average	1990	13.7	1770	8.1	470	3.2	670	5.0	450	3.1	220	2.0
EA934 A/B Average	3370	23.2	3170	22.0	2480	17.1	3510	24.2	2370	16.3	2590	18.0
1524 A/B Average	2380	16.4	3470	24.0	3130	22.0	2790	19.2	2590	18.0	1500	10.3

TABLE 109

PHASE II: STRESS-DURABILITY TEST RESULTS ON 5052-H34 ADHERENDS
EXPOSED AT 200°F (93°C), 95-100% R.H.

Adhesive	Exposure Stress		Stress Durability		Residual Lap Shear Strength	
	% of Baseline	Level (psi) (MPa)	No. of Spec.	Avg. Time (Hours)	No. of Spec.	% of Baseline
EA9320	50	840	2	0.5	---	---
	40	670	2	2.5	---	---
	30	500	2	0.75	---	---
	25	420	1	10.0	---	---
	20	330	4	131.0	---	---
	15	250	3	283.0+	1	61.0
EA9324	50	1280	2	0.5	---	---
	40	1020	2	1.5	---	---
	30	770	3	33.0	---	---
	25	640	1	47.0	---	---
	20	510	4	289.0	---	---
	15	380	1	281.0	---	---
EC3501	50	290	2	0.5	---	---
	40	230	3	225.0+	1	86.0
	35	200	2	337.0+	1	100.9
	30	170	3	448.0+	2	79.0
	20	120	3	672.0+	3	93.0
	50	1270	2	0.5	---	---
EA934	40	1010	2	1.5	---	---
	30	760	4	427.0+	1	72.0
	25	630	2	423.0	---	---
	20	510	3	672.0+	3	78.0
	50	1580	2	0.5	---	---
	40	1260	2	1.5	---	---
1524	30	950	3	172.0	---	---
	25	790	3	357.0	---	---
	20	630	4	416.0	---	---
	20	630	4	416.0	---	---

NOTE: Bonding surfaces prepared with Phosphoric Acid Anodize and primed with BR-127.
Residuals were tested at 200°F (93°C) after 10 minutes at 200°F (93°C).

TABLE 110

PHASE II: STRESS-DURABILITY TEST RESULTS ON 6061-T6 ADHERENDS
EXPOSED AT 200°F (93°C), 95-100% R.H.

Adhesive	Exposure Stress		Stress Durability		Residual Lap Shear Strength	
	% of Baseline	Level (psi) (MPa)	No. of Spec.	Avg. Time (Hours)	No. of Spec.	% of Baseline
EA9320	20	460	3.2	4	11	---
	15	350	2.4	5	49	---
	10	230	1.6	2	672+	30
EA9324	30	670	4.6	5	50	---
	25	560	3.9	4	168	---
	20	450	3.1	5	492+	91
EC3501	45	210	1.5	1	672+	121
	40	190	1.3	3	449+	113
	35	160	1.1	2	672+	116
	30	140	1.0	1	672+	113
	25	120	0.8	1	672+	121
	20	90	0.6	4	672+	111
EA934	35	870	6.0	6	126	---
	30	740	5.1	3	487+	57
	25	620	4.3	1	672+	69
	20	500	3.4	4	672+	73
1524	25	780	5.4	1	375	---
	20	630	4.3	6	253	---
	15	470	3.2	5	502+	66
	10	310	2.2	1	280	---

NOTE: Bonding surfaces prepared with Phosphoric Acid Anodize and primed with BR-127.
Residuals were cested at 200°F (93°C) after 10 minutes at 200°F (93°C).

TABLE III

PHASE III: STRESS-DURABILITY TEST RESULTS ON 5052-H34 ADHERENDS
EXPOSED AT 140°F (60°C), 95-100% R.H.

Adhesive	Exposure Stress		Stress Durability		Residual Lap Shear Strength	
	% of Baseline	Level (psi) (MPa)	No. of Spec.	Avg. Time (Hours)	No. of Spec.	% of Baseline
EA9320	50	1710 11.8	3	12	---	---
	45	1540 10.6	4	35	---	---
	40	1370 9.4	8	396+	---	---
EA9324	50	1640 11.3	2	0.5	---	---
	45	1470 10.1	3	452+	2	111
	40	1310 9.0	8	575+	6	116
EC3501	50	655 4.5	2	0.5	---	---
	40	524 3.6	2	1.5	---	---
	30	393 2.7	2	2.0	---	---
	25	328 2.3	3	231+	1	76
	20	262 1.8	3	271+	1	64
EA934	50	1640 11.3	2	1	---	---
	45	1480 10.2	3	516+	2	99
	40	1310 9.0	8	574+	6	99
1524	50	1680 11.6	2	7	---	---
	45	1510 10.4	3	672+	3	92
	40	1340 9.2	8	623+	7	96

NOTE: Bonding surfaces prepared with Phosphoric Acid Anodize and primed with BR-127.
Residuals were tested at 200°F (93°C) after 10 minutes at 200°F (93°C).

TABLE 112

PHASE III: STRESS-DURABILITY TEST RESULTS ON 6061-T6 ADHERENDS
EXPOSED AT 140°F (60°C), 95-100% R.H.

Adhesive	Exposure Stress		Stress Durability		Residual Lap Shear Strength	
	% of Baseline	Level (psi) (MPa)	No. of Spec.	Avg. Time (Hours)	No. of Spec.	% of Baseline
EA9320	40	1670	11.5	4	24	---
	35	1460	10.1	2	150	---
	33	1380	9.5	1	262	---
	30	1250	8.6	4	210	---
	25	1050	7.2	3	396	---
EA9324	55	1880	12.9	1	3.5	---
	50	1710	11.7	4	407+	113
	45	1530	10.6	3	283	---
	40	1360	9.4	4	672+	132
EC3501	40	470	3.2	3	2.5	---
	35	410	2.8	1	2.0	---
	30	350	2.4	5	272+	68
	25	290	2.0	3	449+	61
EA934	60	1900	13.1	3	171	---
	55	1740	12.0	3	325	---
	50	1590	10.9	2	560	---
	45	1430	9.8	1	672+	106
	40	1270	8.7	4	672+	117
1524	50	1740	12.0	1	672+	110
	45	1560	10.8	3	451+	99
	40	1390	9.6	8	389+	113

NOTE: Bonding surfaces prepared with Phosphoric Acid Anodize and primed with BR-127.
Residuals were tested at 140°F (60°C) after 10 minutes at 140°F (60°C).

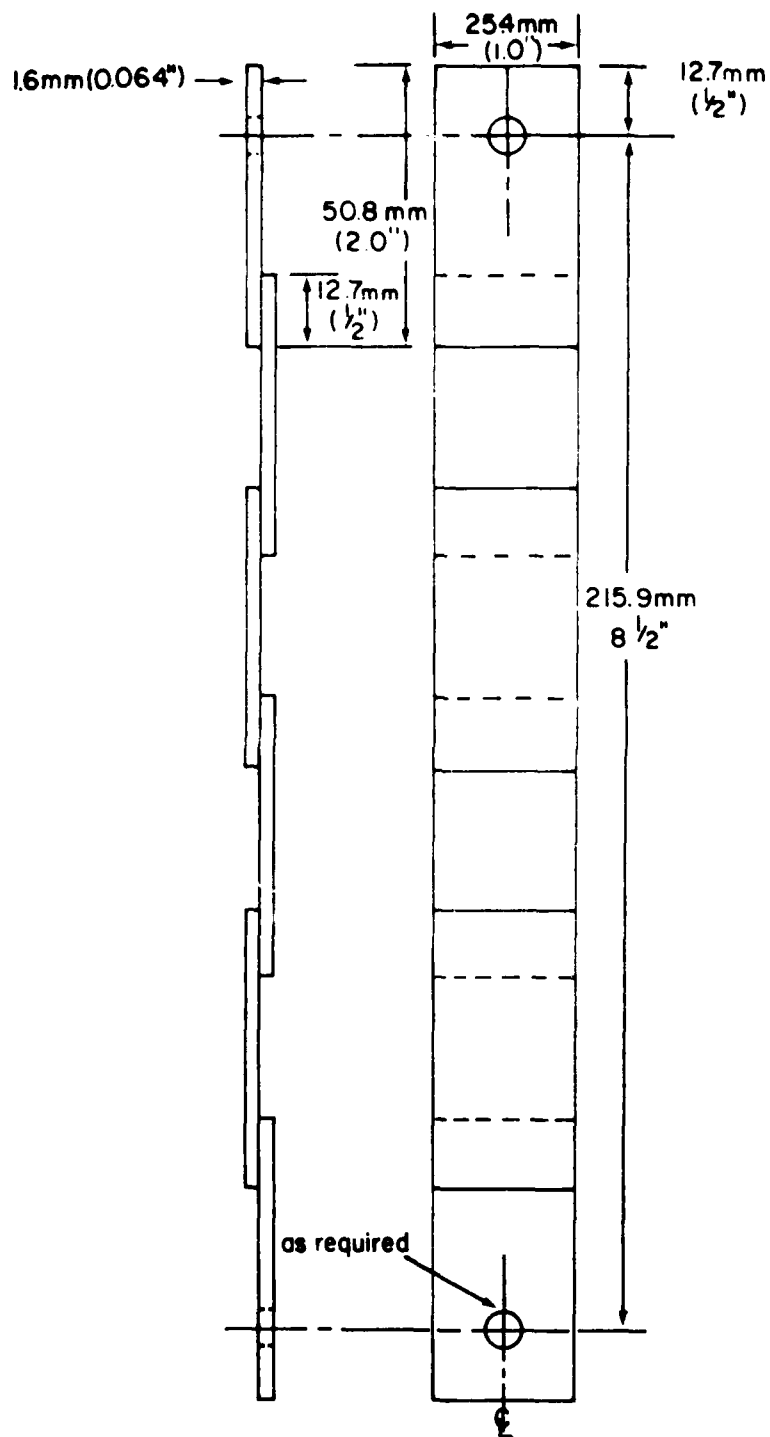


Figure 69. SCAR Specimen.

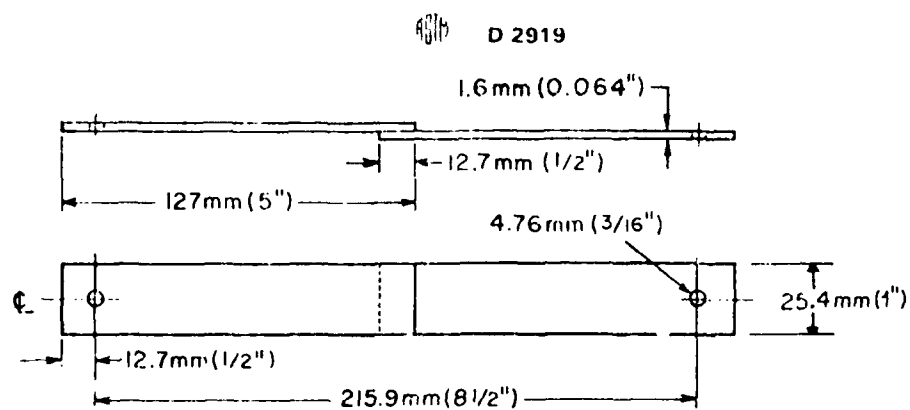


Figure 70. Form and Dimensions of Test Specimen.

consists of a chain of five single lap-joints as illustrated in Figure 69. The two types of loading fixtures are the spring-loaded "Sharpe" fixture illustrated in Figure 71, and the hydraulically loaded cells in the Durability Test Apparatus, (see AFML-TR-78-35).

The test plan consists of the following:

Adhesive - Reliabond 398

Adherend Alloy - 2024-T81 bare aluminum

Surface Preparation - Phosphoric Acid Anodized (APF 1524)

Primer - Reliabond 500

Test Conditions - five replicates each

Static Tests - 72°F (23°C) dry, as fabricated, and
140°F (60°C) dry, as fabricated

Durability Tests - Stress level to be 50 percent of the 140°F (60°C) dry static ultimate strength. Aging condition to be 140°F (60°C), 95-100 percent R.H. Durability tests to continue until specimen failure or until aging time reaches 2,400 hours, whichever occurs first.

SCAR joints which fail will be drilled and bolted back together and the chain will be returned to the aging cycle. Joints surviving 2,400 hours will be tested for residual strength at 140°F (60°C) dry, after ten minutes at 140°F (60°C). Half of the specimens will be loaded with Sharpe Fixtures (five fixtures for single lap-shear specimens and one fixture for the SCAR specimen) and half will be loaded with Durability Test Apparatus (five cells for the single lap-shear specimen and one cell for the SCAR specimen).

If the failures observed during the testing of these specimens are predominantly cohesive within the adhesive layer, the program will be repeated with the MB 329 as the adhesive in place of Reliabond 398. If the observed failures are predominantly in the primer layer, the program will be repeated with an optimized FPL etch surface preparation in place of phosphoric acid anodizing.

The test results obtained to date are reported in Tables 113, 114, and 115.

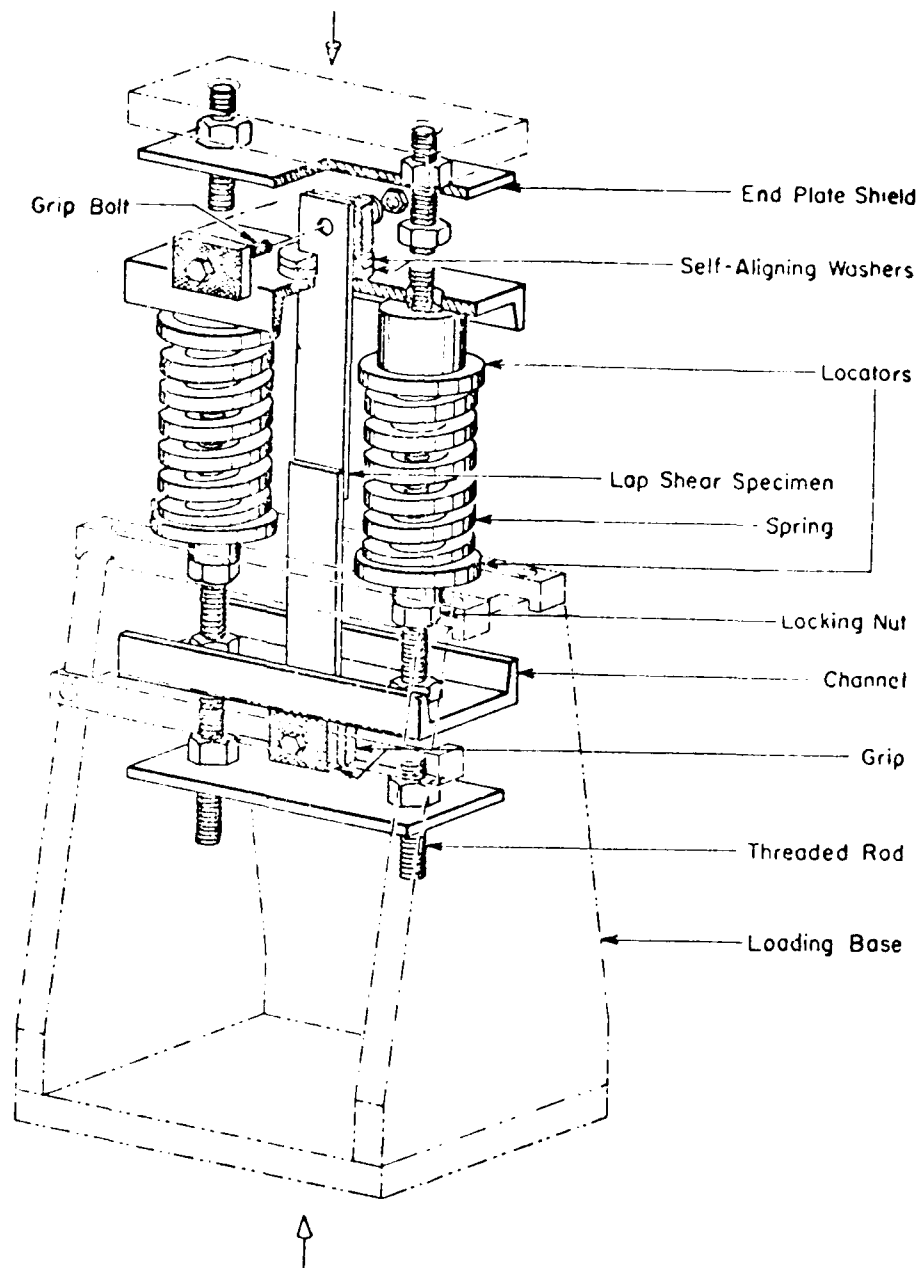


Figure 71. Durability Test Apparatus.

TABLE 113
STATIC LAP SHEAR TEST RESULTS FOR
SCAR DESIGN EVALUATION

Specimen Type	Test Temperature		Ultimate Strength		Failure Sequence	Failure Mode(%) ¹			
	(°F)	(°C)	(psi)	(MPa)		M/P	P	P/A	A
Std. Single Lap	72	22	3180+ 190 ² -	(21.9+ 1.3)	N.A.	0	0	95	5
	140	60	3200+ 150 ² -	(22.0+ 1.0)	N.A.	0	0	85	15
"SCAR"	140	60	3080		1	0	0	80	20
			3080		1	0	0	60	40
			2810		2	0	0	70	30
			2980		3	0	0	80	20
			2780		4	0	0	60	40
			2950+ 140 ² -	(20.3+ 1.0)		0	0	70	30

¹M/P = failure between adherend and primer

P = failure within primer layer

P/A = failure between primer and adhesive

A = failure within adhesive layer

²Average value with standard deviation

TABLE 114

STRESS-DURABILITY TEST RESULTS USING THE SHARP FIXTURE
FOR SCAR DESIGN EVALUATION

Specimen Number	Exposure Stress Level		Stress-Durability		Residual Lap Shear Strength	
	psi	MPa	Ave. Time Hours	Failure Mode M/P-P-P/A-A	% of Baseline	Failure Mode M/P-P-P/A-A
SCAR						
011-4-1-2	1600	11.0	2400+	N.A.	76	0-0-0-100
011-4-1-3	1633	11.3	2400+	N.A.	65	0-0-0-100
011-4-1-4	1600	11.0	2400+	N.A.	62	0-0-0-100
011-4-1-5	1600	11.0	2400+	N.A.	80	0-0-0-100
011-4-1-1	1600	11.0	2400+	N.A.	75	0-0-20-80
Average					71	
Standard Lap-Shear						
011-1-4	1600	11.0	2400+	N.A.	76	0-0-30-70
011-2-1	1600	11.0	2400+	N.A.	74	0-0-20-90
011-2-5	1600	11.0	2400+	N.A.	76	0-0-30-70
011-3-2	1600	11.0	2069	0-0-0-100	N.A.	N.A.
011-3-6	1600	11.0	1478	0-0-5-95	N.A.	N.A.

NOTES: 1. All stress-durability exposures were conducted at 140°F(60°C) and 95-100% R.H.

2. Residual lap shear strengths were obtained at 140°F(60°C) after 10 minutes at 140°F(60°C).

TABLE 115

STRESS-DURABILITY TEST RESULTS USING THE DURABILITY TEST
APPARATUS FOR SCAR DESIGN EVALUATION

Specimen Number	Exposure Stress Level		Stress-Durability		Residual Lap Shear Strength	
	psi	MPa	Ave. Time Hours	Failure Mode M/P-P-P/A-A	% of Baseline	Failure Mode M/P-P-P/A-A
SCAR						
011-5-1-1	1600	11.0	243.1	0-0-0-100	N.A.	N.A.
011-5-1-2	1568	10.8	259.1	0-0-0-100	N.A.	N.A.
011-5-1-4	1633	11.2	360.1	0-0-0-100	N.A.	N.A.
011-5-1-5	1600	11.0	370.85	0-0-0-100	N.A.	N.A.
011-5-1-3	1600	11.0	370.85	0-0-0-100	N.A.	N.A.

NOTES: 1. Standard lap-shear data not available at this time.

2. All stress-durability exposures were conducted at 140°F(60°C) and 95-100% R.H.

3. Residual lap shear strengths were obtained at 140°F(60°C) after 10 minutes at 140°F(60°C).

4.14 COMPATIBILITY OF PHOSPHORIC ACID ANODIZING WITH 350°F (177°C) CURING ADHESIVE PRIMERS

A program was undertaken to determine the compatibility of phosphoric acid anodized (PAA) aluminum surfaces with 350°F (177°C) curing adhesive primers. Some past investigations (Schwartz, Marceau) indicated that the environmental durability of 350°F (177°C) adhesive/primer systems was greater on an FPL etched surface than on a PAA surface. The program reported here consists of conducting surface examinations, lap shear, peel, wedge, and stress-durability tests on a variety of joint combinations. The following alloy/surface preparations/primers/ and adhesives are involved:

1. Adherend alloy - 2024T81 bare;
2. Surface preparations - optimized FPL (OFPL) and PAA;
3. Adhesive/primer combinations - No primer/R398; RB500/R398; No primer/MB329; RB500/MB329; and MB-6725-1/MB329.

The program is organized into three tasks; namely,

Task I - Surface Examination;

Task II - Baseline Values; and

Task III - Surface Effects Tests.

Task I involves preparing both OFPL etched and PAA surfaces and spraying both primers on the surfaces. Scanning electron micrographs (SEM) of both cured and uncured primer samples on each type surface were to be obtained.

Task II involves the preparation of bonds with each combination of alloy/surface prep/adhesive-primer listed above and testing for lap shear and peel strength according to the following test plan:

- (a) Lap shear strength at 72°F (22°C) - ASTM D1002;
- (b) Lap shear strength at 350°F (177°C) - ASTM D1002;
- (c) Peel strength at 72°F (22°C) - ASTM D3167; and
- (d) Peel strength at -65°F (-54°C) - ASTM D3167.

Three replicates of each material combination will be tested, requiring a total of 120 test specimens in Task II (two surface preps x five adhesive/primer combinations x four test conditions x three replicates).

Task III involves the preparation of bonds with each combination of materials listed above and testing for wedge crack-propagation and environmental stress-durability according to the following test plan:

(a) Wedge crack-propagation in a 95°F (35°C)/five percent salt spray environment, and

(b) Stress-durability in a 95°F (35°C)/five percent salt spray environment at a stress level equal to 50 percent of the 72°F (22°C) lap shear strength.

Five replicates of each material combination will be tested, requiring a total of 100 test specimens in Task III (two surface preps x five adhesive/primer combinations x two test conditions x five replicates).

The surface examinations conducted in Task I provided no evidence of non-wetting for either surface preparation method or for either the cured or non-cured primer condition for the RB500 primer. No evidence of rubber inclusions was present either. Small lumps which were dispersed throughout the primer were shown to be strontium chromate particles, which are blended into the primer to impart corrosion resistance. Surface inspection for the MB-6725-1 primer are not yet completed.

The results of the lap-shear and peel tests conducted in Task II are presented in Tables 116 and 117. It will be noted in these two tables that two different data values are presented for some of the adhesive/primer combinations. These represent values obtained from specimens made about three months apart but with the same materials and processing procedures. As can be observed, the data differs substantially in some cases. The places where the data differs most substantially are also those

TABLE 116
LAP SHEAR DATA SUMMARY

Adhesive	Surface Prep.	Primer	72°F (22°C) Strength		350°F (177°C) Strength	
			(psi)	(MPa)	(psi)	(MPa)
R398	OPT	None	3320	22.9	2300	15.8
		500	3300	22.7	2380	16.4
R398	PAA	None	3890	26.8	2840	19.6
		500	2490	17.2	2300	15.8
		500	3130	21.6	2570	17.7
MB329-1	OPT	None	3150	21.7	2710	18.7
		500	2610	18.0	2880	19.4
		500	2690	18.5	3230	22.3
		6725-1	3260	22.5	3110	21.4
MB329-1	PAA	None	3370	23.2	3250	22.4
		500	2690	18.5	3170	21.8
		500	3020	20.8	3250	22.4
		6725-1	3040	20.9	3200	22.0

- NOTES: 1. All tests were on 2024T81 aluminum adherends.
 2. The two surface preparations are:
 OPT - optimized FPL etch
 PAA - phosphoric acid anodized.

TABLE 117
FLOATING ROLLER PEEL DATA SUMMARY

Adhesive	Surface Prep.	Primer	Peel Strength (lb/in width) [N/cm width]			
			72°F (22°C)		-65°F (-54°C)	
R398	OPT	None	(8.31)	[14.55] - 4	(6.95)	[12.24] - 4
		500	(6.58)	[11.52] - 3	(5.50)	[9.63] - 3
R398	PAA	None	(5.62)	[9.84] - 2	(5.34)	[9.35] - 2
		None	(8.98)	[15.72] - 2	(8.03)	[14.06] - 2
		500	(12.94)	[22.66] - 3	(13.93)	[24.30] - 2
		500	(3.66)	[6.41] - 3	(3.40)	[5.95] - 2
MB329-1	OPT	None	(5.60)	[9.81] - 4	(8.60)	[15.06] - 4
		500	(5.03)	[8.81] - 4	(3.14)	[5.50] - 4
		6725-1	(4.88)	[8.54] - 4	(6.23)	[10.91] - 4
MB329-1	PAA	None	(5.01)	[8.77] - 2	(4.38)	[7.67] - 2
		None	(8.20)	[14.36] - 2	(5.58)	[9.77] - 2
		500	(6.43)	[11.26] - 3	(5.92)	[10.37] - 2
		500	(3.97)	[6.95] - 3	(5.94)	[10.40] - 2
		6725-1	(4.95)	[8.67] - 4	(4.74)	[8.30] - 4

- NOTES: 1. Numbers behind hyphens in each column represent the numbers of specimens tested.
2. All tests were on 2024T81 aluminum adherends.
3. The two surface preparations are:
- OPT - optimized FPL etch
- PAA - phosphoric acid anodized.

where the failure mode differed markedly. At this time no explanation for this variability can be offered.

One-half of the wedge crack-propagation tests required in Task III are completed and the balance are underway. These results are presented in Table 118.

TABLE 118
WEDGE CRACK-PROPAGATION DATA SUMMARY

Adhesive	Primer	Initial	Cumulative Crack Length (inches)				
			1 hour	4 hours	24 hours	168 hours	672 hours
R398	None	1.970	2.175	2.202	2.217	2.229	2.320
R398	RB500	1.917	2.068	2.070	2.095	2.146	2.208
MB329-1	None	1.698	1.759	1.787	1.799	1.865	1.916
MB329-1	RB500	1.740	1.831	1.840	1.866	1.942	1.987

The stress-durability testing required in Task III was delayed because of a specimen corrosion problem around the gripping clamp. While not a problem in normal humidity aging, this corrosion proved quite severe in the salt spray environment. This problem has been overcome by coating the gripped area of each specimen with a corrosion inhibiting coating before assembly into the loading fixture. These durability exposures are currently underway.

4.15 AEDC END CAP ADHESIVE EVALUATION

This evaluation was accomplished in two phases. Phase I required the fabrication and testing of "T"-type tension specimens using polyimide adherends. The "stem" and "cross" of the "T" specimen were bonded together with AF-143 adhesive, by 3M, and DC 3145 adhesive, by Dow Corning. Table 119 shows the test results obtained with these specimens after exposure to various conditions. Phase I also involved the fabrication and testing of polyimide to aluminum lap shear specimens bonded with DC 3145 adhesive. The results of these tests are shown in Table 120.

TABLE 119
"T"-TYPE TENSION TEST RESULTS

Adhesive	Aging Condition	Test Temperature		Strength ¹	
		°F	(°C)	psi	(MPa)
AF-143	72°F (22°C)	72	22	1945	13.4
AF-143	48 hrs.@420°F (216°C)	72	22	1438	9.9
AF-143	48 hrs.@420°F (216°C)	420	216	810	5.6
AF-143	48 hrs.@420°F (216°C)	450	232	366	2.5
DC 3145	72°F (22°C)	72	22	229	1.6
DC 3145	48 hrs.@420°F (216°C)	72	22	187	1.3
DC 3145	48 hrs.@420°F (216°C)	420	216	68	0.5
DC 3145	48 hrs.@420°F (216°C)	450	232	78	0.5

¹Average of three specimens.

TABLE 120
LAP SHEAR TEST RESULTS ON POLYIMIDE/ALUMINUM SPECIMENS
BONDED WITH DC 3145 ADHESIVE

Aging Condition	Test Temperature		Lap Shear Str. ¹	
	°F	(°C)	psi	(MPa)
72°F (22°C)	72	22	181	1.2
48 hrs.@ 420°F (216°C)	72	22	52	0.4 ²
48 hrs.@ 420°F (216°C)	420	216	30	0.2

¹Average of three specimens.

²Two of the three specimens fell apart before testing.
Value represents only one specimen.

Phase II involved long-term agings of both the "T"-type tension specimens and lap shear specimens using polyimide adherends and AF-143 adhesive. The results of these tests are shown in Tables 121 and 122.

4.16 DURABILITY TESTING OF ADHESIVES

The University of Dayton Research Institute has been conducting investigations into the durability of adhesives and adhesive bonded structures for several years. Much of this work in recent years has involved the use of environmental stress-rupture testing of lap shear joints. The test apparatus which permits the measurement of the durability of bonded joints while exposed to elevated temperature and humidity under a controlled stress level was designed and constructed by the University of Dayton and has been in service for several years. It permits time-to-failure measurements on stressed adhesive bonds in adverse environments and also has the capability of measuring joint deformation as a function of exposure time. AFML-TR-78-35, Parts I and II, described investigations of the durability of two 350°F (177°C) curing adhesive systems and one 250°F (121°C) curing adhesive system on acid etched and anodized adherend surfaces.

In the investigation reported here, another 350°F (177°C) curing adhesive system (Reliabond 398) has been investigated on an optimized Forest Products Laboratory (OFPL) acid etched adherend surface (2024T3 bare aluminum). Durability tests using stressed lap shear joints in the environmental stress-rupture apparatus have been conducted at 140°F (60°C). A second type of durability test in which unstressed lap shear joints are soaked in water at 140°F (60°C) has also been conducted to provide a comparison of results obtained from the two different test procedures. A complete description and discussion of this investigation has been published in AFML-TR-78-35, Part III, "Environmental Durability Testing of Structural Adhesives, Part III, Reliabond 500/Reliabond 398."

TABLE 121
TEST RESULTS OBTAINED ON AF-143
ADHESIVE BONDED JOINTS

"T" Type Tension Specimen
BPI 373 to BPI 373 Adherends

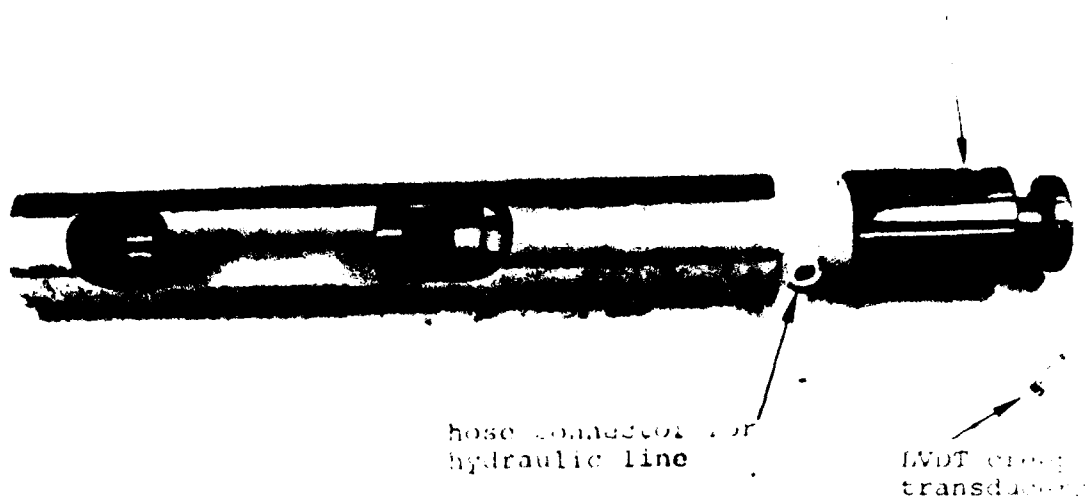
Specimen Number	Aging Condition	Test Temperature	Strength	
			(psi)	(MPa)
A1	R.T.	R.T.	2017	13.91
A2			1864	12.85
A3			1954	13.47
Average			1945	13.41
A4	48 hrs @ 420°F (216°C)	R.T.	1623	11.19
A5			1188	8.19
A6			1504	10.37
Average			1438	9.92
A7	48 hrs @ 420°F (216°C)	420°F(216°C)	785	5.41
A8			813	5.61
A9			831	5.73
Average			810	5.58
A10	48 hrs @ 420°F (216°C)	450°F(232°C)	415	2.86
A11			303	2.09
A12			380	2.62
Average			366	2.52
D4	1000 hrs @ 420°F(216°C)	R.T.	600	4.14
D5			762	5.25
D6			815	5.62
Average			726	5.01
D1	1000 hrs @ 420°F(216°C)	420°F(216°C)	747	5.15
D2			521	3.59
D3			512	3.53
Average			593	4.09

TABLE 122
TEST RESULTS OBTAINED ON AF-143
ADHESIVE BONDED JOINTS

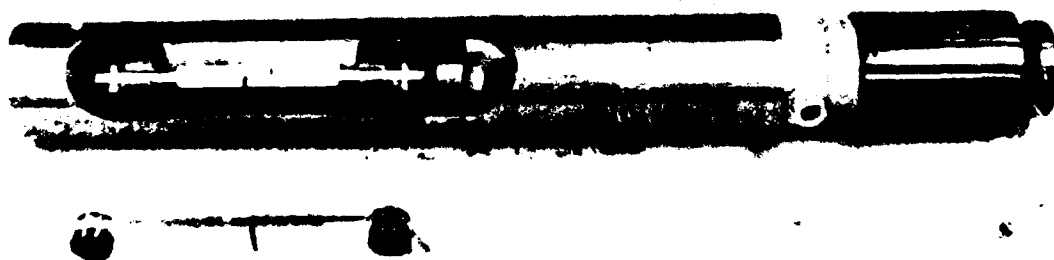
Lap Shear Specimens
BPI 373 to BPI 373 Adherends

Specimen Number	Aging Condition	Test Temperature	Strength	
			(psi)	(MPa)
E1	1000 hrs @ 420°F (216°C)	R.T.	622	4.29
E3			689	4.75
E5			525	3.62
Average			612	4.22
E2	1000 hrs @ 420°F (216°C)	420°F (216°C)	254	1.75
E4			250	1.72
E6			270	1.86
Average			258	1.78

The durability test apparatus provides the capability of conducting environmental exposures on specimens subjected to a constant tensile load during the exposure period. The environment can be controlled between 95°F (35°C) and 200°F (93°C) and between 40 and 95 percent R.H. Loads are applied hydraulically and can be controlled to within ± 10 lbs (± 44 N) over a range from 0 to 1,500 lbs (0 to 6,675 N). Figures 72 to 74 illustrate the test apparatus and specimen mounting cells. An adhesive lap shear specimen of the type used in this program is shown mounted and also lying beside the test cell in Figure 72b. The tester can accommodate 12 specimens simultaneously. Although all 12 are exposed to the same temperature and humidity conditions, the load on each can be independently controlled. The exposure cabinet is a standard Blue M humidity cabinet, Model AC-7502HA-1, which has 12 holes cut through the door for insertion of the test cells. Each test cell permits free access of the environment to the test specimen. Small Linear-Virable-Differential-Transformers (LVDT) transducers are mounted in the hydraulic loading heads of each cell. These transducers permit continuous recording of specimen creep deformation during exposure. The



(a) Empty Cell



(b) Cell with Mounted Specimen

Figure 72. Specimen Mounting Cells For the Durability Test Apparatus.



Figure 73. Specimen Mounting Cell Being Inserted Into Humidity Cabinet.

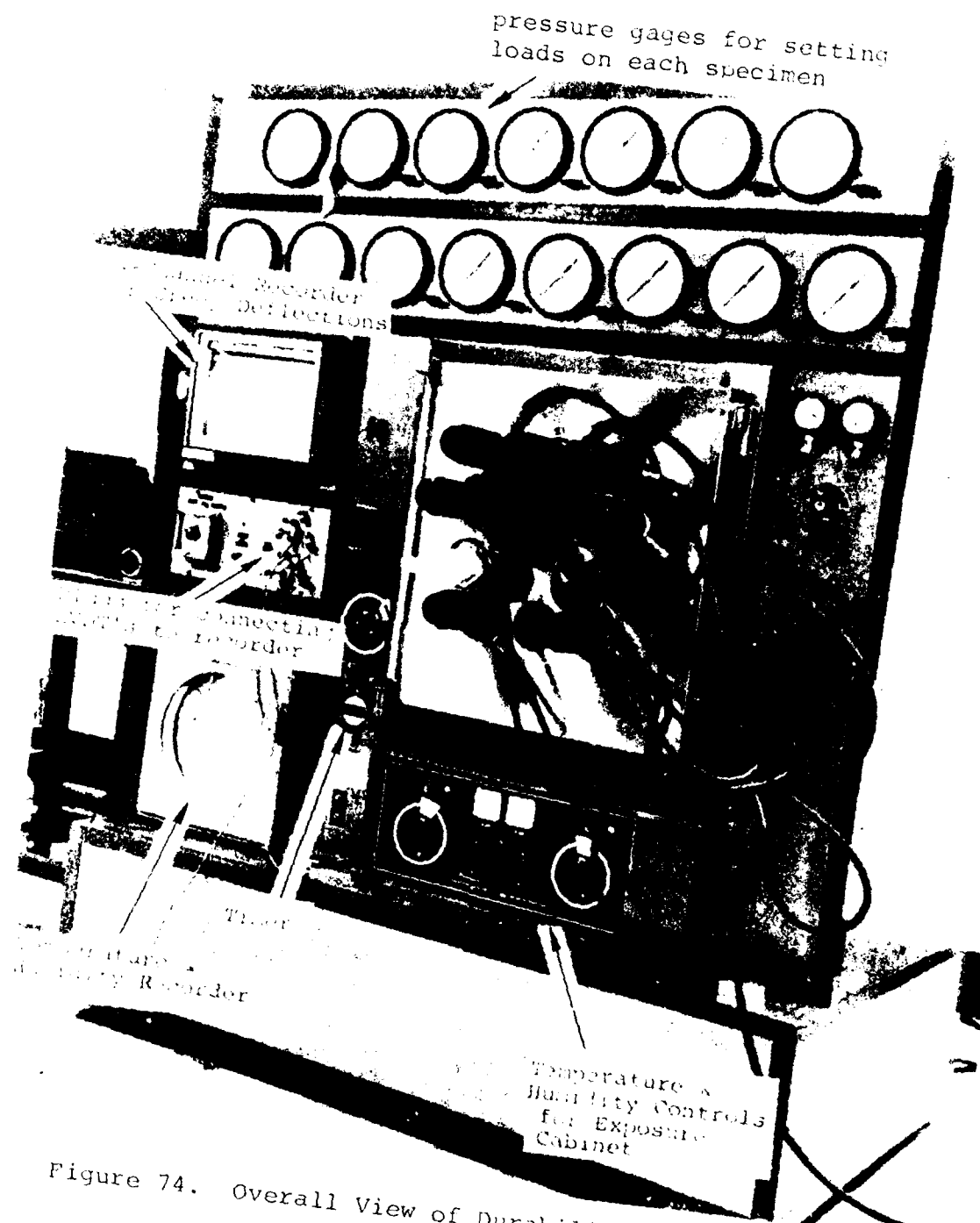


Figure 74. Overall View of Durability Test Apparatus.

creep measurement capability was not utilized in this investigation, however; only time-to-rupture was recorded.

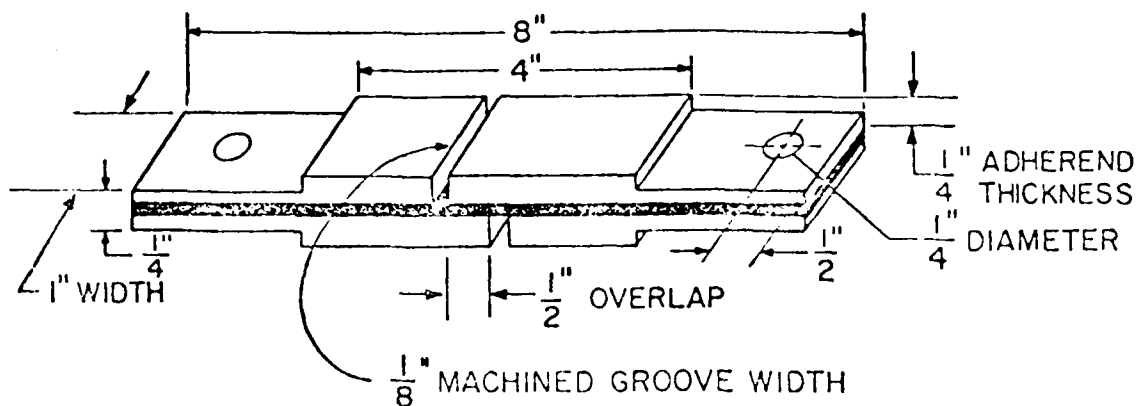
A 350°F (177°C) curing modified epoxy structural adhesive (Reliabond 398 by Reliable, division of Ciba-Geigy) has been evaluated. The adhesive is nominally 0.090 lb/ft² (0.439 Kg/m²) and is nominally 0.012 inch (0.030 cm) thick. It is supported on a synthetic woven fabric carrier. This adhesive was used in combination with a high temperature resistant, corrosion inhibiting primer (Reliabond 500 by Reliable, division of Ciba-Geigy).

All of the specimens in this investigation were prepared with 2024T3 bare aluminum adherends. These adherends were 0.250 inch (0.64 cm) thick and were used to prepare machined single lap shear specimens (also known as blister shear specimens). Figure 75 illustrates this specimen.

An optimized FPL etch surface preparation was used for this program. This is the same as that described in Boeing process specification BAC 5514.

Specimen fabrication procedures can be separated into three general phases. The first phase deals with adherend surface preparation, the second with the panel bonding operation, and the third with the machining of the bonded panel into individual test specimens.

Four types of tests were conducted on the lap shear specimens in this investigation. The first was a simple static test on the as-fabricated, dry specimens at three different temperatures; 72°F (22°C), 140°F (60°C), and 250°F (121°C). The second type was also a simple static test at 72°F (22°C) on specimens which had been exposed to elevated temperature, high-humidity aging [140°F (60°C) and 95 to 100 percent R.H.] for 30 and 100 days prior to testing. The third type of test was also a simple static test at 140°F (60°C) on specimens which had been soaked in water at 140°F (60°C) for 100 and 1,000 hours prior to testing. The fourth type of test was an environmental



0.250 inch (0.64cm), thick adherend, machined single lap shear specimen

Figure 75. Single Lap Shear Adhesive Specimen.

stress-rupture test in which the lap shear specimens were loaded to various stress levels and exposed to a 140°F (60°C), 95 to 100 percent R.H. environment until failure. If no failure had occurred within 2,400 hours, the specimens were removed from the environmental durability tester and tested statically at 72°F (22°C) for residual strength. The stresses imposed during the environmental durability exposures varied between 20 and 60 percent of the ultimate strength obtained in the dry static tests at 140°F (60°C). All of the lap shear tests conducted on specimens which had been humidity aged (either the static or residual strength tests) or water were completed within 30 minutes after the specimen was removed from the environment. Additionally, each of these specimens were wrapped with a wet cloth to prevent dryout during this period.

Tables 123 and 124 present the test results obtained during this investigation. The environmental stress-rupture durability data are graphically illustrated in Figure 76.

As can be seen from the data in Table 123, the static lap shear strength and failure mode of dry specimens is little affected by temperature from 72°F (22°C) to 250°F (121°C). In fact, the strength of the bonds made with the R398/R500 system in this investigation retained a considerably higher fraction

TABLE 123
SINGLE LAP SHEAR STRENGTH OF ADHESIVE JOINTS

Adherends: 2024T3 bare aluminum
 Surface Preparation: Optimized FPL etch
 Surface Primer: Reliabond 500
 Adhesive: Reliabond 398

Test Temperature (°F) (°C)		Pre-Test Conditioning	Ultimate Strength (psi) (MPa)		Failure Mode (% Coh)	No. of Specimens Represented
72	22	None	6430	44.3	85	5
140	60	None	6160	42.5	98	5
250	121	None	5610	38.7	75	5
72	22	30 days at 140°F (60°C) and 95-100% R.H. - unstressed	5630	38.8	65	5
72	22	100 days at 140°F (60°C) and 95-100% R.H. - unstressed	5040	34.7	40	5
140	60	100 hr. soak in water at 140°F (60°C)-unstressed	5920	40.8	85	5
		1000 hr. soak in water at 140°F (60°C)-unstressed	4790	33.0	40	5

TABLE 124
ENVIRONMENTAL STRESS-RUPTURE LAP SHEAR
BEHAVIOR OF ADHESIVE JOINTS

Adherends: 2024T3 bare aluminum
Surface Preparation: Optimized FPL etch
Surface Primer: Reliabond 500
Adhesive: Reliabond 398
Exposure Environment: 140°F(60°C) and 95-100% R.H.

Joint Shear Stress During Exposure (% of 140°F ³ (psi) (MPa) dry ultimate)			Time to Failure (hrs)	Residual Lap Shear Strength (psi) (MPa)		Failure Mode (% Coh)	No. of Specimens Represented
3700	25.5	60	560	---	---	40	3
2460	16.9	40	2010 ¹	5950	41.0	60	3
1850	12.7	30	2400 ²	5280	36.4	55	3
1230	8.5	20	2400 ²	5960	41.1	75	3

¹Two specimens survived 2400-hour exposure period.

²All specimens survived 2400-hour exposure period.

³Base strength at 140°F - 6160 psi (42.4 MPa).

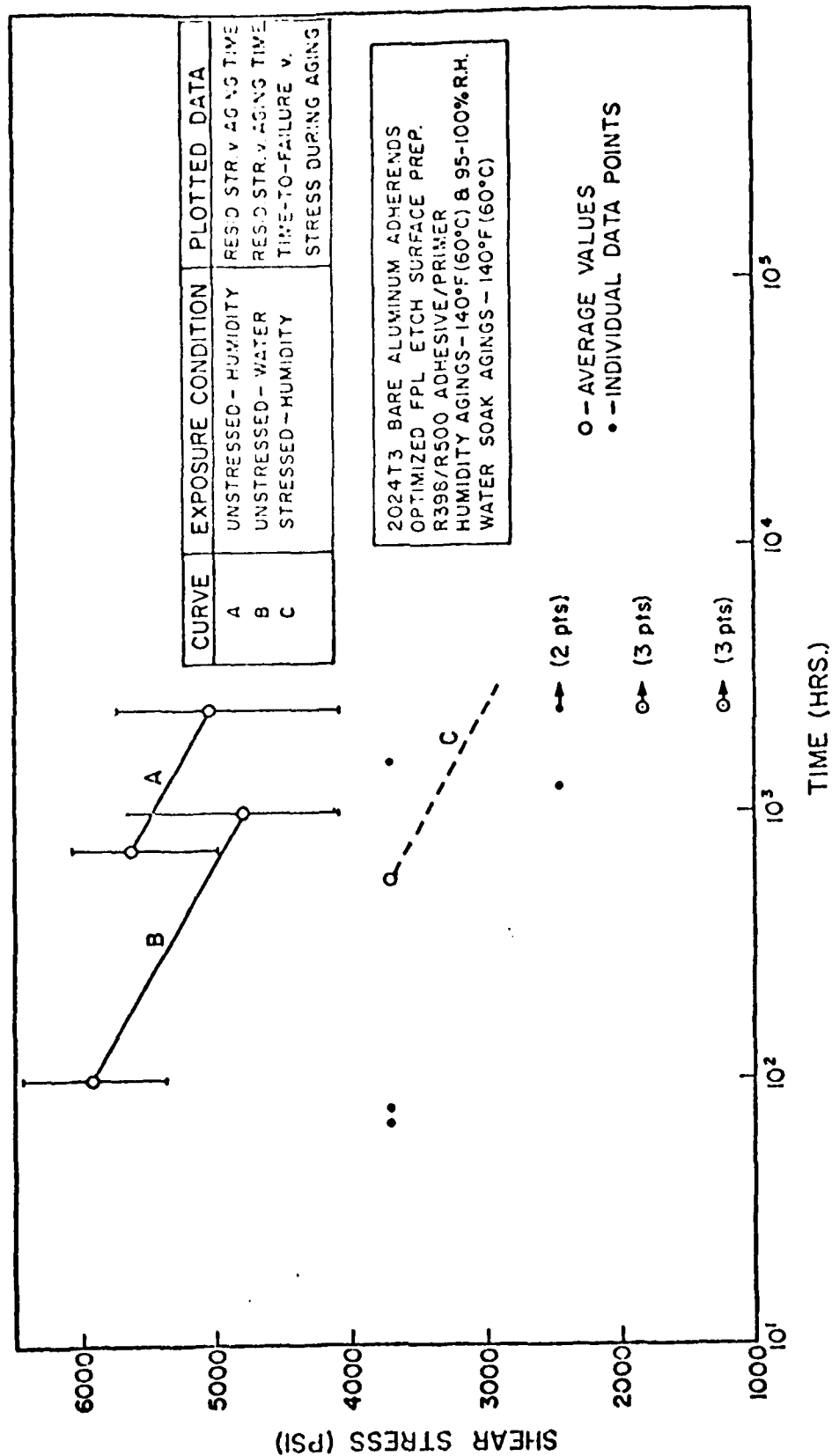


Figure 76. Environmental Degradation Behavior of Machined Single Lap Shear Adhesive Joints.

of their room temperature value than those previously reported in AFML-TR-78-35, Part I, for two other 350°F (177°C) curing adhesive systems (PL-729-3/PL-728 and AF-143-2/EC-3917). Failure modes for all three of these adhesive systems on OFPL etched surfaces and 2024T3 bare aluminum adherends was predominantly cohesive for the dry static tests.

The unstressed specimens aged in a humidity cabinet at 140°F (60°C) and 95 to 100 percent R.H. exhibited a residual strength reduction of about 12 percent after 30 days and 22 percent after 100 days (based on original 72°F (22°C) dry static strength). The failure mode of these specimens becomes progressively more adhesive (interfacial) in nature as aging time increases.

The unstressed specimens aged in a water bath at 140°F (60°C) exhibited a residual strength reduction of about 8 percent after 100 hours and 25 percent after 1,000 hours (again based on original 72°F (22°C) dry static strength). The failure mode of these specimens also becomes progressively more adhesive in nature as aging time increases.

An interesting point to note in comparing the residual strength characteristics of unstressed specimens aged in the humidity cabinet and in a water bath is that the slope of the residual strength versus aging time curves plotted in Figure 76 have the same slope. The relative location of these two curves (A and B) is probably the result of two factors. First, the residual strengths of the water soaked specimens (curve B) were obtained at 140°F (60°C) test temperature, while those for the humidity aged specimens (curve A) were obtained at a 72°F (22°C) test temperature. This difference in test temperature caused about a 5 percent decrease in strength on the dry unaged specimens (Table 123). Since the difference in the positions of curves A and B in Figure 76 represents a difference of about 10 percent in strength for equivalent aging time, it would appear that the difference in aging conditions may also

be contributing to this difference. The progressive decrease in the amount of cohesive failure (alternatively, the progressive increase in the amount of adhesive or interfacial failure) with increasing exposure time indeed indicates a progressive degradation of the interfacial bond, leading to reduced strengths for longer exposures. Since it is reasonable that water would diffuse into the bondline more rapidly in a water immersion exposure than in a high humidity exposure, it is also reasonable that the differences in exposure conditions between curves A and B would indeed contribute to a shift in their relative positions.

The specimens which were exposed to a 140°F (60°C) and 95 to 100 percent R.H. under stress exhibited no failures at all for aging times of up to 2,400 hours at stresses of 1,850 psi (12.7 MPa) and below. Two of the three specimens subjected to a 2,460 psi (16.9 MPa) stress level also survived for 2,400 hours without failure. Since this only provides one good data point for purposes of plotting a stress versus time-to-failure curve in Figure 76, a broken curve, C, has been plotted through the single real average value with a slope arbitrarily equal to curves A and B. Wegman, et al.^[24] have developed evidence that, for some adhesives, this procedure provides a reasonably valid method of prediction of time-to-failure for stressed joints in environmental aging. There is insufficient evidence to establish what the true slope of curve C should be. To do this, substantially more time would have had to have been expended in carrying the exposures completely out to joint failure.

The levels of durability observed are very comparable to those reported for the AF-143-2/EC-3917 and PL-729-3/PL-728 systems in AFML-TR-78-35, Part I, particularly below 2,800 psi (19.3 MPa) where the stress is low enough that the adherend surface oxide layer should not fracture (see pp. 27-30 of AFML-TR-78-35, Part I). A comparison of the environmental stress-rupture time-to-failure behavior of these two systems

with the R398/R500 system, tested here, is presented in Figure 77. Here both the broken curve plotted in Figure 76 as well as the relevant data points for the R398/R500 system are presented for comparison with the AF-143-2 and PL-729-3 curves. At worst it is evident that the R398 system is at least equal to the two previously tested. If the broken curve, obtained as described above, is indeed a reasonable estimate of the R398 behavior, then this system would appear to be more durable than the previous two for this type of test condition.

While the residual strength of the aged unstressed specimens consistently decreases with increasing aging times, as would be expected, the residual strength behavior of the specimens aged under stress is more difficult to explain. While one might normally expect that the residual strength of those specimens which survived the entire 2,400-hour aging period would be higher for the specimens which were at a lower stress and lower for those specimens which were at higher stress, this is not the case, nor has it been for any of the previously tested materials (AFML-TR-78-35, Parts I and II), so long as the stress during exposure is low enough that the surface oxide layer does not fracture (less than about 2,800 psi (19.3 MPa) for 0.250 inch (0.64 cm) thick adherends). For stresses below this level, the residual stress of specimens which survive the 2,400-hour exposure are all about equivalent regardless of the stress level during exposure, and also about equivalent to the original dry room temperature control strength.

Four conclusions were drawn from the results of this investigation.

1. Unstressed aging of lap shear adhesive joints made with the Reliabond 398/Reliabond 500 (R398/R500) adhesive/primer systems on optimized FPL etched 2024T3 bare aluminum adherends in both a 140°F (60°C)/95 to 100 percent R.H. environment and a 140°F (60°C) water soak results in a progressive loss of residual strength with increased aging time and a progressive

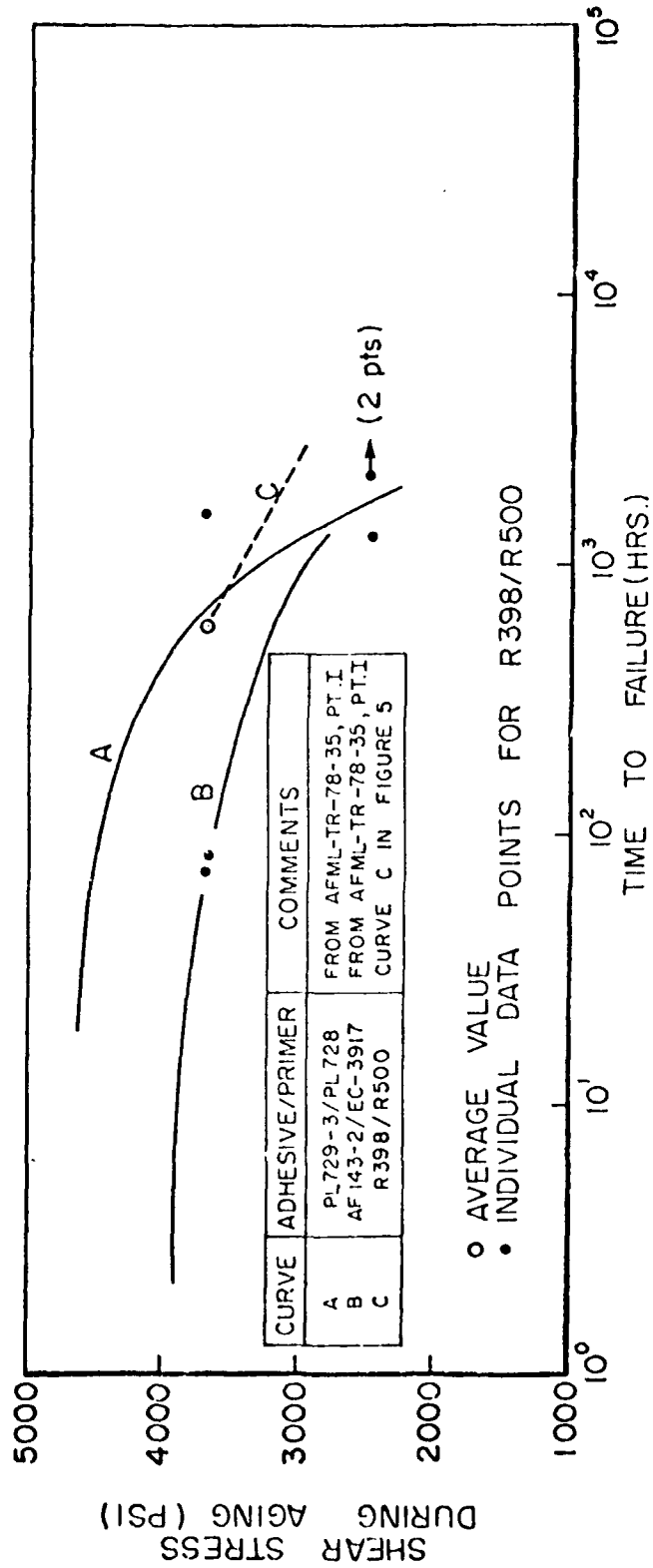


Figure 77. Comparative Environmental Stress-Rupture Time-to-Failure Behavior of Three 350°F(177°C) Curing Adhesive Systems at 140°F(60°C) and 95-100% Relative Humidity.

increase in the amount of adhesive (interfacial) failure with increased aging time.

2. Unstressed agings in the 140°F (60°C) water soak produce about a 10 percent lower residual strength, for equivalent aging time, than unstressed agings in a 140°F (60°C)/95 to 100 percent R.H. environment.

3. Specimens made with the R398/R500 adhesive/primer system and subjected to shear stress during aging in a 140°F (60°C)/95 to 100 percent R.H. environment produced time-to-failure comparable to those obtained previously (AFML-TR-78-35, Part I) for the PL-729-3/PL-728 and AF-143-2/EC-3917 adhesive/primer systems on the same substrates. It is possible, had aging times been carried out beyond 2,400 hours, that the R398/R500 system would have produced longer times-to-failure than either of the other two systems for shear stress levels during exposure of less than about 2,800 psi (19.3 MPa). This is the approximate level at which oxide fracture occurs on this type specimen (see AFML-TR-78-35, Part I - Appendix D).

4. The R398/R500 system loses less strength during a 250°F (121°C) test on dry unaged specimens than either the PL-729-3/PL-728 or AF-143-2/EC-3917 systems tested earlier.

4.17 FLEXURAL TESTING OF PMR-15/GLASS PANELS

This investigation was aimed at determining the value of a Skybond 705 coating for preventing oxidative degradation in glass reinforced PMR-15 polyimide laminates.

Flexure specimens were cut from two glass/PMR-15 laminates. Some of the specimens were coated with Skybond 705 from a solution of 15 percent solids in toluol. The coated specimens were sanded, wiped with methyl ethyl ketone, and blown dry with nitrogen. They were then wiped with methanol and again blown dry with nitrogen. Two coats of the Skybond 705 varnish were brushed onto the coated samples and cured.

Both coated and uncoated specimens were tested at room temperature and 550°F (288°C) after no aging and after aging for 1,000 hours at 550°F (288°C) at one and two atmospheres air pressure. The flexural test results are presented in Table 125.

TABLE 125
FLEXURAL PROPERTIES OF PMR-15/GLASS LAMINATES

Specimen Condition	Pretest Aging Conditions		Test		Flexure Strength (ksi) (MPa)	Flexure Modulus (Msi) (GPa)
	Temperature (°F) (°C)	Pressure (atm)	Temperature (°F) (°C)			
Uncoated	Unaged	Unaged	72	22	51.5 (355)	4.01 (27.7)
Uncoated	Unaged	Unaged	550	288	30.0 (207)	2.33 (16.1)
Uncoated	1000 hrs @ 550 288	1	550	288	27.9 (192)	1.25 (8.6)
Coated	1000 hrs @ 550 288	1	550	288	30.5 (210)	1.31 (9.0)
Uncoated	1000 hrs @ 550 288	2	550	288	34.0 (234)	1.33 (9.2)
Coated	1000 hrs @ 550 288	2	550	288	33.9 (234)	1.36 (9.4)

REFERENCES

1. Cervay, R. R., "Tensile Properties of Six Slack-Quenched Aluminum Alloy Rolled Plates," UDR-TM-79-23, November 1979.
2. "Hardness and Conductivity Inspection of Heat Treated Aluminum Alloy Parts," Aerospace Material Specification Proposed Draft, January 1979.
3. Fudge, K. A. and Jones, R. E., Engineering Design Data for Aluminum Alloy 2124-T851 Thick Plate, AFML-TR-73-310, January 1974.
4. "Investigation of Improperly Quenched (Soft) Aluminum Plate," AFML-TR-79-4205, Harmsworth and Petrak, December 1979.
5. Ruschau, J. J., Complete Fatigue Crack Growth Rate Curves for Aluminum Alloy 2124-T851 including Typical Crack Growth Models, AFML-TR-78-155, November 1978.
6. Hadak, S. J., et al., Development of Standard Methods of Testing and Analyzing Fatigue Crack Growth Rate Data, AFML-TR-78-40, 1978.
7. Anis, C. J., Jr., et al., An Interpolative Model for Elevated Temperature Fatigue Crack Propagation, AFML-TR-76-176, November 1976.
8. Fudge, K. A. and Jones, R. E., Engineering Design Data for Aluminum Alloy 2124-T851 Thick Plate, AFML-TR-73-310, January 1974.
9. Cervay, R. R., Temperature Effects on the Mechanical Properties of Aluminum Alloy 2124-T851, AFML-TR-75-208, December 1975.
10. Walker, K., "The Effect of Stress Ratio During Crack Propagation and Fatigue for 2024-T3 and 7075-T6 Aluminum," ASTM STP 426, 1970.
11. Forman, R. G., et al., "Numerical Analysis of Crack Propagation in Cyclically Loaded Structures," J. of Basic Eng., Trans. ASME, Vol. 89, Series D, September 1967.
12. Corbly, D. M., Air Force Materials Laboratory, Wright-Patterson Air Force Base, Ohio, Personal Communication to John J. Ruschau, July 1978.

13. Variability in Fatigue Crack Growth Testing, Clark, W. G., et al., Journal of Testing and Evaluation, JTEVA, Vol. 3, No. 6, 1975.
14. Development of Standard Methods of Testing and Analyzing Fatigue Crack Growth Rate Data, Hudak, S. J., et al., Westinghouse R&D Center, February 1978.
15. Crack Length Determination for the Compact Tension Specimen Using a Crack-Opening Displacement Calibration, Sullivan, A. M., NRL Report 7888, June 1975.
16. Petrak, G. J., "Lubricating Characteristics of Aerospace Greases on Fasteners," UDR-TM-77-23, December 1977.
17. Petrak, G. J., "Torque/Tension Relationships for High Strength Threaded Fasteners Lubricated with Graphite Grease and Moly-D Grease," UDR-TM-78-11, October 1978.
18. Petrak, G. J., "Comparison of Manually and Machine Developed Torque/Tension Data," UDR-TM-78-16, December 1978.
19. Petrak, G. J., "Some Torque/Tension Data for Threaded Fasteners," UDR-TM-79-01, January 1979.
20. Ruschau, J. J., "Determination of Test Technique Influence on K_{ISCC} Values for Aluminum 7075-T651," AFML-TR-79-4117, August 1979.
21. Sprowls, D. O., et al., Evaluation of Stress-Corrosion Cracking Susceptibility Using Fracture Mechanics Techniques, Alcoa Research Laboratories, May 1973.
22. Staley, J. T., Investigation to Develop a High Strength Stress-Corrosion Resistant Naval Aircraft Aluminum Alloy, Alcoa Research Laboratories, November 1970.
23. Hyatt, M. V. and Speidel, M. O., Stress Corrosion Cracking of High Strength Aluminum Alloys, Boeing D6-24840, June 1970.
24. Wegman, R. F., Bodnar, M. J., and Ross, M. C., "A New Technique for Assessing the Durability of Structural Adhesives," SAMPE Journal, Vol. 14, No. 1, January/February 1978.

END

DATE
FILMED

8-80

DTIC